FURTHER STUDIES OF THE UNDERWATER NOISE PRODUCED BY RAINFALL

National Center
for
Physical Acoustics

The University of Mississippi

Institute for Technology Development

A joint venture

(4)

FURTHER STUDIES OF THE UNDERWATER NOISE PRODUCED BY RAINFALL

BY

PAUL A. ELMORE
HUGH C. PUMPHREY
and
LAWRENCE A. CRUM

National Center for Physical Acoustics
University, MS 38677

August 1989

Technical Report
prepared for:

Office of Naval Research
Contract # N0014-87-K-0019

NCPA LC.02.89

UNCLASSIFIED
SECURITY CLASSIFICATION OF THIS PAGE

REPORT DOCUMENTATION PAGE

Form Approved
OMB No. 0704-0188

1a. REPORT SECURITY CLASSIFICATION Unclassified	1b. RESTRICTIVE MARKINGS
2a. SECURITY CLASSIFICATION AUTHORITY	3. DISTRIBUTION/AVAILABILITY OF REPORT Approved for public release distribution unlimited
2b. DECLASSIFICATION/DOWNGRADING SCHEDULE	
4. PERFORMING ORGANIZATION REPORT NUMBER(S) NCPA LC.02.89	5. MONITORING ORGANIZATION REPORT NUMBER(S)
6a. NAME OF PERFORMING ORGANIZATION National Center for Physical Acoustics 6b. OFFICE SYMBOL (If applicable) LC	7a. NAME OF MONITORING ORGANIZATION Office of Naval Research
6c. ADDRESS (City, State, and ZIP Code) NCPA P.O.Box 847 University, MS 38677	7b. ADDRESS (City, State, and ZIP Code) Department of the Navy Arlington, VA 22217
8a. NAME OF FUNDING/SPONSORING ORGANIZATION 8b. OFFICE SYMBOL (If applicable)	9. PROCUREMENT INSTRUMENT IDENTIFICATION NUMBER N0014-87-K-0019
8c. ADDRESS (City, State, and ZIP Code)	10. SOURCE OF FUNDING NUMBERS PROGRAM ELEMENT NO. / PROJECT NO. / TASK NO. / WORK UNIT ACCESSION NO.

11. TITLE (Include Security Classification)
Further Studies of the Underwater Noise Produced by Rainfall

12. PERSONAL AUTHOR(S)
Elmore, Paul A., Pumphrey, Hugh C., and Crum, Lawrence A.

13a. TYPE OF REPORT	13b. TIME COVERED	14. DATE OF REPORT (Year, Month, Day)	15. PAGE COUNT
Techincal	FROM 89/5/15 TO 89/8/17	1989 August 17	110

16 SUPPLEMENTARY NOTATION

17. COSATI CODES			18. SUBJECT TERMS (Continue on reverse if necessary and identify by block number)
FIELD	GROUP	SUB-GROUP	Physical Acoustics; Underwater Acoustics; Ambient Noise

19. ABSTRACT (Continue on reverse if necessary and identify by block number)

A study of the sound produced by water drops striking a water surface has confirmed some earlier results (Pumphrey, Crum, and Bjørnø, J. Acoust. Soc. Am. 85, 1518 (1989)). In particular, for a well defined range of impact velocities, drops will predictably and repeatedly entrain bubbles; this phenomenon has been named regular entrainment. In the present study, various drop diameters have been used to investigate how bubble frequency, dipole strength, and time between drop impact and bubble formation vary with impact velocity. It is found that as impact velocity is increased through the point where entrainment begins, both frequency and dipole strength decrease to a minimum value and then rise again as the highest velocity at which entrainment occurs is approached. Both terms show increased variability near the critical upper and lower velocities. The frequency tends to increase monotonically as drop size is reduced; drops that entrain bubbles at their terminal velocities tend to produce freqeuncies near 14 kHz, which is also the peak frequency of the natural

20. DISTRIBUTION/AVAILABILITY OF ABSTRACT ☐ UNCLASSIFIED/UNLIMITED ☒ SAME AS RPT. ☐ DTIC USERS	21. ABSTRACT SECURITY CLASSIFICATION Unclassified
22a. NAME OF RESPONSIBLE INDIVIDUAL Lawrence A. Crum	22b. TELEPHONE (Include Area Code) (601) 232-5815 22c. OFFICE SYMBOL LC

DD Form 1473, JUN 86 Previous editions are obsolete.

SECURITY CLASSIFICATION OF THIS PAGE
UNCLASSIFIED

19. (cont.) rainfall spectrum. Finally, the time between drop impact and bubble formation was found to increase monotonically as drop size or impact velocity increases.

TABLE OF CONTENTS

ABSTRACT

Further studies of the underwater noise produced by rainfall. Paul A. Elmore, Hugh C. Pumphrey, and Lawrence A. Crum; National Center for Physical Acoustics; University of Mississippi; University, MS 38677

A study of the sound produced by water drops striking a water surface has confirmed some earlier results [Pumphrey et al. J. Acoust. Soc. Am. 85, 1518 (1989)]. In particular, for a certain well-defined range of drop sizes and impact velocities, drops will predictably and repeatedly entrain bubbles; this phenomenon has been named regular entrainment. In the present study, various fixed drop diameters have been used to investigate how bubble frequency, dipole strength, and time between drop impact and bubble formation vary with impact velocity. It is found that as impact velocity is increased through the point where entrainment begins, both frequency and dipole strength decrease to a minimum value and then rise again as the highest velocity at which entrainment occurs is approached. Both terms show increased variability near the critical upper and lower velocities. The frequency tends to increase monotonically as drop size is reduced; drops that entrain bubbles at their terminal velocities tend to produce frequencies near 14 kHz, which is also the peak frequency of the natural rainfall spectrum. Finally, the time between drop impact and bubble formation was found to increase monotonically as drop size or impact velocity increases.

INTRODUCTION

This study further investigates the underwater noise of rainfall and the phenomenon known as regular entrainment. Previous studies (Pumphrey, Crum, and Bjørnø, 1989a; Pumphrey and Crum, 1989b) have shown that the impact of a single drop on a plane surface of water can make two sounds: first, an impact noise and then a bubble noise, which originates from the oscillations of a bubble entrained underneath the surface by a drop. Therefore, the spectrum of underwater rain noise, which is shown in Fig. 1, can only be caused by these two effects. However, the impact noise is not believed to be a major contributor to the total spectrum. Although not every drop entrains a bubble, the individual contribution by the bubbles are much larger than that due to the impact alone. The majority of these bubbles are thought to be oscillating at 14 kHz because the spectrum has a large peak at that frequency.

These studies have also shown that drops will entrain bubbles predictably and repeatedly within a well defined range of impact velocities and drop sizes, as shown in Fig. 2a. Entrainment that occurs in this manner is called "regular entrainment." Also shown in this figure are data from Scrimger, which give the sizes and number of raindrops measured in three different rainfalls (Scrimger et al., 1987). The comparisons indicate that the drops which regularly entrain drops at terminal velocity are found in abundance in natural rain. Thus, in order to understand the mechanism of rain noise, we must first learn about regular entrainment.

The regular entrainment process starts with the entraining drop striking the water and forming a conically shaped cavity. This cavity will eventually stop growing and collapse after a few milliseconds. As it does, the bottom part is pinched off from the rest of the cavity, forming a damped radially oscillating bubble underneath the surface. This bubble has a dipole radiation pattern because it is very close to a pressure release surface. Another process, which has been named "irregular entrainment" by Pumphrey and Crum, can create bubbles as well but by unpredictable cavity deformations underneath the water or entrainment by drops formed from jets erupting from the cavity (Franz, 1959; Longuet-Higgins, 1989; Pumphrey and Crum, 1989b; Oguz and Prosperetti, 1989).

The present experiment's purpose has been to reproduce these earlier findings and to examine more closely the role of regular entrainment in the underwater noise produced by rainfall. Thus, the experiment investigated the characteristics of bubbles over the entire entrainment region. The bubbles' radii, frequencies, and initial dipole strengths were measured along with the amount of time between drop impact and bubble formation. The measurements were made by keeping the drop size constant but varying the impact velocity. The study was then conducted over a wide range of drop sizes. Using the results of the study, we can conclude whether or not rain noise is caused by regular entrainment.

METHODS

The experiments were conducted in a water tank measuring a cubic meter in volume filled with tap water to a depth between 0.85 and 0.9 meters. The transducer system used for measuring acoustic frequency and pressure was a miniature hydrophone (Brüel & Kjær 8103) and a charge amplifier (Brüel & Kjær 2635). The signal was then read on a digital oscilloscope (LeCroy 9400) which is capable of analyzing the signal in various ways (FFT's, averages, integration, etc.). The oscilloscope was interfaced by a GPIB to a computer (DEC MINC-73) for additional signal analysis. A diagram of the experimental set-up is shown in Fig. 3.

Drops of tap water were dropped into the water tank from a syringe suspended above the center of the tank. Various tubings or hypodermic needles were attached to it to create different sizes of drops. Drops larger than 1.71 mm in diameter were produced from allowing them to drip from the end of a needle, glass pipet, or piece of tubing. Smaller drops had to be produced by feeding the water from the syringe to a 30-gauge needle attached to the cone of a loudspeaker. The speaker-needle system was then vibrated with a square wave signal while allowing water to flow freely from the syringe to the needle's tip (this method gave the drops some but negligible amounts of horizontal velocity). The actual size of the drops, assuming that they are spherical, was determined by measuring the volumes of ten or fifteen captured samples with a microliter syringe, converting the each volume to a corresponding diameter, and then averaging the diameters. The standard deviation of the measured diameters was found to be quite small.

The impact velocity, v_i, of the drops was determined by measuring the height of the fall, z, and calculating v_i by using the equation

$$v_i = v_t\sqrt{1-\exp\left(\frac{-2gz}{v_t^2}\right)}, \qquad (1)$$

where v_t is the terminal velocity. The value of v_t for a given drop size was found by computing it from a polynomial fit (Dingle and Lee, 1972) of earlier experimental data (Gunn and Kinser, 1949). The polynomial fit and equation (1) were programmed into the MINC-73 computer to ease the computation. The error of impact velocity based on the error in measuring the height of fall was not found to be significant.

Using the impact velocities, the kinetic energy, T, of each drop at impact can be found from its classical form:

$$T = \frac{1}{2} m v_i^2 , \tag{2}$$

where m is the drop's mass. Since the drop's radius, not mass, was directly measured, it was more convenient to express T in terms of the drop's radius, R, and v_i. The drop's mass is related to it's radius by the relation

$$m = \rho V = \left(1.0 \times 10^3 \frac{kg}{m^3}\right)\left(\frac{4}{3}\pi R^3\right) , \tag{3}$$

where ρ is the water density, V the drop's volume. Substituting this expression for mass into equation (2) gives the desired form,

$$T = \left(\frac{2\pi}{3} \times 10^3 \frac{kg}{m^3}\right) R^3 v_i^2 . \tag{4}$$

The frequency of the bubble's oscillation was measured by either of two methods. One method was to measure the time between the second and seventh positive voltage peaks (to make sure transient behavior was excluded) directly from the oscilloscope screen, as shown in Fig. 4, and then multiply the reciprocal of the time by five. The LeCroy 9400 measures the temporal difference and its reciprocal between any two points along the trace. The other method was to interface the oscilloscope to the computer and use a program that displays numerical values of the oscillation's frequency and initial amplitude. The latter method was more precise than the first, but comparisons between the two showed no significant difference. The damped signals produced usually had quality factors of ten or higher.

From these readings the frequency was converted to a bubble radius, a, by the relation

$$a = \frac{\sqrt{3\kappa P_o/\rho}}{2\pi f} , \tag{5}$$

where P_o is the static pressure of the bubble, ρ the water density, and f the bubble's frequency. Since the value of these variables were known for the environmental conditions during the experiment, the equation reduces to

$$a \approx \frac{3.28}{f} . \tag{6}$$

Measurements of the initial dipole strength began with the measurements of the initial amplitude. These measurements were also done by either measuring initial voltage directly on the oscilloscope screen or by using the program. When reading it directly from the oscilloscope, the voltage difference was measured between the first negative voltage peak and the second positive peak (again, to exclude any transient behavior), as shown in Fig. 5. The initial voltage was then converted to initial dipole strength, D, by solving for D in the formula

$$p = \frac{D \cos \theta \, e^{if(t - r/c)} e^{-\beta(t - r/c)}}{r} \tag{7}$$

where p is acoustic pressure, and θ is the angle between the bubble and the hydrophone with respect to the perpendicular of the plane of the water surface going through the hydrophone. f is the bubble frequency, t the time from bubble formation, c the velocity of sound underwater ($\approx$ 1500 m/s), ß the damping factor, and r the distance from the hydrophone to the bubble. This distance was set at five centimeters. Since $\theta = 0$, $\cos \theta = 1$. Also, $t - r/c \approx 0$, so $e^{-\beta(t - r/c)} \approx 1$, and $e^{if(t - r/c)} = 1$ at a peak. Therefore,

$$p \approx \frac{D}{r} = 5 \, V_{pp} \tag{8}$$

for the equipment that was used. Since r = 0.05 m, the above equation reduces to

$$D \approx \frac{V_{pp}}{4} . \tag{9}$$

The temporal measurement between the drop impact and bubble formation was facilitated by a function on the oscilloscope that averages the traces from fifty drop impacts and subsequent bubble noise and displays the average as a single trace. Using this resultant trace, the time measurement was made between the base of the bubble noise and a reference point in the transient behavior of the bubble's formation, as shown in Fig. 6.

The dat^ anaiysis was done using the Cricket Graph software package available for Macintosh ., .nputers.

EXPLANATION OF DATA SET 1

The first set of data shows the final velocity, bubble radius, frequency, and initial dipole strength for each drop size. The drop diameter, measured in millimeters, is listed above each table. The dates and times shown at the top of each sheet are not of any significance. The first column is the drop's impact velocity in meters per second. The columns following it are the measured values of the bubble's frequency in kilohertz, initial dipole strength in newtons per meter, and radius in millimeters. The standard deviations of each value follow it. Each row represents the average of thirty trials, except when noted.

There are four graphs that follow each data page. The first three plot the relationships between impact velocity and bubble size, frequency, and initial dipole strength. The fourth graph plots the initial dipole strength versus the frequency.

DATA SET 1

drop diameter = 0.79mm   Tue, Aug 8, 1989 2:45 PM

	impact vel.	f (kHz)	sd of f	D (N/m)	sd of D	Bubble rad/mm	sd of rad
1	3.235	48.350	16.422	0.532	0.185	0.200	0.068
2	[illegible]33	52.088	21.562	0.955	0.330	0.152	0.063
3	3.231	58.626	25.267	0.730	0.290	0.130	0.056
4	3.240	40.875	12.521	0.723	0.290	0.262	0.080

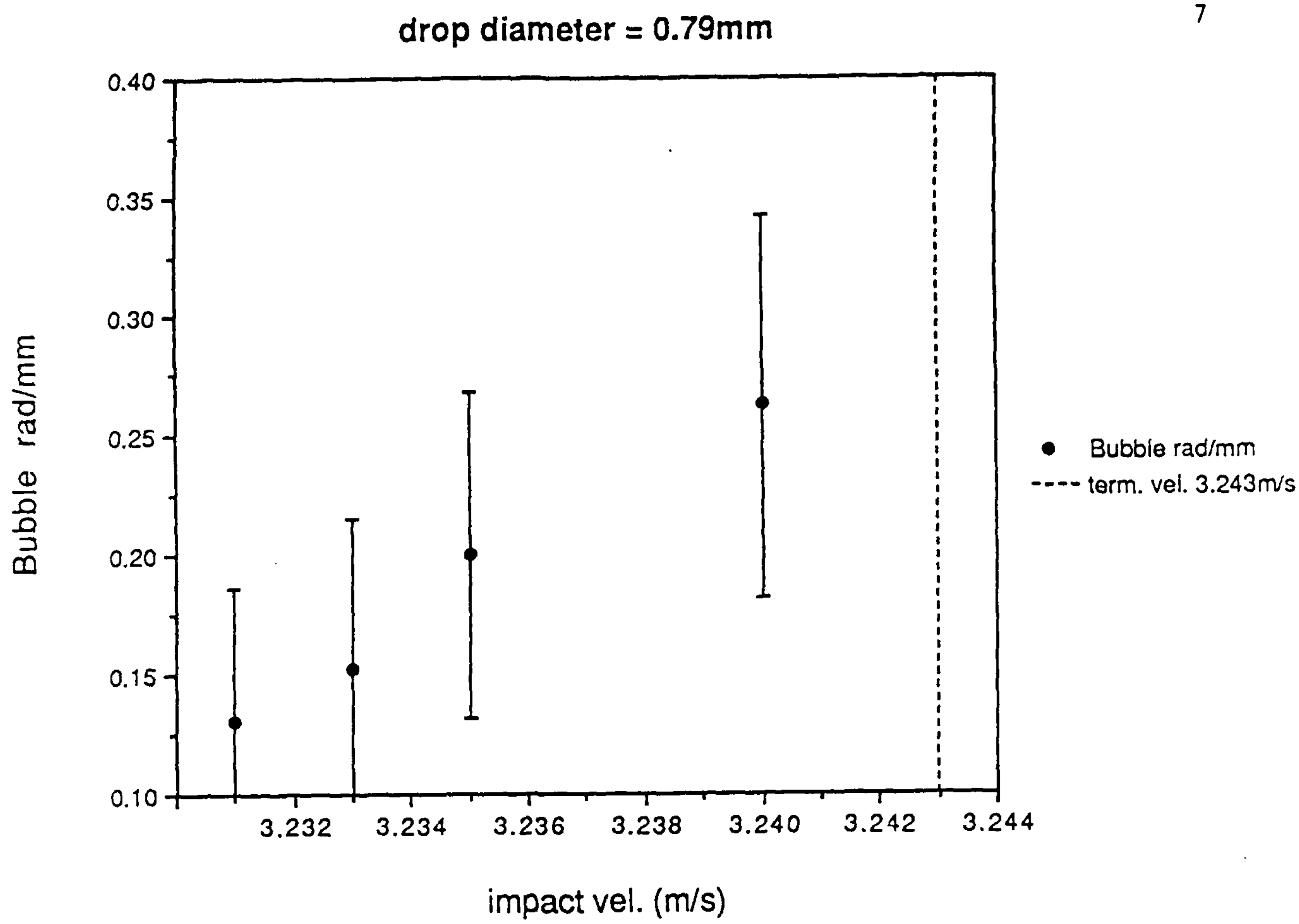
drop diameter = 0.79mm
Bubble rad/mm
0.40
0.35
0.30
0.25
0.20
0.15
0.10
3.232
3.234
3.236
3.238
3.240
3.242
3.244
impact vel. (m/s)
Bubble rad/mm
term. vel. 3.243m/s

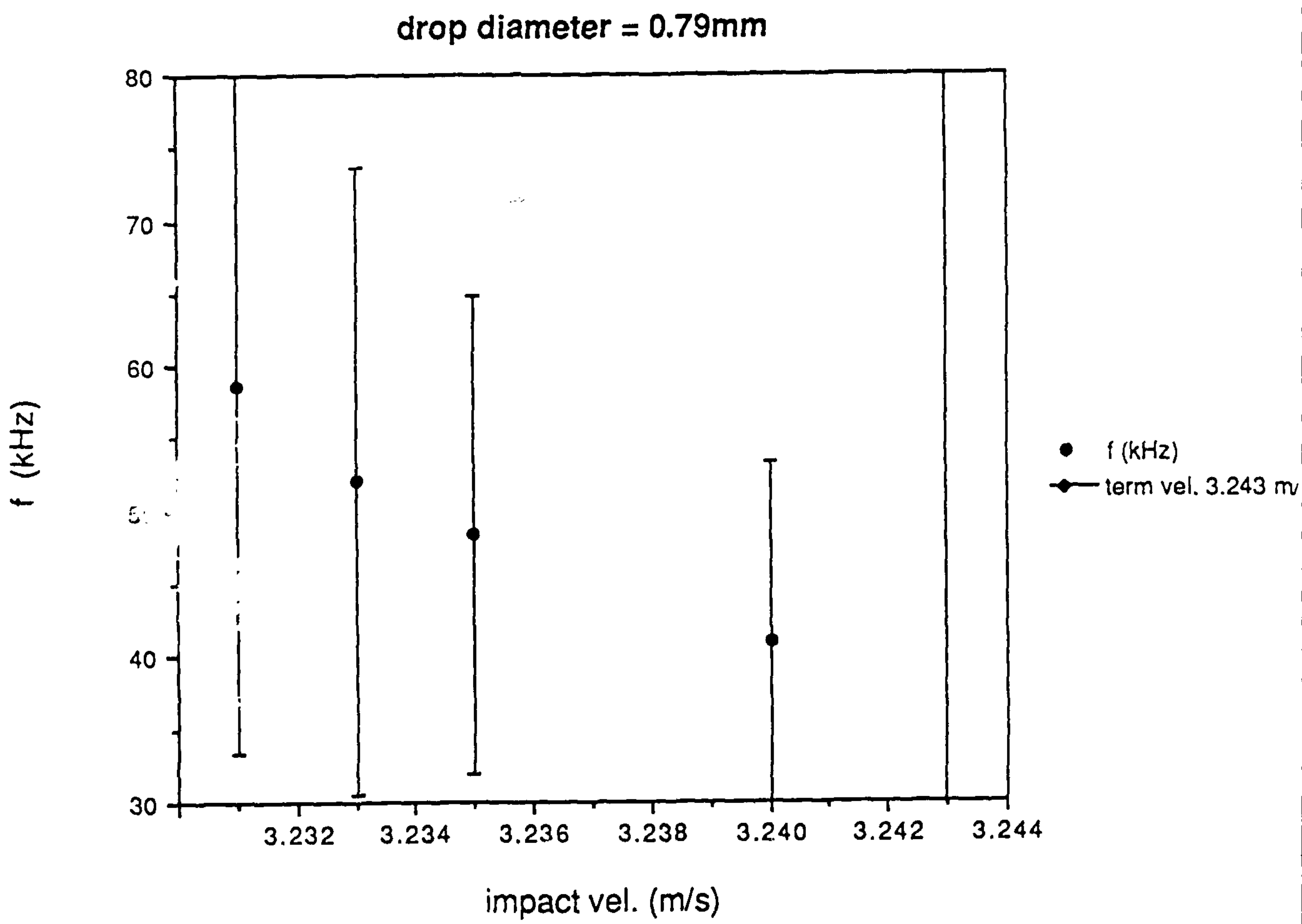
drop diameter = 0.79mm
f (kHz)
80
70
60
40
30
3.232
3.234
3.236
3.238
3.240
3.242
3.244
impact vel. (m/s)
f (kHz)
term vel. 3.243 m/

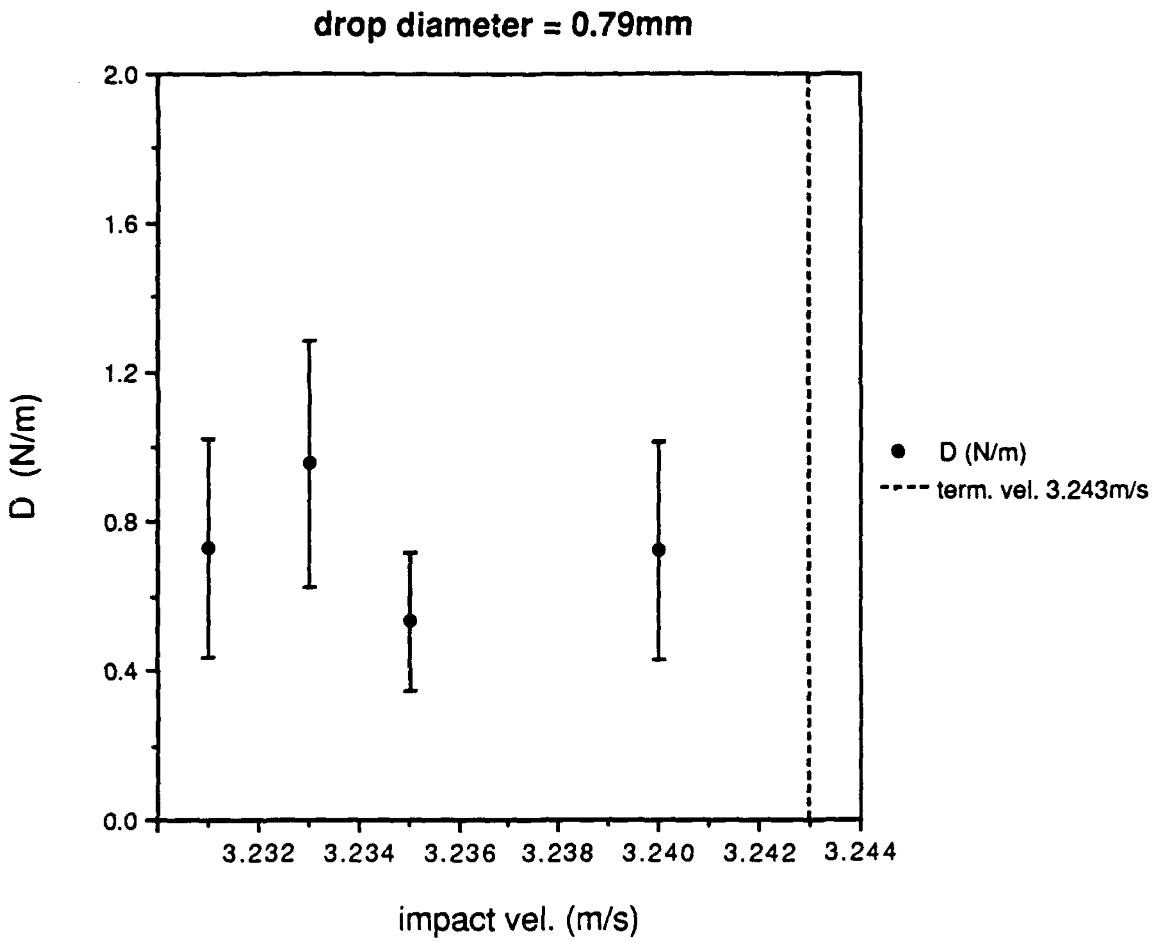
drop diameter = 0.79mm
2.0
1.6
1.2
0.8
0.4
0.0
D (N/m)
3.232
3.234
3.236
3.238
3.240
3.242
3.244
impact vel. (m/s)
D (N/m)
term. vel. 3.243m/s

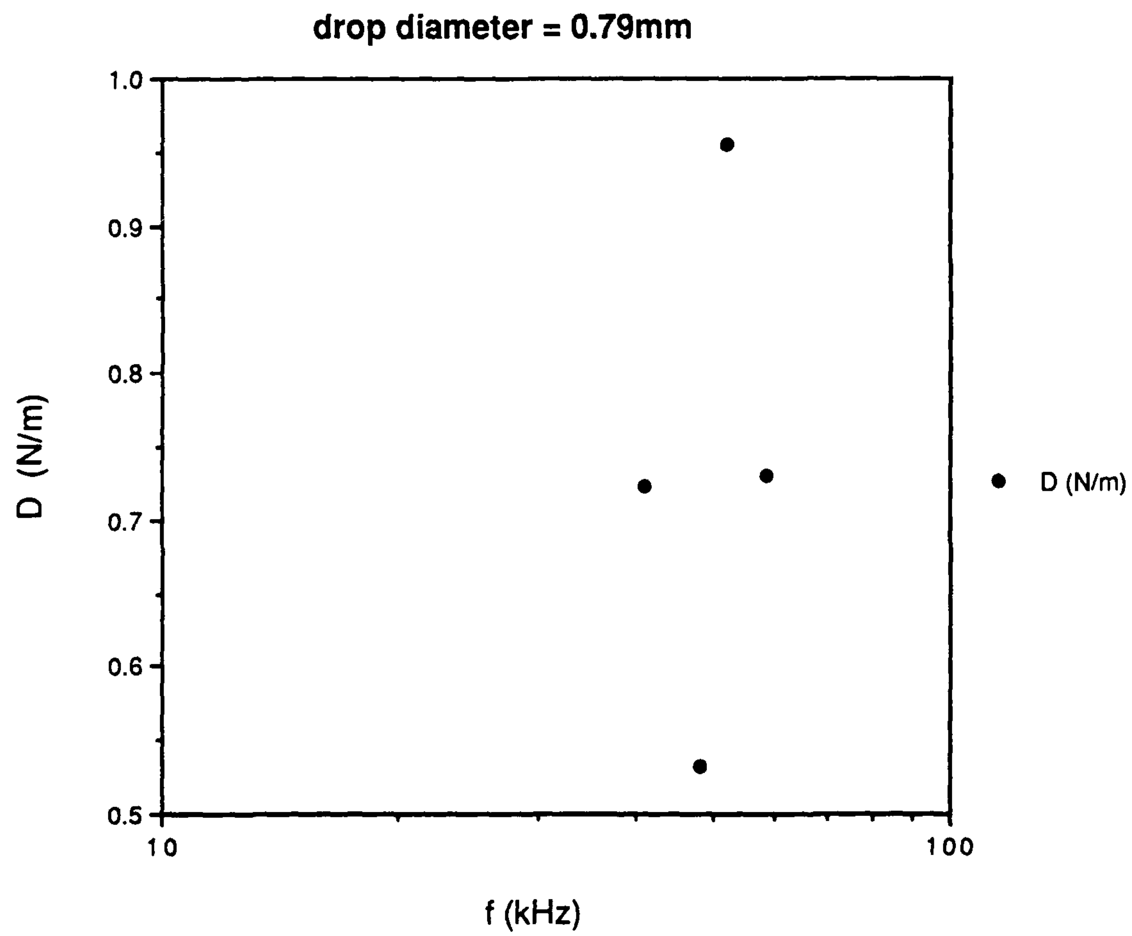
drop diameter = 0.79mm
1.0
0.9
0.8
0.7
0.6
0.5
D (N/m)
10
100
f (kHz)
D (N/m)

drop diameter = 0.87mm   Thu, Jul 20, 1989 7:44 PM

	impact vel.	f (kHz)	sd of f	D (N/m)	sd of D	Bubble rad/mm	sd of rad
1	3.539	14.331	0.612	0.422	0.070	0.229	0.010
2	3.526	16.852	3.581	0.318	0.065	0.195	0.041
3	3.521	15.029	1.197	0.385	0.075	0.218	0.017
4	3.517	17.973	16.704	0.362	0.080	0.182	0.170
5	3.511	16.975	6.032	0.350	0.095	0.193	0.069
6	3.505	18.329	6.341	0.438	0.092	0.179	0.062
7	3.498	16.899	1.213	0.407	0.058	0.194	0.014
8	3.489	18.698	1.690	0.492	0.107	0.175	0.016
9	3.479	21.115	7.920	0.652	0.163	0.155	0.058
10	3.467	20.579	2.743	0.340	0.060	0.159	0.021
11	3.454	20.749	1.315	0.463	0.075	0.158	0.010
12	3.439	23.081	2.084	0.472	0.075	0.142	0.013
13	3.421	19.439	1.285	0.365	0.045	0.169	0.011
14	3.401	18.447	1.460	0.405	0.065	0.178	0.014
15	3.373	27.705	7.600	0.873	0.223	0.118	0.032
16	3.342	30.355	5.319	1.005	0.170	0.108	0.019

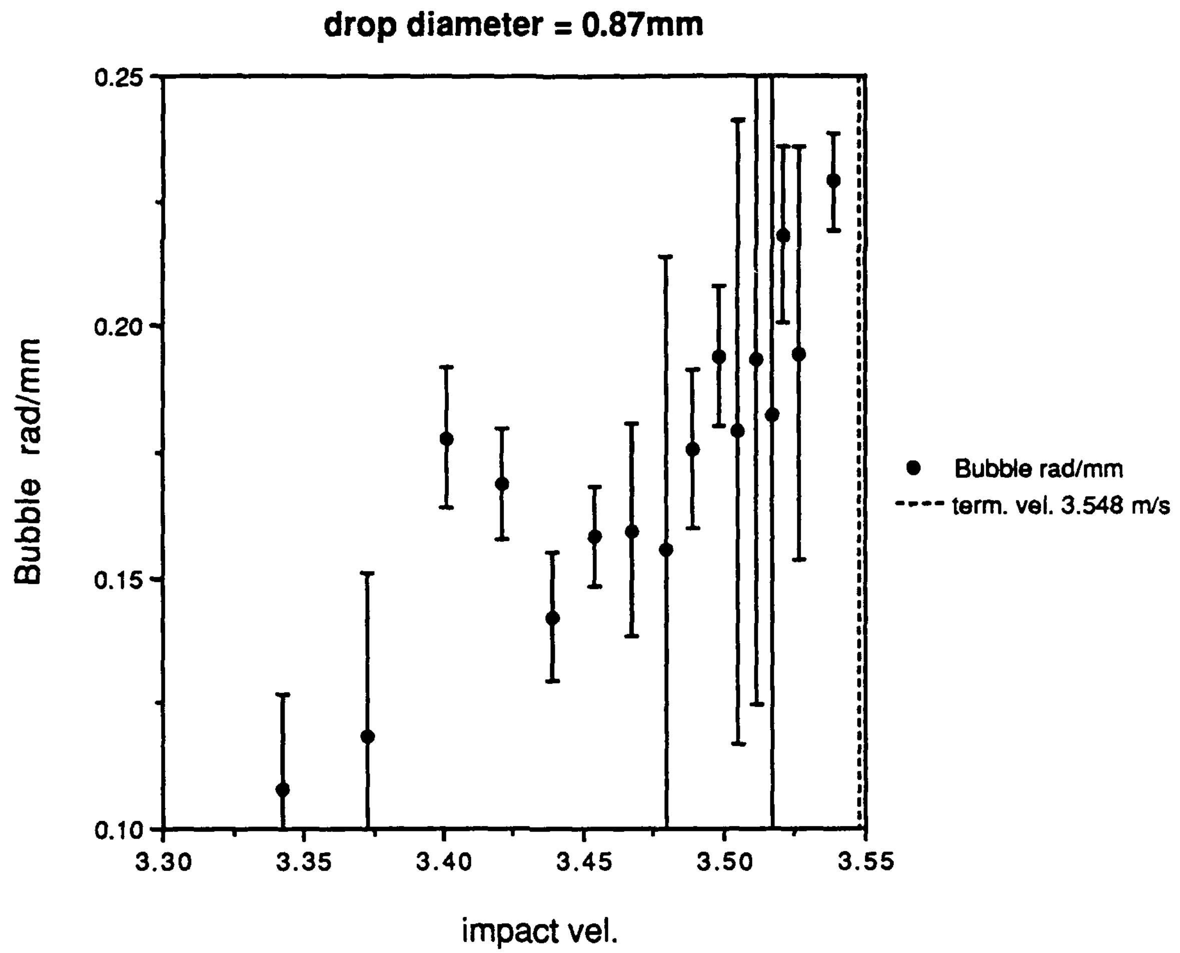
drop diameter = 0.87mm
0.25
0.20
0.15
0.10
3.30
3.35
3.40
3.45
3.50
3.55
Bubble rad/mm
impact vel.
Bubble rad/mm
term. vel. 3.548 m/s

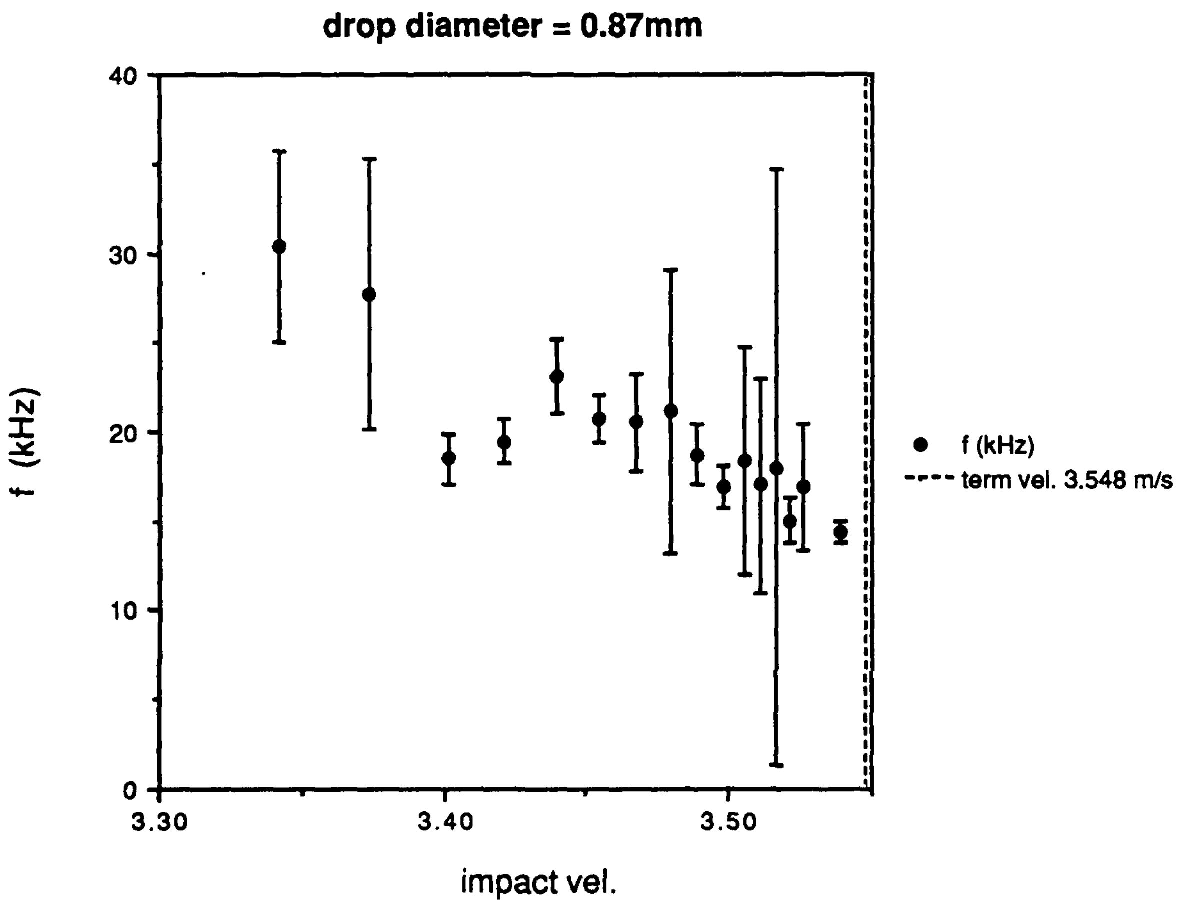
drop diameter = 0.87mm
40
30
20
10
0
3.30
3.40
3.50
f (kHz)
impact vel.
f (kHz)
term vel. 3.548 m/s

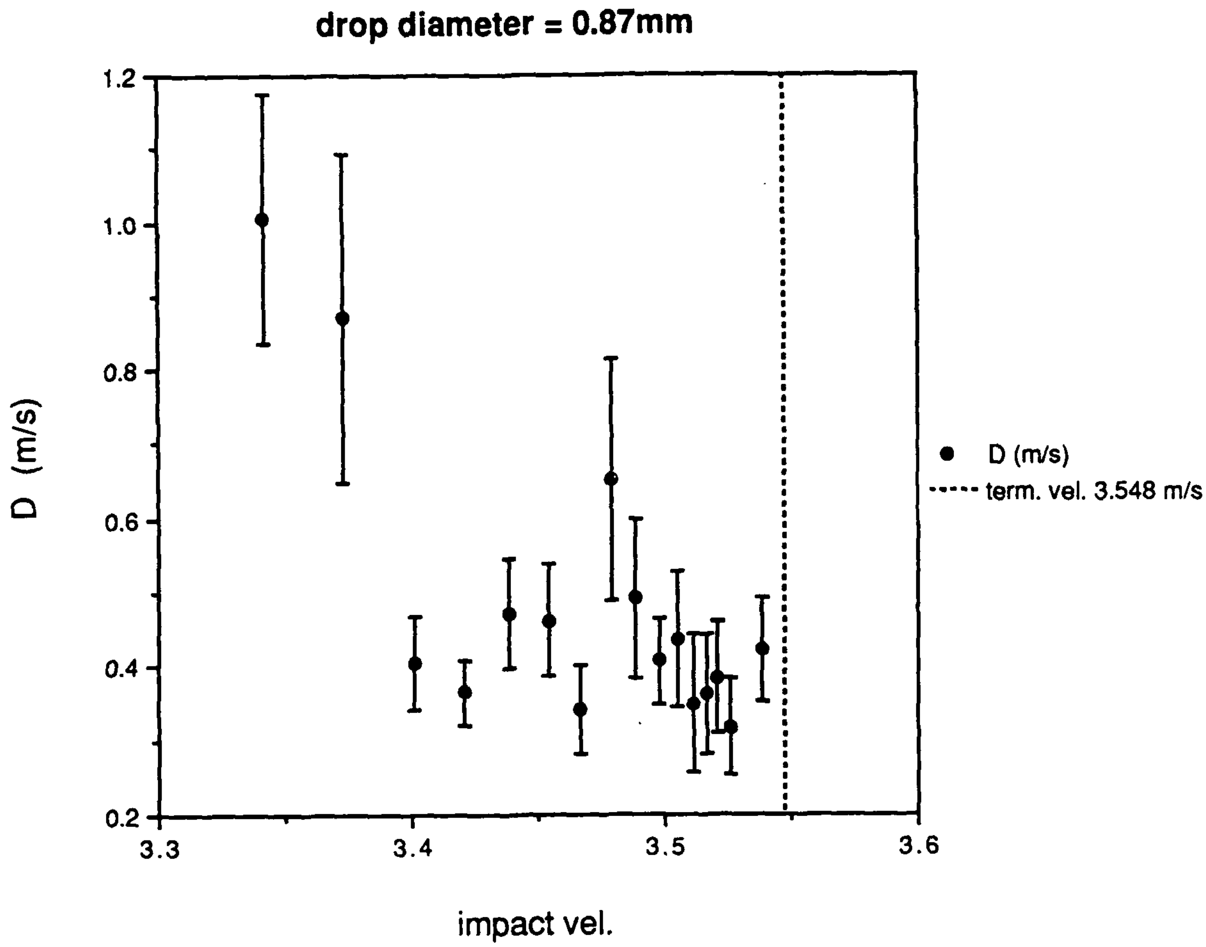
drop diameter = 0.87mm
D (m/s)
impact vel.
1.2
1.0
0.8
0.6
0.4
0.2
3.3
3.4
3.5
3.6
D (m/s)
term. vel. 3.548 m/s

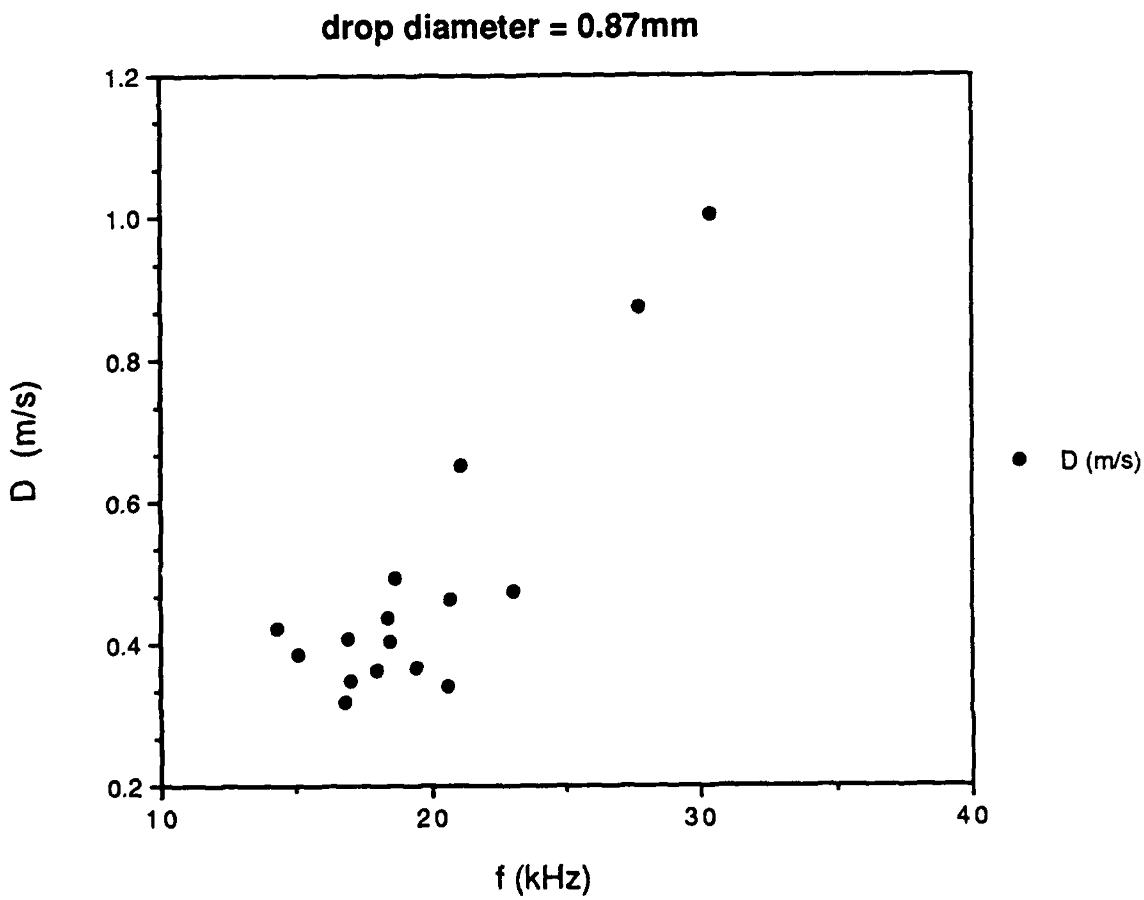
drop diameter = 0.87mm
D (m/s)
f (kHz)
1.2
1.0
0.8
0.6
0.4
0.2
10
20
30
40
D (m/s)

drop diameter = 0.93mm   Thu, Jul 20, 1989 9:12 AM

	impact vel.	f (kHz)	sd of f	D (N/m)	sd of D	Bubble rad/mm	sd of rad
1	3.103	49.786	10.003	0.917	0.350	0.066	0.013
2	3.196	25.592	7.621	0.980	0.138	0.128	0.038
3	3.276	22.220	8.228	0.820	0.155	0.148	0.055
4	3.343	16.426	1.734	0.573	0.055	0.200	0.021
5	3.441	14.933	2.395	0.417	0.150	0.220	0.035
6	3.390	14.808	3.837	0.378	0.147	0.222	0.057
7	3.485	13.216	1.205	0.307	0.065	0.248	0.023
8	3.523	12.866	2.104	0.388	0.100	0.255	0.042
9	3.558	15.878	18.225	0.345	0.072	0.207	0.237
10	3.583	12.190	0.948	0.323	0.052	0.269	0.021
11	3.608	12.662	1.079	0.378	0.055	0.259	0.022
12	3.629	12.145	0.832	0.318	0.043	0.270	0.019
13	3.647	11.535	2.548	0.240	0.060	0.284	0.063
14	3.663	12.143	1.425	0.193	0.077	0.270	0.032
15	3.677	12.584	2.352	0.310	0.117	0.261	0.049
16	3.689	12.167	1.168	0.302	0.070	0.270	0.026
17	3.699	14.336	8.425	0.315	0.117	0.229	0.134
18	3.708	12.731	1.433	0.330	0.068	0.258	0.029
19	3.716	12.021	0.456	0.242	0.043	0.273	0.010
20	3.723	12.126	0.741	0.200	0.062	0.270	0.017
21	3.729	12.024	0.744	0.260	0.045	0.273	0.017
22	3.751	12.156	0.154	0.185	0.040	0.270	0.003

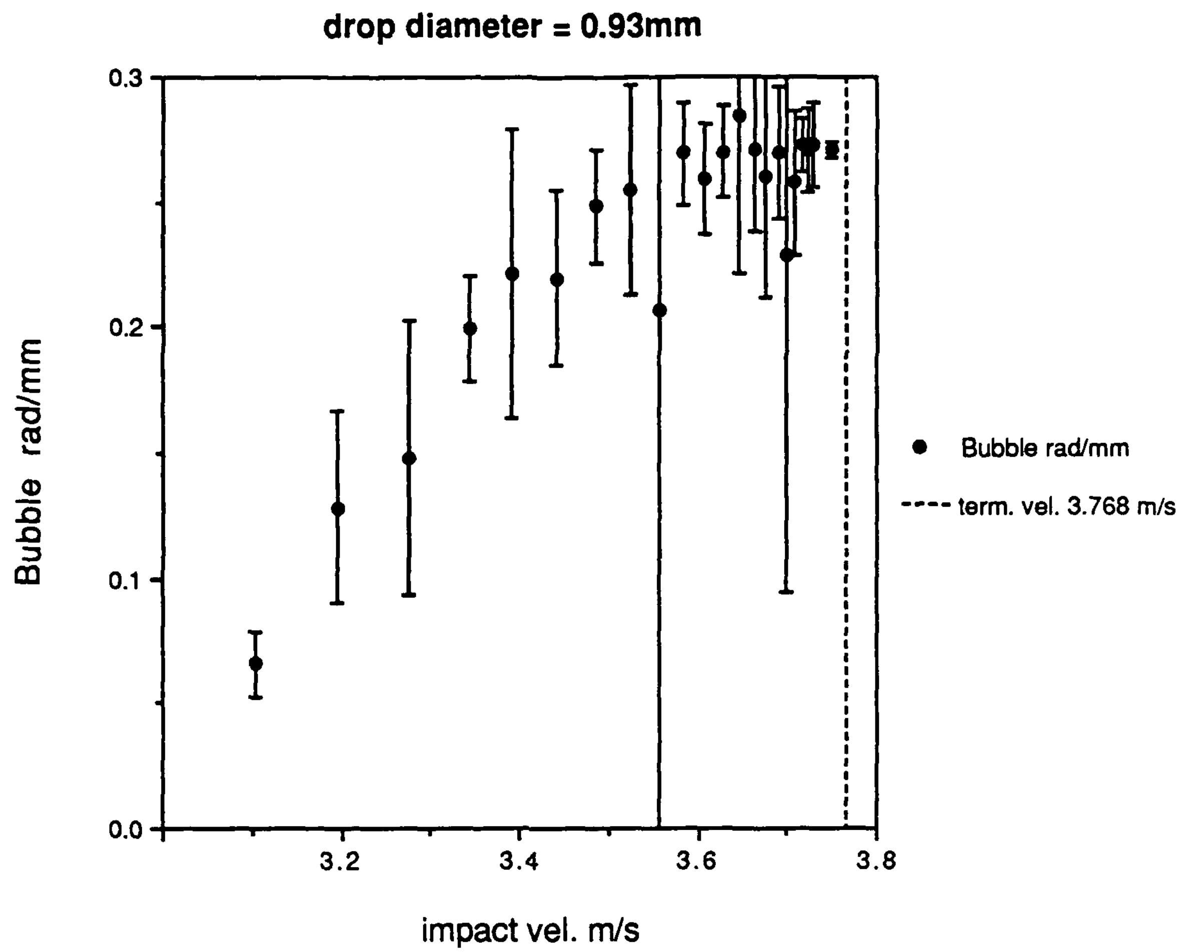
drop diameter = 0.93mm
0.3
0.2
0.1
0.0
3.2
3.4
3.6
3.8
Bubble rad/mm
impact vel. m/s
Bubble rad/mm
term. vel. 3.768 m/s

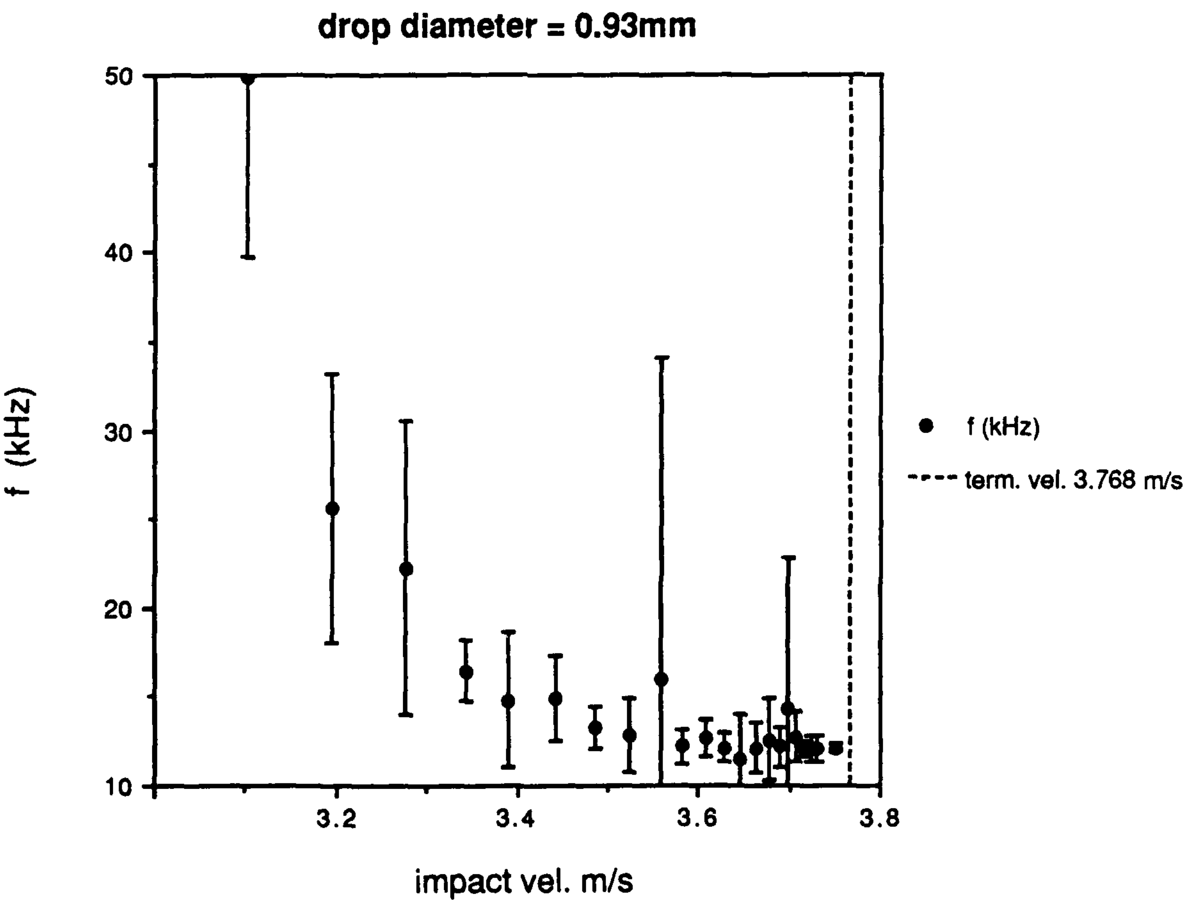
drop diameter = 0.93mm
50
40
30
20
10
3.2
3.4
3.6
3.8
f (kHz)
impact vel. m/s
f (kHz)
term. vel. 3.768 m/s

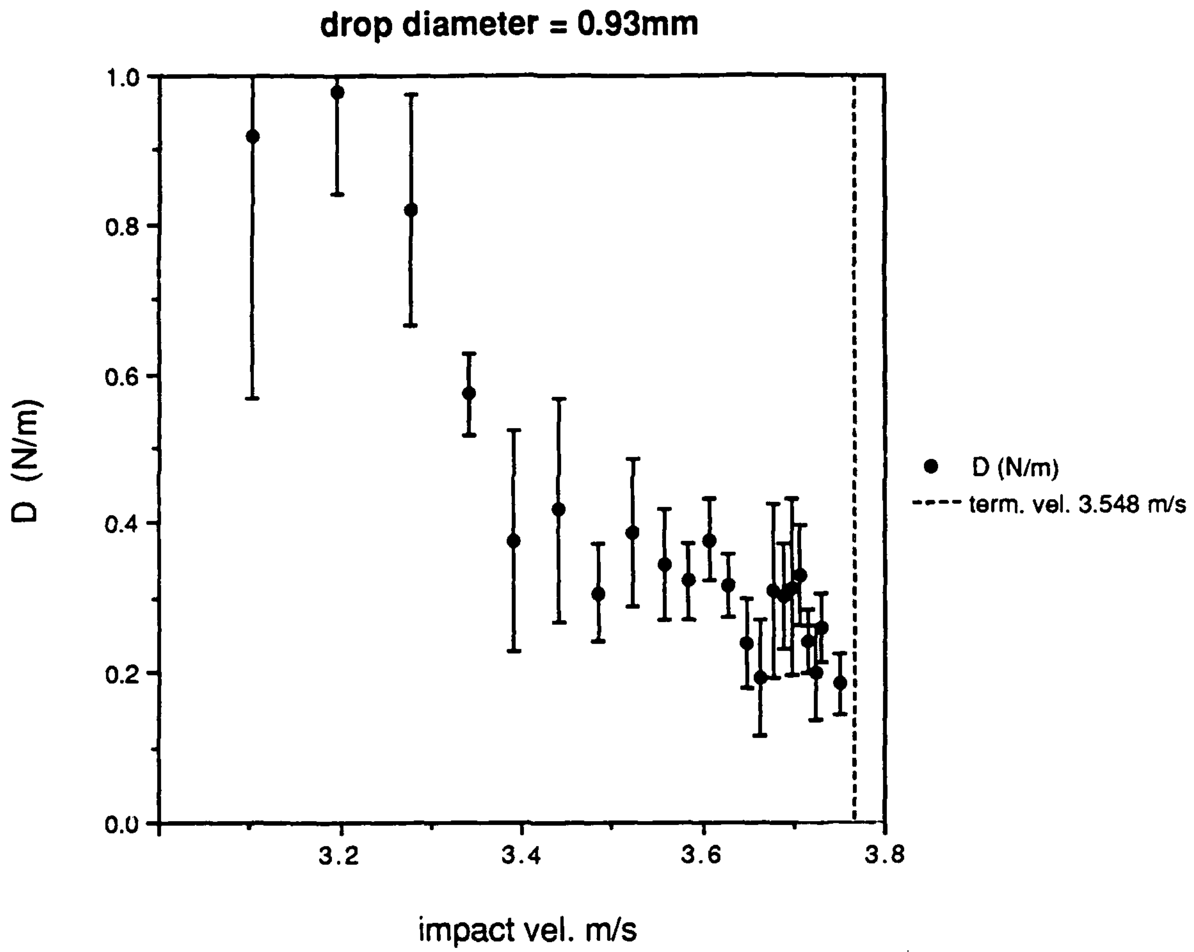
drop diameter = 0.93mm
D (N/m)
impact vel. m/s
1.0
0.8
0.6
0.4
0.2
0.0
3.2
3.4
3.6
3.8
D (N/m)
term. vel. 3.548 m/s

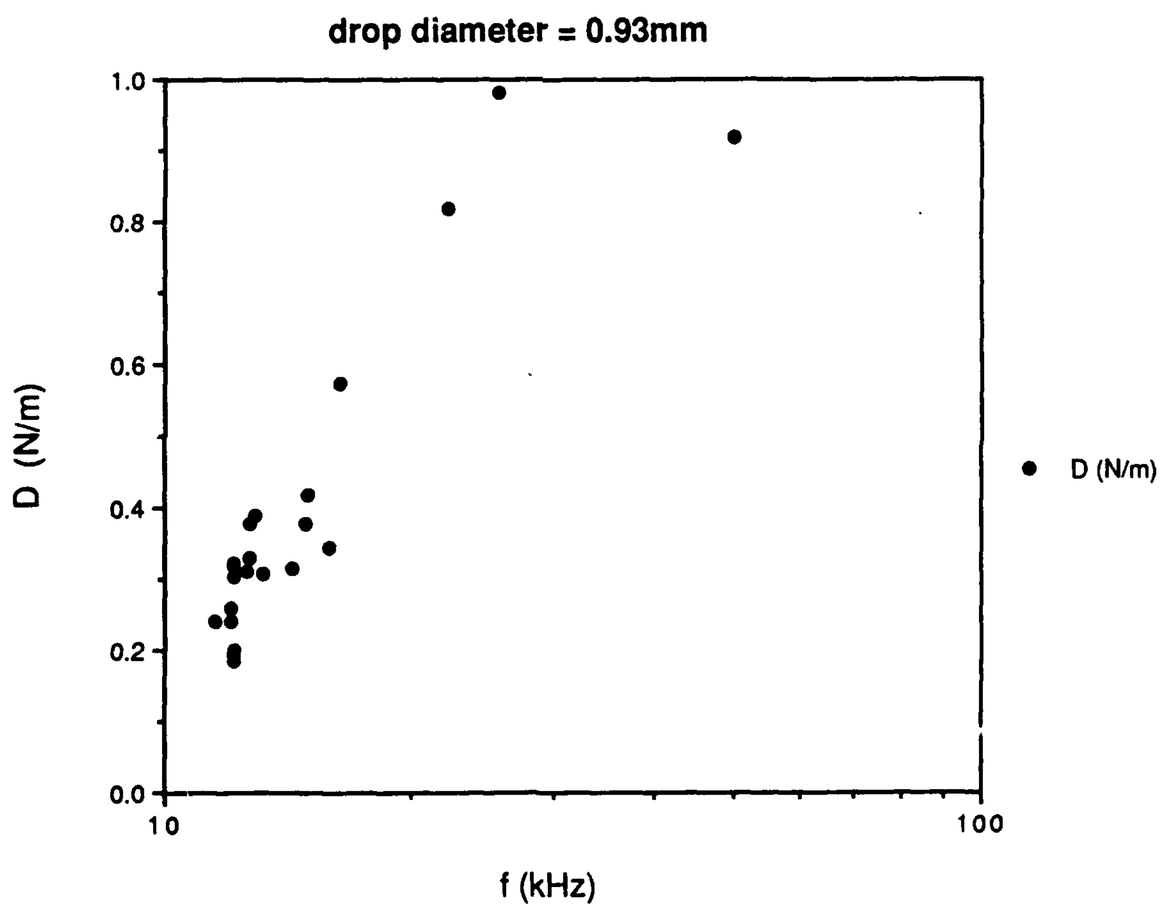
drop diameter = 0.93mm
D (N/m)
f (kHz)
1.0
0.8
0.6
0.4
0.2
0.0
10
100
D (N/m)

drop diameter = 1.00mm Wed, Jul 19, 1989 5:18 PM

	impact vel.	f (kHz)	sd of f	D (N/m)	sd of D	Bubble rad/mm	sd of radius
1	3.167	20.500	5.368	0.980	0.190	0.160	0.042
2	3.275	17.707	5.865	0.500	0.195	0.185	0.061
3	3.368	17.866	12.250	0.405	0.128	0.184	0.126
4	3.449	14.174	3.267	0.545	0.165	0.231	0.053
5	3.518	13.000	2.184	0.435	0.070	0.252	0.042
6	3.579	12.022	0.282	0.378	0.018	0.273	0.006
7	3.631	11.703	0.366	0.350	0.028	0.280	0.009
8	3.677	11.148	0.050	0.307	0.018	0.294	0.001
9	3.717	11.233	0.063	0.265	0.022	0.292	0.002
10	3.753	11.401	0.138	0.210	0.013	0.288	0.003
11	3.784	11.291	0.153	0.021	0.018	0.290	0.004
12	3.784	11.733	0.400	0.193	0.020	0.280	0.010
13	3.811	14.365	2.923	0.350	0.109	0.228	0.046
14	3.835	11.287	1.988	0.240	0.028	0.291	0.051
15	3.556	14.906	4.876	0.378	0.190	0.220	0.072
16	3.874	12.321	1.370	0.282	0.065	0.266	0.030
17	3.891	12.403	2.505	0.253	0.092	0.264	0.053
18	3.905	13.763	8.163	0.275	0.105	0.238	0.141
19	3.918	12.023	0.138	0.275	0.058	0.273	0.003
20	3.929	12.215	1.863	0.193	0.043	0.269	0.041
21	3.938	16.768	16.502	0.182	0.048	0.196	0.193
22	3.983	12.217	0.449	0.233	0.040	0.268	0.099

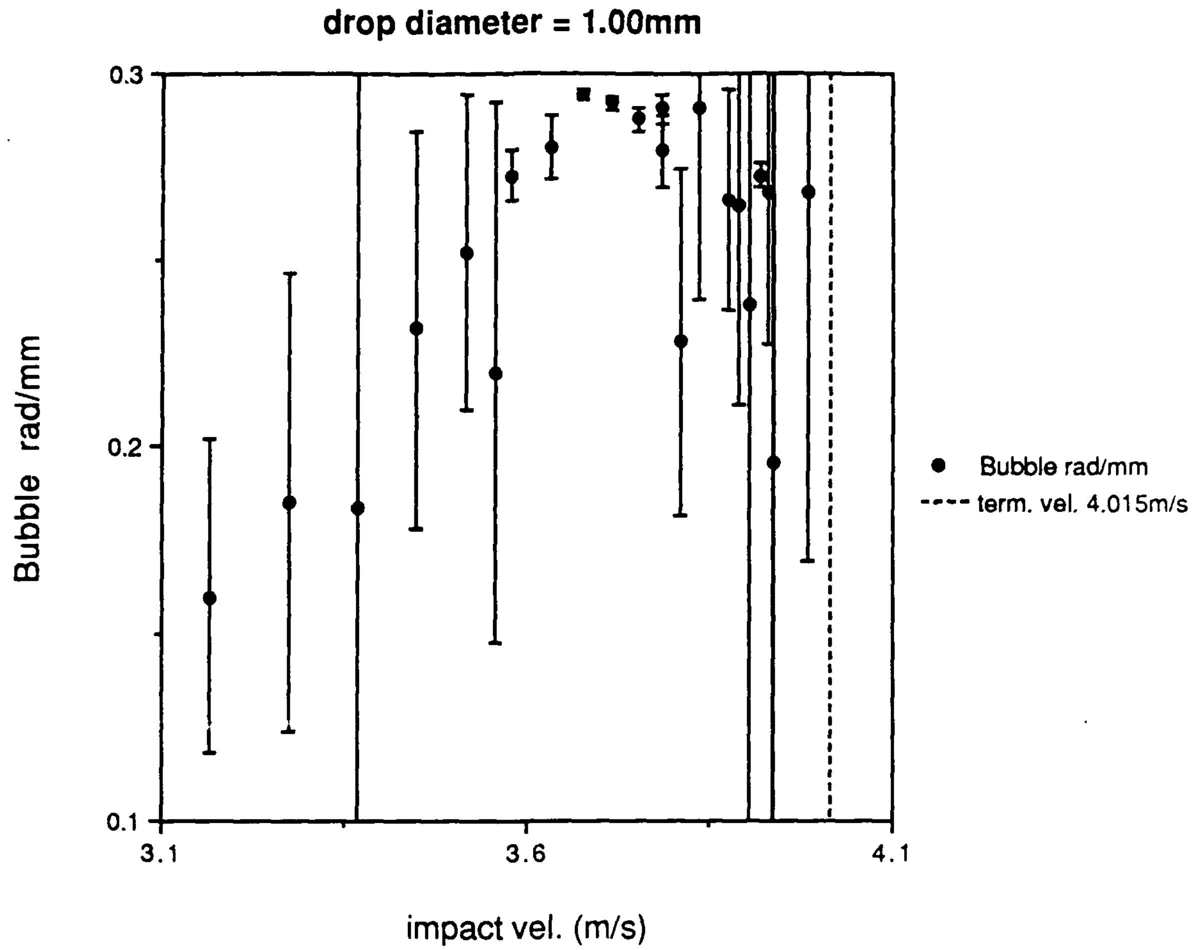
drop diameter = 1.00mm
Bubble rad/mm
0.3
0.2
0.1
3.1
3.6
4.1
impact vel. (m/s)
Bubble rad/mm
term. vel. 4.015m/s

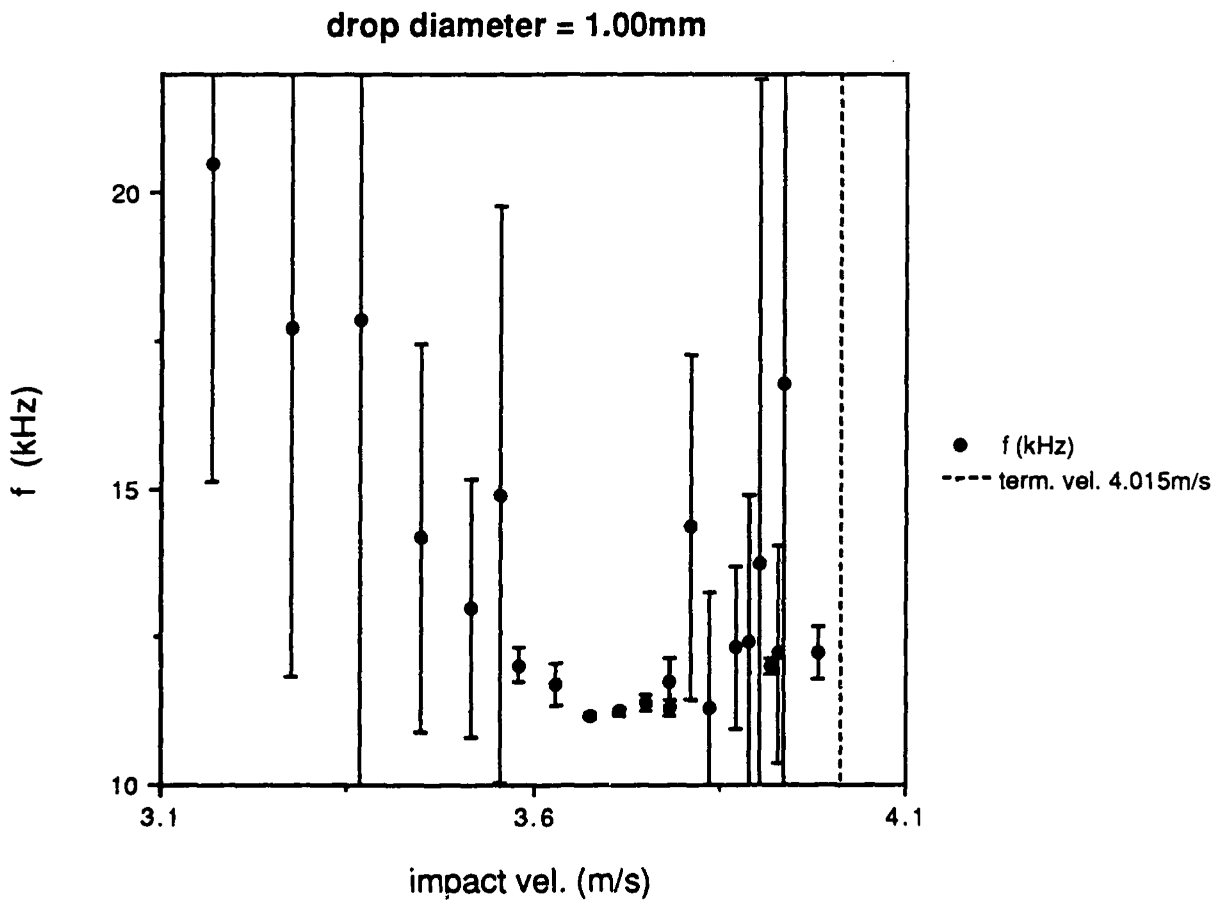
drop diameter = 1.00mm
f (kHz)
20
15
10
3.1
3.6
4.1
impact vel. (m/s)
f (kHz)
term. vel. 4.015m/s

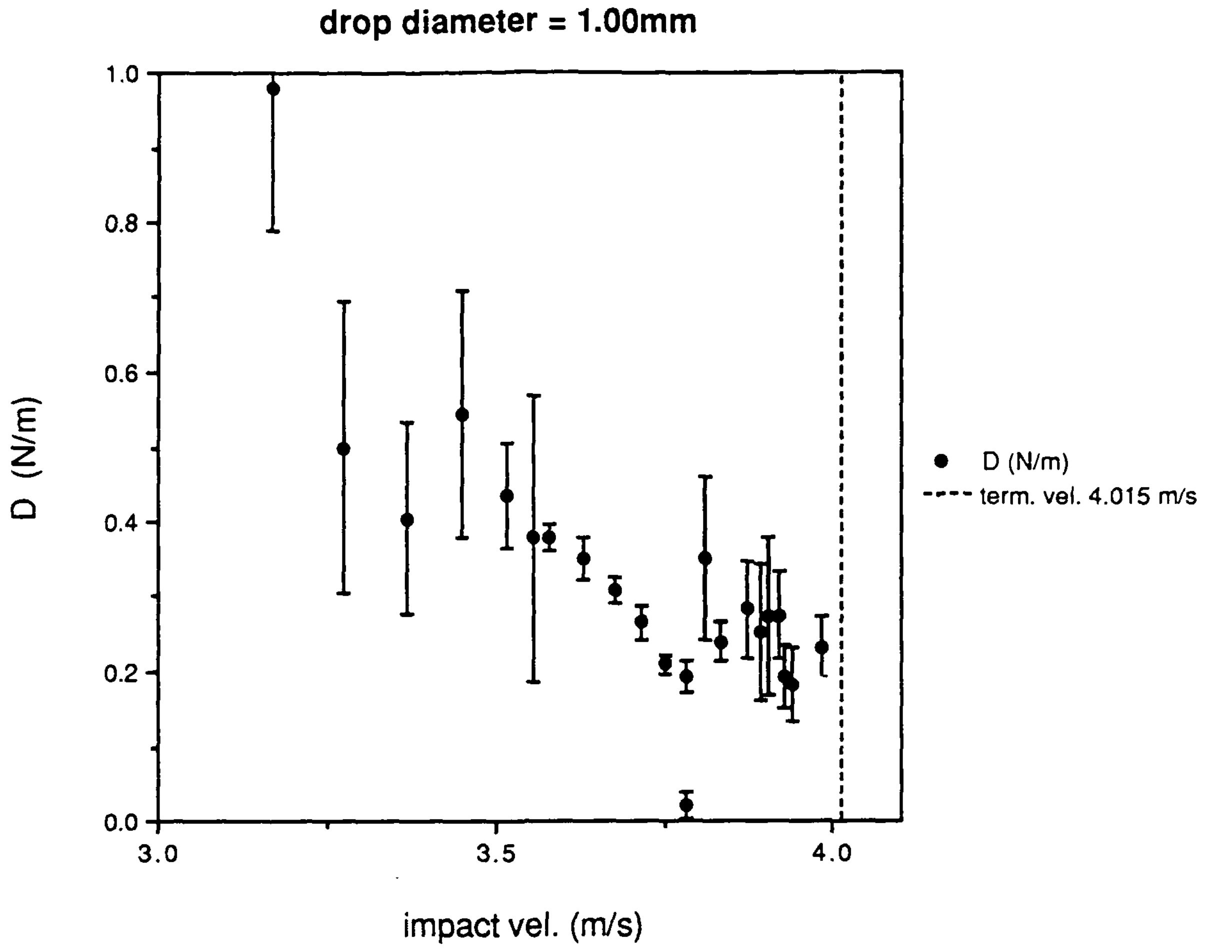
drop diameter = 1.00mm
D (N/m)
impact vel. (m/s)
1.0
0.8
0.6
0.4
0.2
0.0
3.0
3.5
4.0
D (N/m)
term. vel. 4.015 m/s

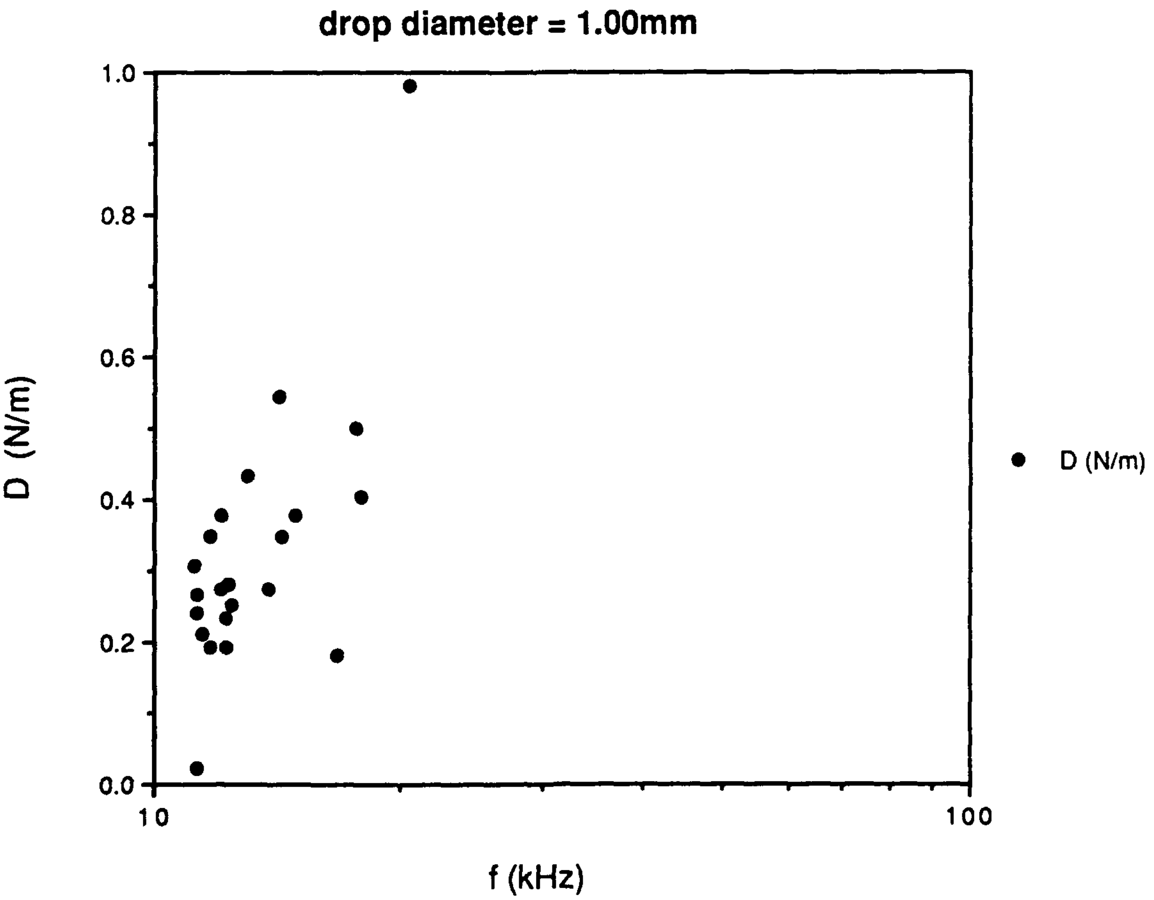
drop diameter = 1.00mm
D (N/m)
f (kHz)
1.0
0.8
0.6
0.4
0.2
0.0
10
100
D (N/m)

drop diameter = 1.07mm Thu, Jul 20, 1989 9:41 AM

	impact vel.	f (kHz)	sd of f	D (N/m)	sd of D	Bubble rad/mm	sd of rad
1	2.941	85.753	24.074	1.218	0.335	0.038	0.011
2	3.101	27.208	14.211	1.050	0.193	0.121	0.063
3	3.238	15.391	17.903	0.398	0.083	0.213	0.248
4	3.356	16.186	18.079	0.378	0.080	0.203	0.226
5	3.459	12.376	1.224	0.318	0.075	0.265	0.026
6	3.549	12.064	1.409	0.300	0.098	0.272	0.032
7	3.627	10.455	1.742	0.235	0.020	0.314	0.052
8	3.696	11.616	0.298	0.320	0.065	0.282	0.007
9	3.757	11.080	0.202	0.233	0.062	0.296	0.005
10	3.810	11.152	0.101	0.275	0.030	0.294	0.003
11	3.858	11.764	0.888	0.235	0.050	0.279	0.021
12	3.900	15.138	9.947	0.372	0.172	0.217	0.142
13	3.937	11.346	0.805	0.318	0.048	0.289	0.021
14	3.971	14.851	10.727	0.280	0.117	0.221	0.160
15	4.000	11.506	1.139	0.270	0.050	0.285	0.028
16	4.027	18.925	18.821	0.275	0.050	0.173	0.172
17	4.050	11.097	0.359	0.292	0.030	0.296	0.010
18	4.090	12.949	2.745	0.287	0.138	0.253	0.054
19	4.071	11.599	0.524	0.195	0.030	0.283	0.013
20	4.106	21.123	11.572	0.138	0.060	0.155	0.085
21	4.121	32.643	18.186	0.117	0.060	0.100	0.056
22	4.136	24.655	10.258	0.102	0.045	0.133	0.055
23	4.147	30.209	14.412	0.092	0.025	0.109	0.052

drop diameter = 1.07mm

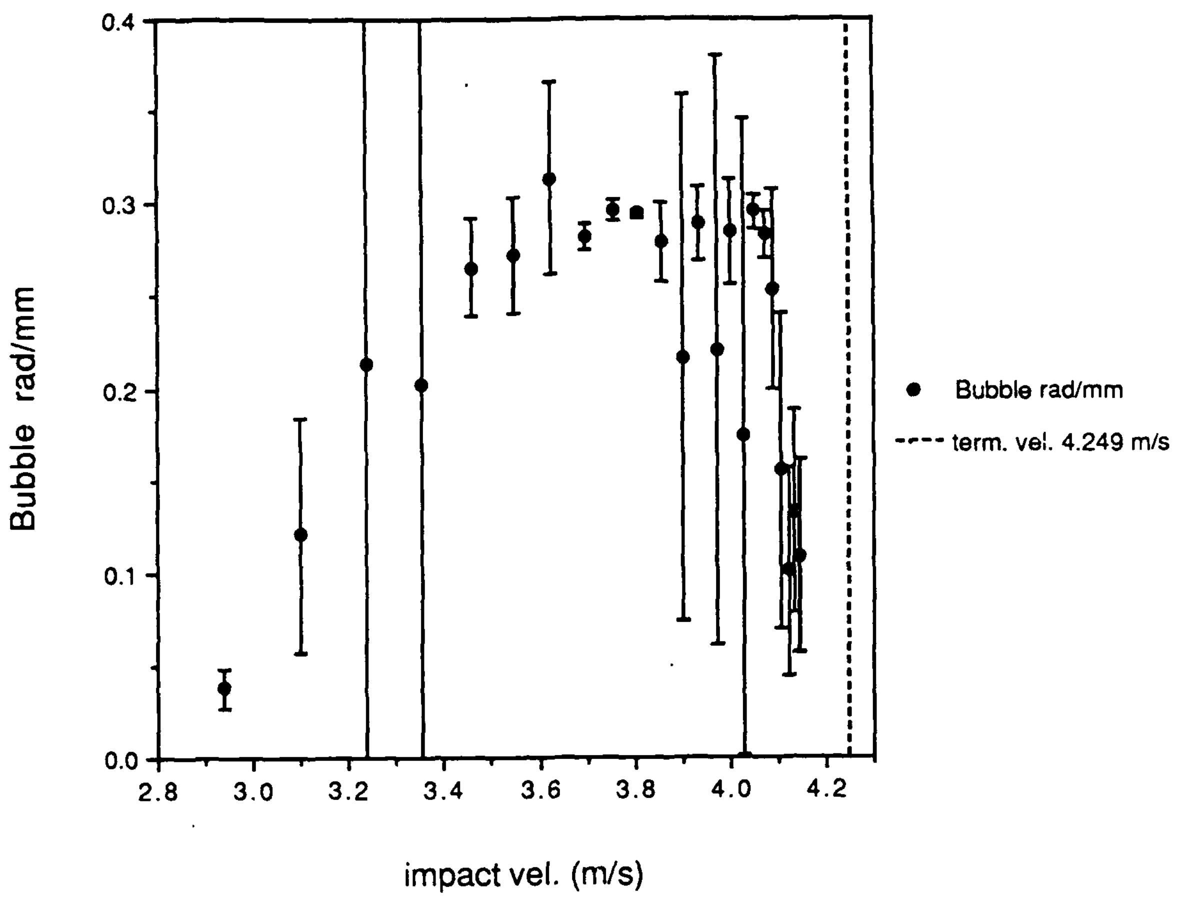

drop diameter = 1.07mm

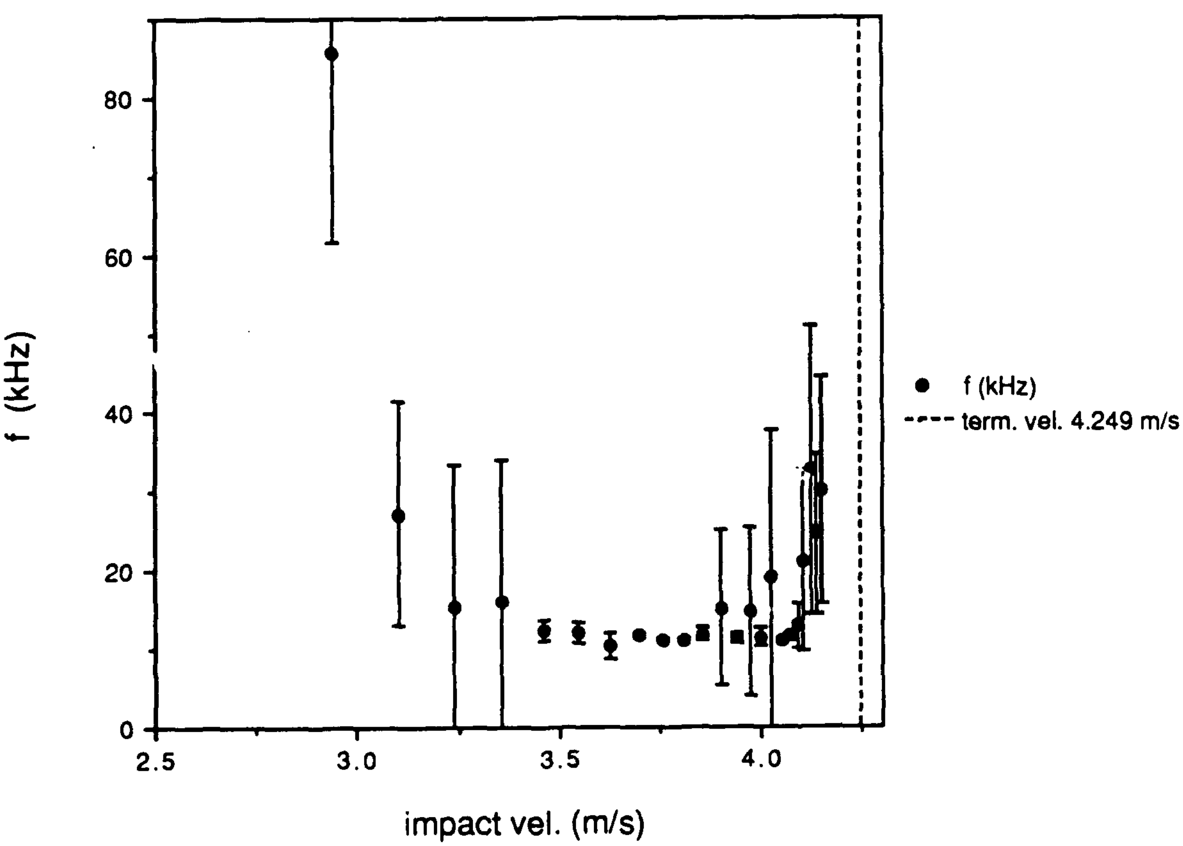

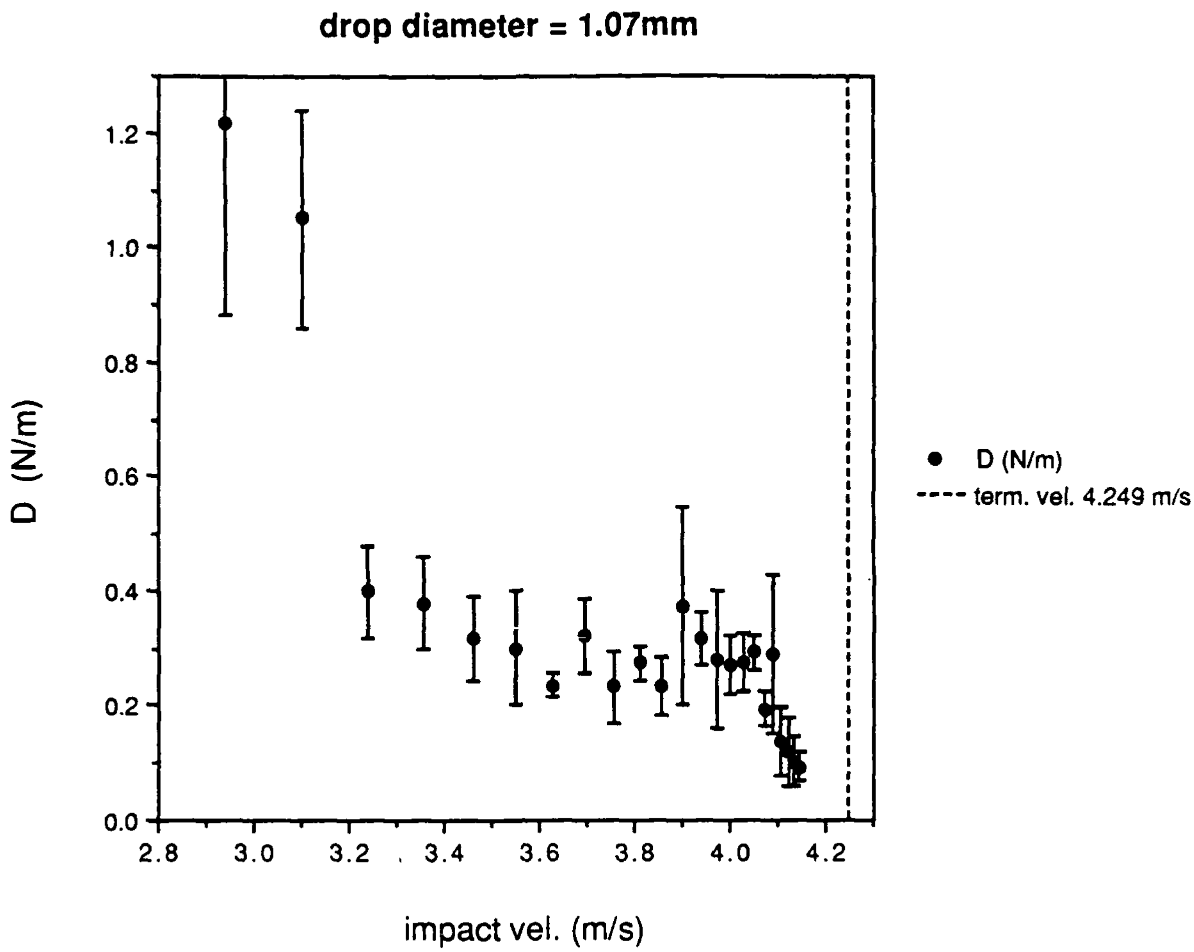
drop diameter = 1.07mm
D (N/m)
1.2
1.0
0.8
0.6
0.4
0.2
0.0
2.8
3.0
3.2
3.4
3.6
3.8
4.0
4.2
impact vel. (m/s)
D (N/m)
term. vel. 4.249 m/s

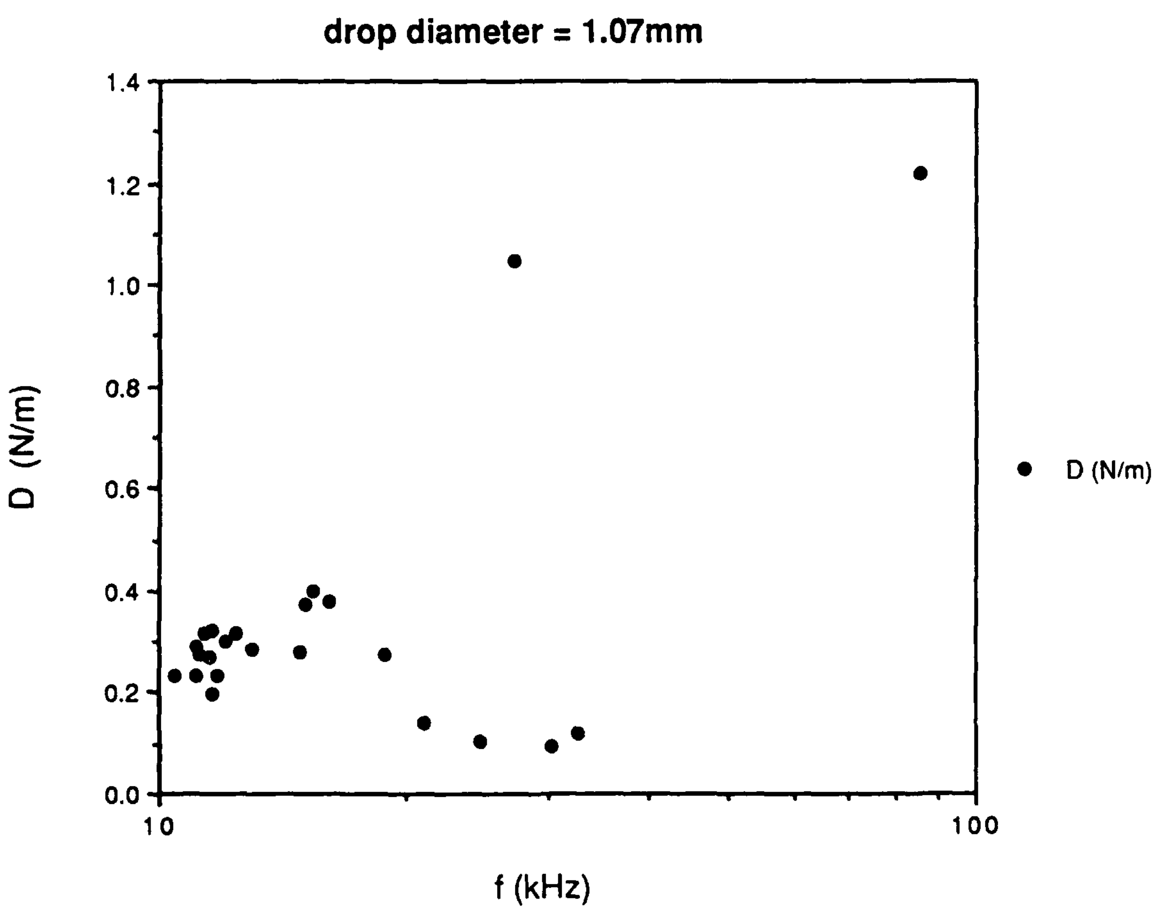
drop diameter = 1.07mm
D (N/m)
1.4
1.2
1.0
0.8
0.6
0.4
0.2
0.0
10
100
f (kHz)
D (N/m)

drop diameter = 1.22mm Thu, Jul 20, 1989 10:07 AM

	impact vel	f (khz)	sd of f	D (N/m)	sd of D	Bubble rad/mm	sd of rad
1	2.610	30.372	12.849	1.917	0.149	0.108	0.046
2	2.711	19.664	9.813	1.186	0.230	0.167	0.083
3	2.804	15.230	5.225	0.922	0.193	0.215	0.074
4	2.891	15.389	4.861	0.925	0.229	0.213	0.067
5	2.943	12.266	2.049	0.747	0.158	0.267	0.045
6	3.022	11.996	2.139	0.461	0.178	0.273	0.049
7	3.114	10.558	1.343	0.554	0.124	0.311	0.040
8	3.188	10.505	1.695	0.502	0.097	0.312	0.050
9	3.508	10.312	0.370	0.985	0.166	0.318	0.011
10	3.625	11.857	1.483	0.731	0.158	0.277	0.035
11	3.729	12.894	2.298	0.988	0.218	0.254	0.045
12	3.294	9.814	1.794	0.394	0.063	0.334	0.061
13	3.436	10.630	0.515	0.769	0.115	0.309	0.015
14	3.562	10.923	0.610	0.599	0.076	0.300	0.017
15	3.673	11.363	1.547	0.702	0.086	0.289	0.039
16	3.772	11.094	0.809	0.470	0.119	0.296	0.022
17	3.817	12.056	2.968	0.823	0.189	0.272	0.067
18	3.860	18.911	10.219	0.785	0.211	0.173	0.094
19	3.900	32.727	21.765	0.635	0.247	0.100	0.067
20	3.935	30.154	21.827	0.740	0.290	0.109	0.079

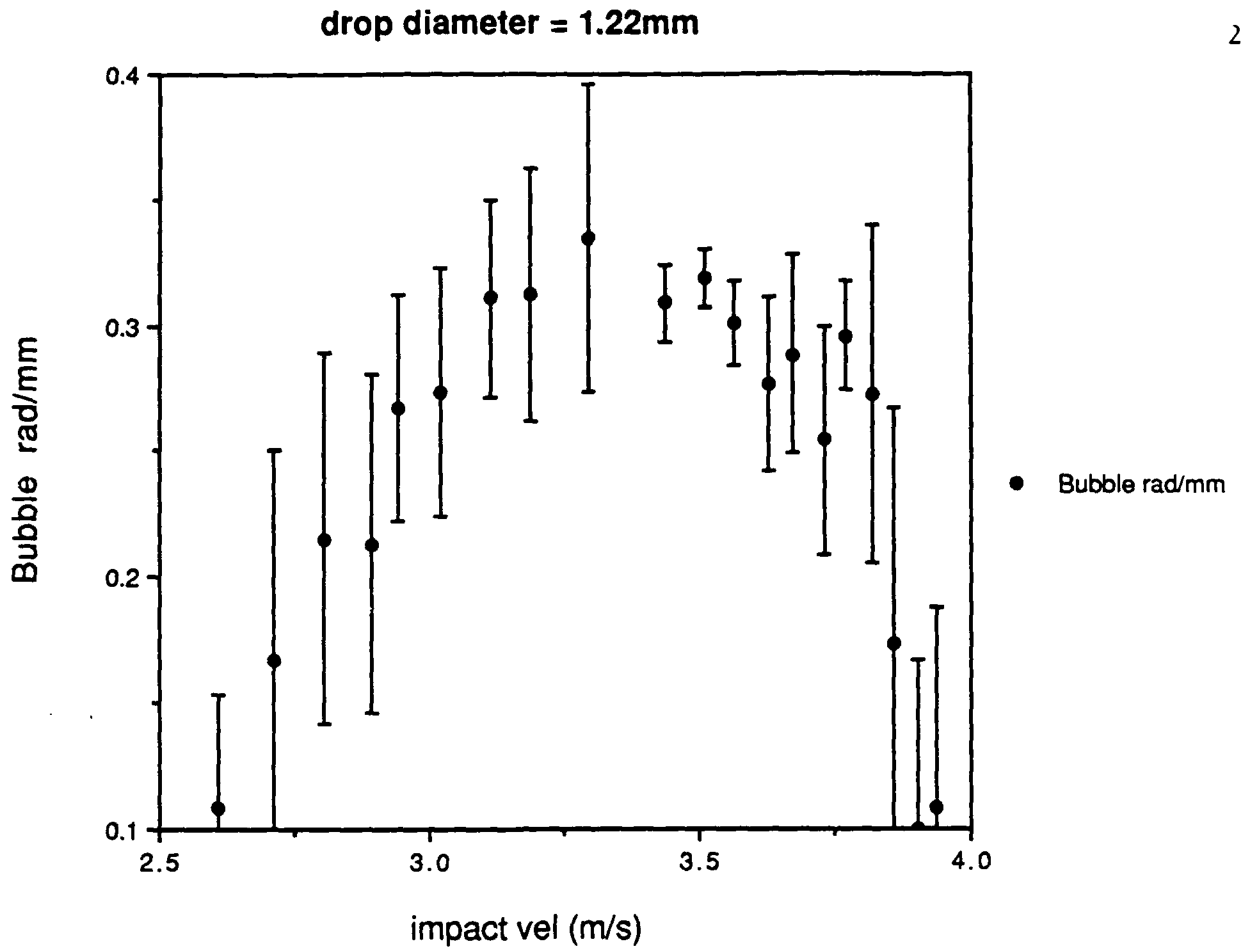
drop diameter = 1.22mm
Bubble rad/mm
0.4
0.3
0.2
0.1
2.5
3.0
3.5
4.0
impact vel (m/s)
Bubble rad/mm

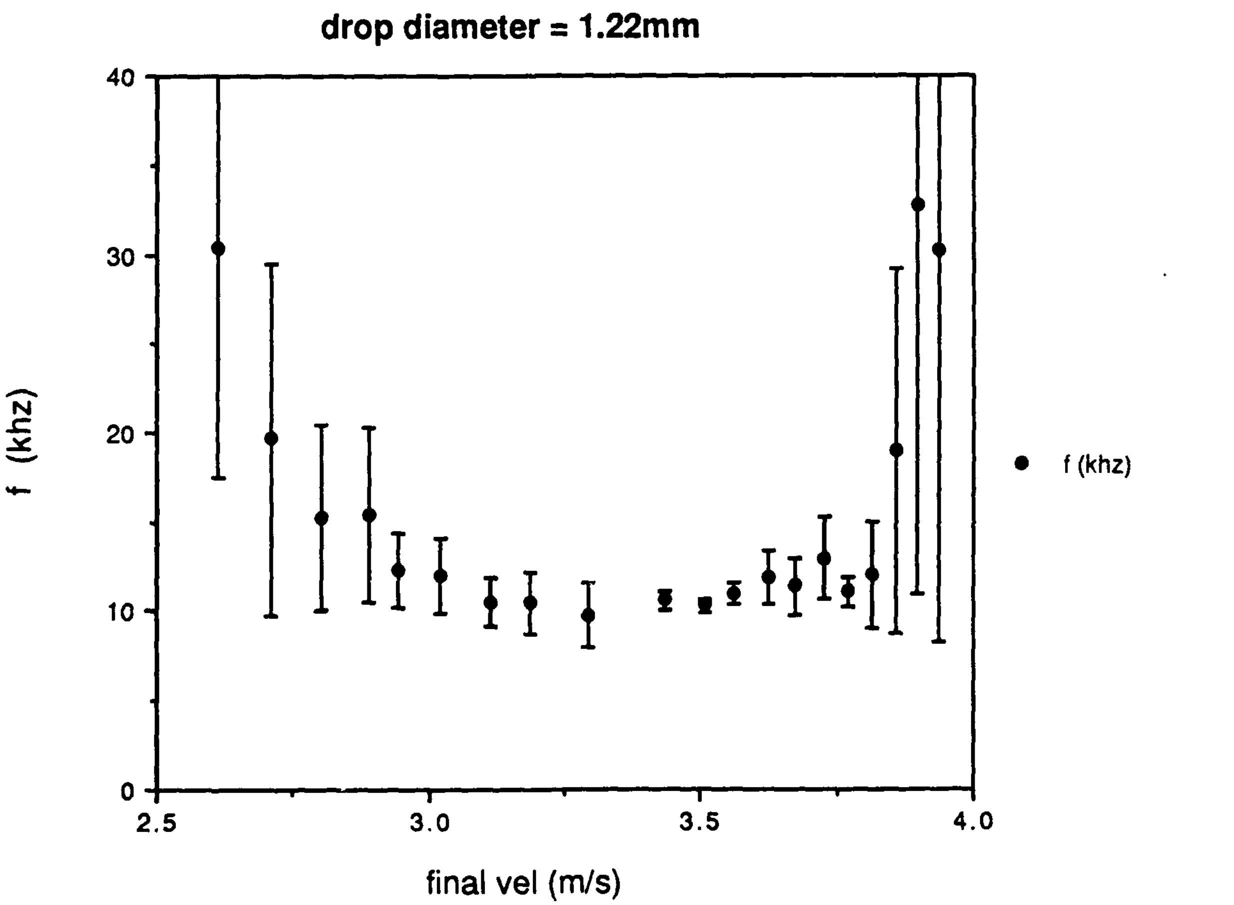
drop diameter = 1.22mm
f (khz)
40
30
20
10
0
2.5
3.0
3.5
4.0
final vel (m/s)
f (khz)

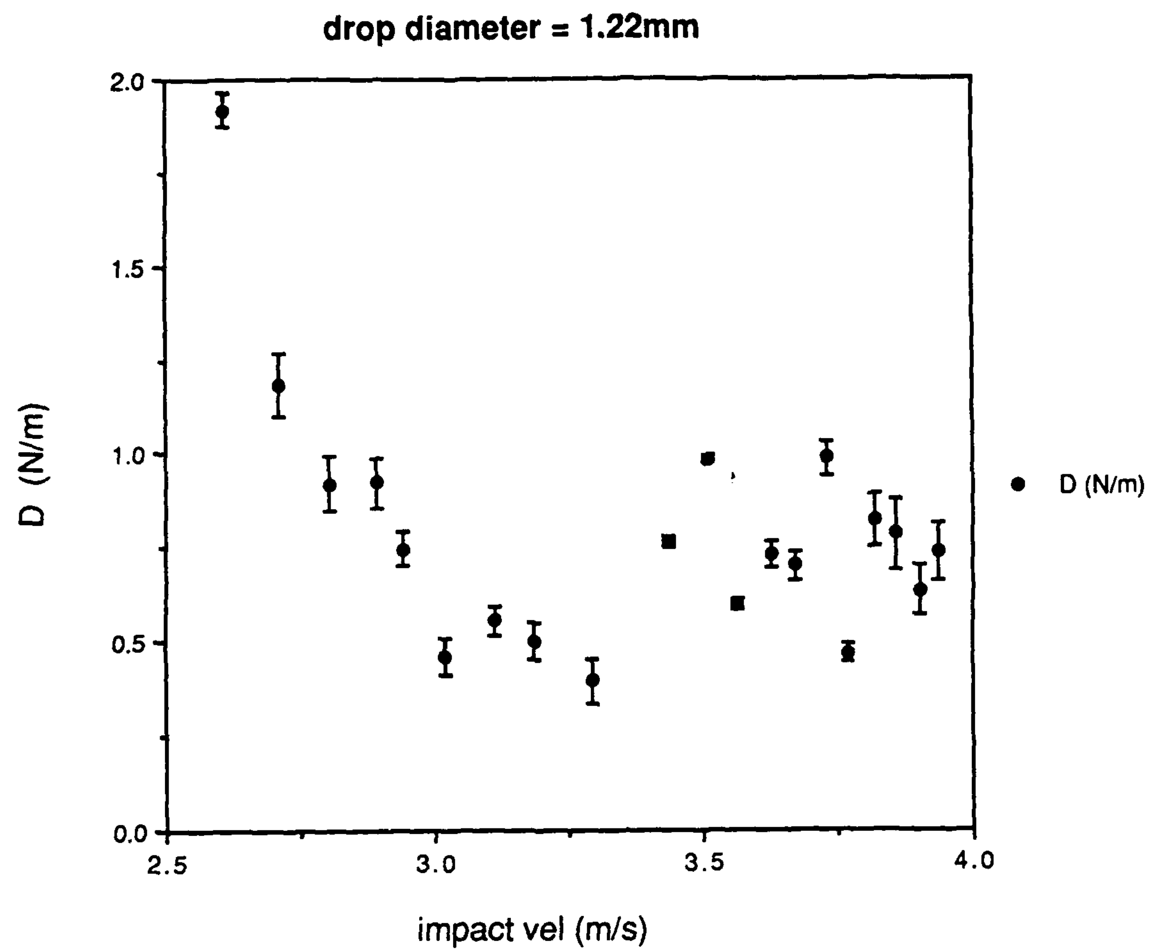
drop diameter = 1.22mm
D (N/m)
2.0
1.5
1.0
0.5
0.0
2.5
3.0
3.5
4.0
impact vel (m/s)
D (N/m)

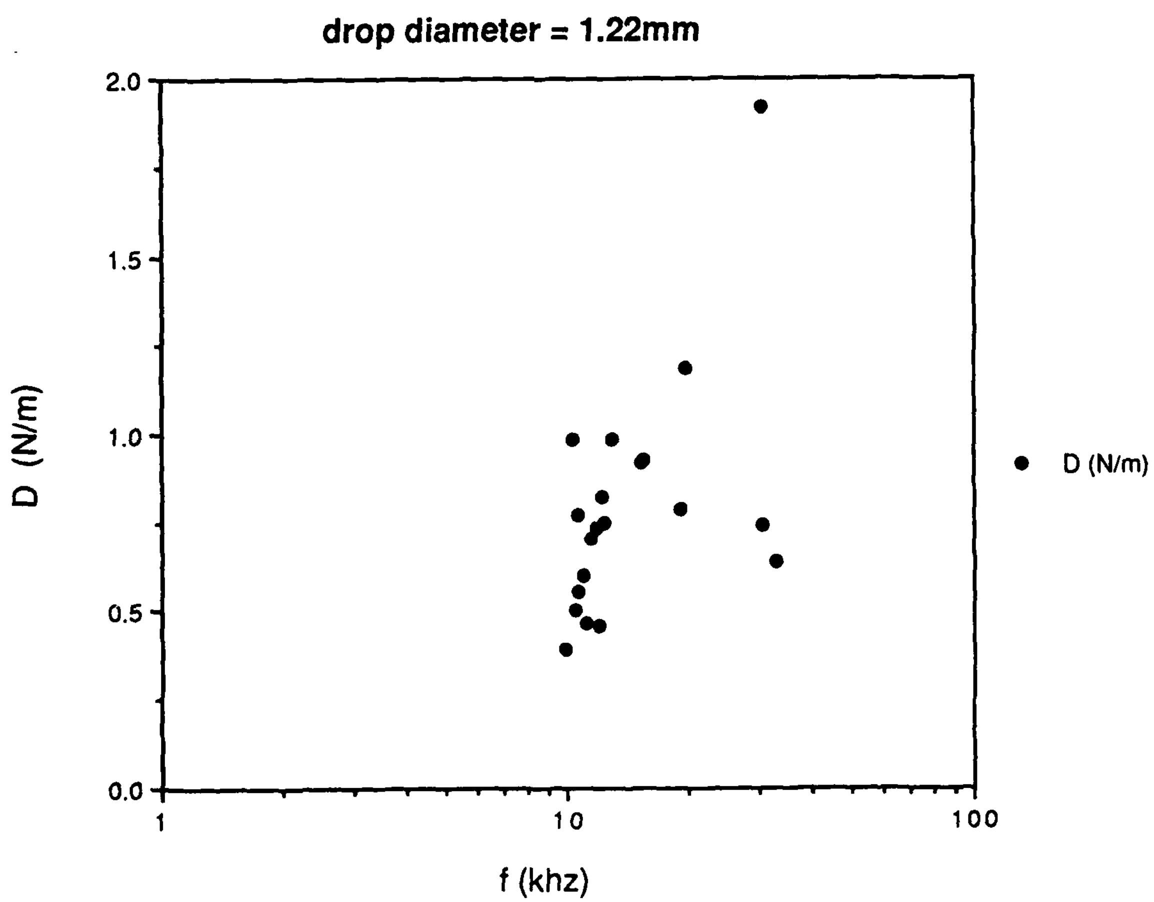
drop diameter = 1.22mm
D (N/m)
2.0
1.5
1.0
0.5
0.0
1
10
100
f (khz)
D (N/m)

drop diameter = 1.71mm Thu, Jul 20, 1989 10:20 AM

	final vel.	f (kHz)	sd of f	D (N/m)	sd of D	Bubble rad/mm	sd of rad
1	2.004	46.174	22.574	1.897	0.155	0.071	0.035
2	2.058	16.600	1.505	1.383	0.147	0.198	0.018
3	2.099	12.964	0.705	1.160	0.117	0.253	0.014
4	2.130	11.639	0.538	1.055	0.058	0.282	0.013
5	2.179	10.637	0.418	0.927	0.058	0.308	0.012
6	2.217	10.140	0.423	0.883	0.060	0.323	0.013
7	2.255	9.492	0.365	0.765	0.058	0.346	0.013
8	2.292	9.718	0.526	0.775	0.072	0.338	0.018
9	2.328	9.362	0.340	0.740	0.065	0.350	0.013
10	2.363	9.233	2.850	0.715	0.065	0.355	0.110
11	2.397	9.211	0.317	0.600	0.052	0.356	0.012
12	2.431	9.029	0.169	0.635	0.048	0.363	0.007
13	2.465	8.482	1.582	0.623	0.033	0.387	0.072
14	2.497	9.657	2.164	0.620	0.102	0.340	0.076
15	2.529	9.954	2.579	0.682	0.122	0.330	0.085
16	2.561	8.807	0.199	0.552	0.028	0.372	0.008
17	2.591	11.070	10.737	0.585	0.050	0.296	0.287
18	2.622	10.069	4.126	0.723	0.152	0.326	0.133
19	2.652	10.294	2.728	0.745	0.205	0.319	0.084
20	2.695	10.048	2.780	0.690	0.150	0.326	0.090
21	2.738	11.946	7.300	0.875	0.480	0.275	0.168
22	2.766	11.141	3.031	0.787	0.190	0.294	0.080
23	2.794	13.340	4.817	0.938	0.172	0.246	0.089
24	2.821	11.810	2.631	0.925	0.225	0.278	0.062
25	2.847	20.767	18.640	1.160	0.295	0.158	0.142
26	2.874	27.478	19.067	1.143	0.453	0.119	0.083
27	2.900	27.783	15.139	1.228	0.417	0.118	0.064
28	2.925	37.226	22.462	1.180	0.485	0.088	0.053

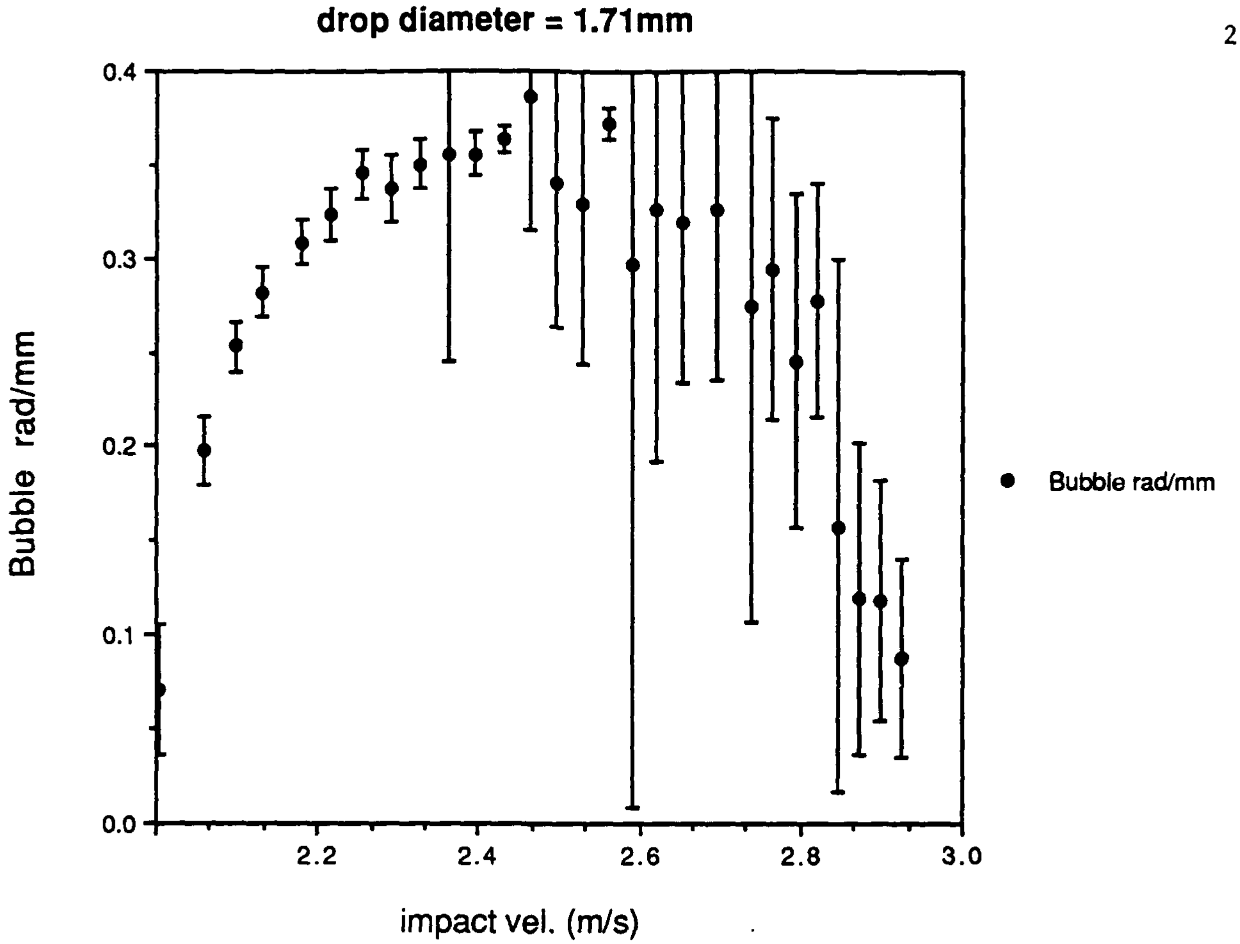
drop diameter = 1.71mm
0.4
0.3
0.2
0.1
0.0
Bubble rad/mm
2.2
2.4
2.6
2.8
3.0
impact vel. (m/s)
Bubble rad/mm

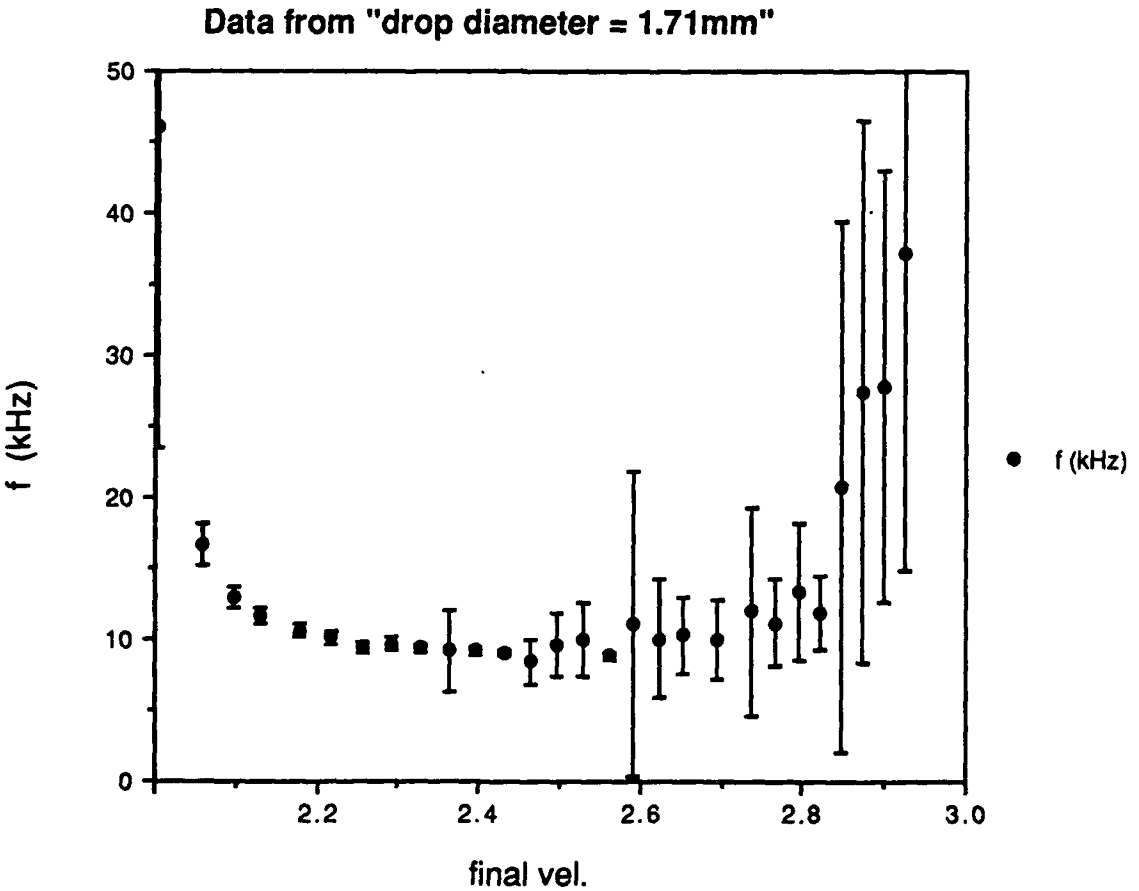
Data from "drop diameter = 1.71mm"
50
40
30
20
10
0
f (kHz)
2.2
2.4
2.6
2.8
3.0
final vel.
f (kHz)

drop diameter = 1.71mm

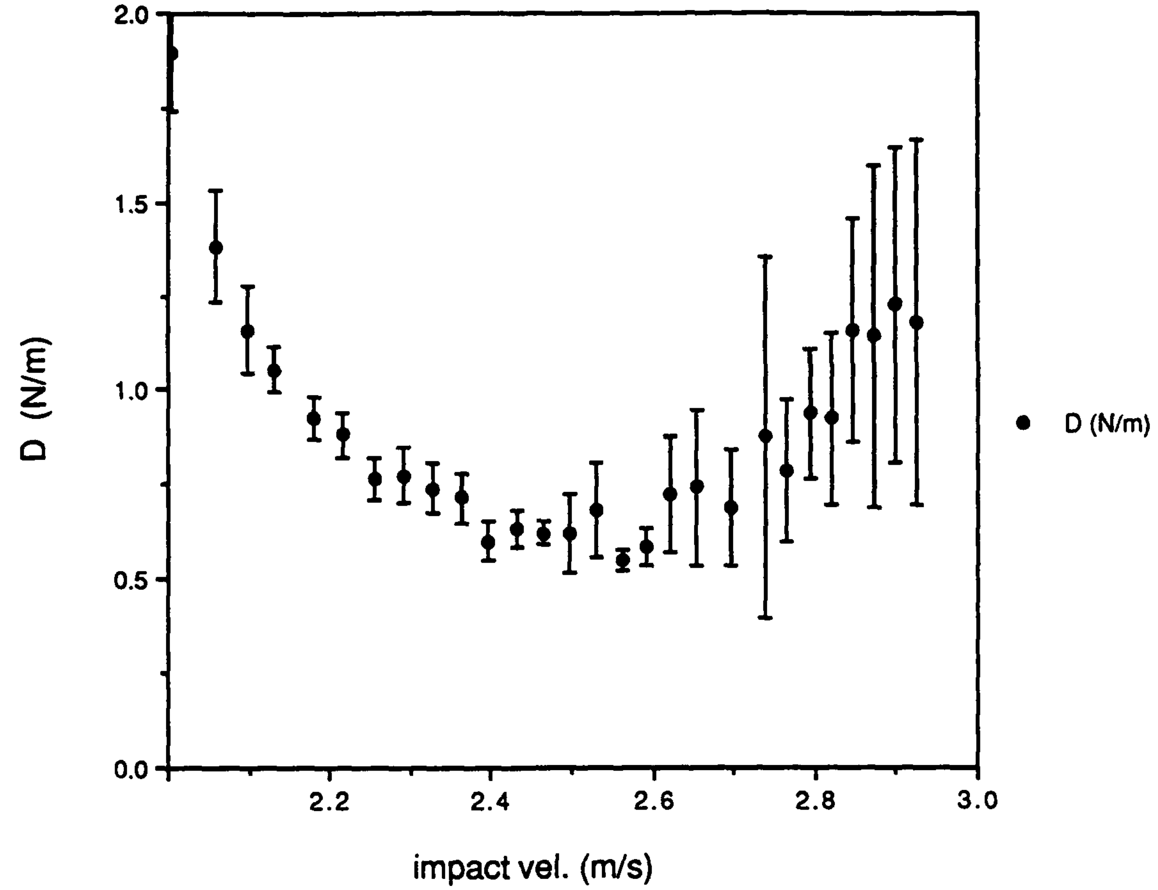

drop diameter = 1.71mm

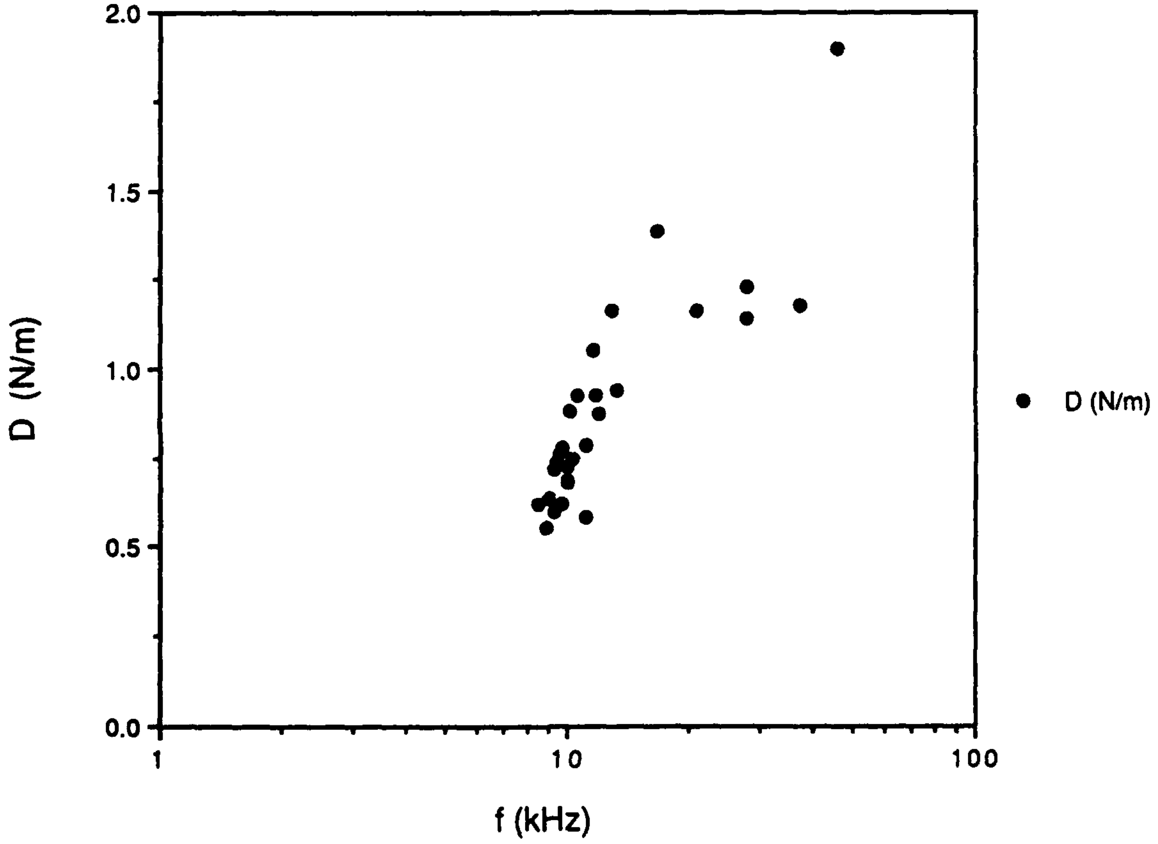

drop diameter = 2.17mm Thu, Jul 20, 1989 10:40 AM

	impact vel.	f (kHz)	sd of f	D (N/m)	sd of D	Bubble rad/mm	sd of rad
1	1.716	24.796	6.820	0.510	0.155	0.132	0.036
2	1.794	12.134	0.390	0.613	0.022	0.270	0.009
3	1.845	9.786	0.487	0.603	0.033	0.335	0.017
4	1.893	8.827	0.530	0.647	0.022	0.372	0.022
5	1.940	9.573	0.346	0.647	0.028	0.343	0.012
6	1.986	8.580	0.615	0.657	0.025	0.382	0.027
7	2.031	8.496	0.723	0.640	0.033	0.386	0.033
8	2.074	8.389	0.850	0.585	0.055	0.391	0.040
9	2.117	8.325	0.307	0.600	0.052	0.394	0.015
10	2.158	8.346	0.262	0.713	0.040	0.393	0.012
11	2.199	8.128	0.238	0.735	0.035	0.404	0.012
12	2.238	8.115	0.219	0.708	0.022	0.404	0.011
13	2.277	8.745	0.413	0.743	0.028	0.375	0.018
14	2.315	9.510	0.731	0.760	0.058	0.345	0.027
15	2.352	8.905	0.493	0.762	0.037	0.368	0.020
16	2.389	9.558	0.696	0.818	0.030	0.343	0.025
17	2.424	11.381	3.320	0.843	0.065	0.288	0.084
18	2.459	12.179	8.389	0.828	0.110	0.269	0.186
19	2.494	19.439	17.760	0.825	0.230	0.169	0.154
20	2.528	15.525	5.281	0.973	0.215	0.211	0.072

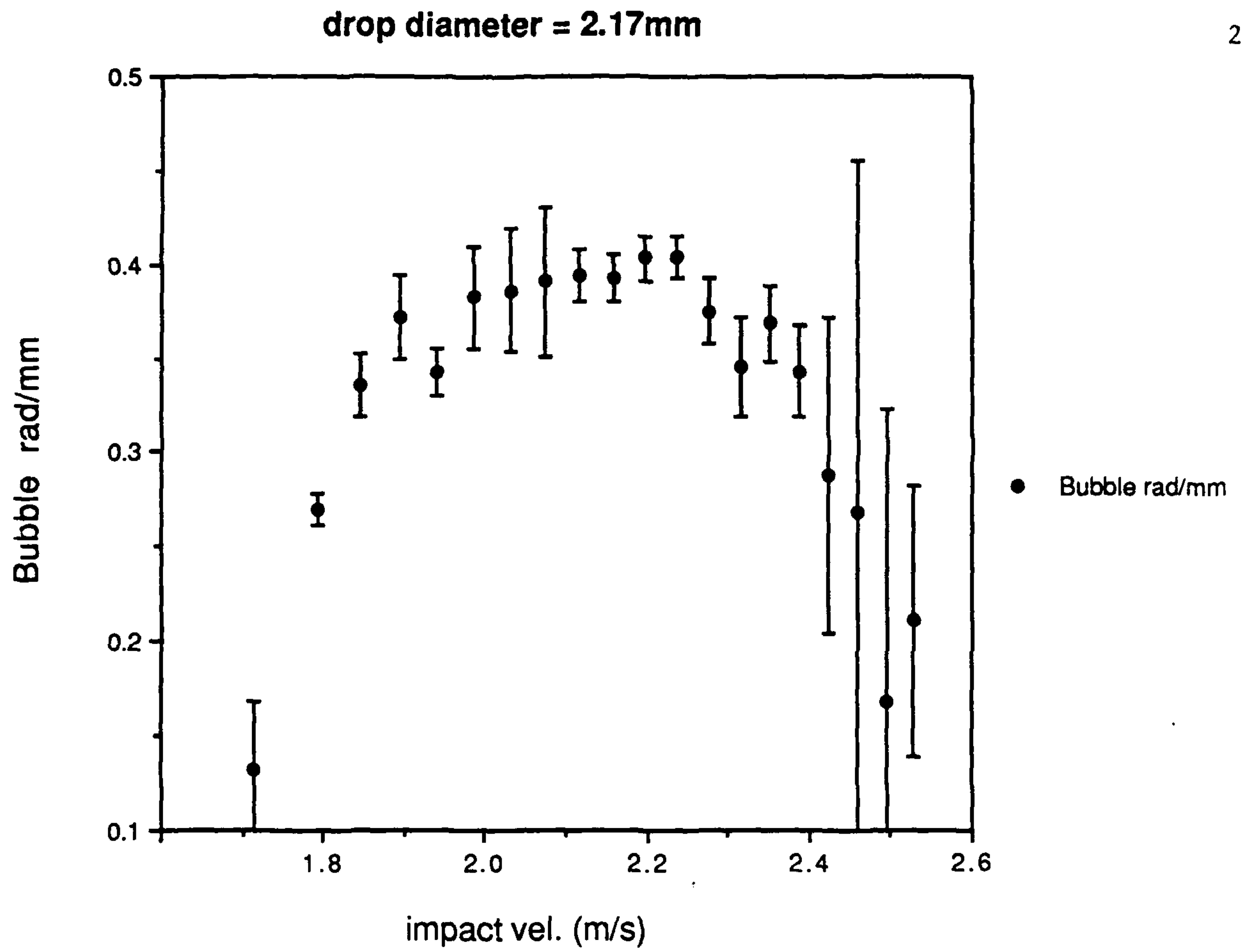
drop diameter = 2.17mm
Bubble rad/mm
0.5
0.4
0.3
0.2
0.1
1.8
2.0
2.2
2.4
2.6
impact vel. (m/s)
Bubble rad/mm

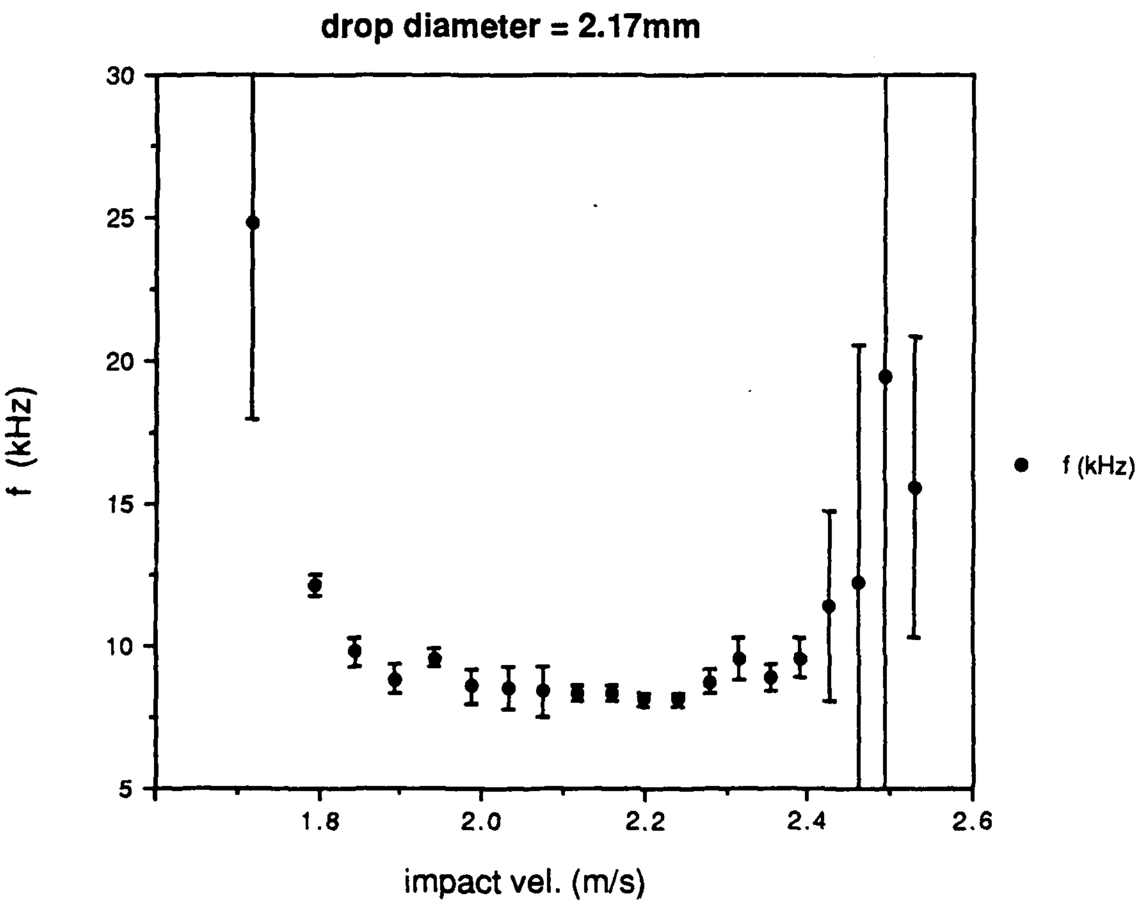
drop diameter = 2.17mm
f (kHz)
30
25
20
15
10
5
1.8
2.0
2.2
2.4
2.6
impact vel. (m/s)
f (kHz)

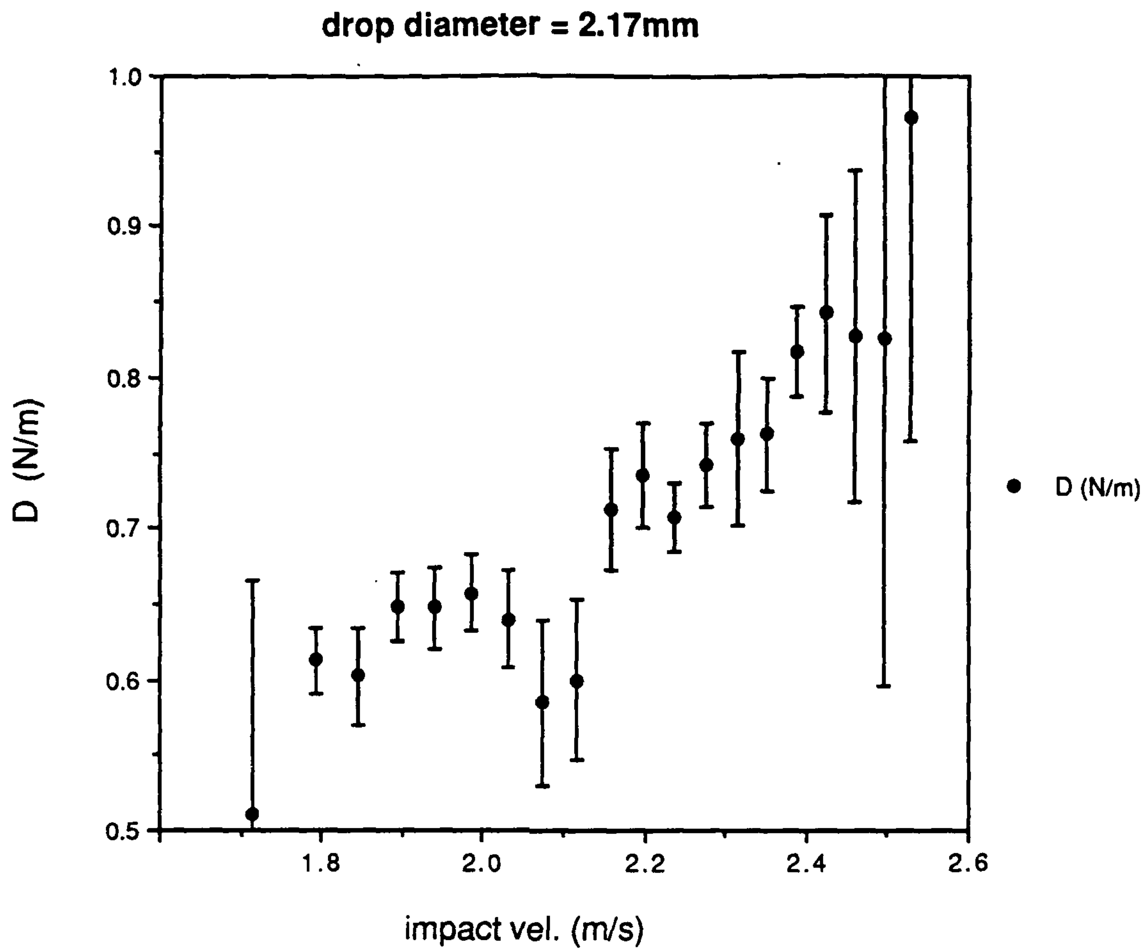
drop diameter = 2.17mm
D (N/m)
1.0
0.9
0.8
0.7
0.6
0.5
1.8
2.0
2.2
2.4
2.6
impact vel. (m/s)
D (N/m)

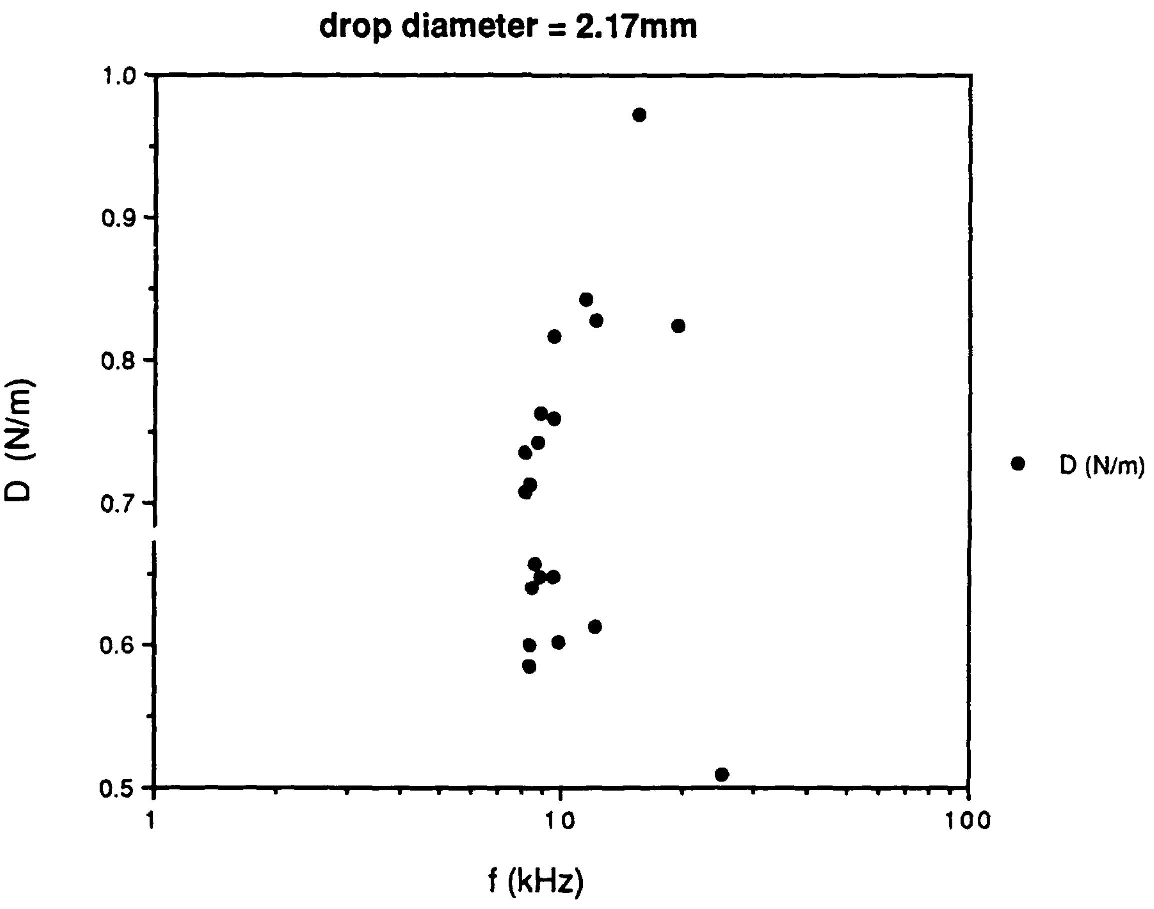
drop diameter = 2.17mm
D (N/m)
1.0
0.9
0.8
0.7
0.6
0.5
1
10
100
f (kHz)
D (N/m)

drop diameter = 2.23mm Thu, Jul 20, 1989 11:03 AM

	impact vel.	f (kHz)	sd of f	D (N/m)	sd of D	Bubble rad/mm	sd of rad
1	1.846	14.300	1.117	1.288	0.130	0.229	0.018
2	1.894	11.881	0.836	1.062	0.058	0.276	0.019
3	1.941	11.406	0.920	1.095	0.095	0.288	0.023
4	1.987	9.563	0.506	0.910	0.077	0.343	0.018
5	2.032	9.306	0.314	0.873	0.045	0.352	0.012
6	2.076	8.891	0.383	0.810	0.058	0.369	0.016
7	2.118	8.533	0.278	0.775	0.033	0.384	0.013
8	2.160	8.269	2.940	0.743	0.030	0.397	0.141
9	2.200	8.185	0.179	0.725	0.025	0.401	0.009
10	2.240	8.149	0.207	0.685	0.117	0.403	0.010
11	2.279	8.269	0.363	0.716	0.025	0.397	0.017
12	2.317	8.465	0.402	0.723	0.028	0.387	0.018
13	2.354	8.773	0.304	0.762	0.033	0.374	0.013
14	2.391	9.305	0.708	0.818	0.075	0.352	0.027
15	2.427	9.413	0.682	0.825	0.083	0.348	0.025
16	2.462	9.293	0.573	0.795	0.072	0.353	0.022
17	2.496	24.548	14.274	1.312	0.405	0.134	0.078
18	2.530	27.932	20.458	1.240	0.540	0.117	0.086
19	2.564	31.849	15.423	1.173	0.472	0.103	0.050
20	2.597	35.173	25.170	1.260	0.485	0.093	0.067

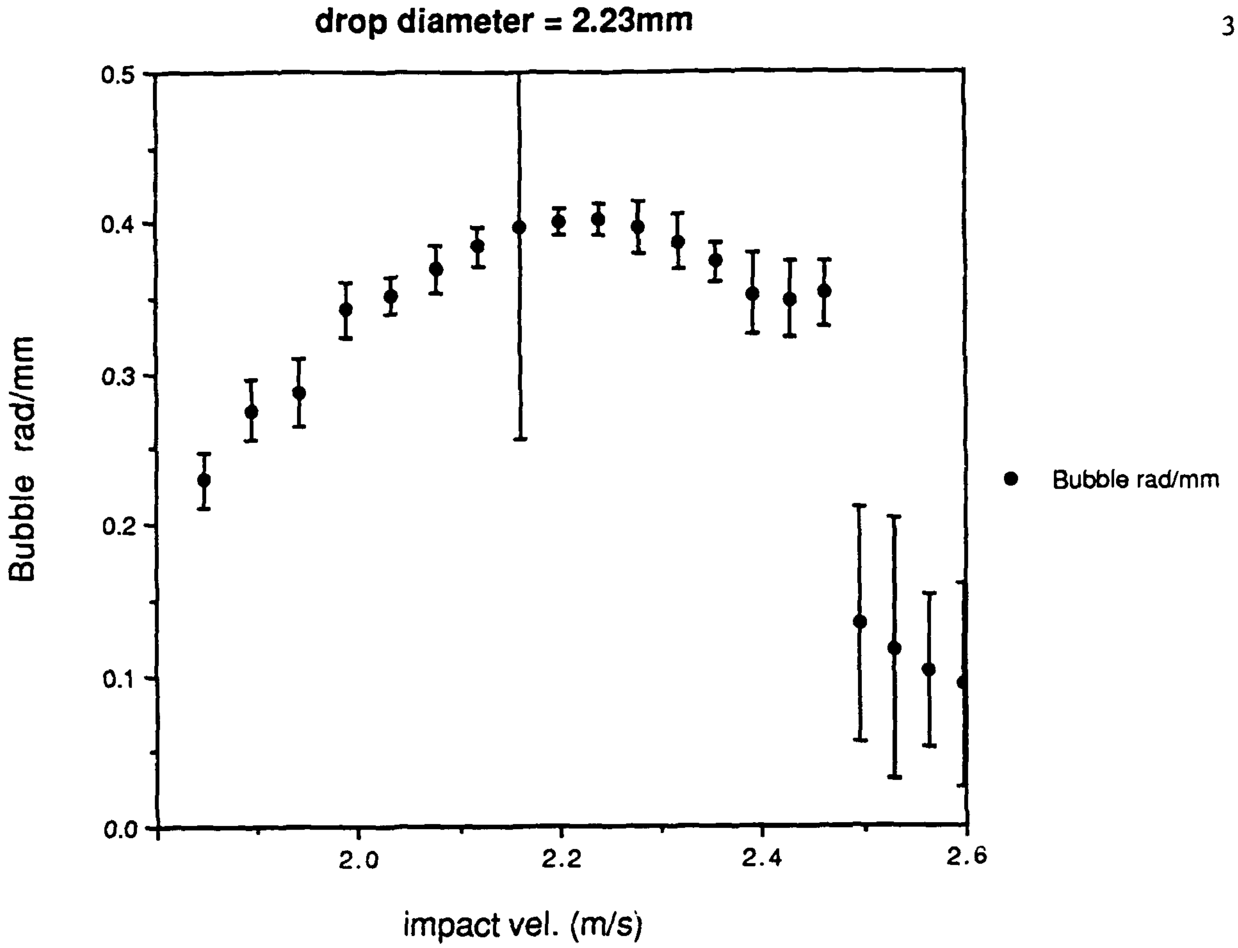
drop diameter = 2.23mm
Bubble rad/mm
impact vel. (m/s)
Bubble rad/mm
0.0
0.1
0.2
0.3
0.4
0.5
2.0
2.2
2.4
2.6

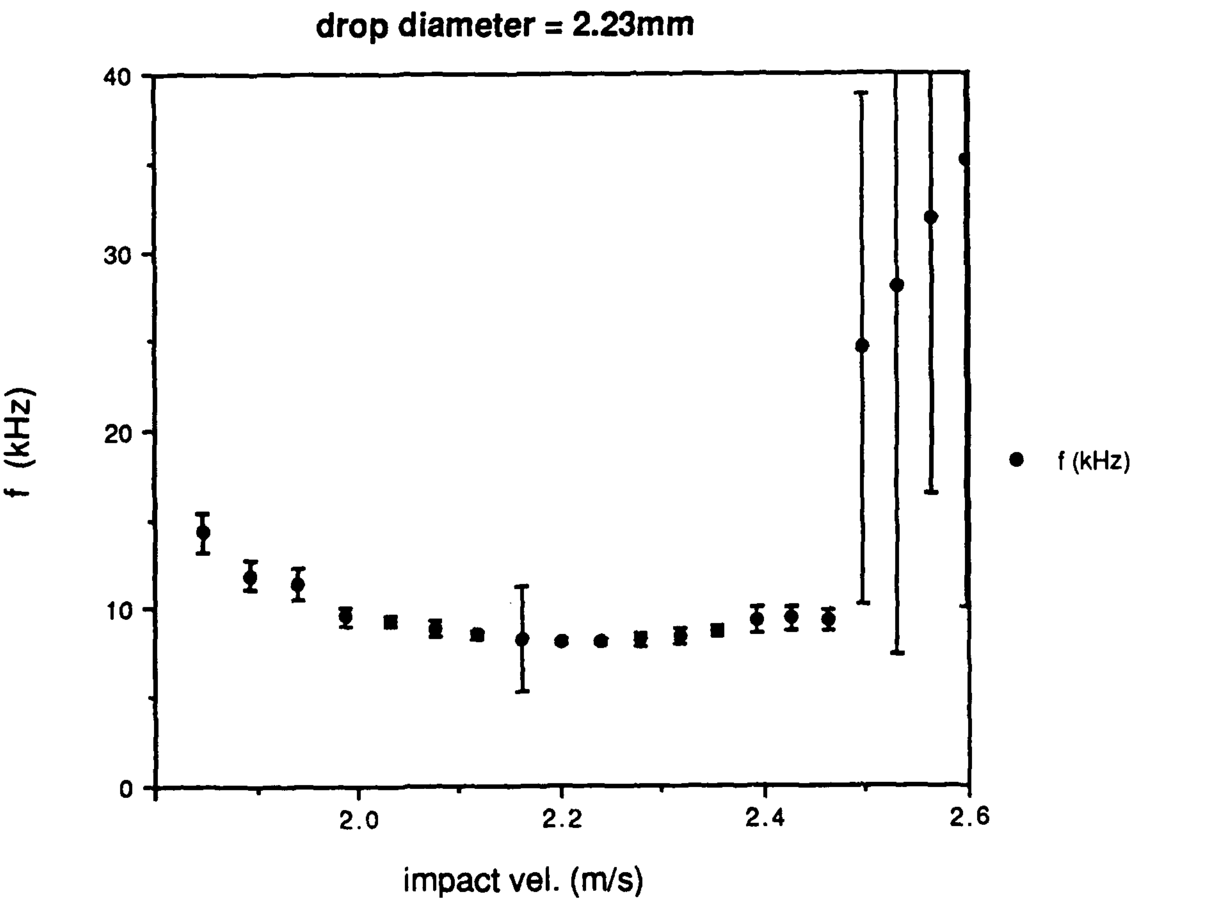
drop diameter = 2.23mm
f (kHz)
impact vel. (m/s)
f (kHz)
0
10
20
30
40
2.0
2.2
2.4
2.6

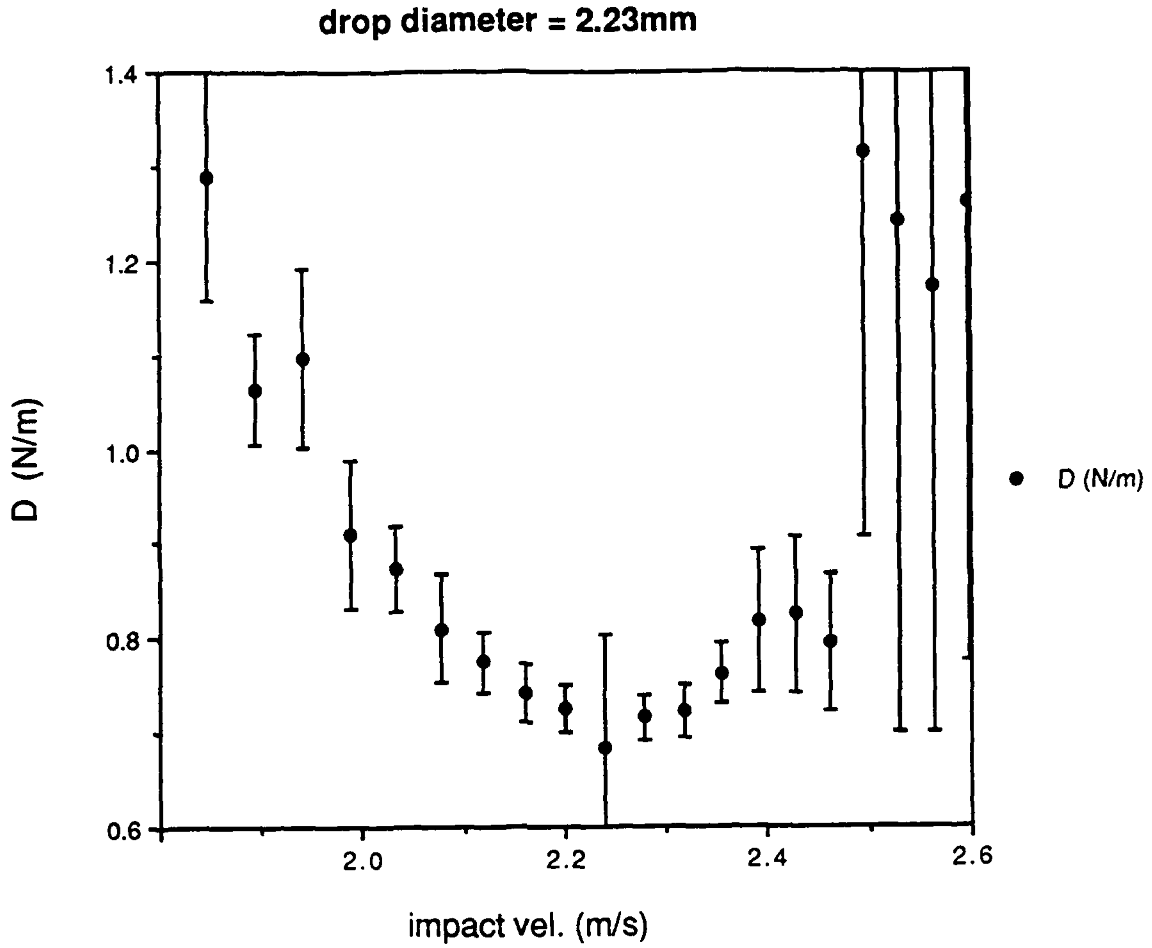
drop diameter = 2.23mm
D (N/m)
impact vel. (m/s)
1.4
1.2
1.0
0.8
0.6
2.0
2.2
2.4
2.6
D (N/m)

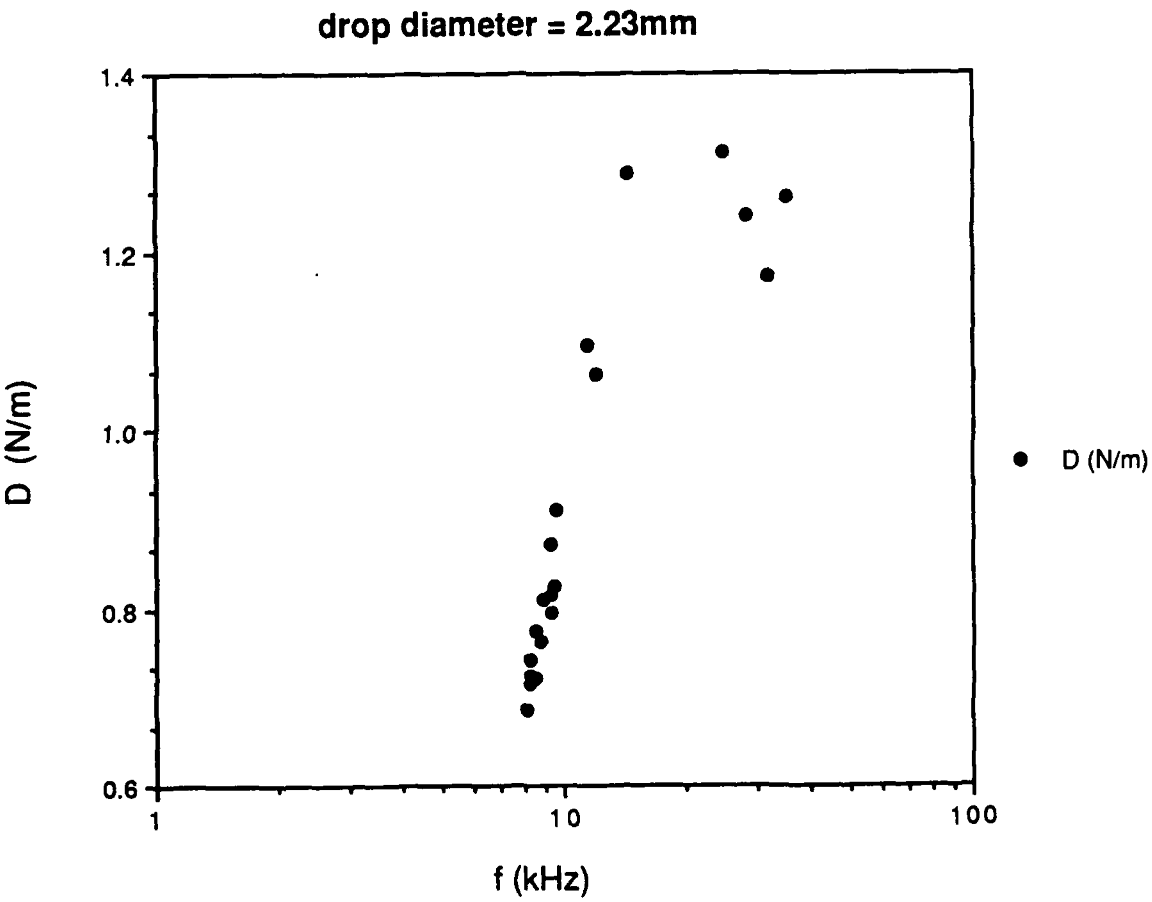
drop diameter = 2.23mm
D (N/m)
f (kHz)
1.4
1.2
1.0
0.8
0.6
1
10
100
D (N/m)

drop diameter = 2.57mm   Thu, Jul 20, 1989 11:24 AM

	impact vel.	f (khz)	sd of f	D (N/m)	sd of D	Bubble rad/mm	sd of rad
1	2.208	9.927	2.770	0.950	0.188	0.330	0.092
2	2.167	11.850	5.573	1.035	0.217	0.277	0.130
3	2.125	9.586	1.993	0.865	0.217	0.342	0.071
4	2.082	9.233	1.400	0.833	0.200	0.355	0.054
5	2.038	8.155	0.671	0.713	0.068	0.402	0.033
6	1.993	7.901	0.354	0.710	0.022	0.415	0.019
7	1.947	7.202	0.640	0.645	0.075	0.455	0.040
8	1.899	7.625	0.314	0.720	0.037	0.430	0.018
9	1.850	7.987	1.030	0.765	0.085	0.411	0.053
10	1.800	8.460	1.116	0.840	0.115	0.388	0.051
11	1.747	9.050	3.498	0.973	0.253	0.362	0.140
12	1.693	8.965	1.546	0.930	0.120	0.366	0.063
13	1.637	11.207	6.241	1.028	0.297	0.293	0.163
14	1.579	14.563	3.944	1.377	0.333	0.225	0.061

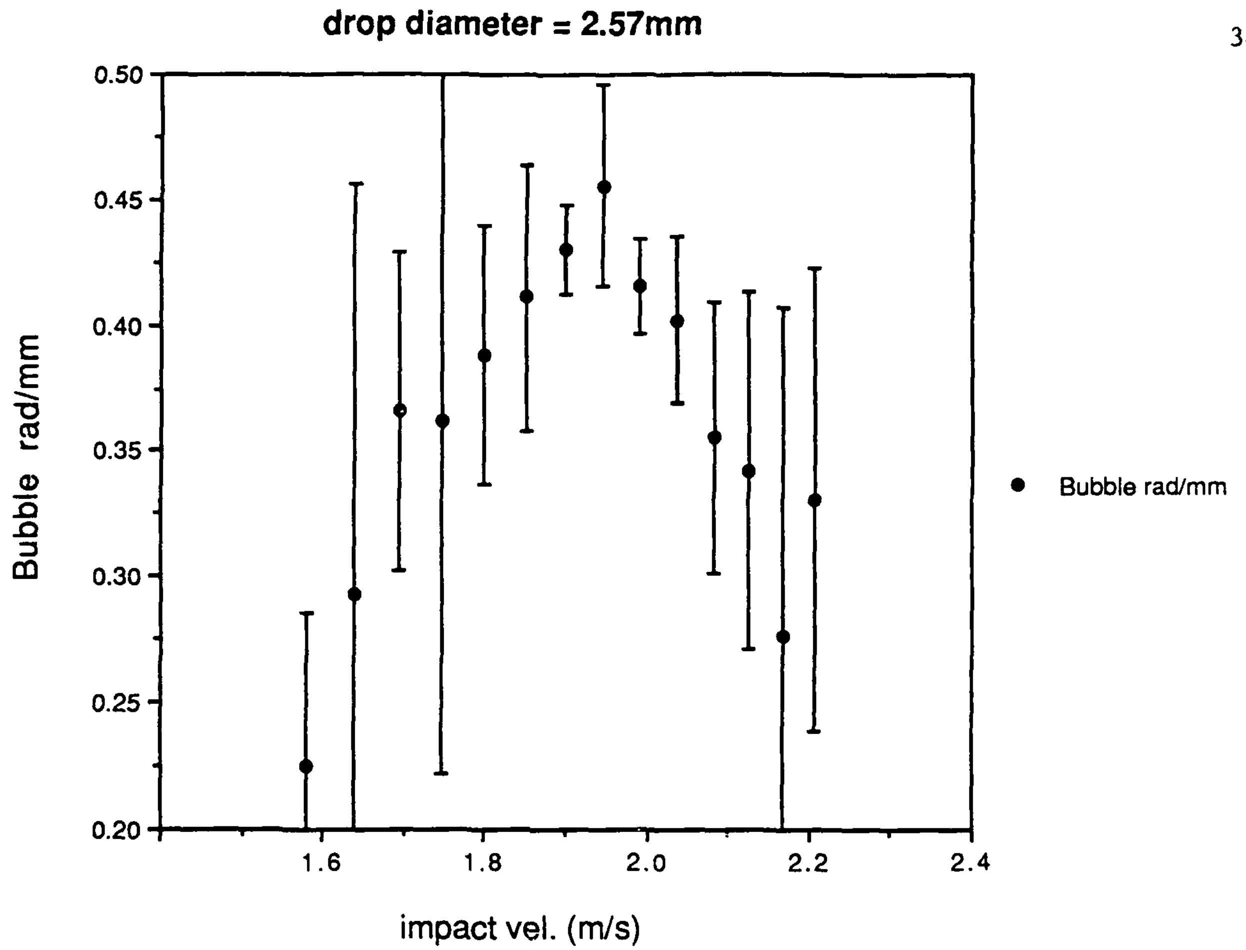
drop diameter = 2.57mm
Bubble rad/mm
0.50
0.45
0.40
0.35
0.30
0.25
0.20
1.6
1.8
2.0
2.2
2.4
impact vel. (m/s)
Bubble rad/mm

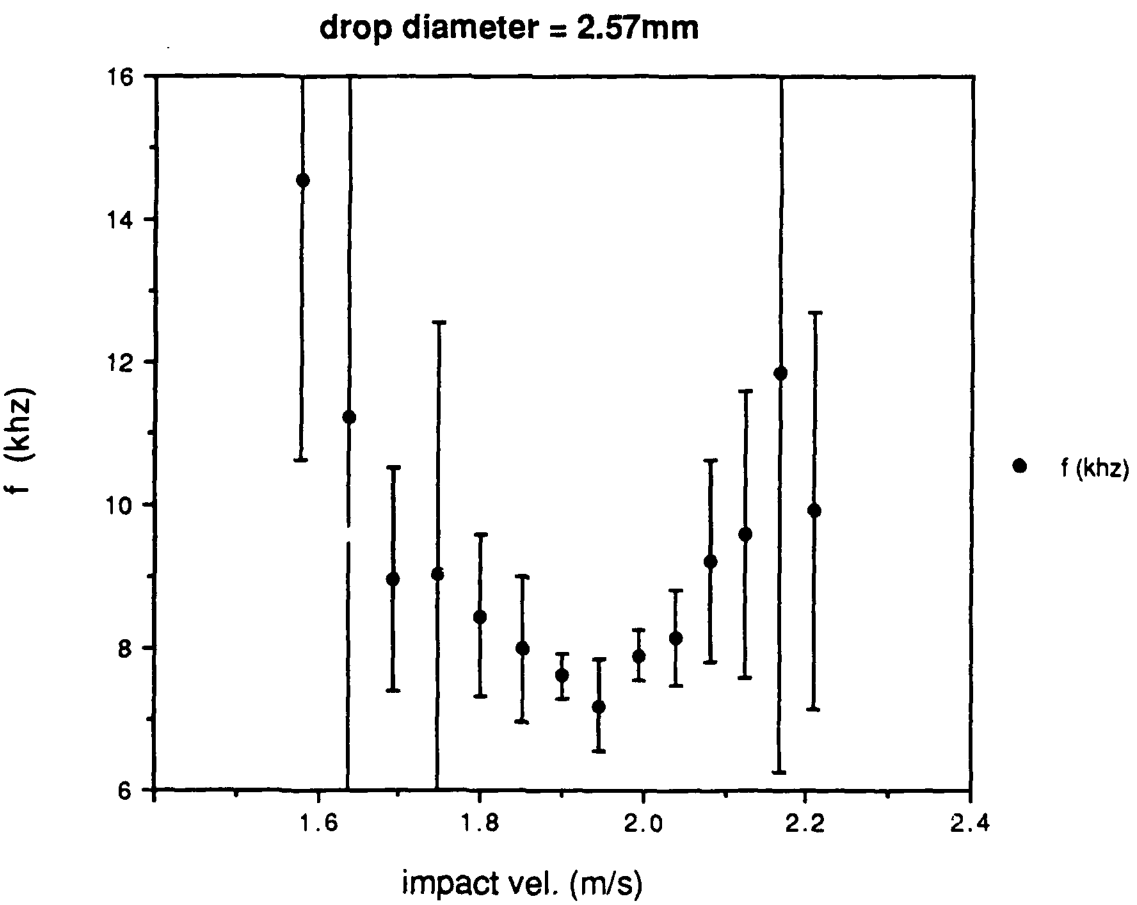
drop diameter = 2.57mm
f (khz)
16
14
12
10
8
6
1.6
1.8
2.0
2.2
2.4
impact vel. (m/s)
f (khz)

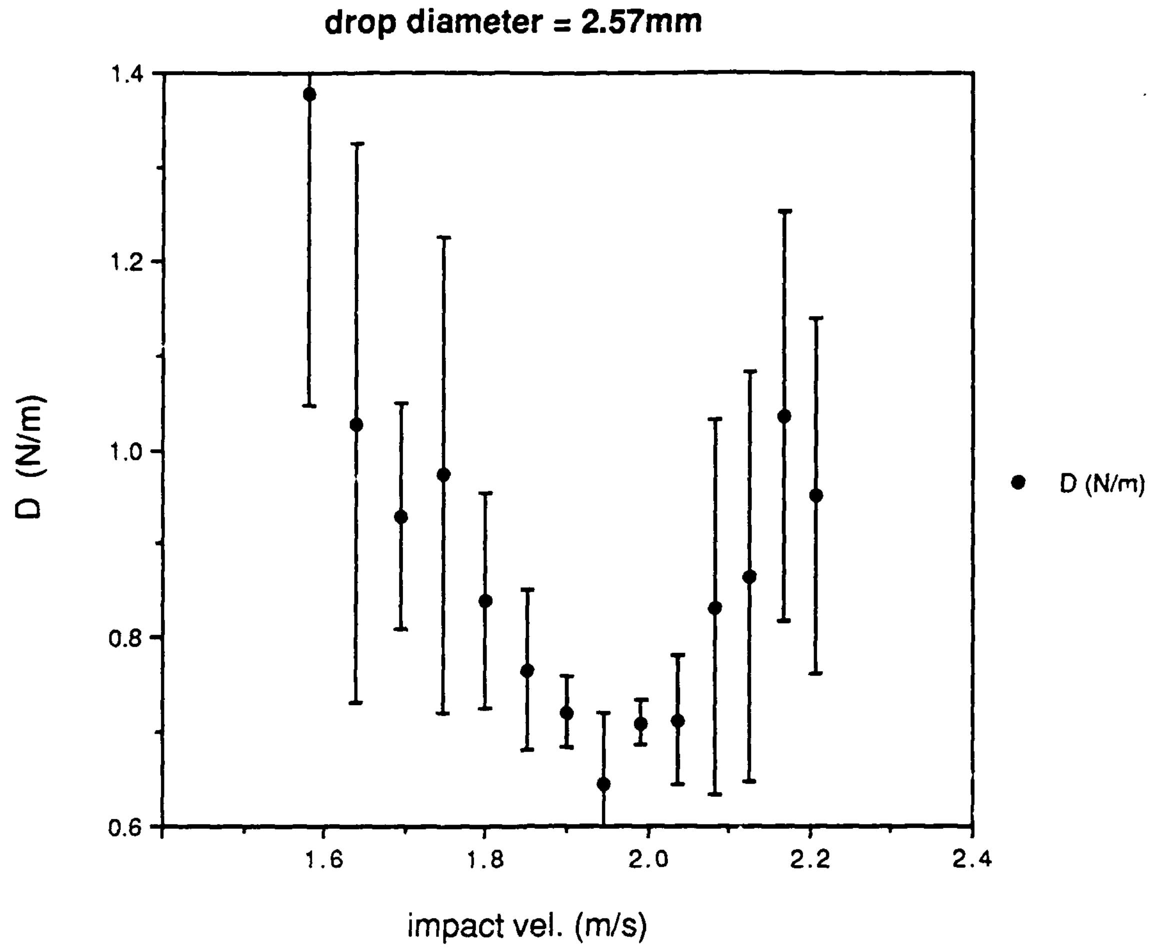
drop diameter = 2.57mm
1.4
1.2
1.0
0.8
0.6
D (N/m)
1.6
1.8
2.0
2.2
2.4
impact vel. (m/s)
D (N/m)

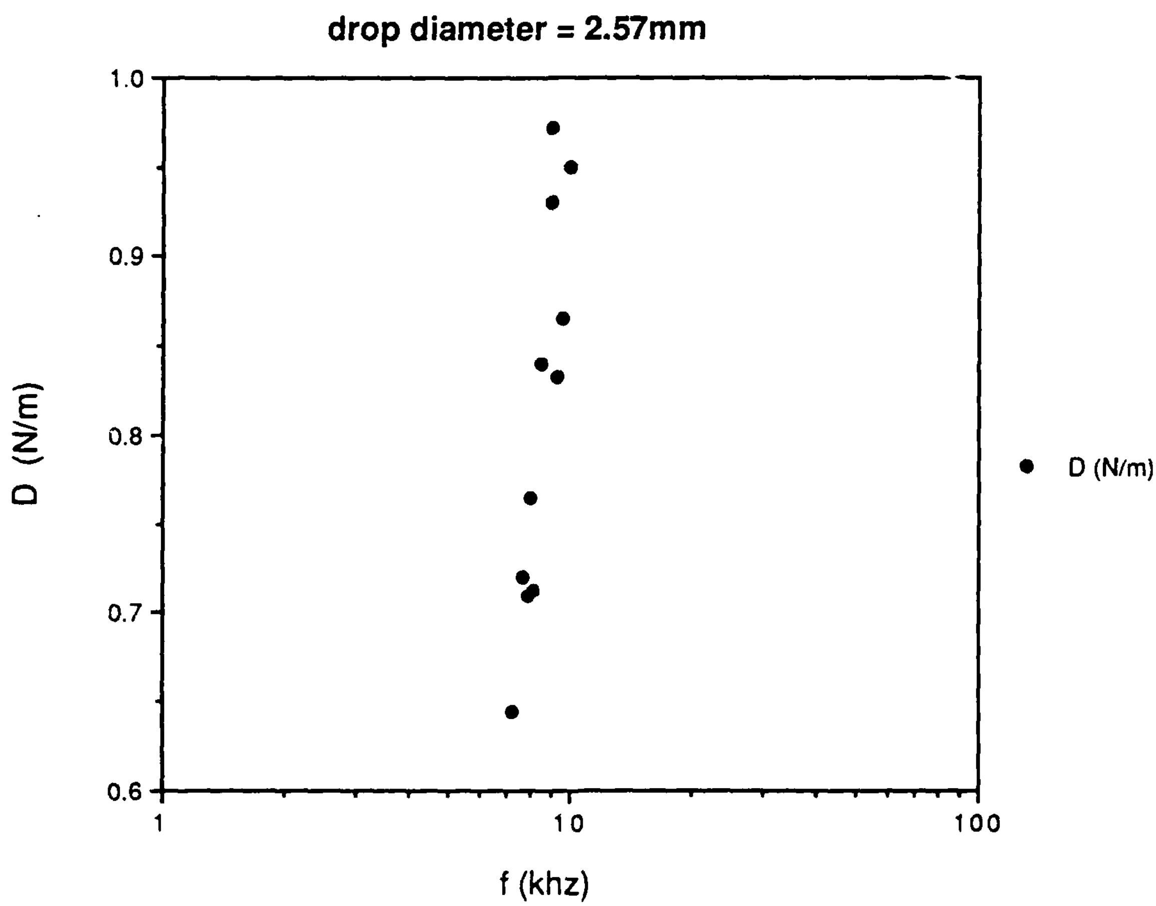
drop diameter = 2.57mm
1.0
0.9
0.8
0.7
0.6
D (N/m)
1
10
100
f (khz)
D (N/m)

drop diameter = 2.78mm Thu, Jul 20, 1989 11:47 AM

	final vel.	f (kHz)	sd of f	D (N/m)	sd of D	Bubble rad/mm	sd of rad
1	2.110	9.506	1.573	0.000	0.000	0.345	0.057
2	2.170	27.714	31.057	0.000	0.000	0.118	0.133
3	2.040	7.595	0.313	0.000	0.000	0.432	0.018
4	2.000	8.280	2.001	0.000	0.000	0.396	0.096
5	1.950	8.423	2.022	0.000	0.000	0.389	0.093
6	1.900	7.909	0.409	0.665	0.048	0.415	0.021
7	2.170	17.070	6.272	0.995	0.362	0.192	0.071
8	1.850	7.246	0.772	0.632	0.092	0.453	0.048
9	1.800	7.201	0.674	0.695	0.085	0.455	0.043
10	1.750	7.126	1.736	0.830	0.092	0.460	0.112
11	1.700	8.236	1.085	0.940	0.080	0.398	0.052
12	1.640	8.980	1.400	0.828	0.130	0.365	0.057
13	1.580	9.871	2.767	0.995	0.223	0.332	0.093
14	1.520	16.567	5.438	1.510	0.320	0.198	0.065
15	1.460	17.174	6.586	1.417	0.263	0.191	0.073

NOTE TO THE USE OF d=2.78mm

The dipole strength values, D, that equal zero are artificial; they were inserted solely to make the graphing work. For impact velocity = 2.170 m/s, N = 75.

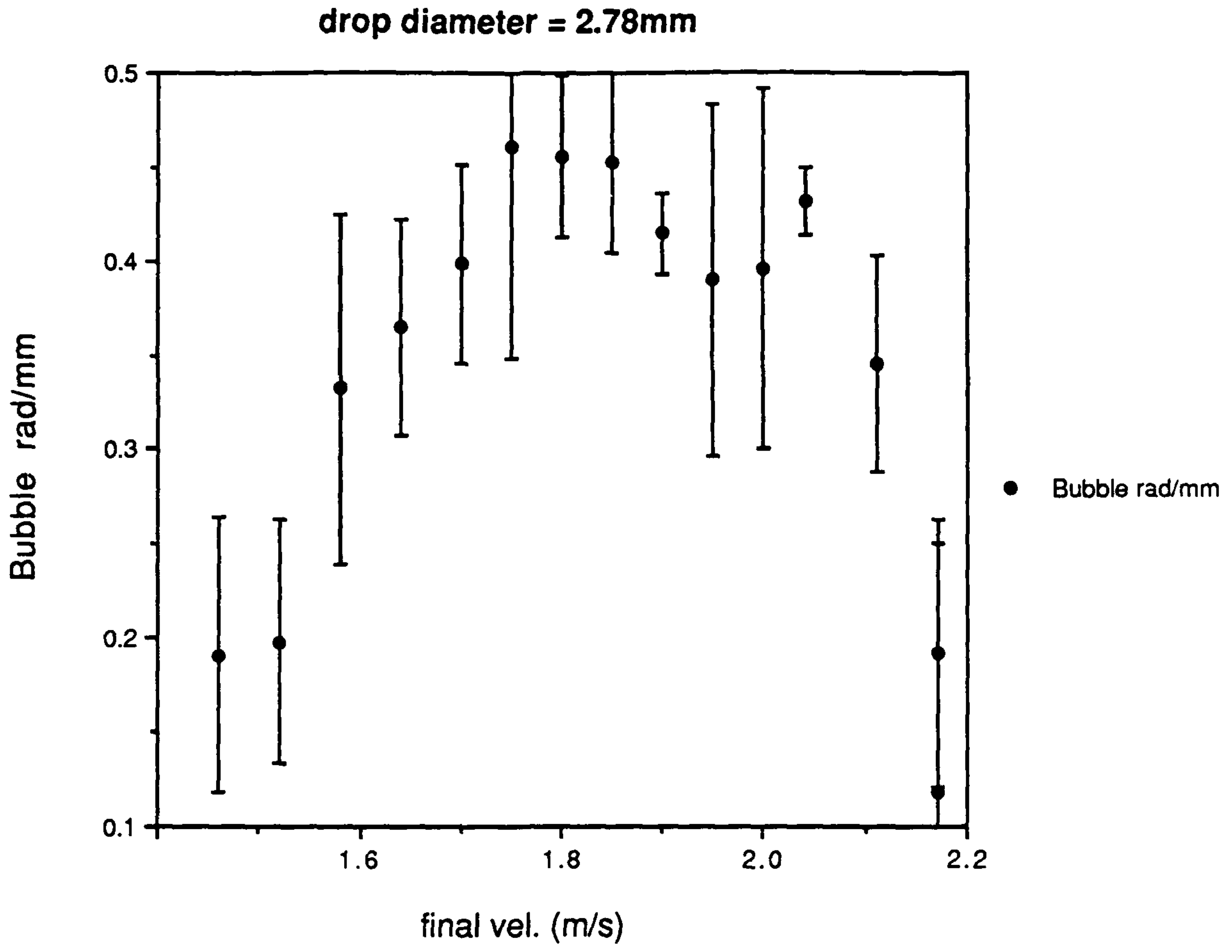
drop diameter = 2.78mm
0.5
0.4
0.3
0.2
0.1
Bubble rad/mm
1.6
1.8
2.0
2.2
final vel. (m/s)
Bubble rad/mm

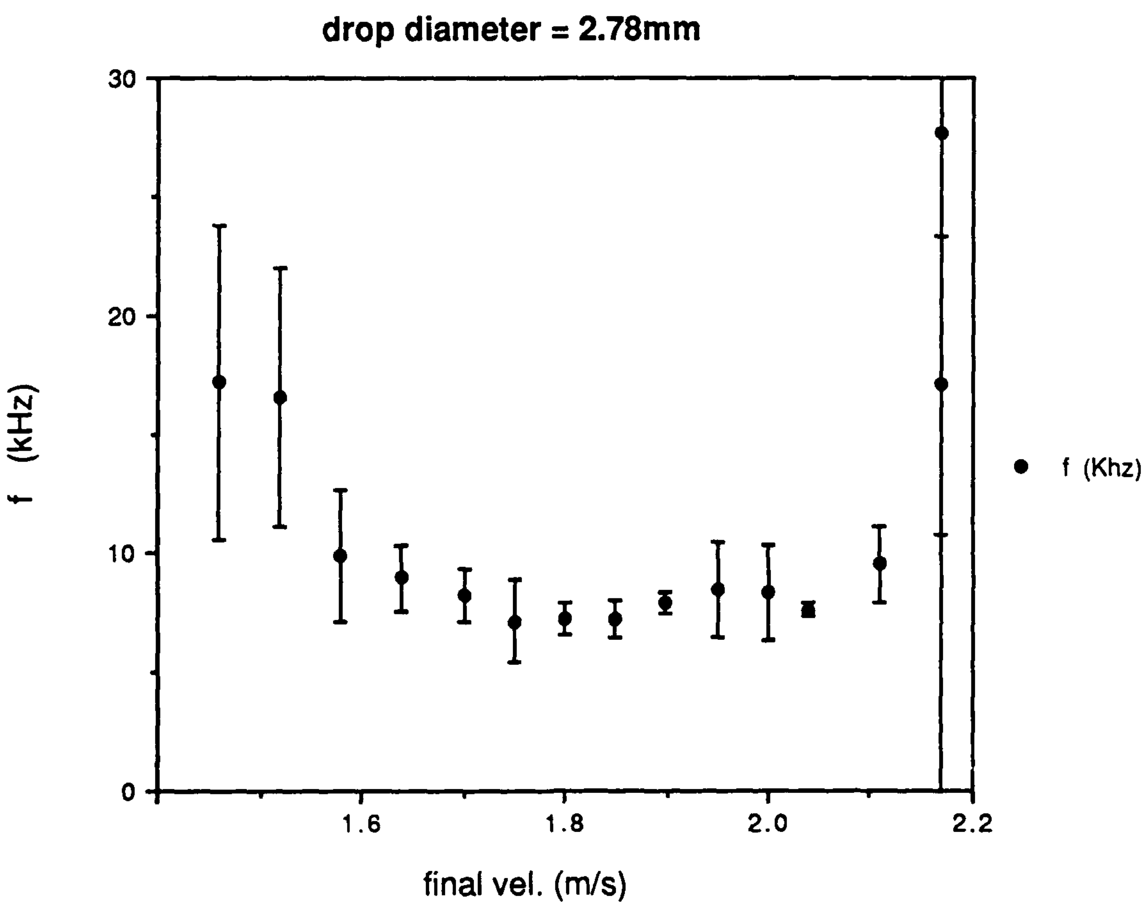
drop diameter = 2.78mm
30
20
10
0
f (kHz)
1.6
1.8
2.0
2.2
final vel. (m/s)
f (Khz)

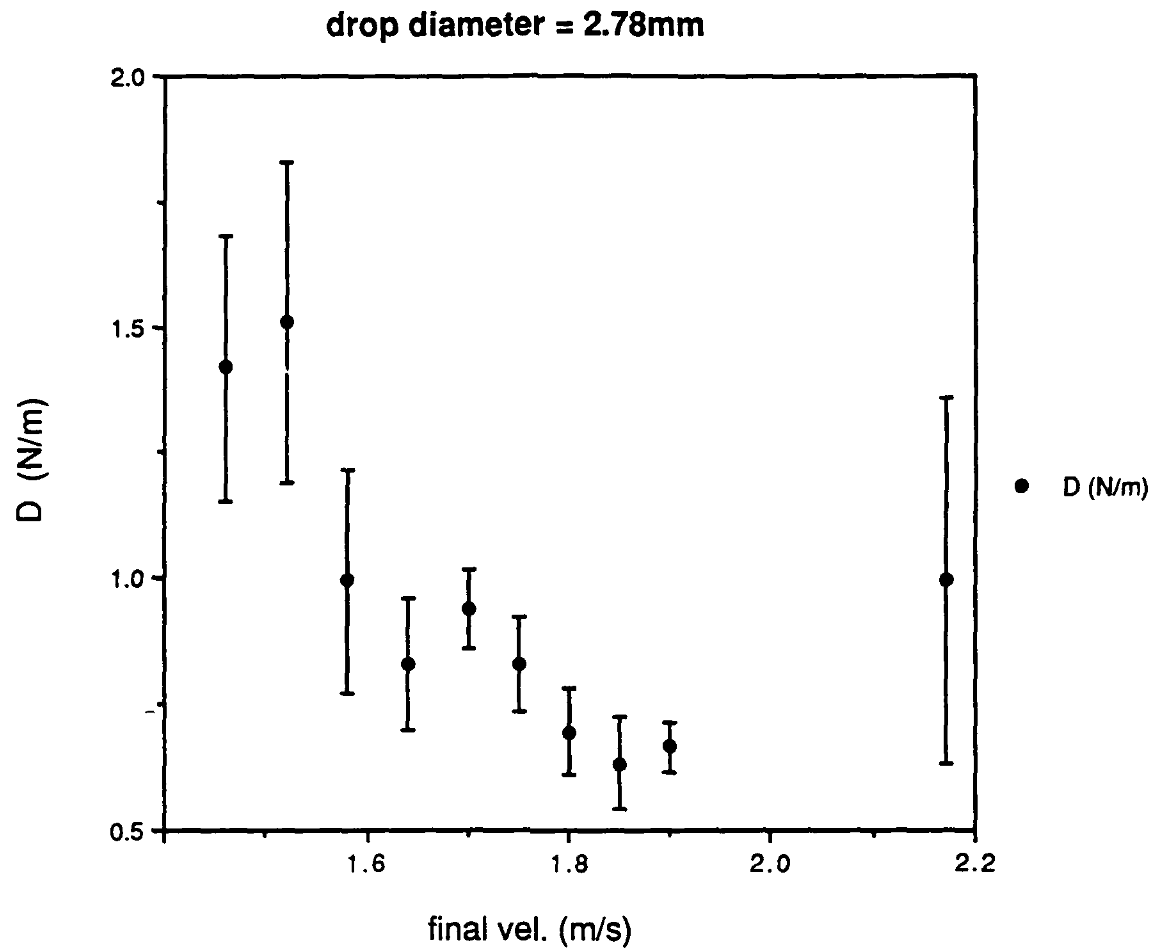
drop diameter = 2.78mm
2.0
1.5
1.0
0.5
D (N/m)
1.6
1.8
2.0
2.2
final vel. (m/s)
D (N/m)

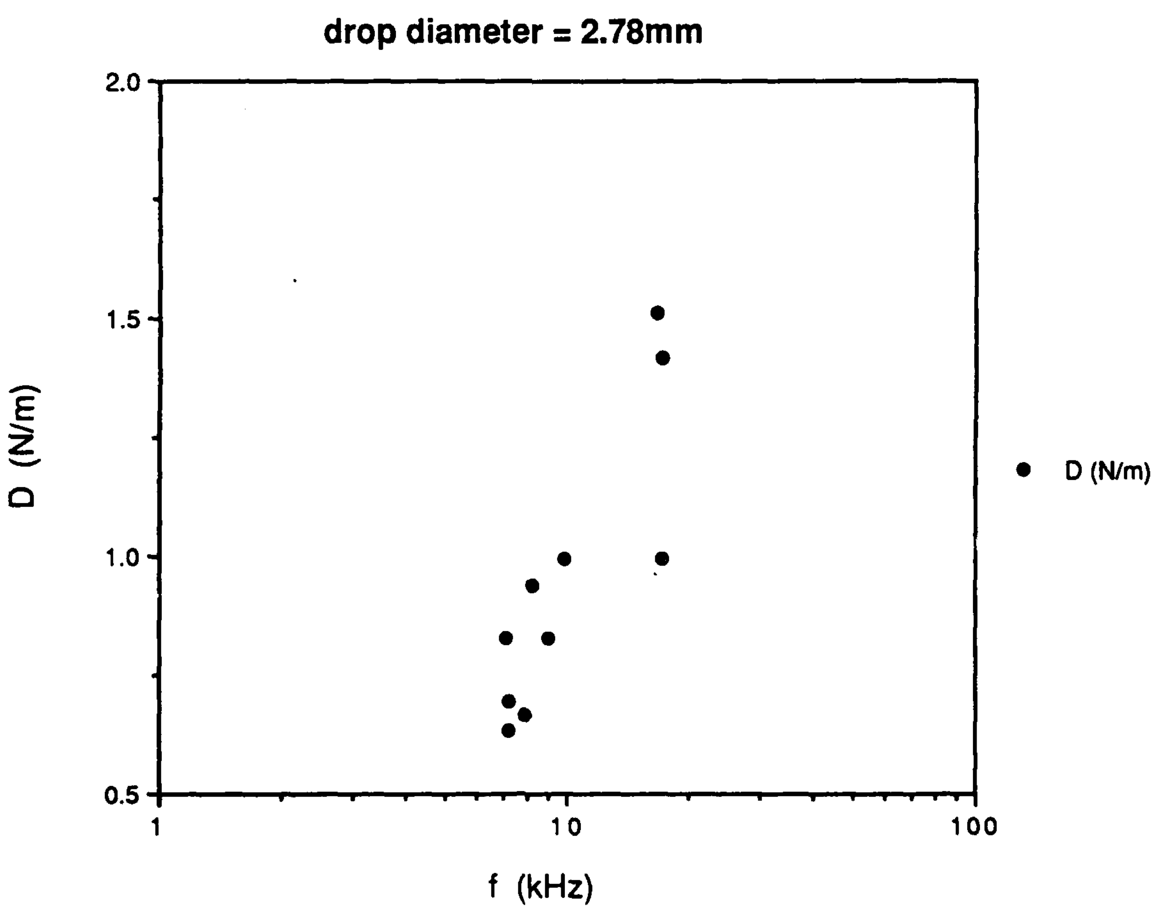
drop diameter = 2.78mm
2.0
1.5
1.0
0.5
D (N/m)
1
10
100
f (kHz)
D (N/m)

	final vel.	f (kHz)	sd of f	Bubble rad/mm	sd of rad
1	1.620	7.233	0.338	0.453	0.021
2	1.740	7.968	0.939	0.412	0.049
3	1.470	8.817	2.520	0.372	0.106
4	1.860	12.950	5.727	0.253	0.112
5	1.470	18.217	9.365	0.180	0.093
6	1.390	8.248	2.943	0.398	0.142
7	1.520	6.611	0.685	0.496	0.051
8	1.640	7.174	0.352	0.457	0.022
9	1.800	7.610	0.322	0.431	0.018
10	1.850	8.228	0.940	0.399	0.046

NOTE TO THE USE OF D=2.86mm

Not all of the data points represent the average of N = 30 measured frequencies. For the two impact velocities = 1.47 m/s, N = 20 and 84. For impact velocity = 1.85 m/s, N = 20.

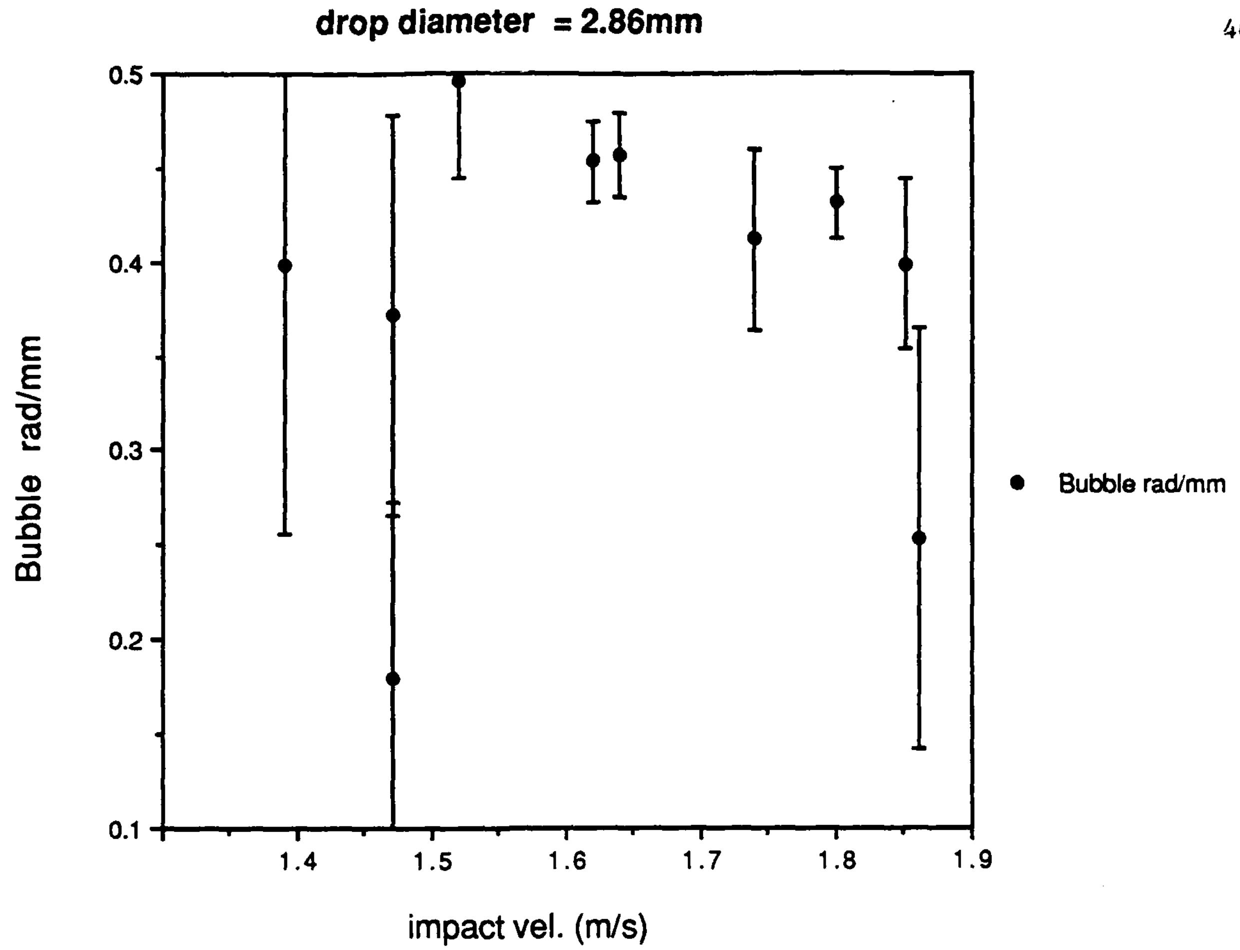
drop diameter = 2.86mm
Bubble rad/mm
0.5
0.4
0.3
0.2
0.1
1.4
1.5
1.6
1.7
1.8
1.9
impact vel. (m/s)
Bubble rad/mm

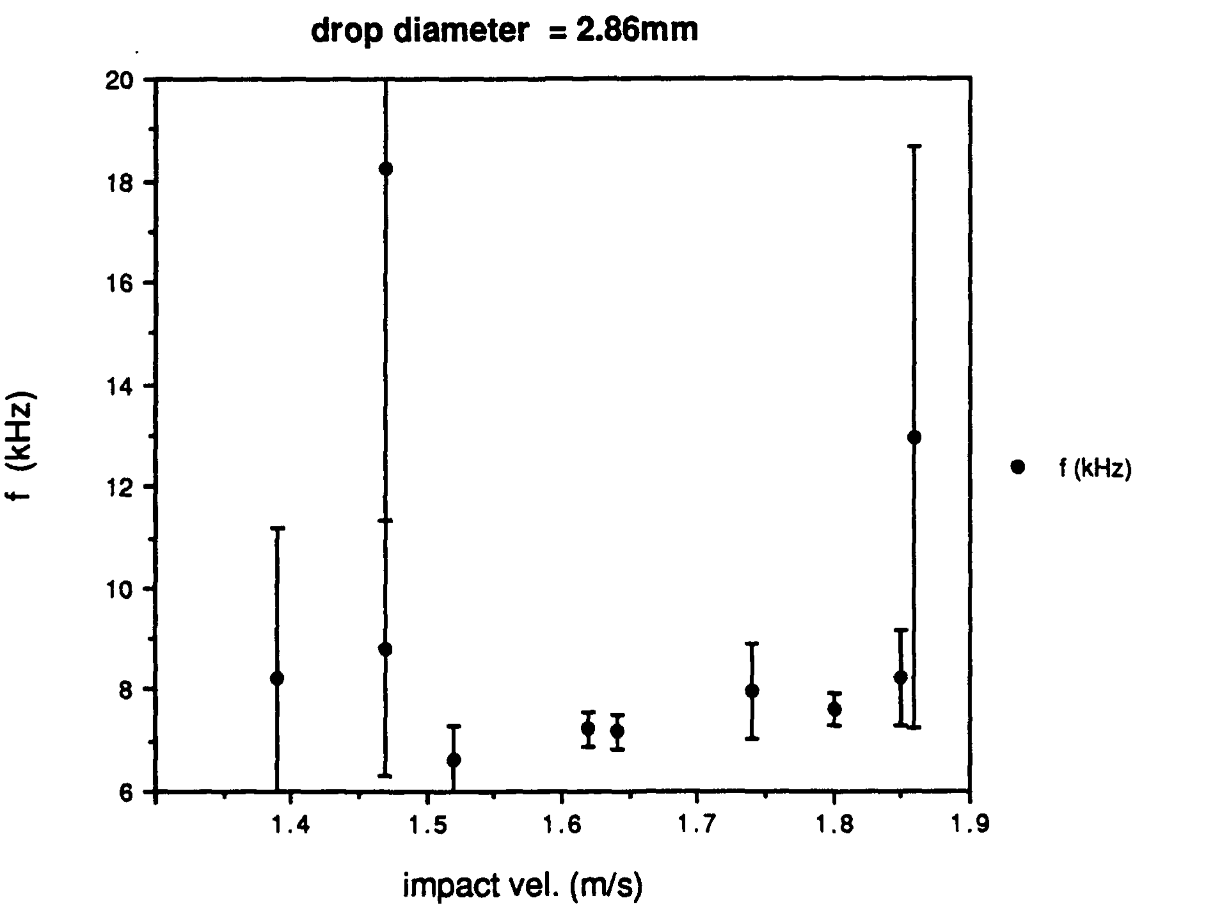
drop diameter = 2.86mm
f (kHz)
20
18
16
14
12
10
8
6
1.4
1.5
1.6
1.7
1.8
1.9
impact vel. (m/s)
f (kHz)

drop diameter = 3.07mm Thu, Jul 20, 1989 1:02 PM

	impact vel.	f (kHz)	sd of f	D (N/m)	sd of D	Bubble rad/mm	sd of rad
1	1.390	11.422	2.271	1.060	0.215	0.287	0.057
2	1.451	8.212	1.883	0.855	0.190	0.399	0.092
3	1.521	7.214	0.422	0.785	0.045	0.455	0.027
4	1.582	6.993	0.620	0.710	0.065	0.469	0.042
5	1.640	6.527	0.420	0.565	0.055	0.503	0.032
6	1.697	7.467	1.425	0.630	0.025	0.439	0.084
7	1.751	7.408	0.233	0.625	0.030	0.443	0.014
8	1.803	8.157	0.484	0.625	0.050	0.402	0.024
9	1.854	9.810	2.311	0.905	0.225	0.334	0.079
10	1.904	13.567	7.235	0.745	0.205	0.242	0.129
11	1.952	16.416	6.594	1.140	0.275	0.200	0.135

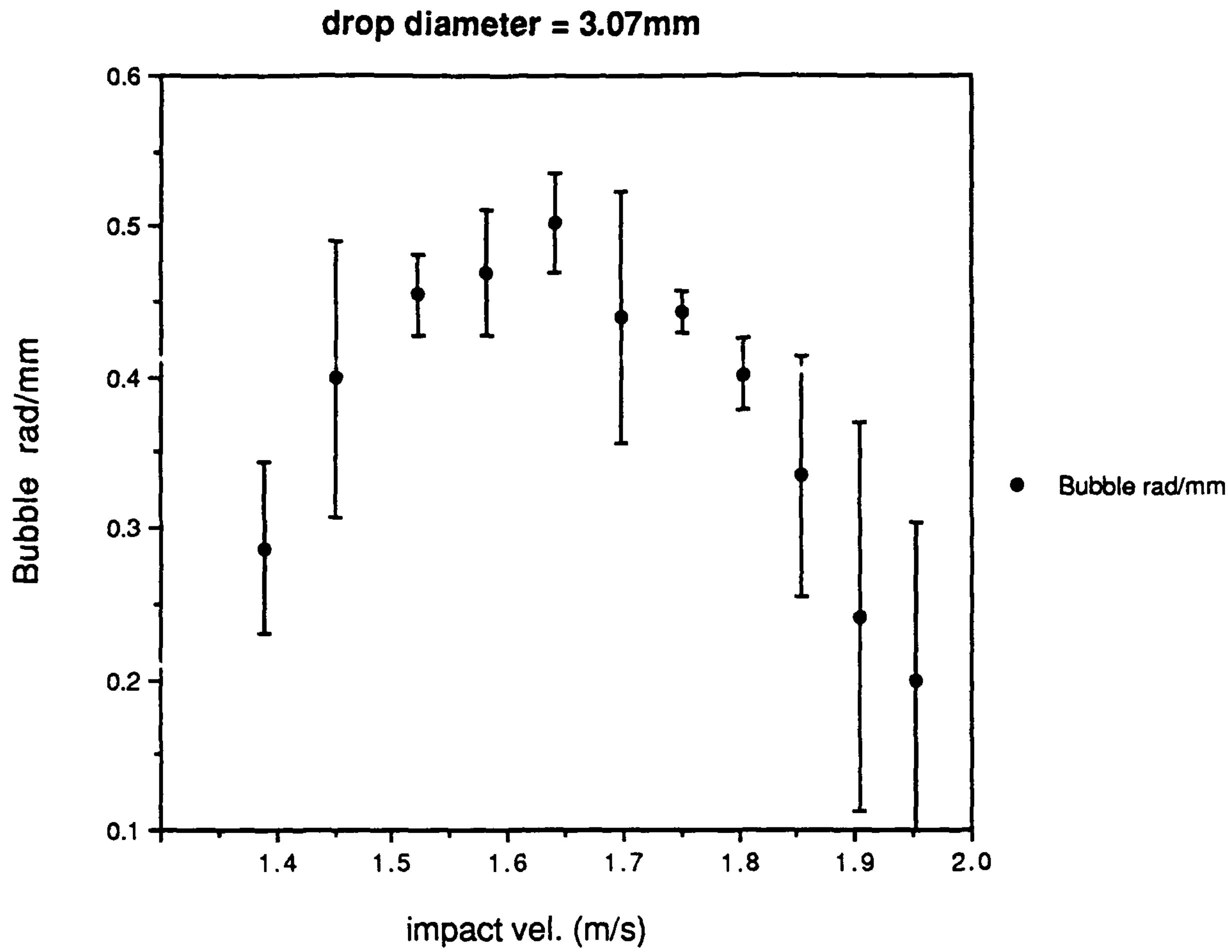
drop diameter = 3.07mm
Bubble rad/mm
0.6
0.5
0.4
0.3
0.2
0.1
1.4
1.5
1.6
1.7
1.8
1.9
2.0
impact vel. (m/s)
Bubble rad/mm

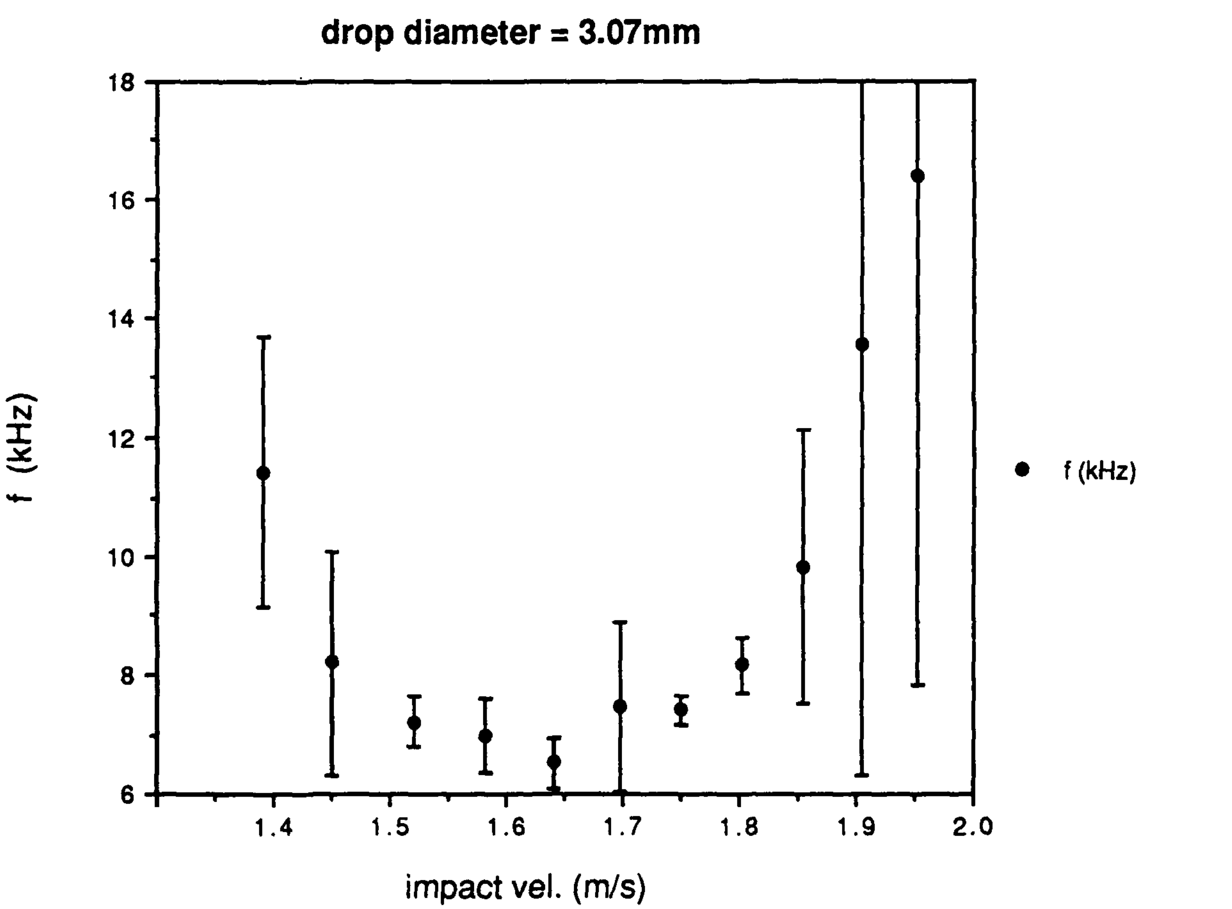
drop diameter = 3.07mm
f (kHz)
18
16
14
12
10
8
6
1.4
1.5
1.6
1.7
1.8
1.9
2.0
impact vel. (m/s)
f (kHz)

drop diameter = 3.07mm

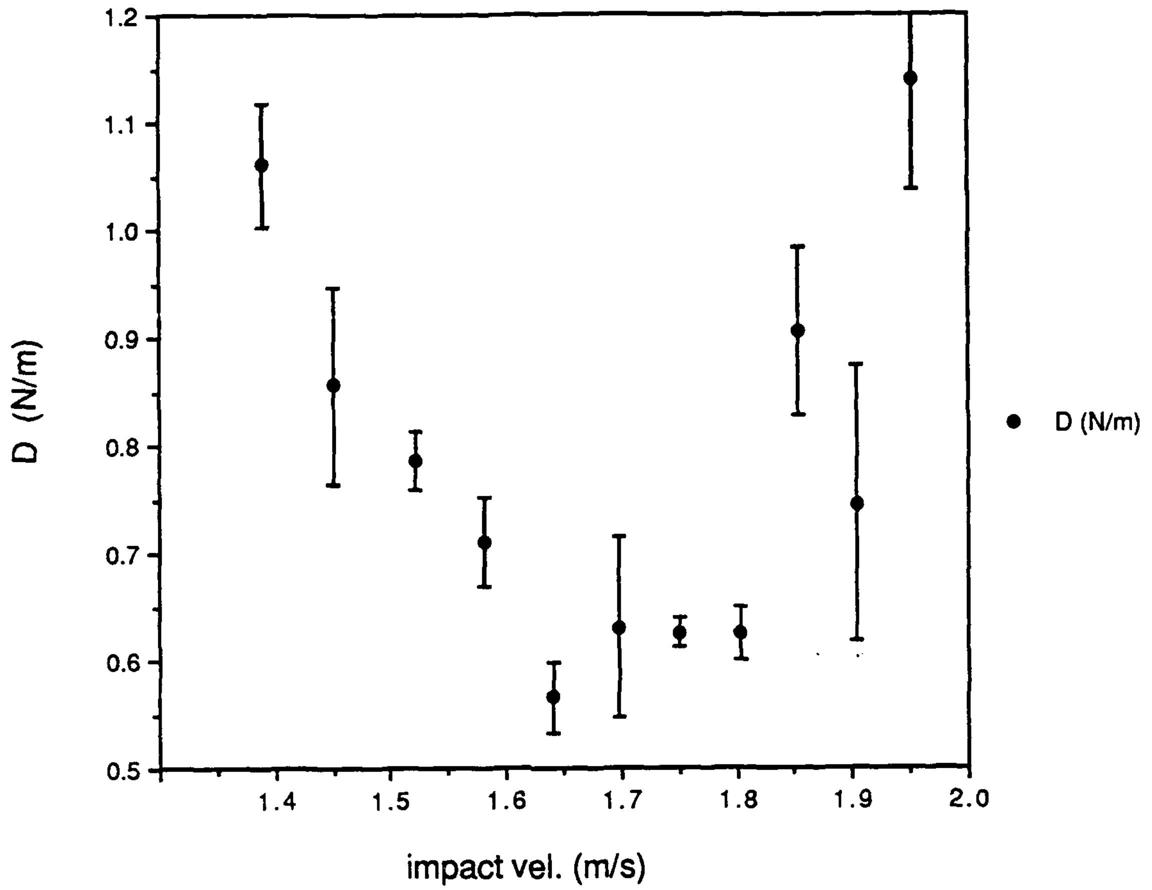

drop diameter = 3.07mm

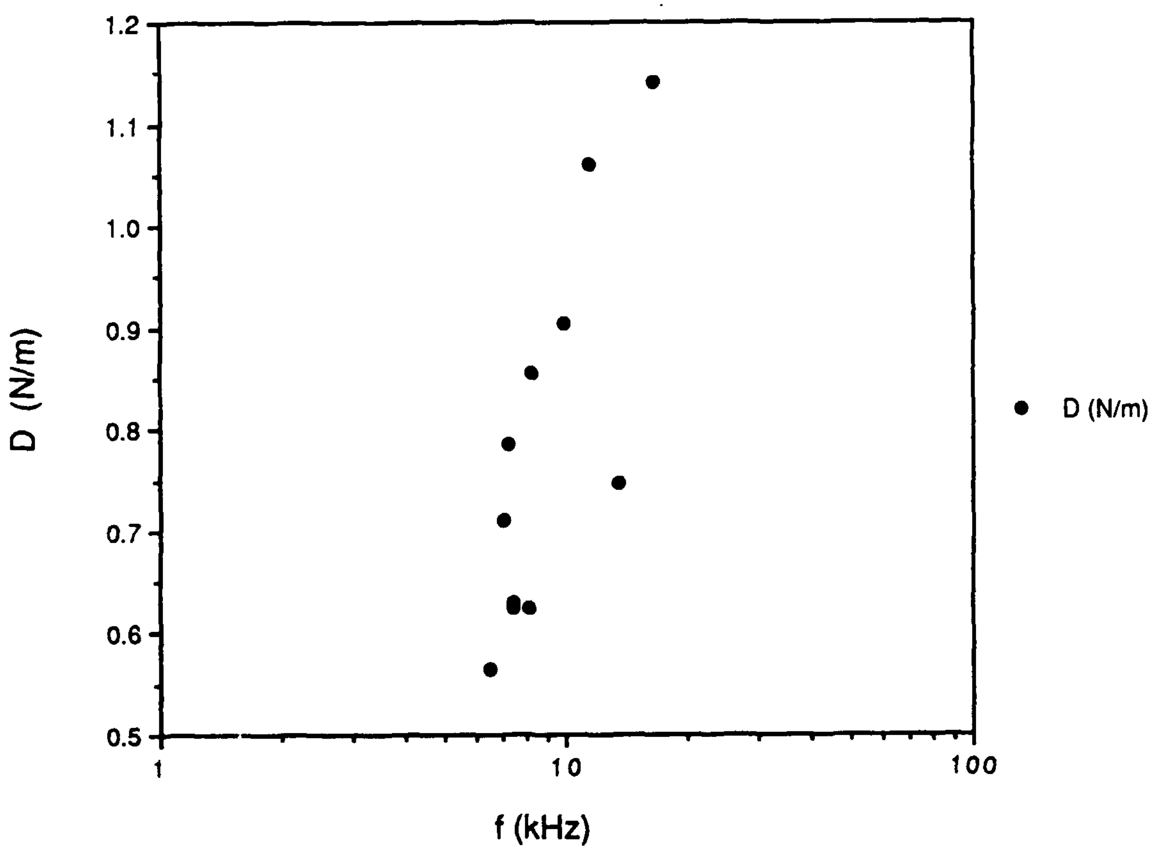

drop diameter = 3.34mm Thu, Jul 20, 1989 1:38 PM

	impact vel.	f (kHz)	sd of f	D (N/m)	sd of D	Bubble rad/mm	sd of rad
1	1.246	21.170	5.790	1.185	0.230	0.155	0.042
2	1.321	10.536	1.551	0.715	0.045	0.311	0.046
3	1.391	7.186	0.357	0.710	0.030	0.456	0.023
4	1.458	7.938	0.630	0.825	0.065	0.413	0.033
5	1.522	7.985	0.311	0.820	0.035	0.411	0.016
6	1.583	12.064	3.968	0.975	0.135	0.272	0.089
7	1.641	9.687	0.427	0.880	0.045	0.339	0.015
8	1.698	17.586	6.049	0.512	0.145	0.187	0.064

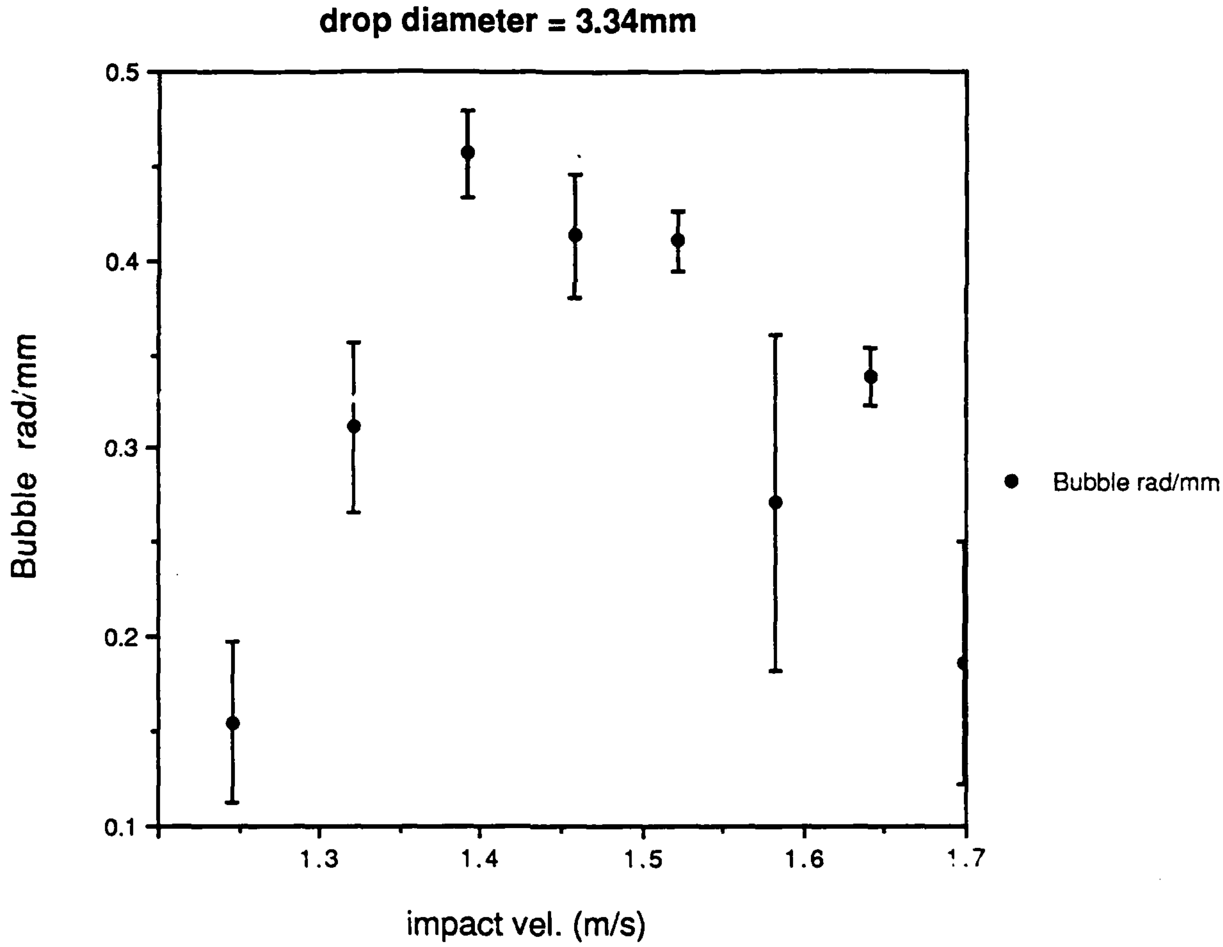

drop diameter = 3.34mm
Bubble rad/mm
0.5
0.4
0.3
0.2
0.1
1.3
1.4
1.5
1.6
1.7
impact vel. (m/s)
Bubble rad/mm

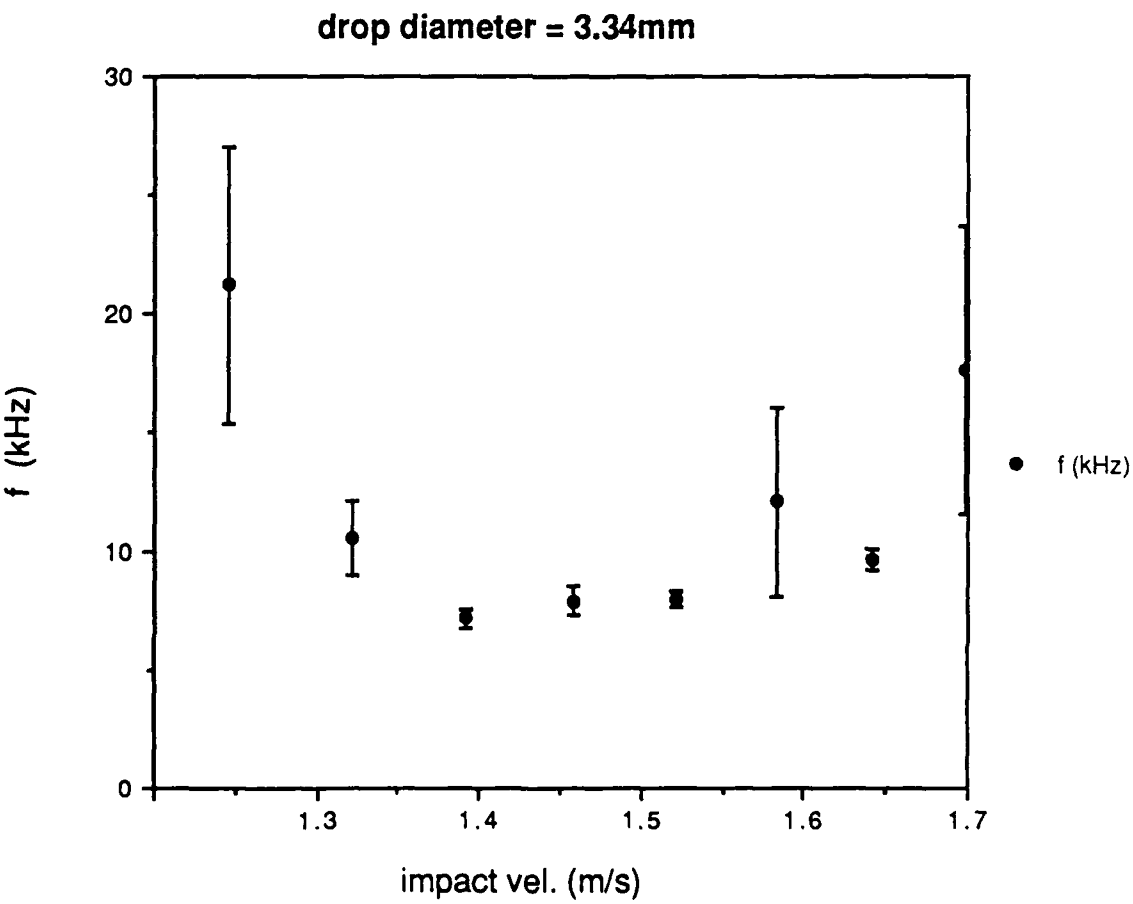

drop diameter = 3.34mm
f (kHz)
30
20
10
0
1.3
1.4
1.5
1.6
1.7
impact vel. (m/s)
f (kHz)

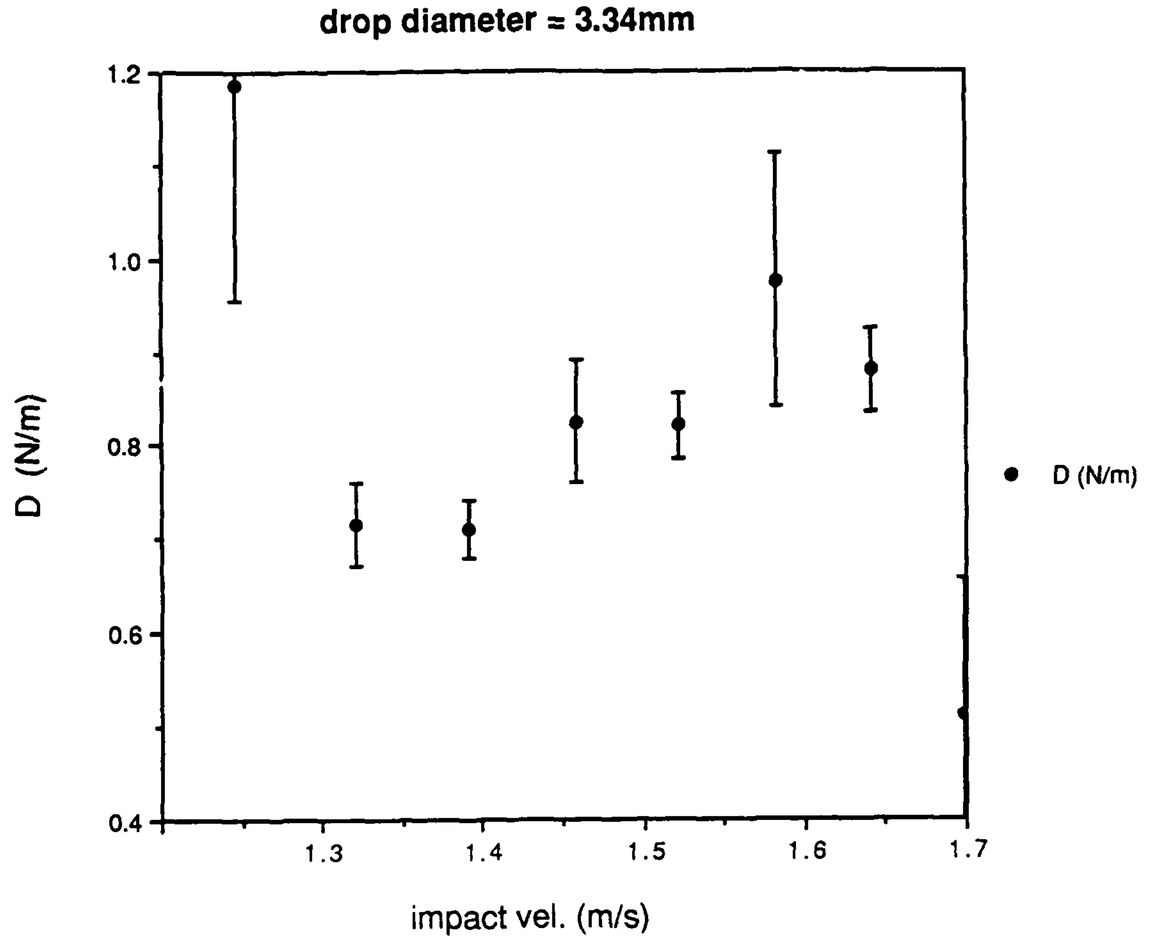
drop diameter = 3.34mm
D (N/m)
1.2
1.0
0.8
0.6
0.4
1.3
1.4
1.5
1.6
1.7
impact vel. (m/s)
D (N/m)

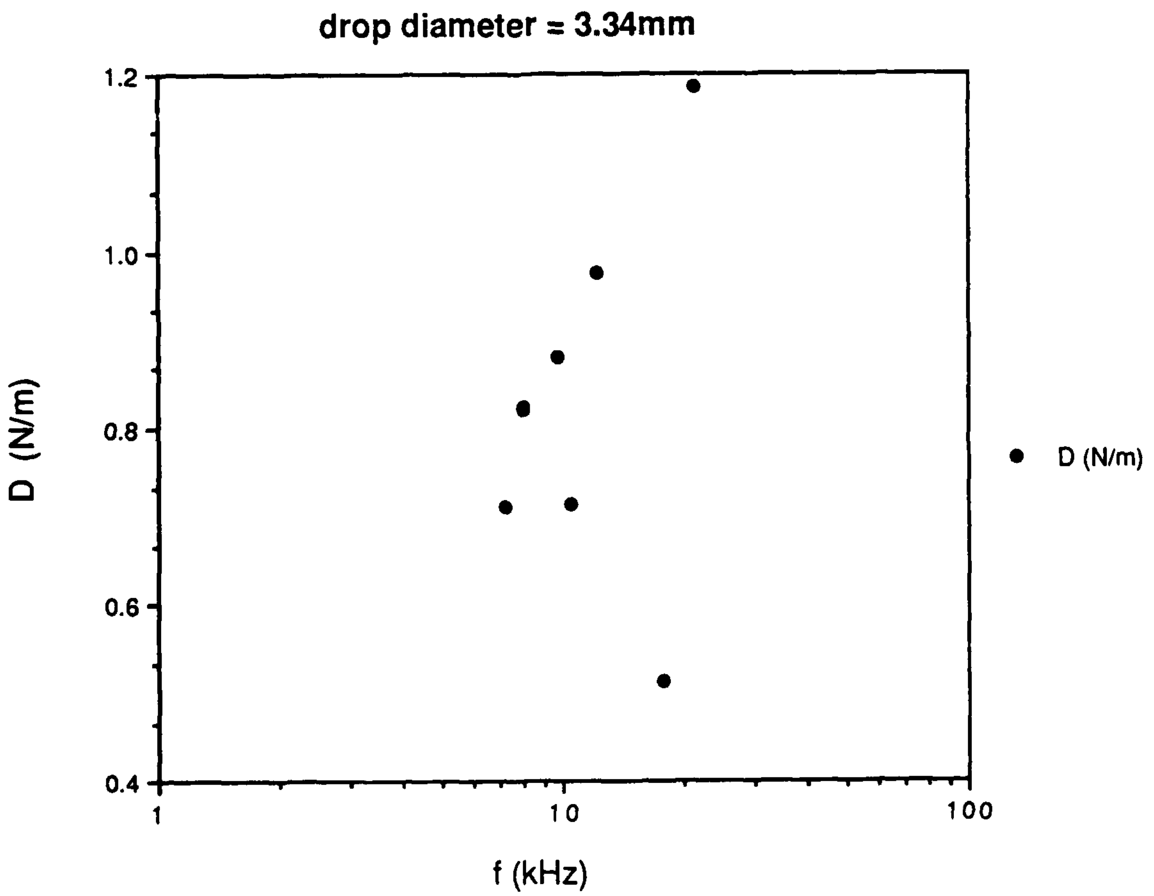
drop diameter = 3.34mm
D (N/m)
1.2
1.0
0.8
0.6
0.4
1
10
100
f (kHz)
D (N/m)

drop diameter = 3.73mm Thu, Jul 20, 1989 1:48 PM

	impact vel.	f (kHz)	sd of f	D (N/m)	sd of D	Bubble rad/mm	sd of rad
1	1.207	9.050	4.809	0.797	0.305	0.362	0.193
2	1.289	6.957	1.017	0.725	0.065	0.471	0.069
3	1.391	6.377	0.767	0.657	0.110	0.514	0.062
4	1.459	6.661	0.247	0.672	0.025	0.492	0.018
5	1.522	7.124	0.244	0.735	0.062	0.460	0.016
6	1.583	13.785	11.822	0.892	0.195	0.238	0.204
7	1.642	15.768	8.605	1.440	0.517	0.208	0.114

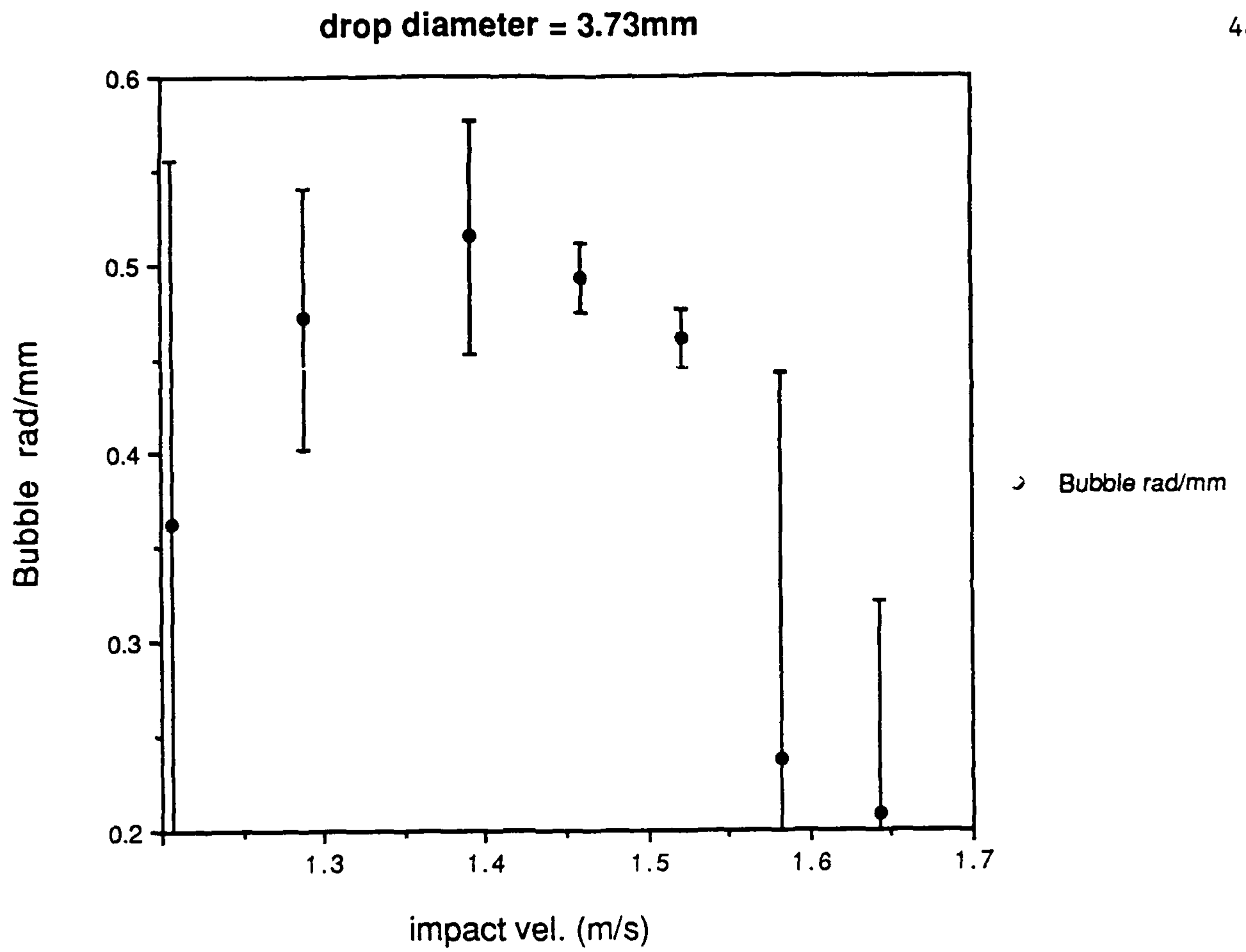
drop diameter = 3.73mm
Bubble rad/mm
0.6
0.5
0.4
0.3
0.2
1.3
1.4
1.5
1.6
1.7
impact vel. (m/s)
Bubble rad/mm

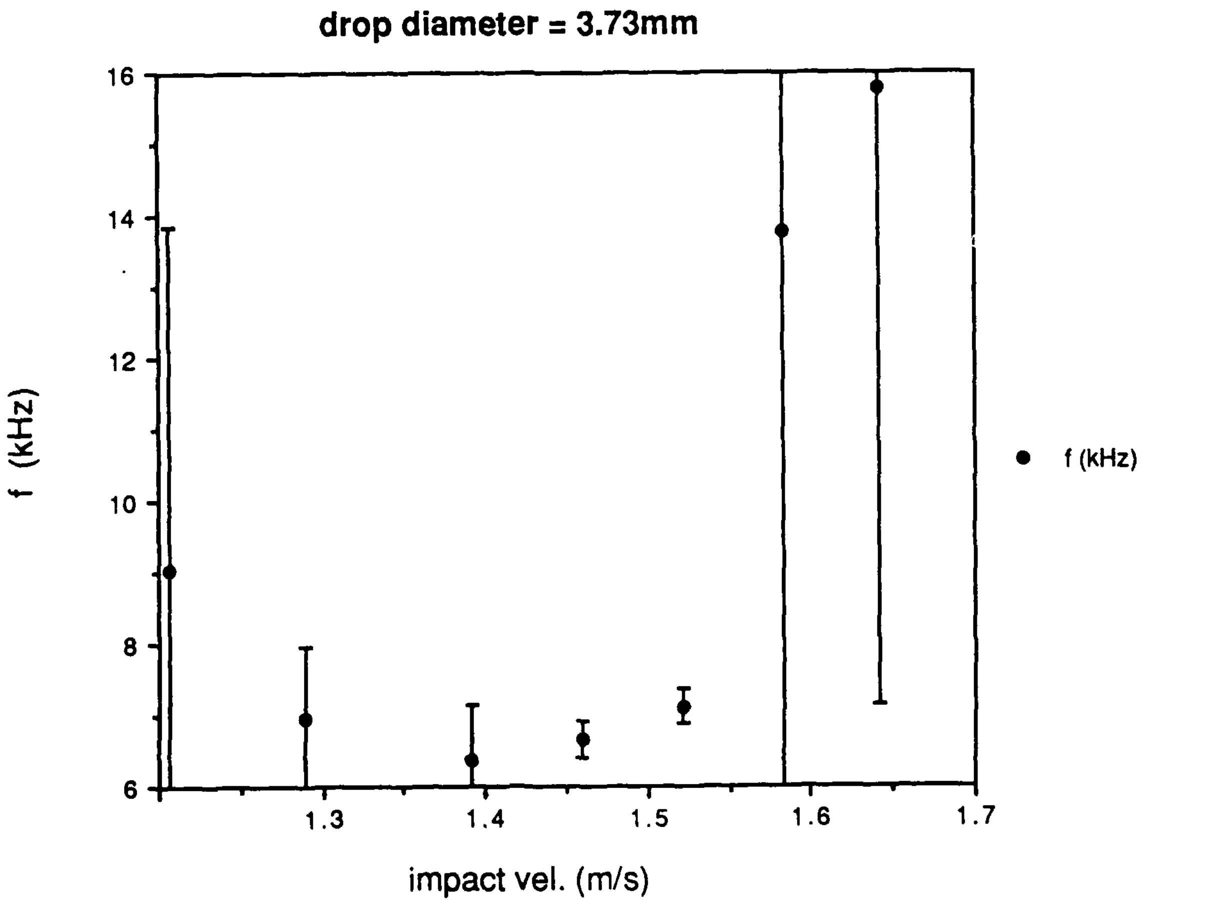
drop diameter = 3.73mm
f (kHz)
16
14
12
10
8
6
1.3
1.4
1.5
1.6
1.7
impact vel. (m/s)
f (kHz)

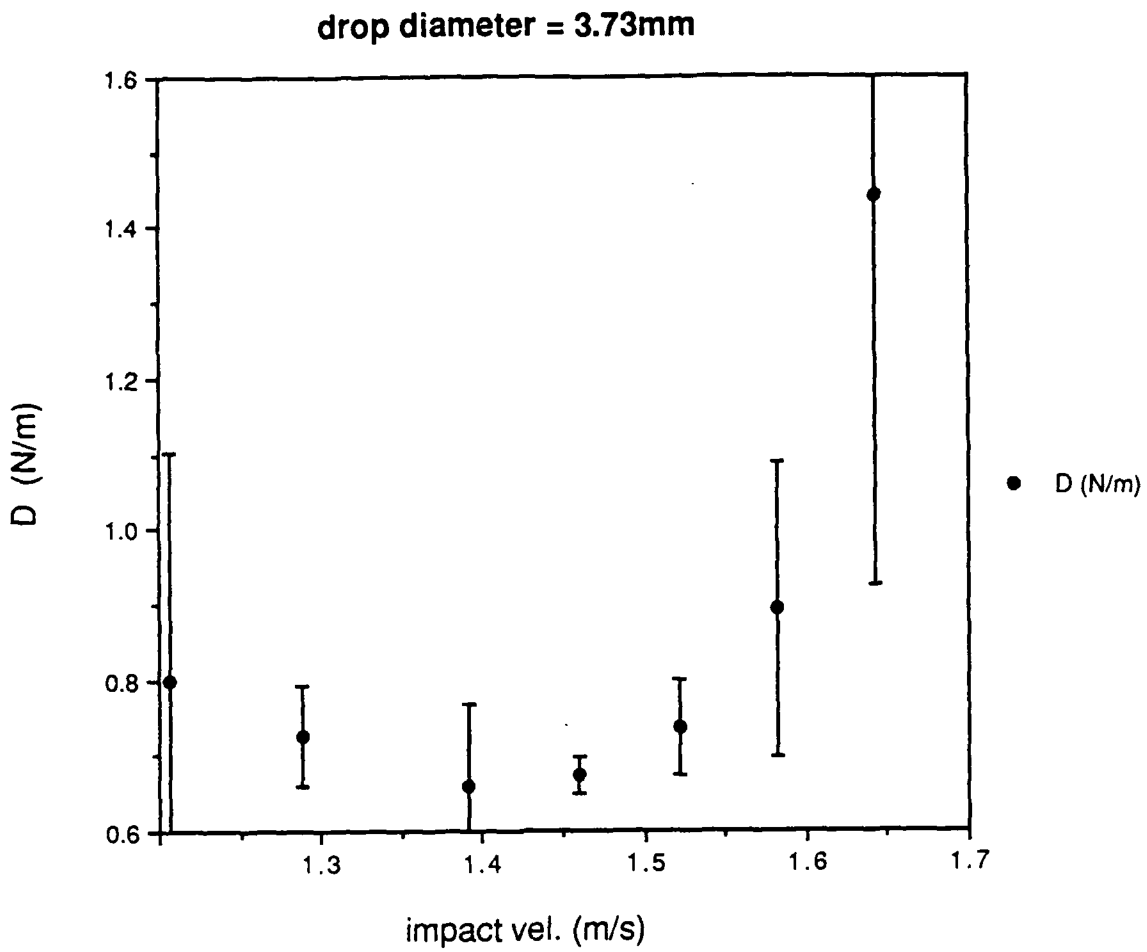
drop diameter = 3.73mm
D (N/m)
impact vel. (m/s)
1.6
1.4
1.2
1.0
0.8
0.6
1.3
1.4
1.5
1.6
1.7
D (N/m)

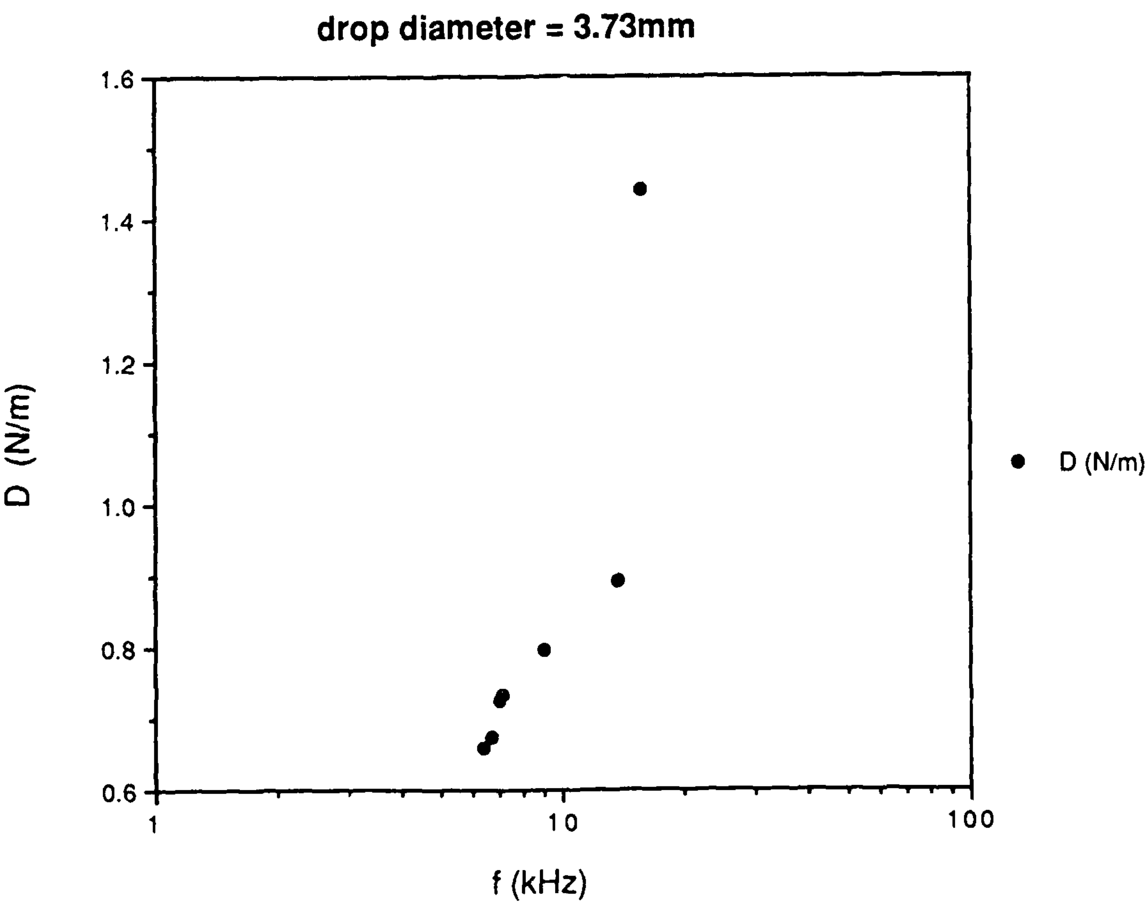
drop diameter = 3.73mm
D (N/m)
f (kHz)
1.6
1.4
1.2
1.0
0.8
0.6
1
10
100
D (N/m)

drop diameter = 3.99mm Thu, Jul 20, 1989 2:04 PM

	impact vel.	f (kHz)	sd of f	D (N/m)	sd of D	Bubble rad/mm	sd of rad
1	1.247	6.265	2.088	0.525	0.070	0.524	0.084
2	1.321	6.761	0.452	0.825	0.080	0.485	0.072
3	1.392	6.842	0.488	0.835	0.110	0.479	0.070
4	1.285	8.240	0.448	0.906	0.510	0.398	0.048
5	1.357	6.085	0.137	0.815	0.025	0.539	0.089
6	1.426	6.749	0.494	0.815	0.055	0.486	0.072
7	1.459	9.331	3.556	0.448	0.150	0.352	0.038

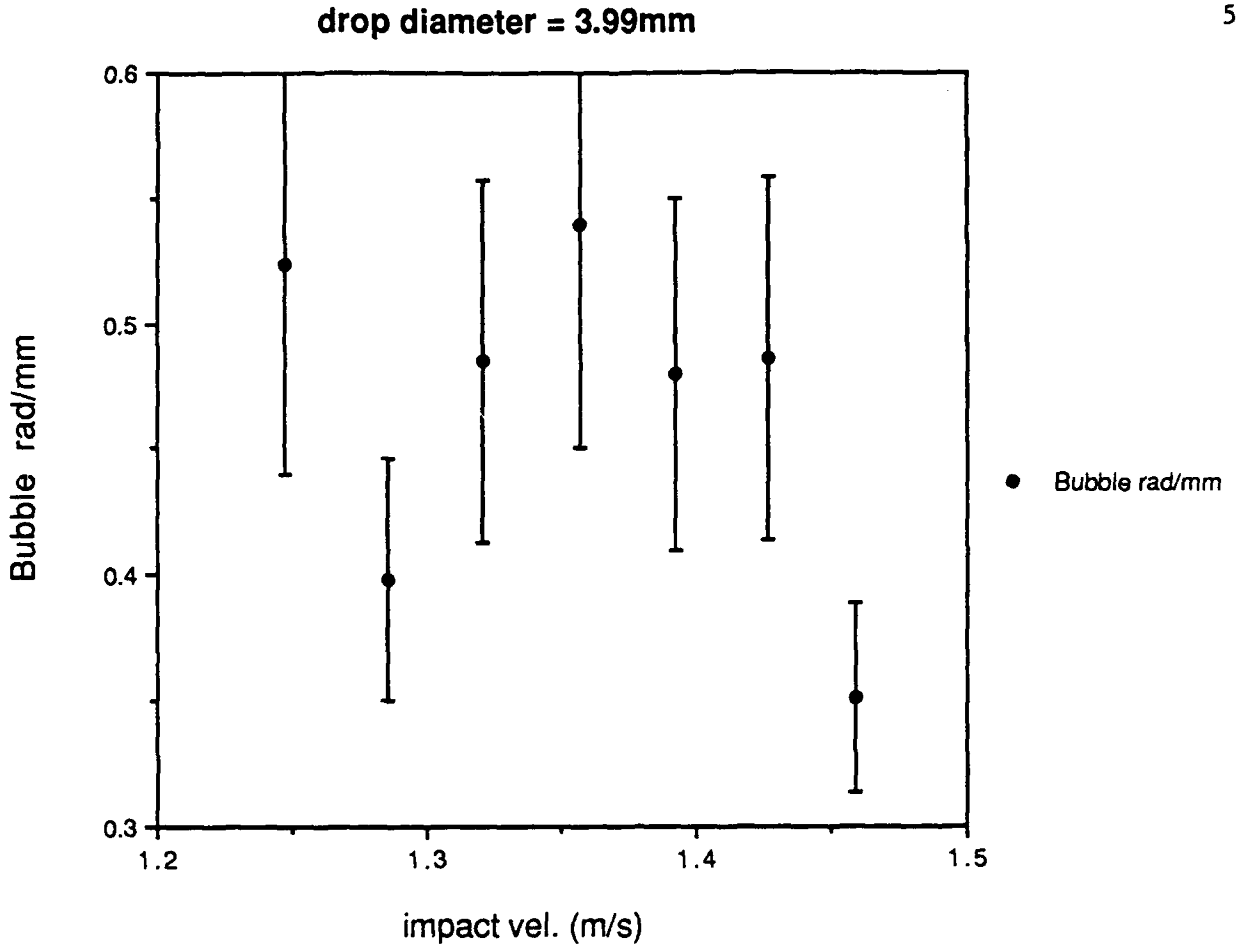
drop diameter = 3.99mm
Bubble rad/mm
0.6
0.5
0.4
0.3
1.2
1.3
1.4
1.5
impact vel. (m/s)
Bubble rad/mm

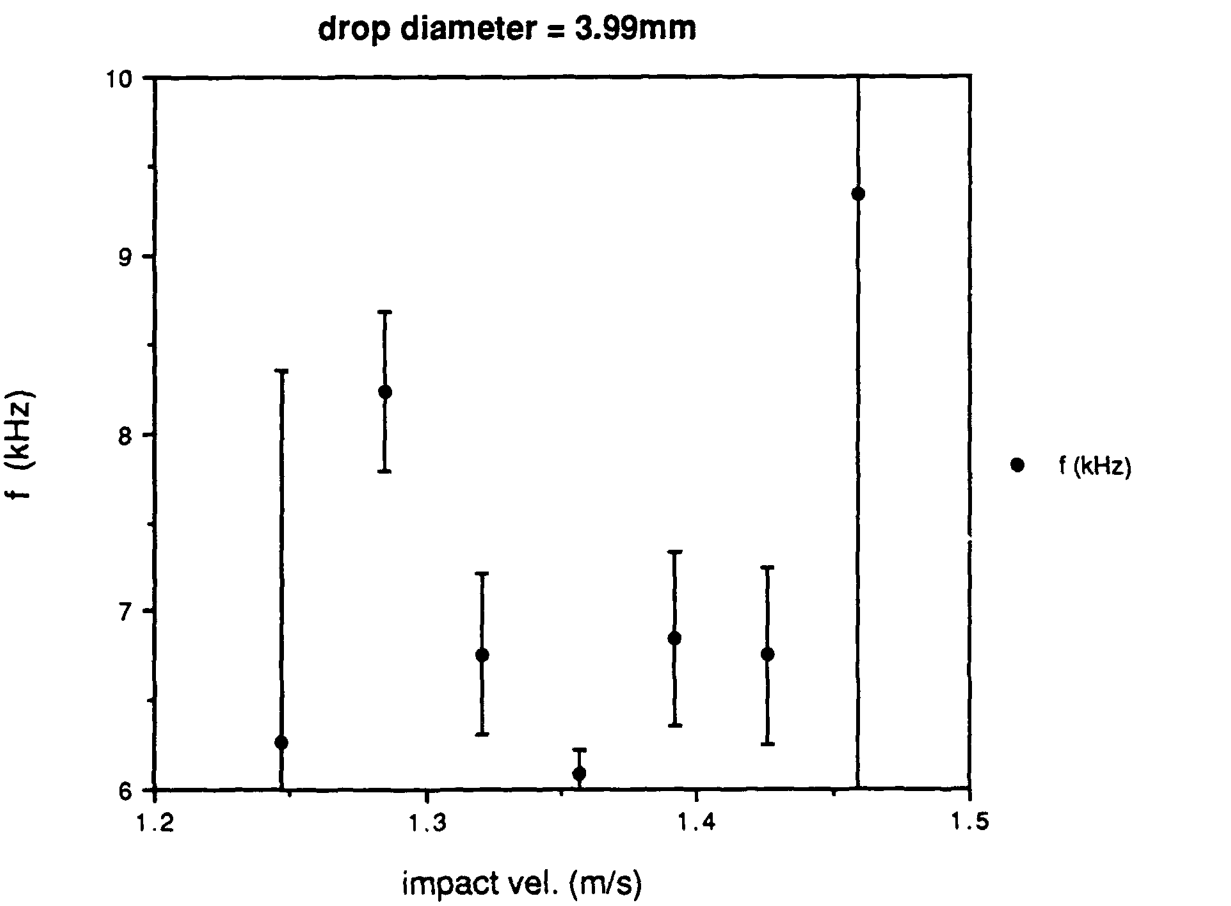
drop diameter = 3.99mm
f (kHz)
10
9
8
7
6
1.2
1.3
1.4
1.5
impact vel. (m/s)
f (kHz)

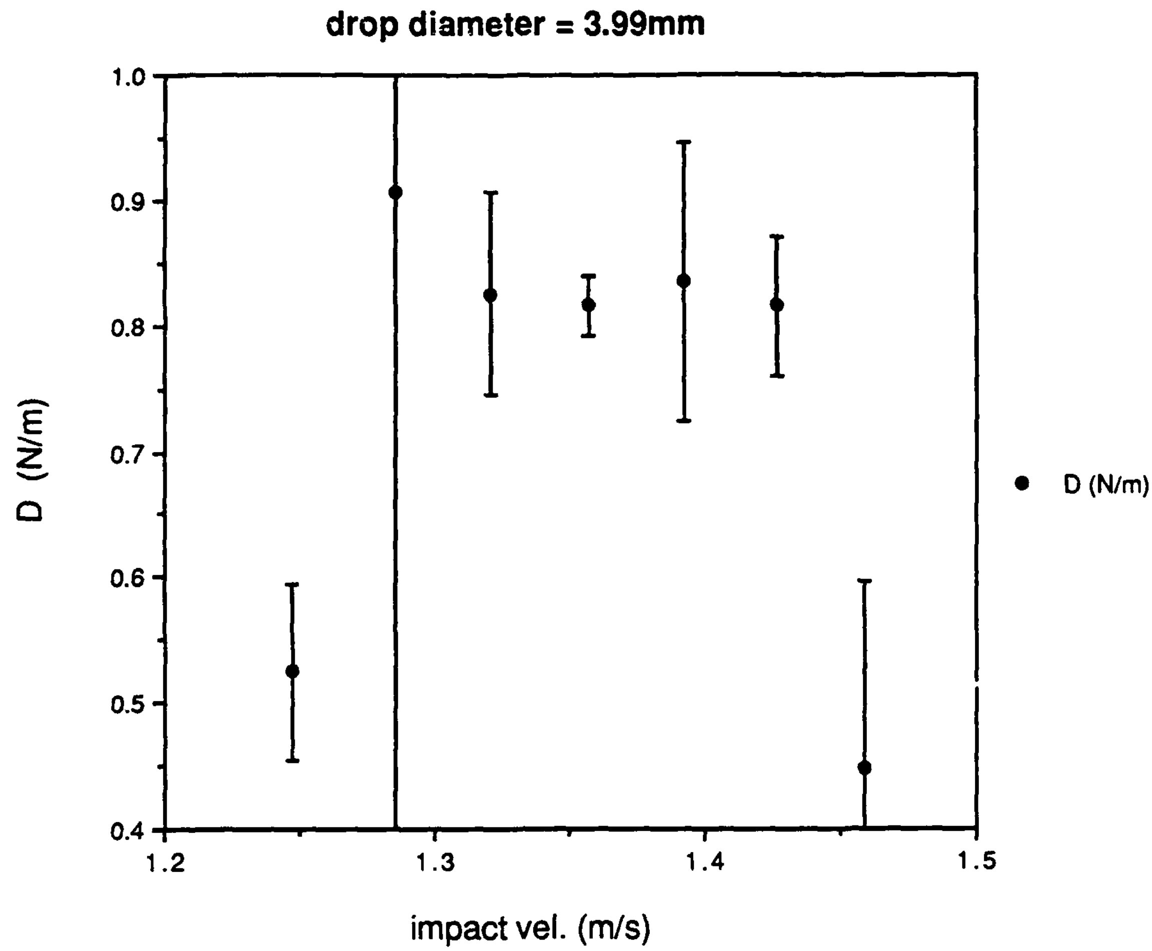
drop diameter = 3.99mm
1.0
0.9
0.8
0.7
0.6
0.5
0.4
D (N/m)
1.2
1.3
1.4
1.5
impact vel. (m/s)
D (N/m)

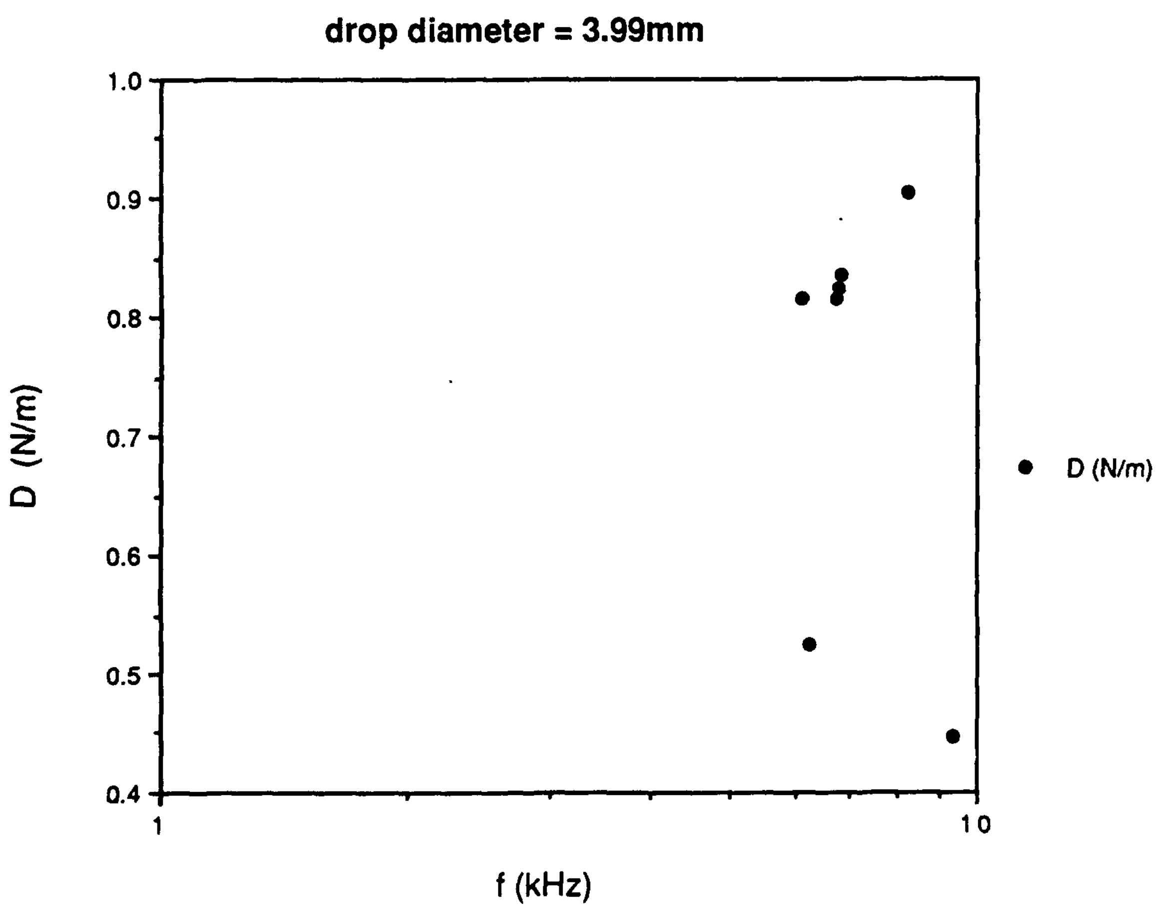
drop diameter = 3.99mm
1.0
0.9
0.8
0.7
0.6
0.5
0.4
D (N/m)
1
10
f (kHz)
D (N/m)

	impact vel.	f (kHz)	sd of f	D (N/m)	sd of D	Bubble rad/mm	sd of rad
1	1.035	12.377	10.077	0.963	0.352	0.265	0.216
2	1.124	8.488	2.826	0.845	0.362	0.386	0.129
3	0.987	10.790	3.400	0.922	0.295	0.304	0.096
4	1.167	8.082	2.680	0.479	0.080	0.406	0.135
5	1.081	8.132	1.576	0.805	0.165	0.403	0.078
6	1.208	21.017	18.564	0.825	0.198	0.156	0.138

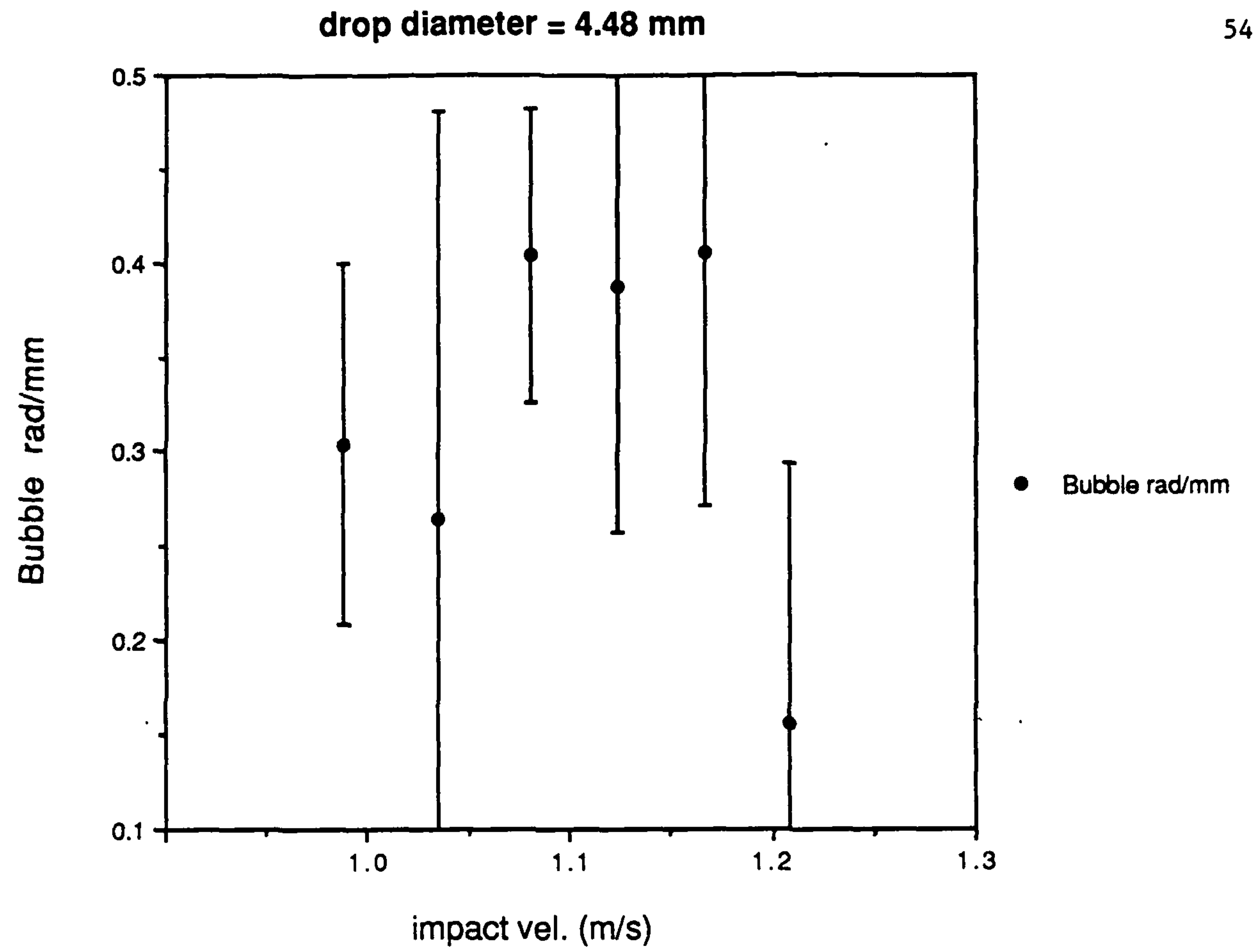
drop diameter = 4.48 mm
Bubble rad/mm
0.5
0.4
0.3
0.2
0.1
1.0
1.1
1.2
1.3
impact vel. (m/s)
Bubble rad/mm

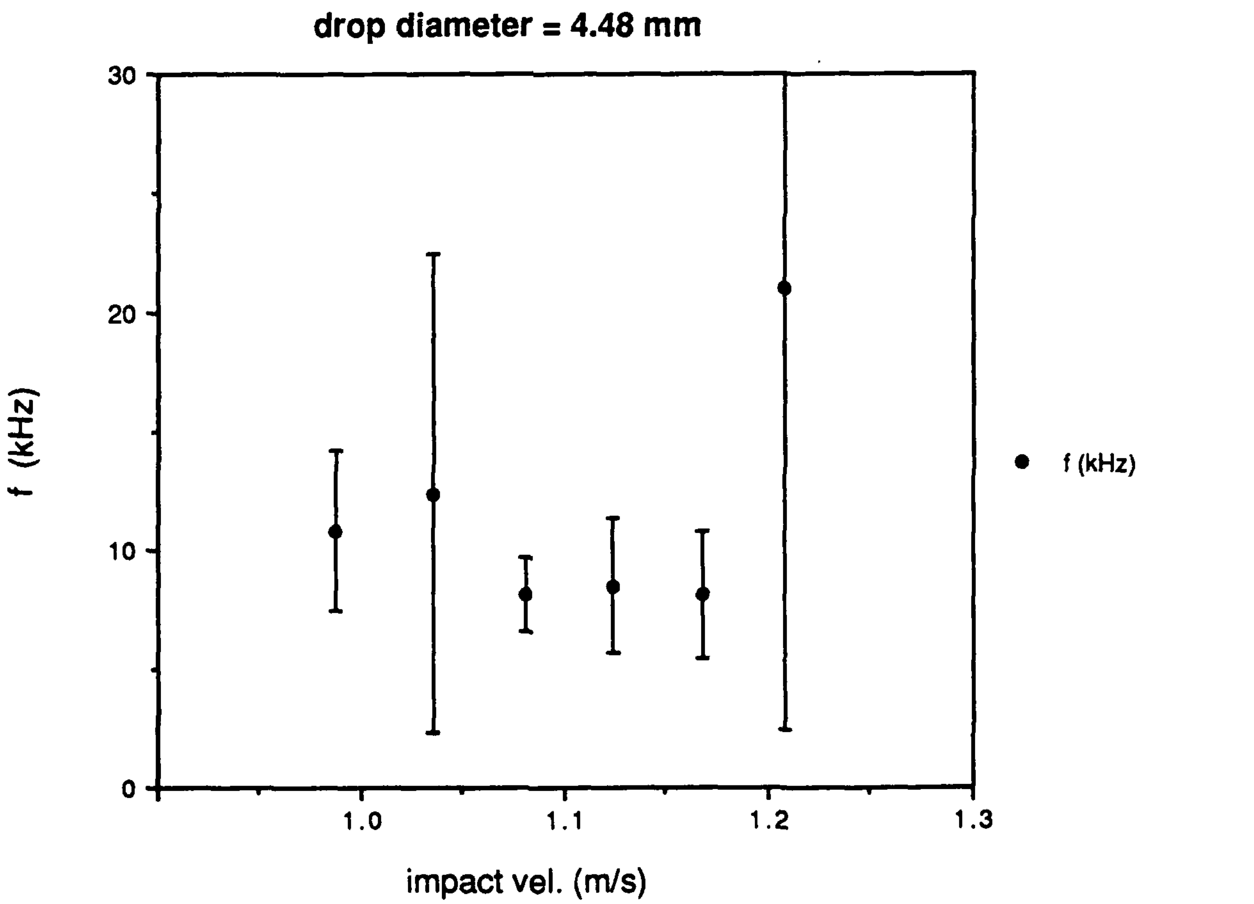
drop diameter = 4.48 mm
f (kHz)
30
20
10
0
1.0
1.1
1.2
1.3
impact vel. (m/s)
f (kHz)

drop diameter = 4.48 mm

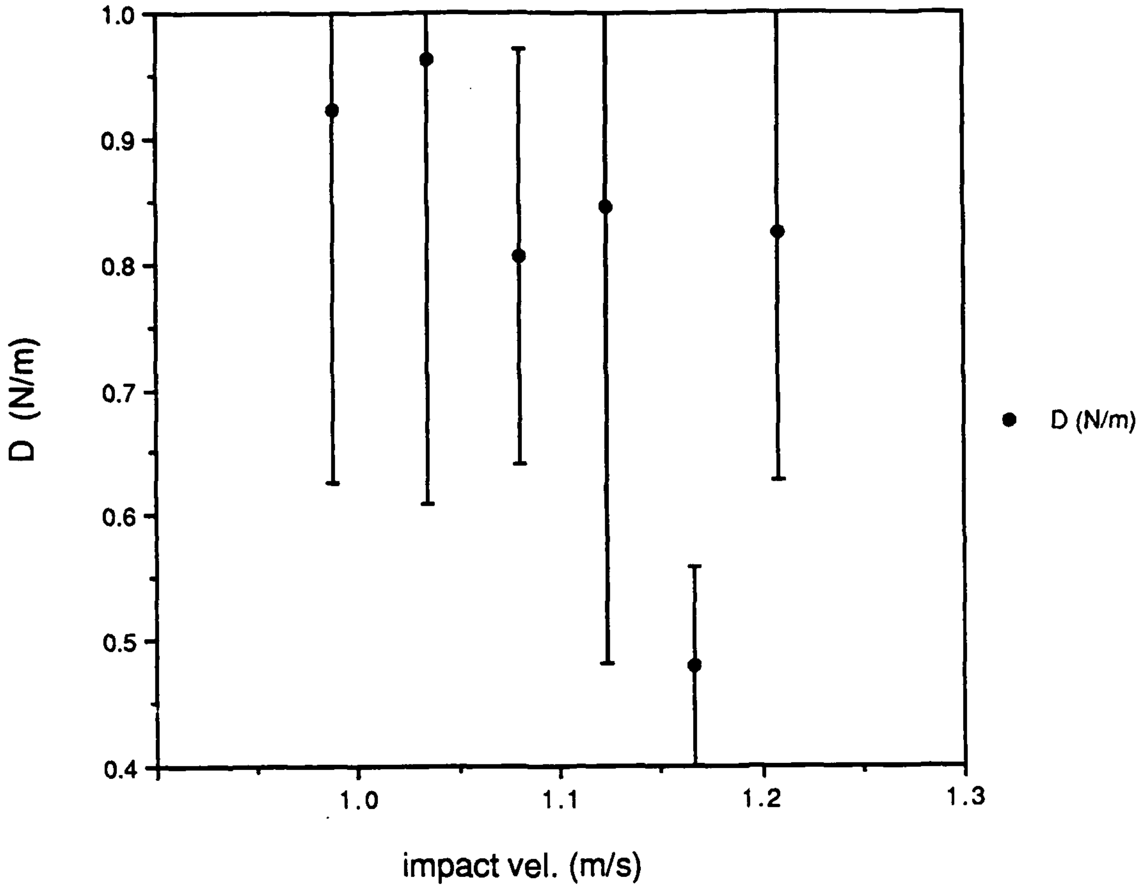

drop diameter = 4.48 mm

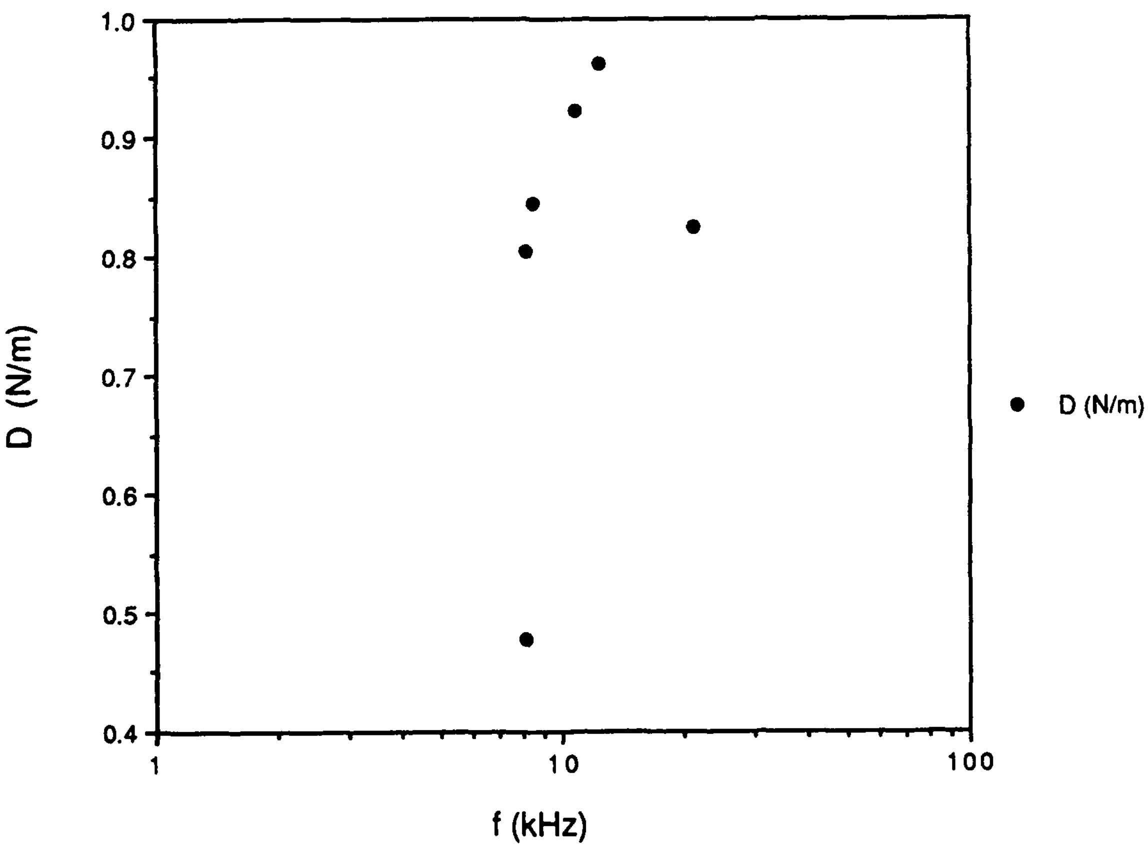

drop diameter = 4.58mm Thu, Jul 20, 1989 2:44 PM

	impact vel.	f (kHz)	sd of f	D (N/m)	sd of D	Bubble rad/mm	sd of rad
1	1.125	7.456	1.788	0.825	0.175	0.440	0.105
2	1.167	7.650	1.864	0.915	0.155	0.429	0.104
3	1.146	6.700	1.128	0.825	0.140	0.490	0.082
4	1.187	7.415	1.759	0.790	0.075	0.442	0.105

drop diameter = 4.58mm

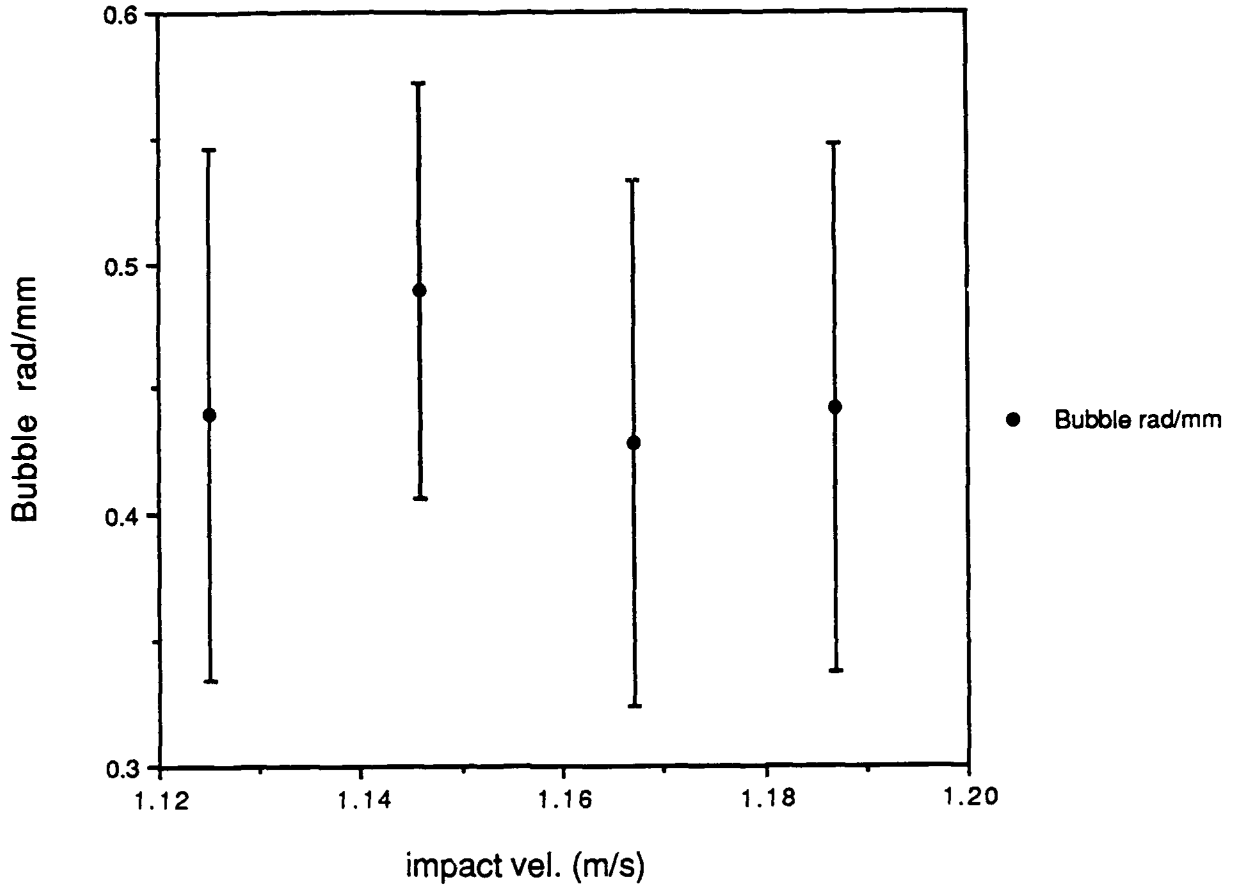

drop diameter = 4.58mm

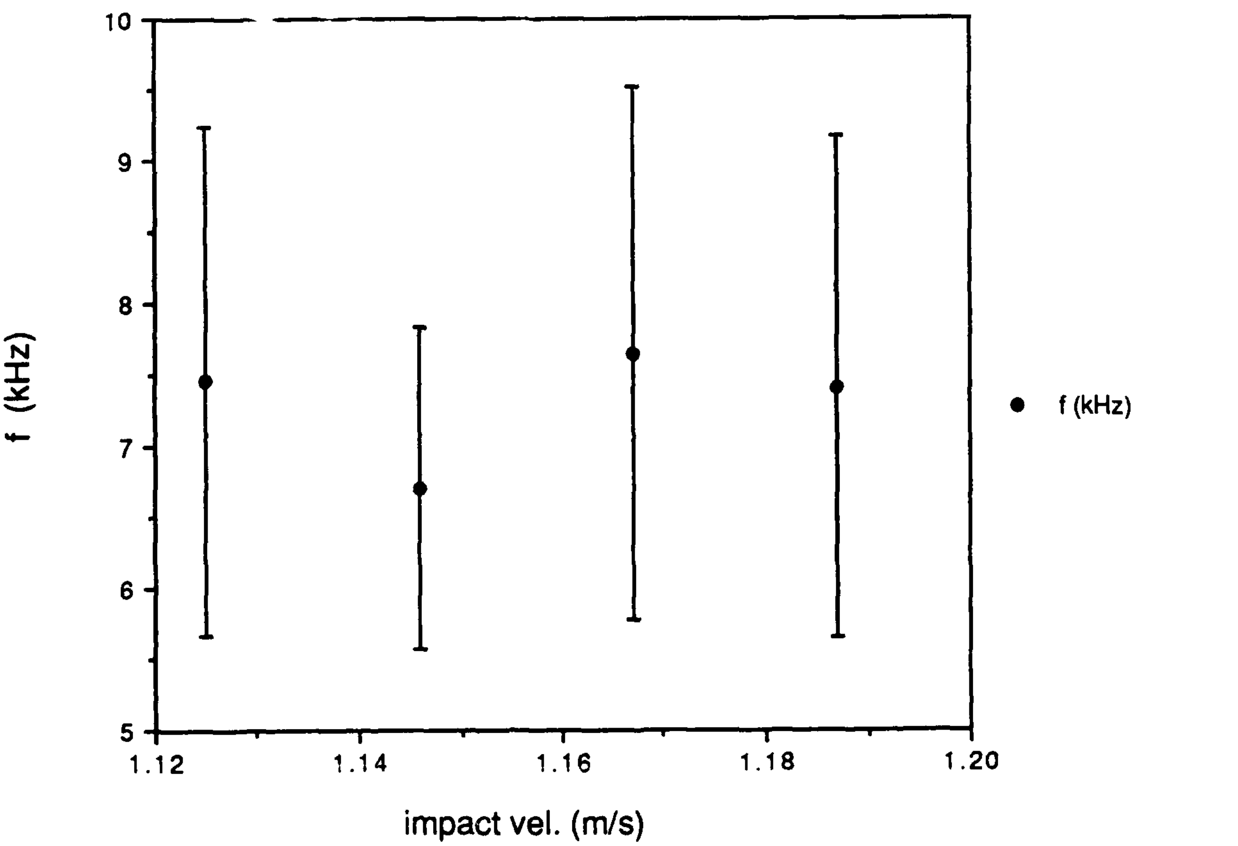

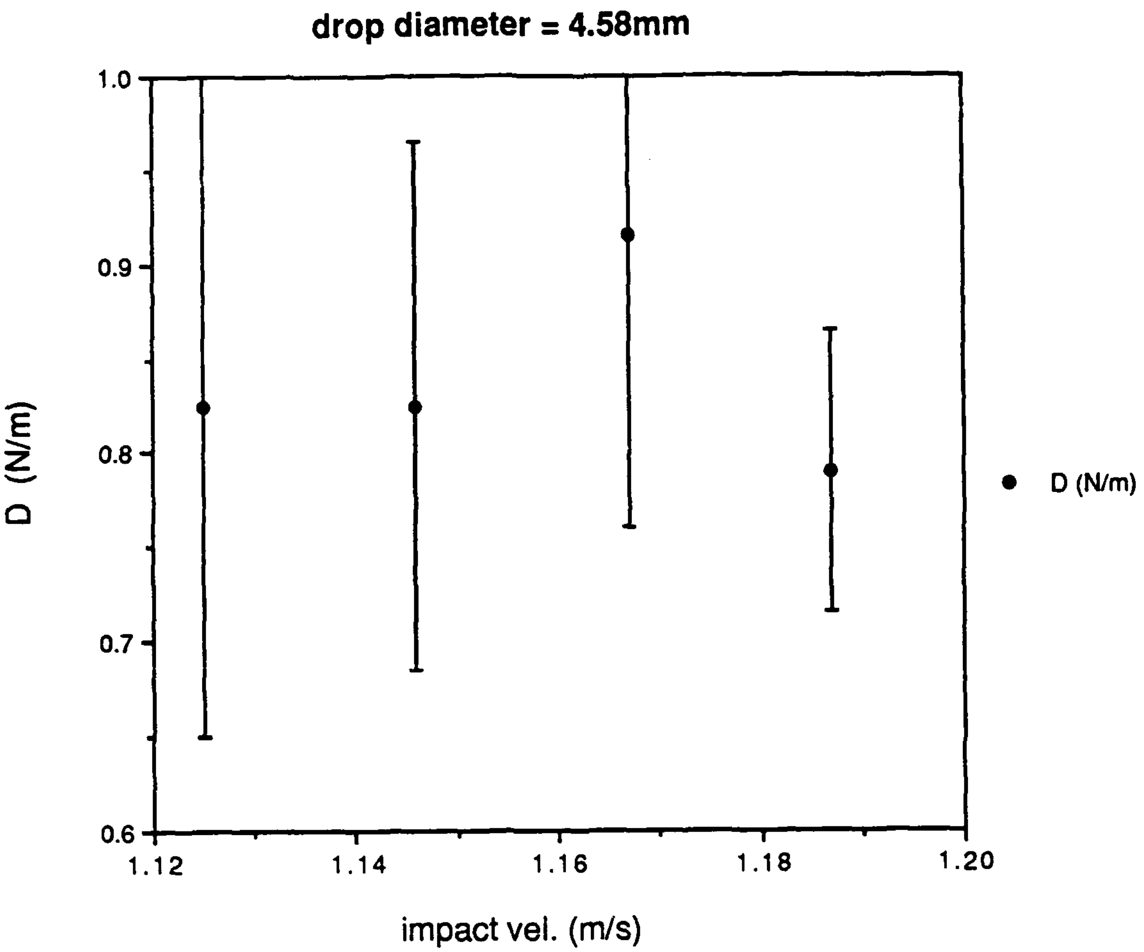
drop diameter = 4.58mm
D (N/m)
1.0
0.9
0.8
0.7
0.6
1.12
1.14
1.16
1.18
1.20
impact vel. (m/s)
D (N/m)

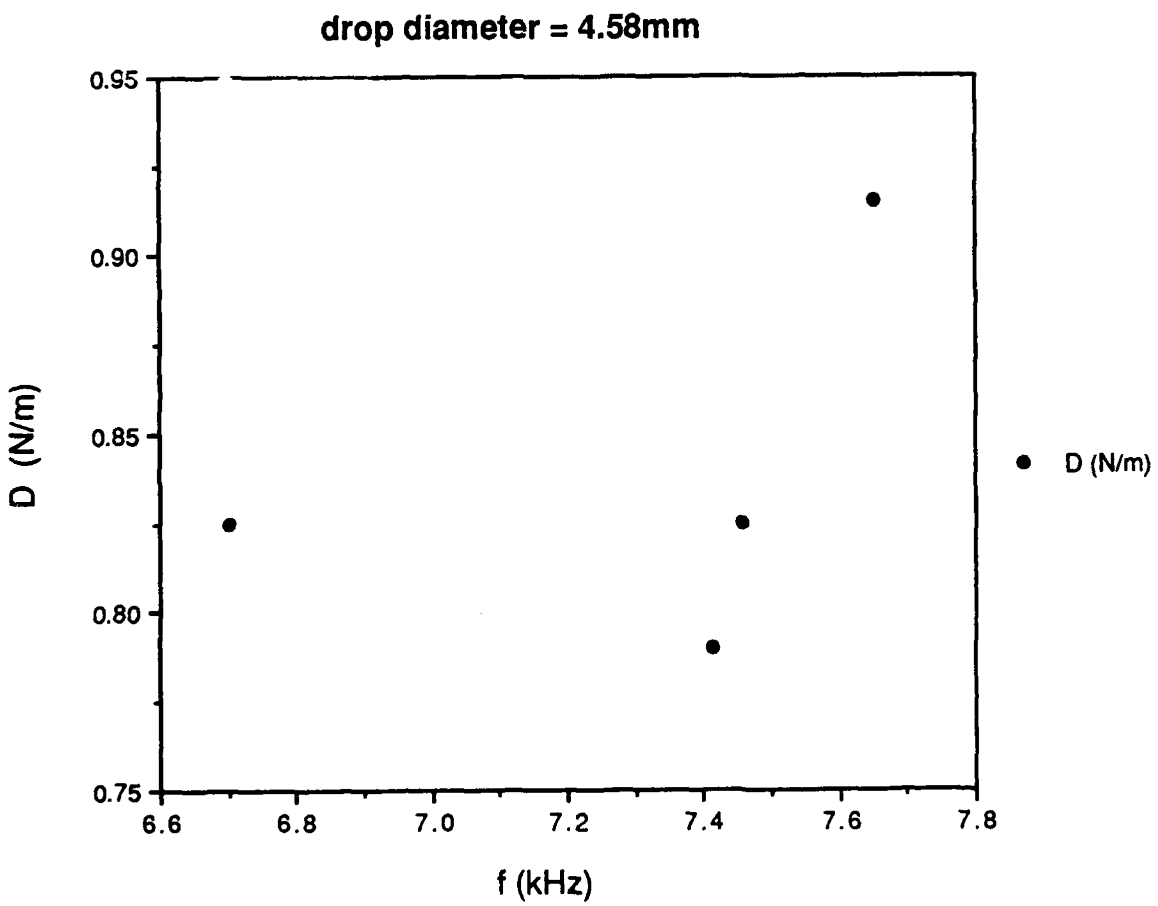
drop diameter = 4.58mm
D (N/m)
0.95
0.90
0.85
0.80
0.75
6.6
6.8
7.0
7.2
7.4
7.6
7.8
f (kHz)
D (N/m)

ANALYSIS OF DATA SET 1

The data seems to divide itself into three subsets. The first group encompasses drops 1.22 to 3.73 mm in diameter, the second for drops larger than 3.73 mm, and the third for drops smaller than 1.22 mm.

For the first group the plot of impact velocity versus bubble radii or frequency resembles a concave "U" shape. As impact velocity increases from zero through the point where entrainment begins, the bubble radius increases in size to a maximum value and then becomes smaller again as the highest entrainment velocity is reached. Regular entrainment discontinues after this point. The same sort of effect occurs with frequency, but since bubble radius is inversely proportional to frequency, the concavity is reversed. The graphs of the initial dipole strength versus impact velocity are similar to those for frequency versus impact velocity but with a "V" shaped rather than a ' U" shaped pattern.* The variability of each data point is dependent on its impact velocity, being high if the impact velocity is near the upper or lower velocity limit and low if the impact velocity is in between the two limits. The final set of graphs in this group--initial dipole strength versus frequency--cannot be analyzed alone because there are not enough data points. However, some features can be determined if they are compared with Fig. 7, which plots 200 drops of the same size hitting the water at a constant speed. These graphs all show a monotonic rise in dipole strength with increased frequency. However, after a certain point the relationship is destroyed and prediction of initial dipole strength based on the knowledge of frequency is impossible.

With the exception of this last graph, the graphic features of the next two groups are different from first. The group consisting of drops larger than 3.73 mm has more of an isotropic behavior. From this point to the point where drops become too big to cause regular entrainment the curvature in the graphs is destroyed and the variance is constant among the points (Thus, one can conclude that entrainment is unstable in this region). The group made of drops smaller than 1.22 mm in diameter only partially displays characteristics of the first group. Since the drops' terminal velocities are lower than their highest entraining velocities, the graphs only show part a "U" or "V". If the drops could fall faster than their terminal velocities, the patterns would probably be complete.

Using the highest and lowest entrainment velocities observed in this study, a second graph of the range of impact velocities and drop diameters is displayed in Fig. 8. This range matches the one done in the earlier study, shown in Fig. 2a. The curves are the best fit curves of the observed lowest and highest entrainment velocities. From the

---

* The marring of this pattern in the graphs for drop diameters = 1.22 mm and 2.17 mm is probably due to contaminates in the water.

knowledge of the impact velocities and drop radii, Fig. 8 can be modified to show the range of regular entrainment based on kinetic energy and drop diameter, which is graphed in Fig. 9. Again, the curves are best fit curves of the highest and lowest entraining kinetic energies.

From the data, a determination of whether or not regular entrainment causes rain noise can be made. Fig. 10 shows an enlargement of Fig. 8 in the area where the upper and lower boundaries of the entrainment intersect the terminal velocity curve. Raindrops entraining bubbles at terminal velocity are symbolized by diamonds; the frequencies of the bubbles are listed beside them. Since most of the bubbles entrained by drops falling at terminal velocity oscillate around 12 to 14 kHz, regular entrainment must be the cause of the 14 kHz peak found in the spectrum of natural rainfall and the source of rain noise underwater.

At one point during the study, the peak was believed to be caused by the 14 kHz bubbles being the most in number and the loudest. However, for bubbles entrained by drops falling at terminal velocity, the dipole strengths of 14 kHz bubbles are usually lower than those oscillating at 20 to 40 kHz. Therefore, the peak must be due only to the amount of bubbles attributed to it.

Figures 11 and 12 display the data in the form of contour graphs. The first one, showing similar regions of initial dipole strength for the entrainment region, indicates that dipole strength weakens as drop diameter is decreased. The other graph, displaying similar areas of frequency or bubble radius, shows that frequency steadily increases as drop diameter decreases.

EXPLANATION OF DATA SET 2

The second set of data measures the impact velocity and time required for the bubble to form after drop impact. Impact velocities are measured in meters per second and time is in milliseconds. As before, each row represents the average of thirty trials. After each data sheet are two graphs which plot both the relationship between the time and the impact velocity. However, the top graph is a logarithmic curve fit to the data while the bottom is a linear fit. Again, the drop diameter is listed at the top of each table, and the dates and times are unimportant.

DATA SET 2

drop diameter = 0.79mm Tue, Aug 15, 1989 2:33 PM

	impact vel.	time (ms)
1	3.240	4.641
2	3.235	4.620
3	3.233	4.584
4	3.231	4.569

drop diameter = 0.79mm

y = - 21.744 + 8.1452x R^2 = 0.914

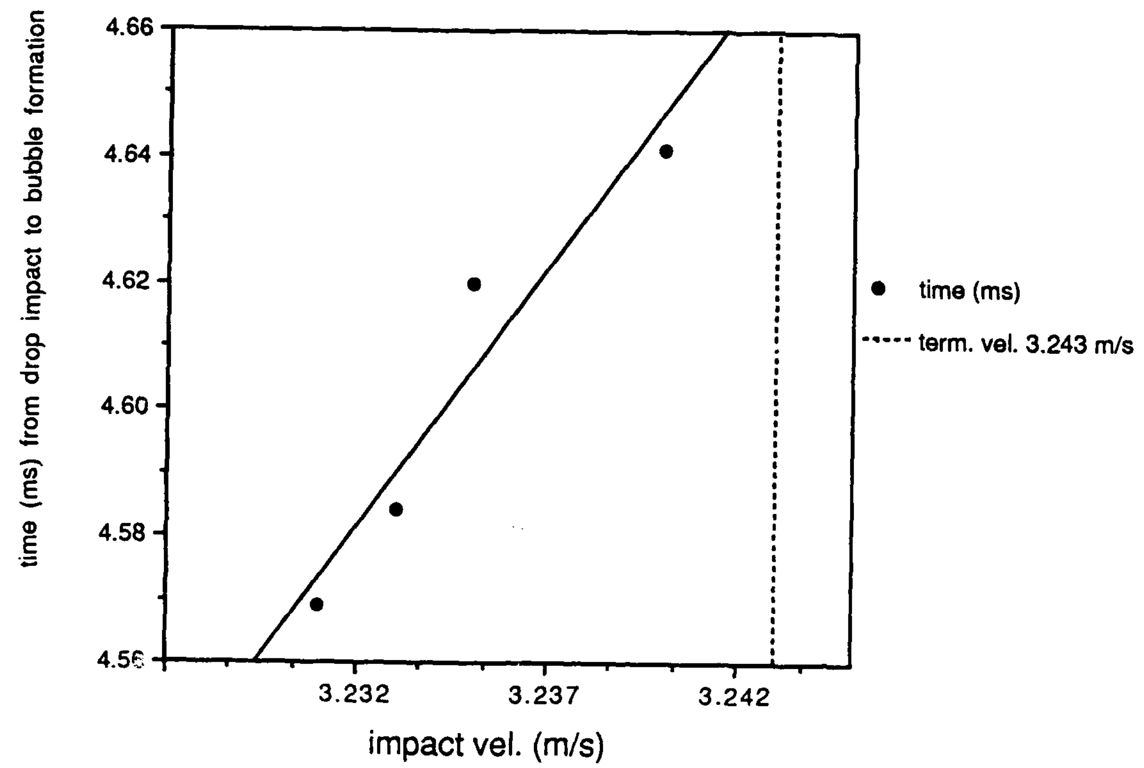

drop diameter = 0.79mm

y = 5.5704e-3 * x^5.7218 R^2 = 0.913

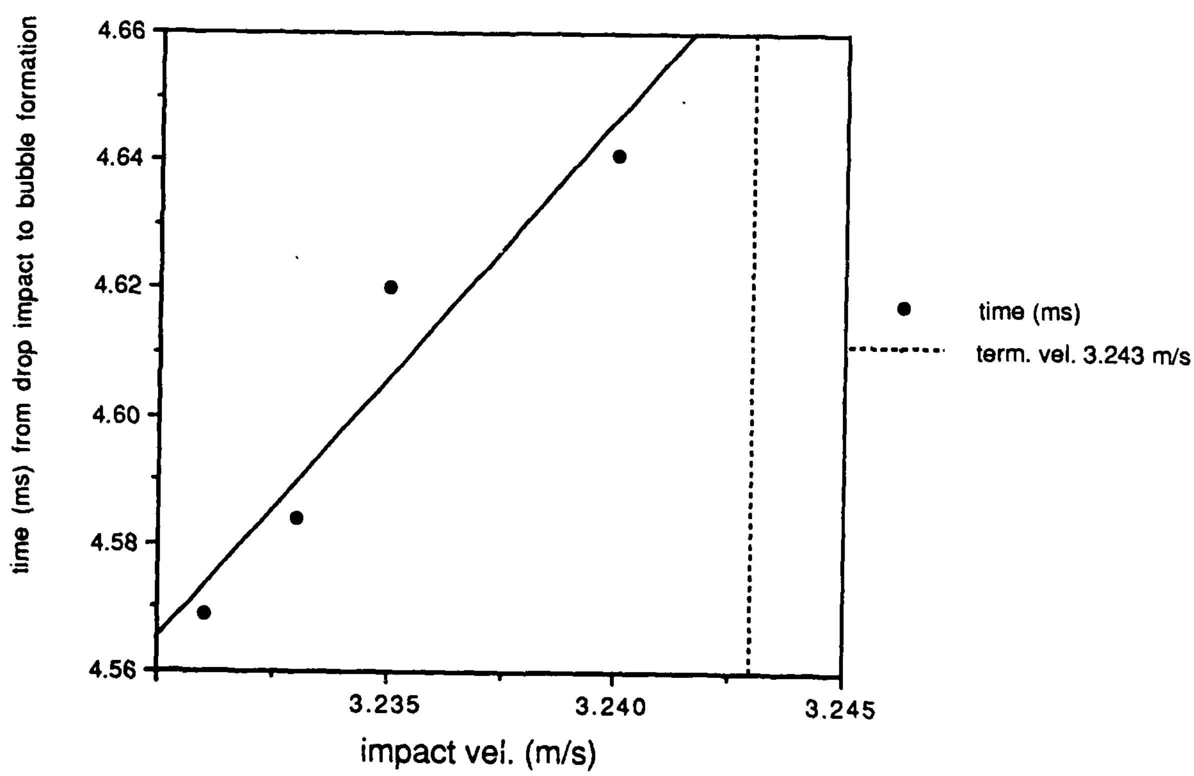

	impact vel.	time (ms)
1	3.526	5.490
2	3.517	5.737
3	3.512	5.708
4	3.506	5.740
5	3.499	5.616
6	3.490	5.558
7	3.480	5.462
8	3.469	5.496
9	3.455	5.506
10	3.439	5.464
11	3.421	5.204
12	3.401	5.263
13	3.373	5.214
14	3.342	5.152
15	3.306	5.108
16	3.263	5.102
17	3.539	5.604

drop diameter = 0.87mm

y = 0.79549 * x^1.5541   R^2 = 0.831

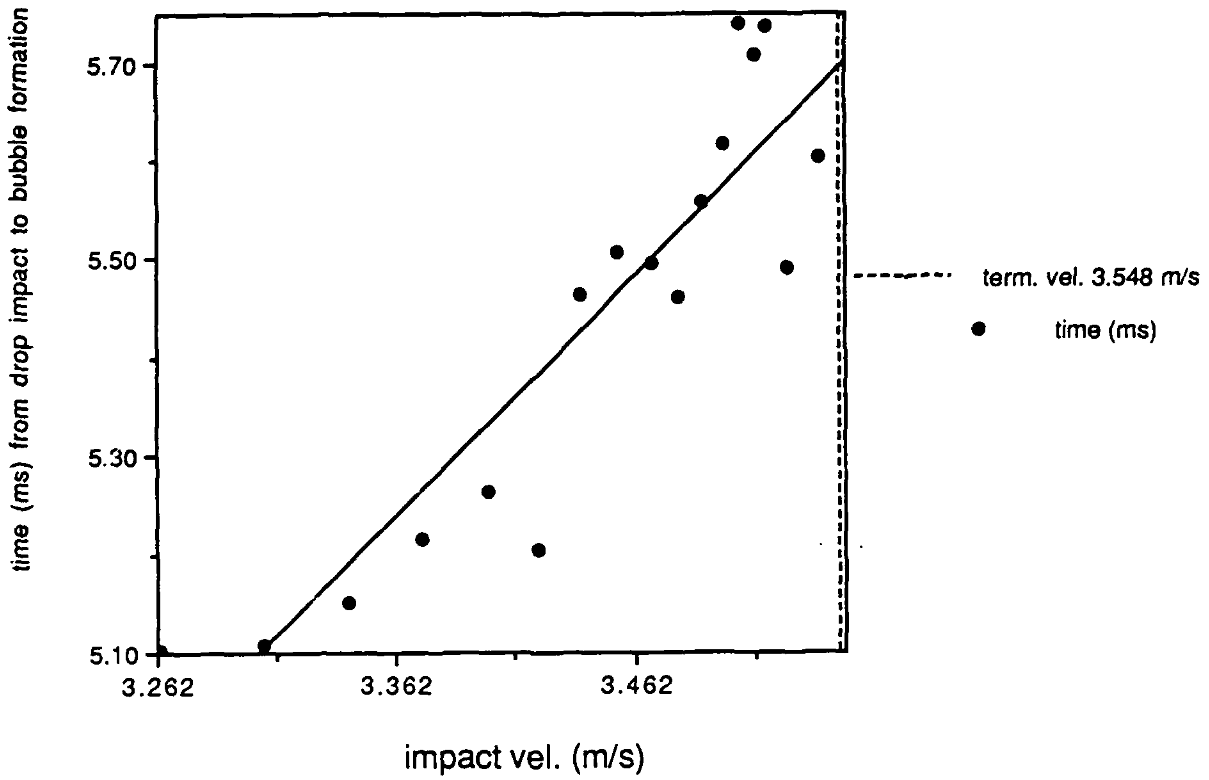

drop diameter = 0.87mm

y = - 3.0285 + 2.4584x   R^2 = 0.826

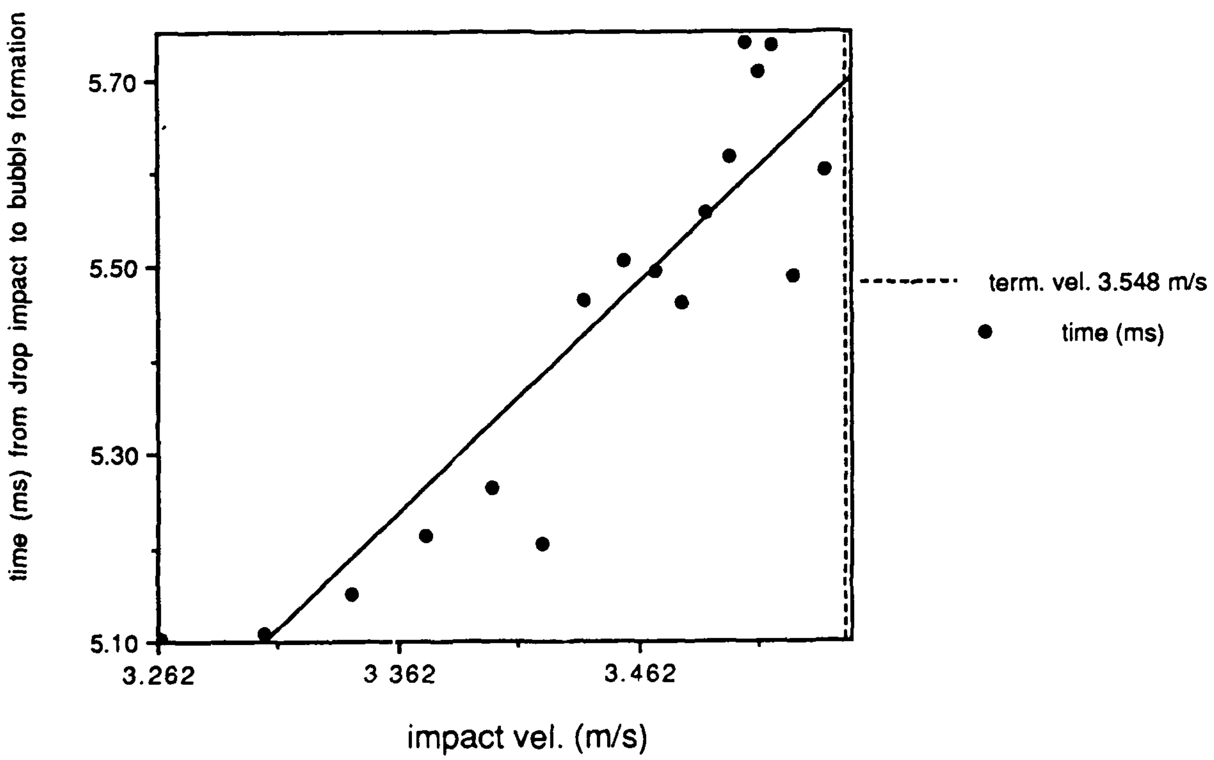

drop diameter = 0.93mm   Thu, Jul 20, 1989 10:01 PM

	imapct vel.	time (ms)
1	3.204	5.847
2	3.253	6.155
3	3.331	6.216
4	3.390	6.265
5	3.485	6.763
6	3.523	6.679
7	3.558	6.881
8	3.583	7.081
9	3.608	6.720
10	3.629	6.769
11	3.647	6.804
12	3.663	6.991
13	3.677	7.044
14	3.689	6.886
15	3.699	6.860
16	3.708	6.847
17	3.716	6.913
18	3.723	6.855
19	3.723	6.937

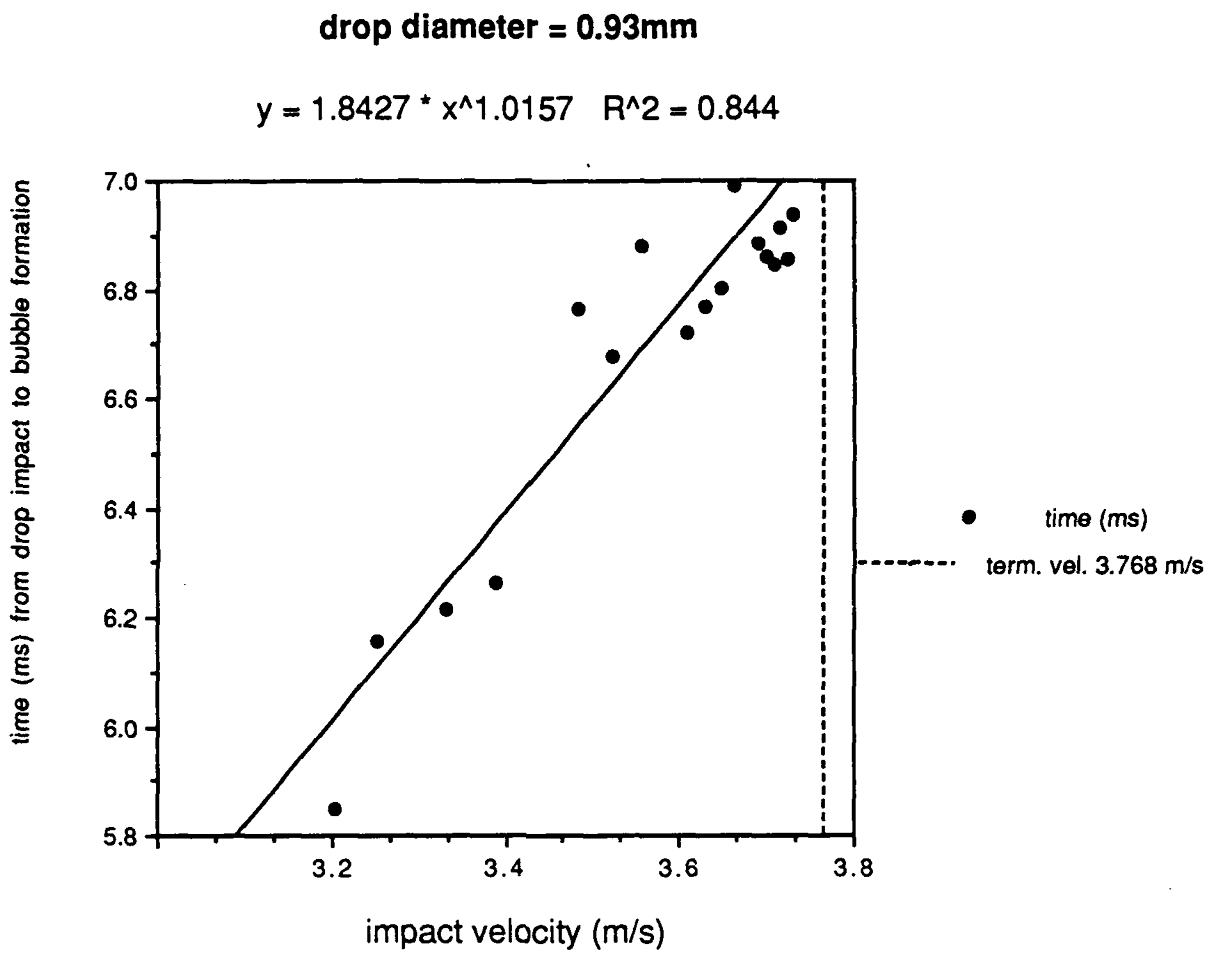
drop diameter = 0.93mm
y = 1.8427 * x^1.0157   R^2 = 0.844
time (ms) from drop impact to bubble formation
7.0
6.8
6.6
6.4
6.2
6.0
5.8
3.2
3.4
3.6
3.8
impact velocity (m/s)
time (ms)
term. vel. 3.768 m/s

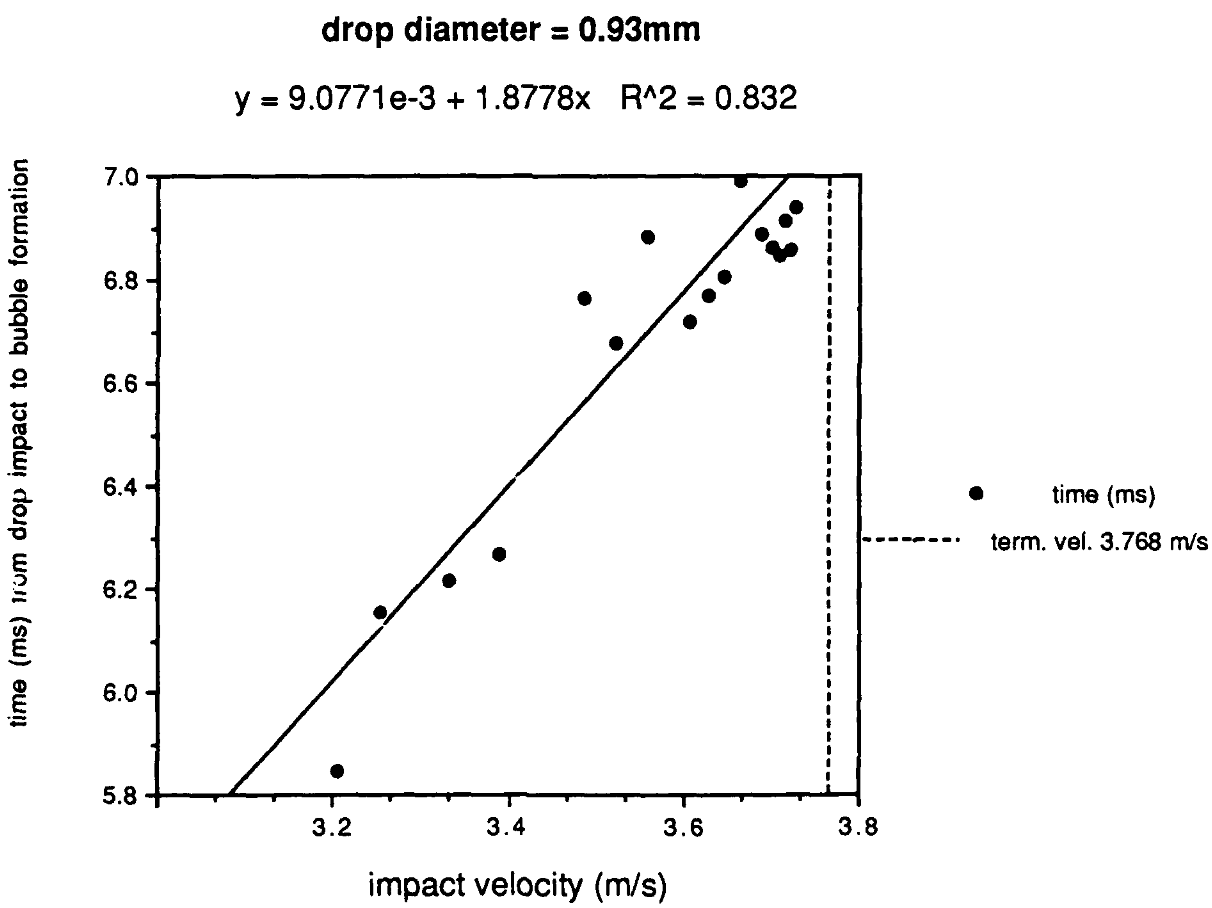
drop diameter = 0.93mm
y = 9.0771e-3 + 1.8778x   R^2 = 0.832
time (ms) from drop impact to bubble formation
7.0
6.8
6.6
6.4
6.2
6.0
5.8
3.2
3.4
3.6
3.8
impact velocity (m/s)
time (ms)
term. vel. 3.768 m/s

	impact vel.	time (ms)
1	3.167	5.847
2	3.275	6.453
3	3.368	6.592
4	3.449	6.714
5	3.518	6.768
6	3.579	6.952
7	3.631	7.030
8	3.677	7.692
9	3.717	7.696
10	3.753	7.826
11	3.784	7.986
12	3.811	8.113
13	3.835	7.848
14	3.856	8.188
15	3.874	8.126
16	3.905	8.075
17	3.918	8.062
18	3.929	7.736
19	3.938	7.627
20	3.983	7.522

drop diameter = 1.00mm

$y = 1.3061 * x^{1.3294}$ $R^2 = 0.846$

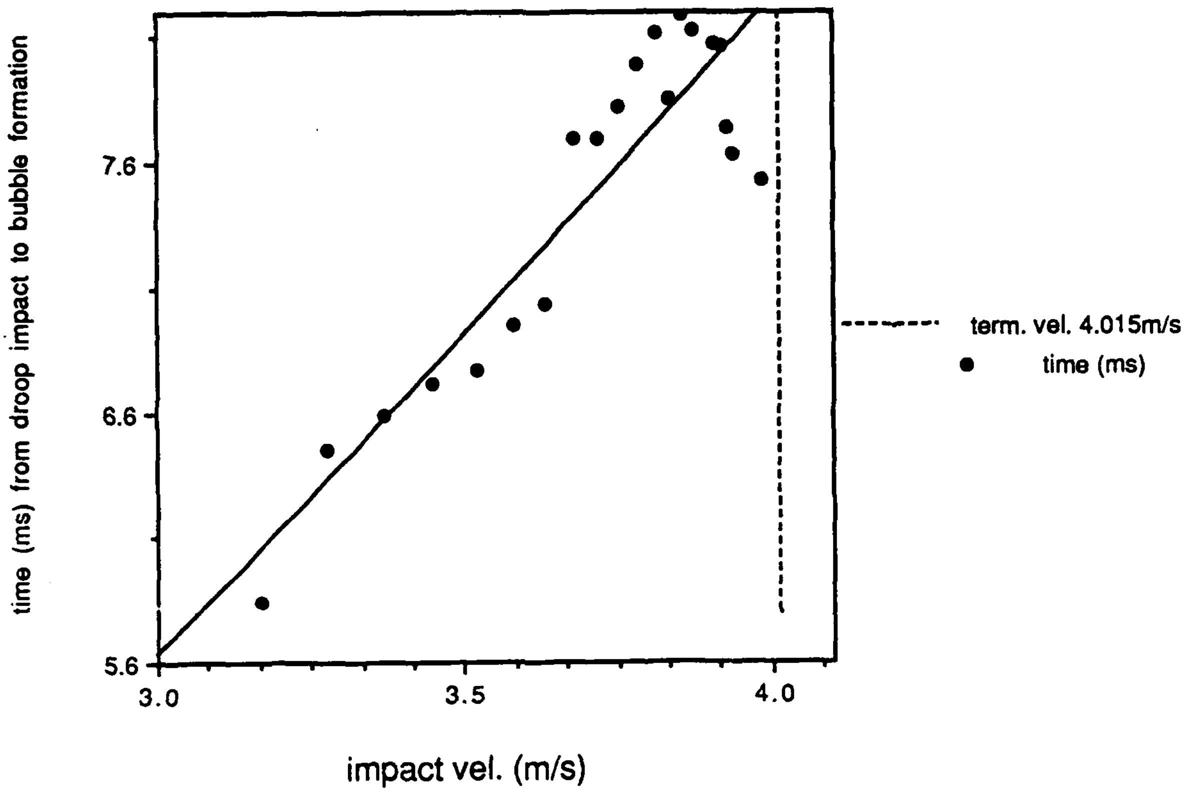

drop diameter = 1.00mm

$y = -2.1907 + 2.6048x$ $R^2 = 0.825$

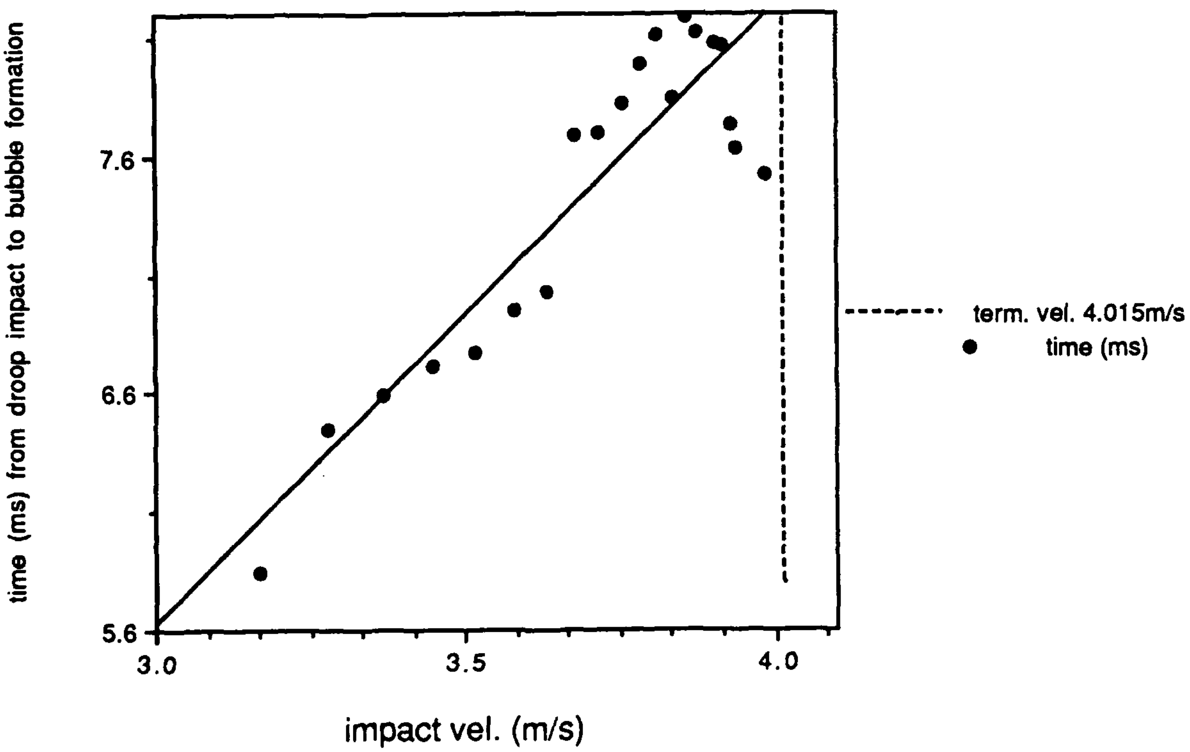

	final vel.	time (ms)
1	3.101	6.573
2	3.238	6.881
3	3.356	7.176
4	3.459	7.232
5	3.549	7.460
6	3.627	7.633
7	3.696	7.257
8	3.757	7.587
9	3.810	7.594
10	3.858	7.903
11	3.900	8.725
12	3.937	8.994
13	3.971	8.639
14	4.000	8.756
15	4.050	8.703
16	4.071	9.261
17	4.090	10.013
18	4.106	9.531
19	4.121	9.607
20	4.138	9.567
21	4.147	9.509

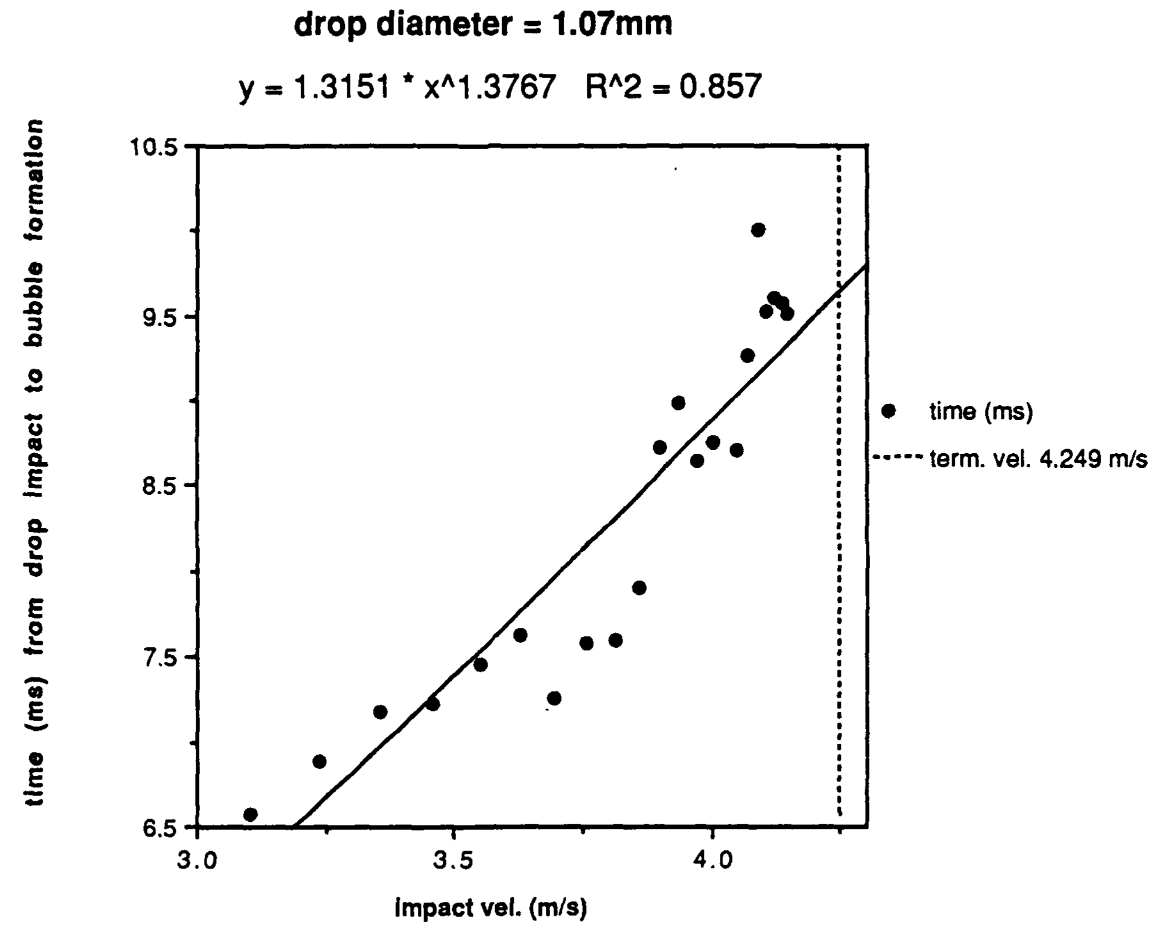
drop diameter = 1.07mm
y = 1.3151 * x^1.3767   R^2 = 0.857
time (ms) from drop impact to bubble formation
10.5
9.5
8.5
7.5
6.5
3.0
3.5
4.0
impact vel. (m/s)
time (ms)
term. vel. 4.249 m/s

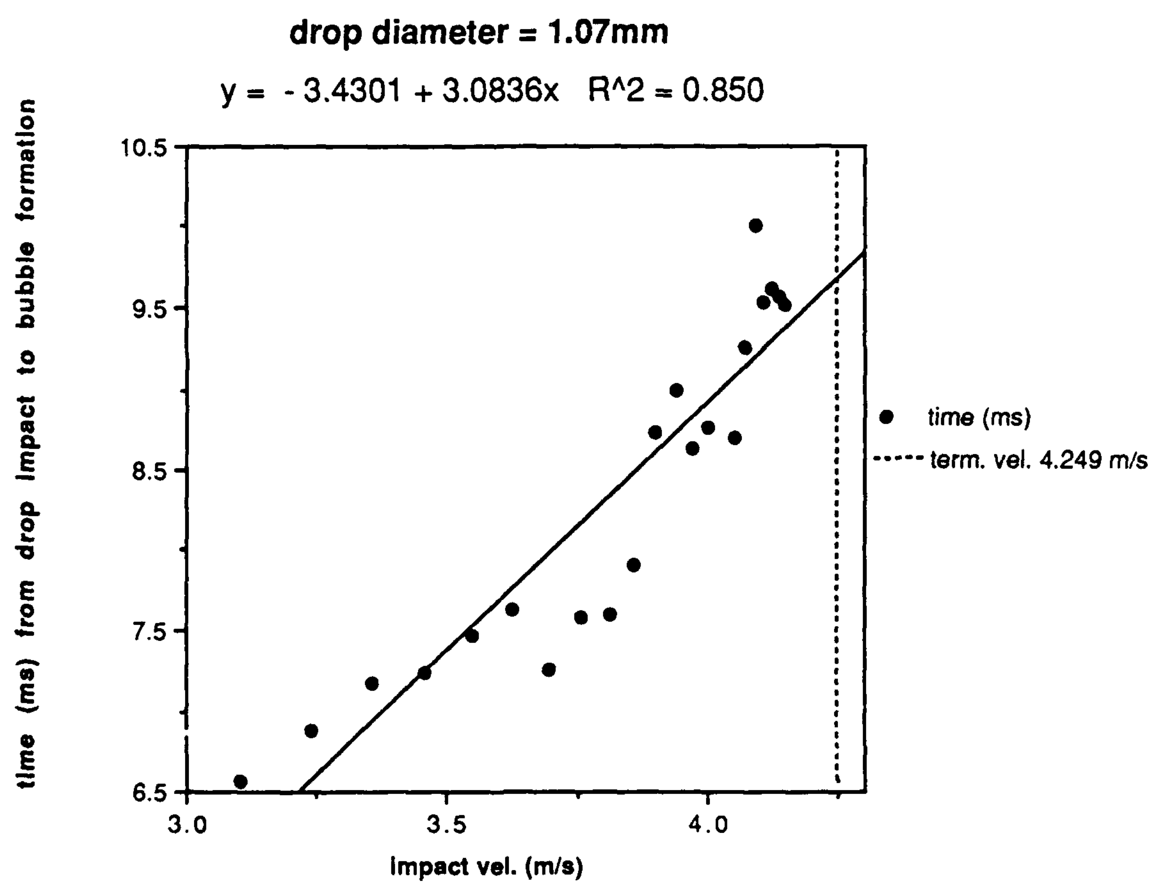
drop diameter = 1.07mm
y = - 3.4301 + 3.0836x   R^2 = 0.850
time (ms) from drop impact to bubble formation
10.5
9.5
8.5
7.5
6.5
3.0
3.5
4.0
impact vel. (m/s)
time (ms)
term. vel. 4.249 m/s

drop diameter = 1.71mm Fri, Jul 21, 1989 11:25 AM

	impact vel	time (ms)
1	2.004	11.560
2	2.058	11.840
3	2.099	12.000
4	2.130	12.220
5	2.179	12.420
6	2.217	12.600
7	2.255	12.760
8	2.292	12.940
9	2.328	13.140
10	2.363	13.240
11	2.397	13.400
12	2.431	13.560
13	2.465	13.700
14	2.497	14.180
15	2.529	14.220
16	2.561	14.360
17	2.591	14.520
18	2.622	14.680
19	2.652	14.780
20	2.695	14.850
21	2.738	14.910
22	2.766	15.030
23	2.794	15.280
24	2.821	15.400
25	2.847	15.370
26	2.874	15.440
27	2.900	15.560
28	2.925	16.140

drop diameter = 1.71mm

y = 6.5009 * x^0.83239   R^2 = 0.992

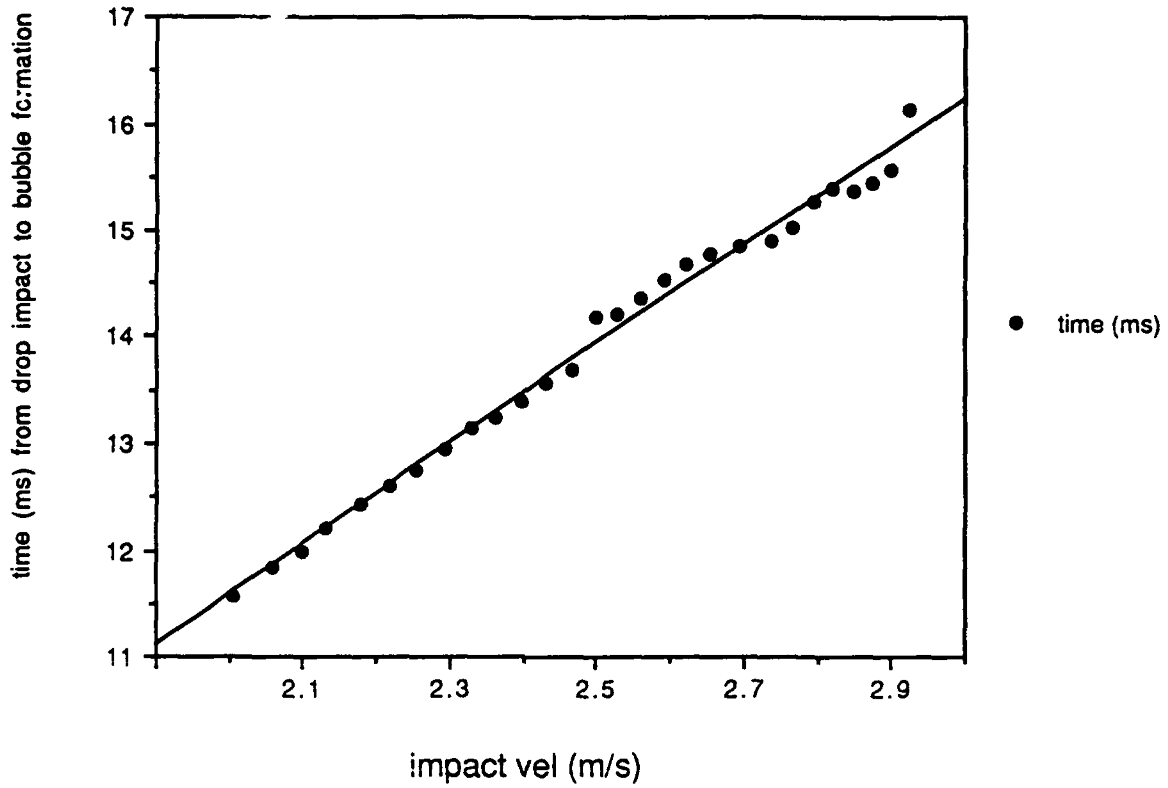

drop diameter = 1.71mm

y = 2.3442 + 4.6332x   R^2 = 0.990

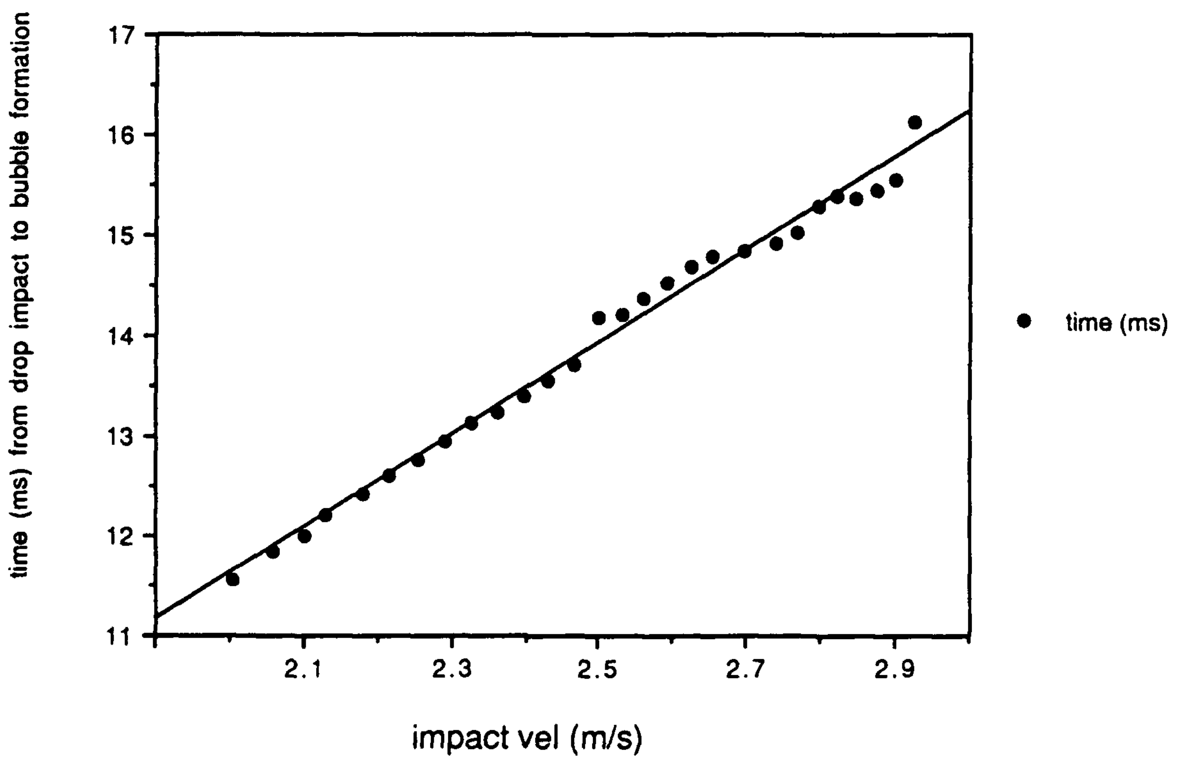

	impact vel.	time (ms)
1	1.794	14.720
2	1.844	15.100
3	1.890	15.500
4	1.940	15.780
5	1.986	15.970
6	2.031	16.230
7	2.074	16.520
8	2.117	16.800
9	2.158	17.000
10	2.199	17.200
11	2.238	17.440
12	2.277	17.640
13	2.315	17.800
14	2.352	18.080
15	2.389	18.280
16	2.424	18.460
17	2.459	18.680
18	2.494	18.800
19	2.527	19.040
20	2.561	19.240
21	2.594	19.400

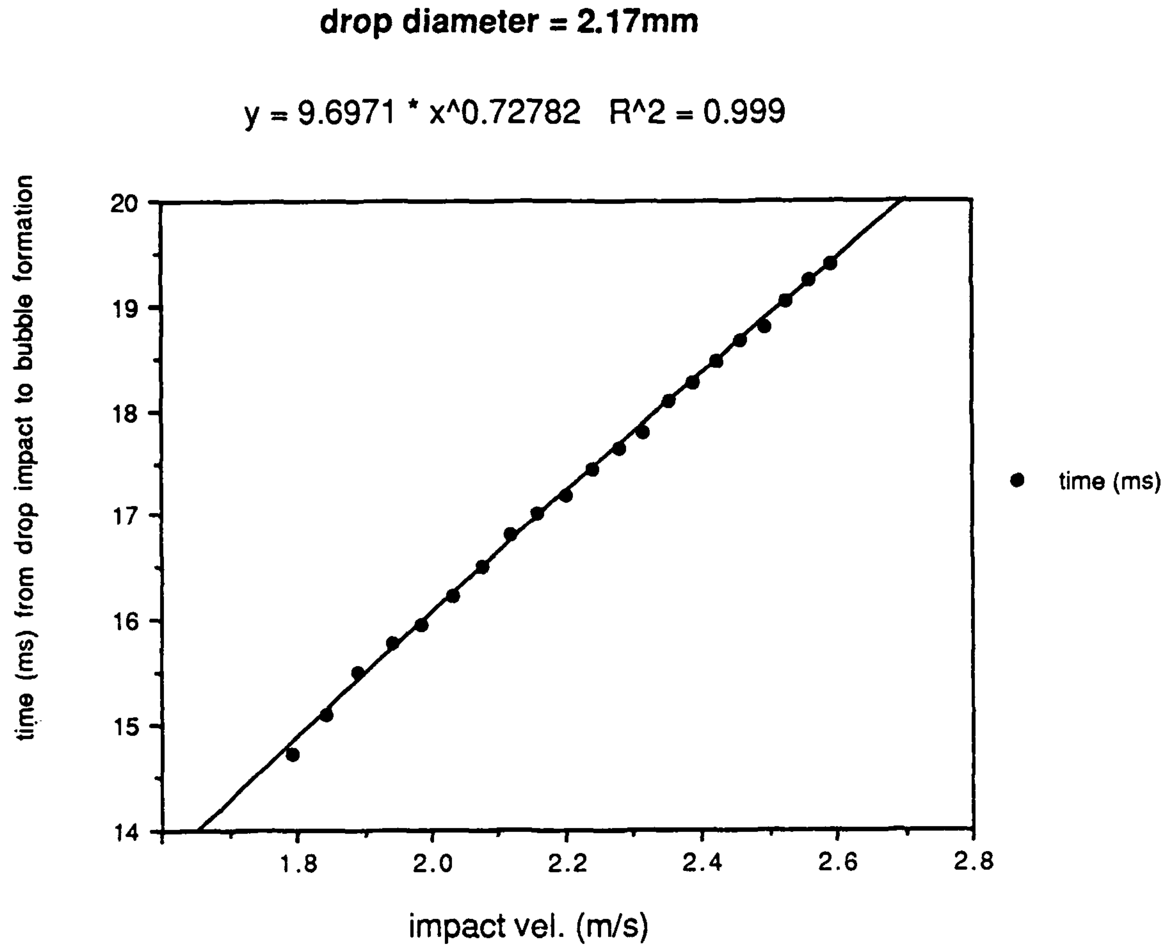

drop diameter = 2.17mm
y = 9.6971 * x^0.72782   R^2 = 0.999
time (ms) from drop impact to bubble formation
20
19
18
17
16
15
14
1.8
2.0
2.2
2.4
2.6
2.8
impact vel. (m/s)
time (ms)

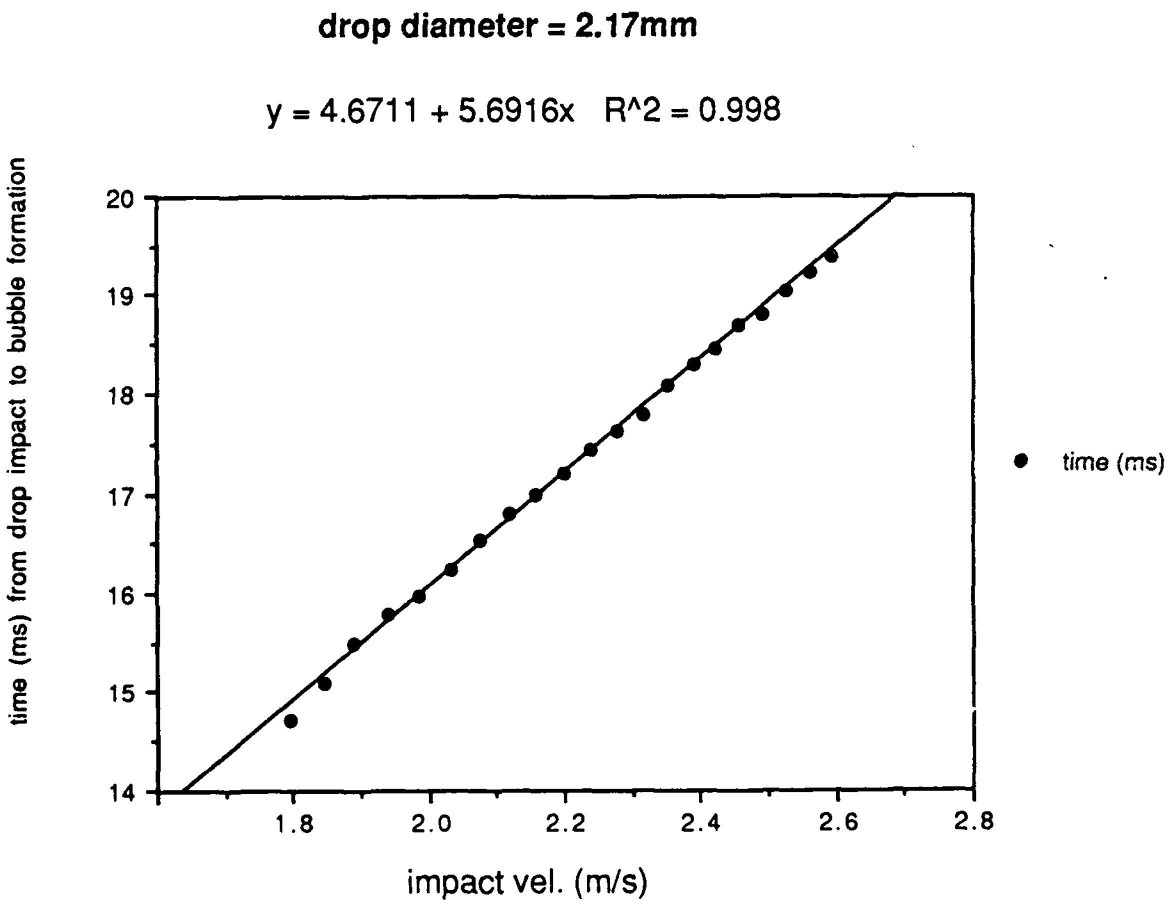

drop diameter = 2.17mm
y = 4.6711 + 5.6916x   R^2 = 0.998
time (ms) from drop impact to bubble formation
20
19
18
17
16
15
14
1.8
2.0
2.2
2.4
2.6
2.8
impact vel. (m/s)
time (ms)

drop diameter = 2.27mm Fri, Jul 21, 1989 11:29 AM

	impact vel.	time (ms)
1	1.760	14.480
2	1.796	14.720
3	1.846	15.180
4	1.895	15.360
5	1.942	15.530
6	1.988	15.890
7	2.033	16.080
8	2.077	16.570
9	2.119	16.750
10	2.161	17.170
11	2.202	17.350
12	2.241	17.640
13	2.280	17.880
14	2.318	18.130
15	2.356	18.280
16	2.392	18.500
17	2.428	18.800
18	2.498	18.980

drop diameter = 2.27mm

$y = 9.2074 * x^{0.80057}$ $R^2 = 0.996$

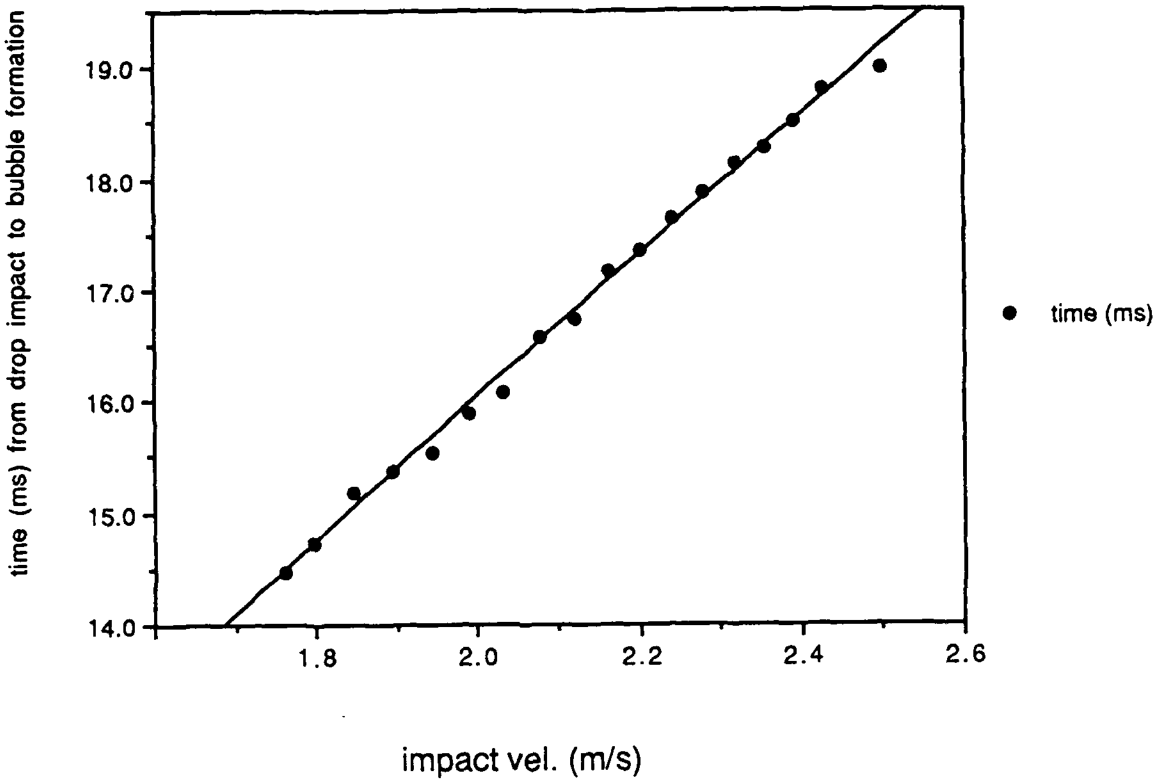

Data from "drop diameter = 2.27mm"

$y = 3.3340 + 6.3466x$ $R^2 = 0.996$

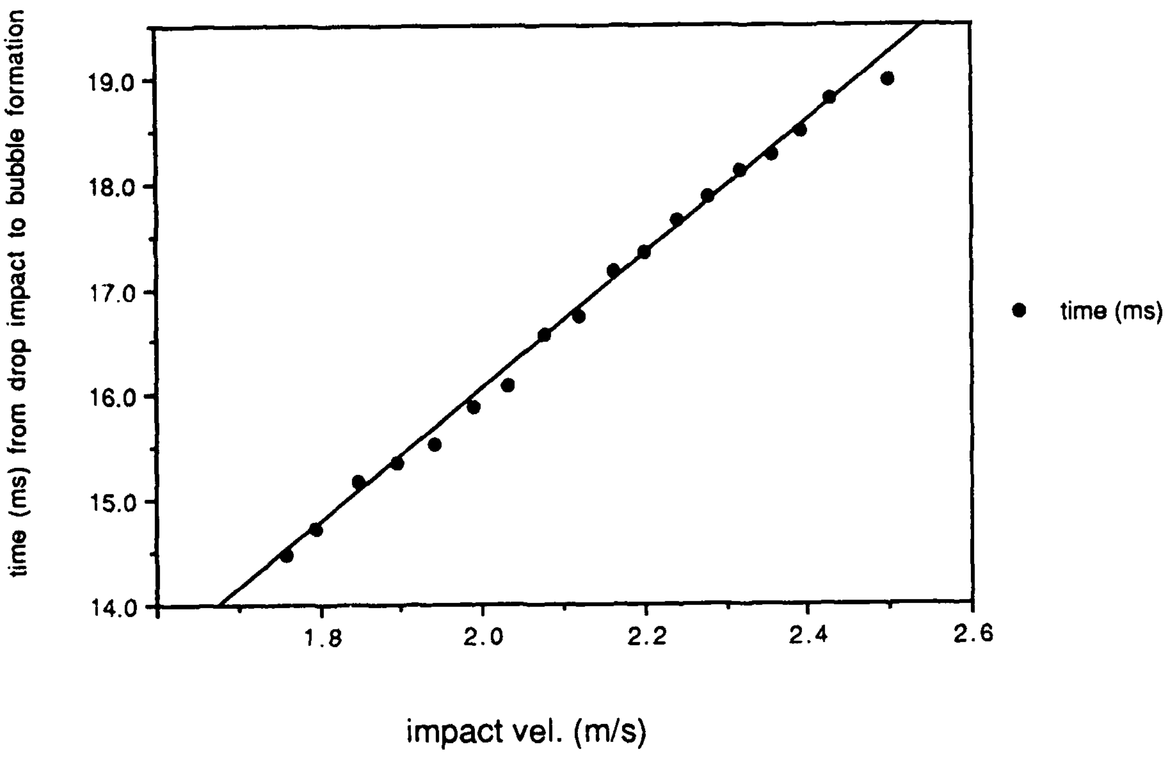

drop diameter = 2.57mm Fri, Jul 21, 1989 11:31 AM

	impact vel.	time (ms)
1	1.519	15.580
2	1.579	16.110
3	1.637	16.710
4	1.693	17.160
5	1.747	17.560
6	1.800	17.930
7	1.850	18.270
8	1.899	18.864
9	1.947	19.088
10	1.993	19.584
11	2.038	19.748
12	2.125	20.424
13	2.164	20.680
14	2.208	20.984

drop diameter = 2.57mm

y = 11.272 * x^0.79038   R^2 = 0.998

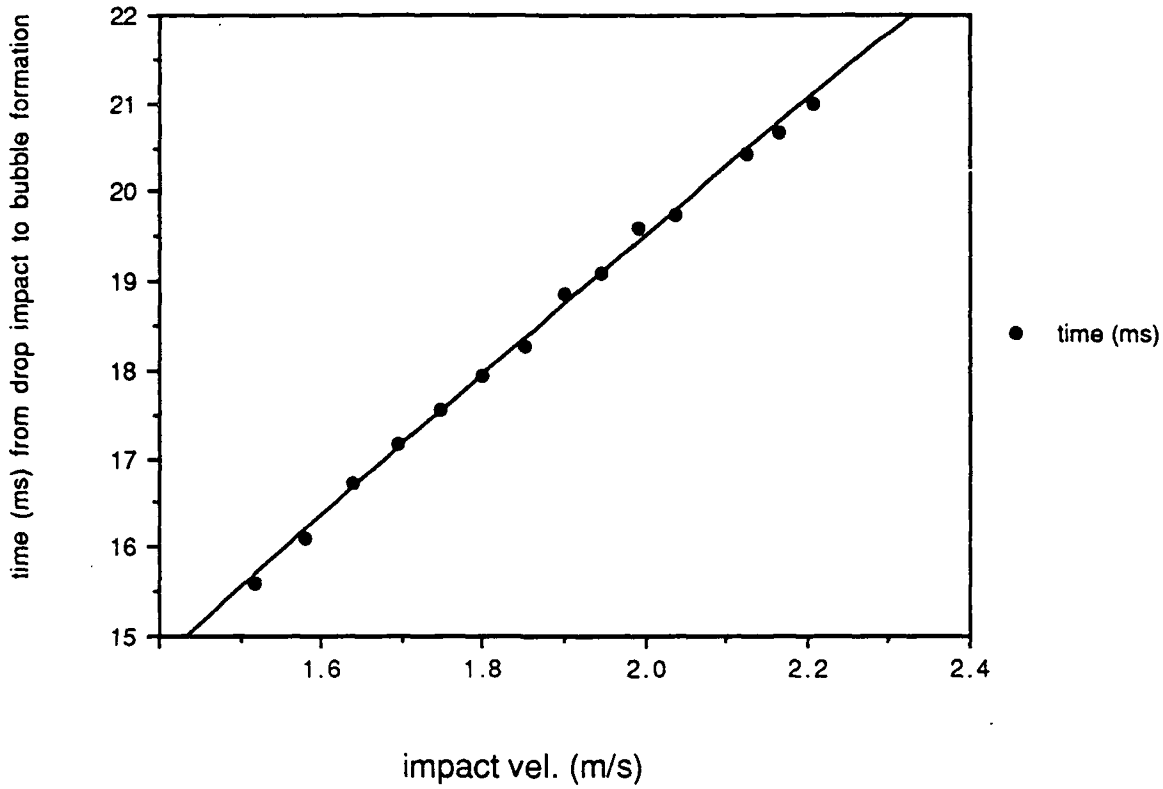

drop diameter = 2.57mm

y = 3.9015 + 7.7893x   R^2 = 0.997

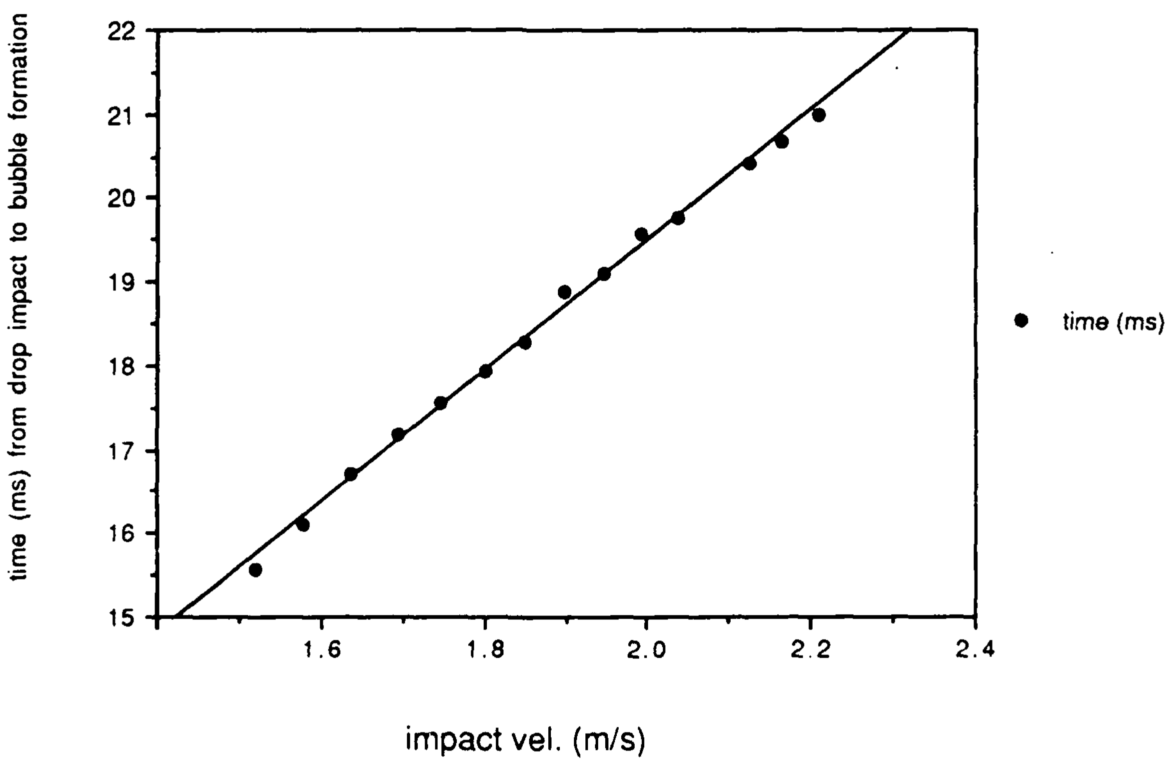

drop diameter = 2.86mm

Fri, Jul 21, 1989 11:36 AM

	impact vel.	time (ms)
1	1.520	17.589
2	1.581	18.532
3	1.639	18.930
4	1.695	19.392
5	1.750	19.772
6	1.802	20.240
7	1.853	20.904
8	1.902	21.238
9	1.950	21.608
10	1.997	21.786
11	2.042	22.188
12	2.086	22.388

drop diameter = 2.86mm

y = 13.056 * x^0.74647   R^2 = 0.991

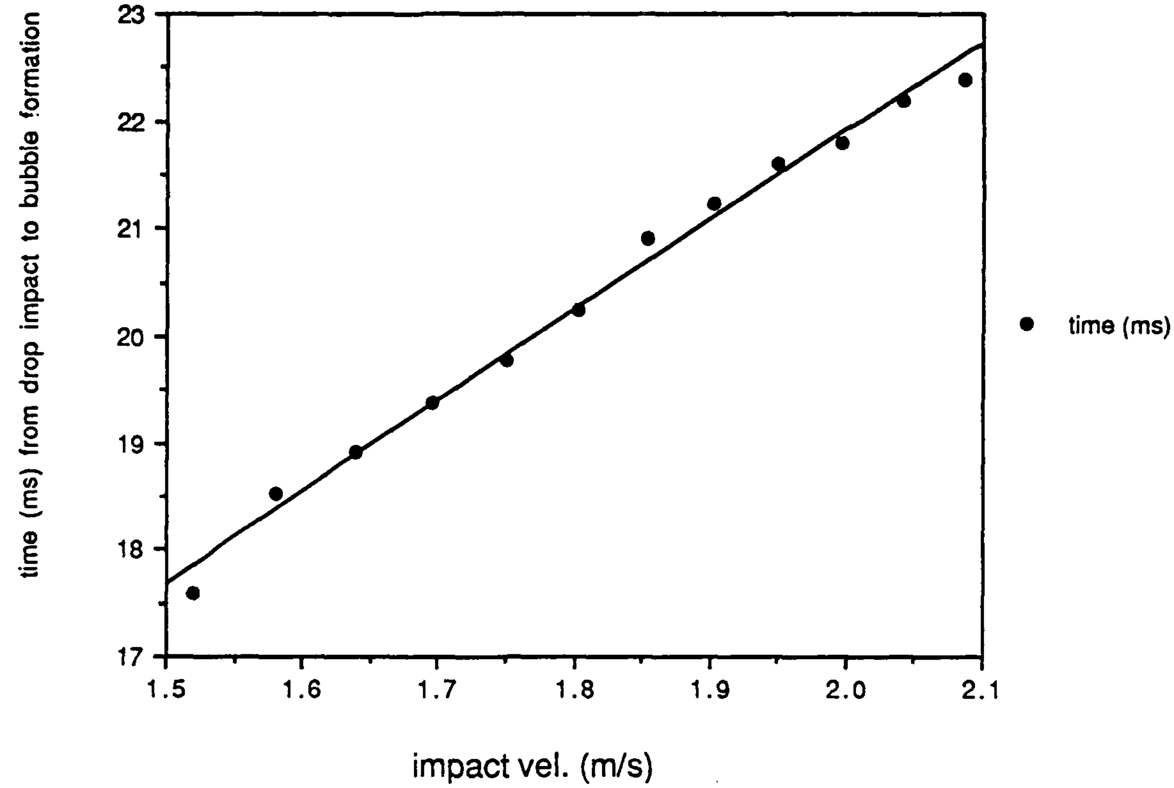

drop diameter = 2.86mm

y = 5.2206 + 8.3385x   R^2 = 0.990

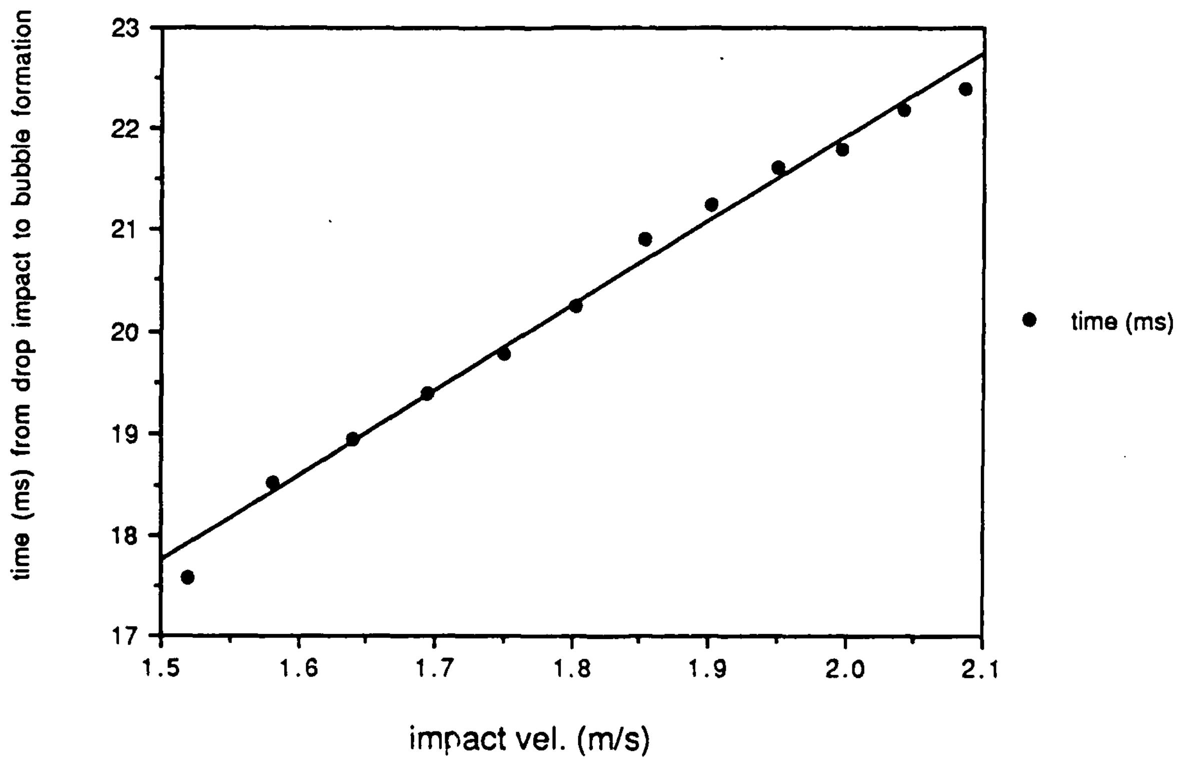

drop diameter = 3.03mm Thu, Jul 20, 1989 9:08 PM

	impact vel	time (ms)
1	1.457	19.040
2	1.521	19.568
3	1.582	20.160
4	1.640	20.880
5	1.696	21.256
6	1.751	21.784
7	1.803	22.180
8	1.879	22.456
9	1.904	22.960
10	1.952	23.232
11	1.998	23.524
12	2.044	23.832

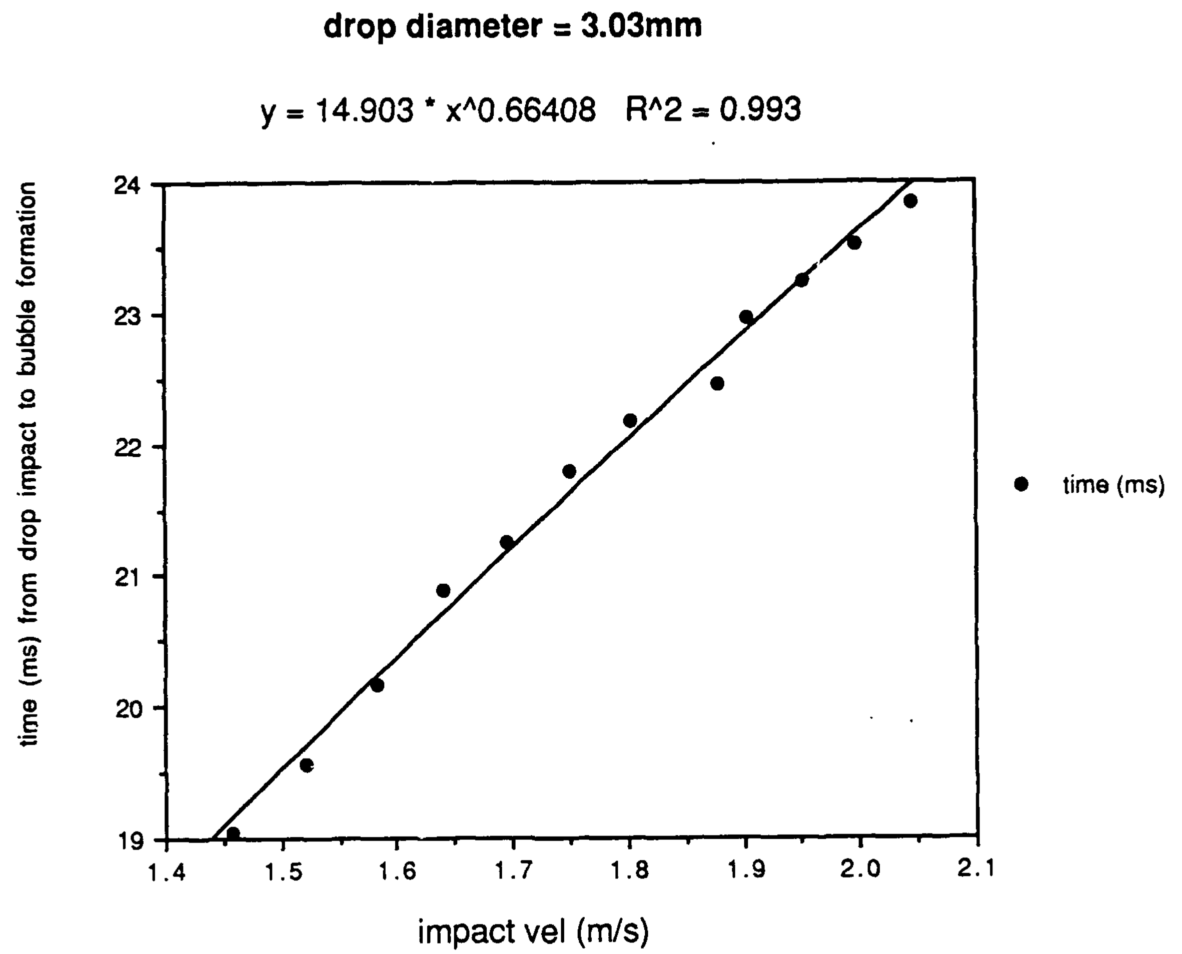

drop diameter = 3.03mm
y = 14.903 * x^0.66408   R^2 = 0.993
time (ms) from drop impact to bubble formation
24
23
22
21
20
19
1.4
1.5
1.6
1.7
1.8
1.9
2.0
2.1
impact vel (m/s)
time (ms)

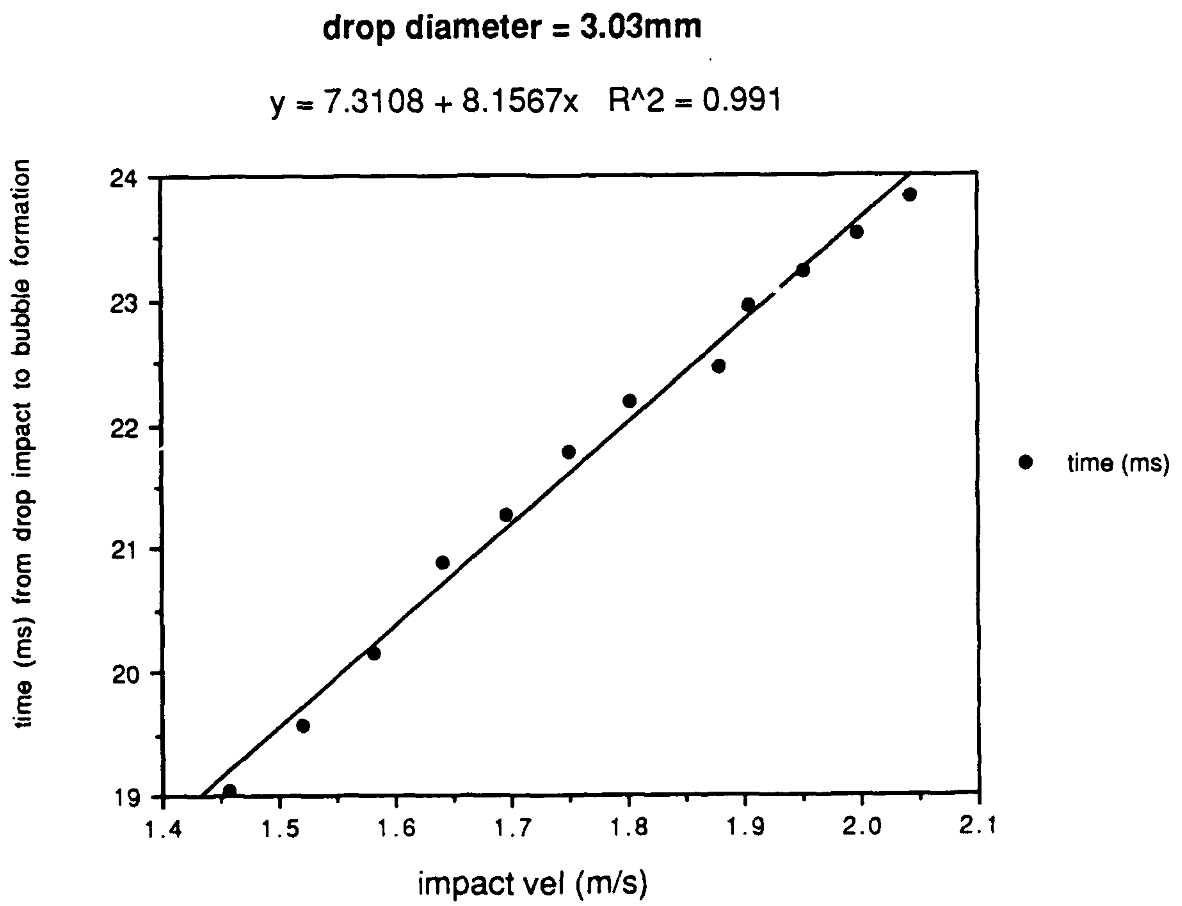

drop diameter = 3.03mm
y = 7.3108 + 8.1567x   R^2 = 0.991
time (ms) from drop impact to bubble formation
24
23
22
21
20
19
1.4
1.5
1.6
1.7
1.8
1.9
2.0
2.1
impact vel (m/s)
time (ms)

	impact vel.	time (ms)
1	1.321	20.032
2	1.391	20.844
3	1.458	21.384
4	1.522	22.036
5	1.583	22.916
6	1.641	23.476
7	1.698	23.968

drop diameter = 3.13mm

y = 14.697 * x^0.67948   R^2 = 0.993

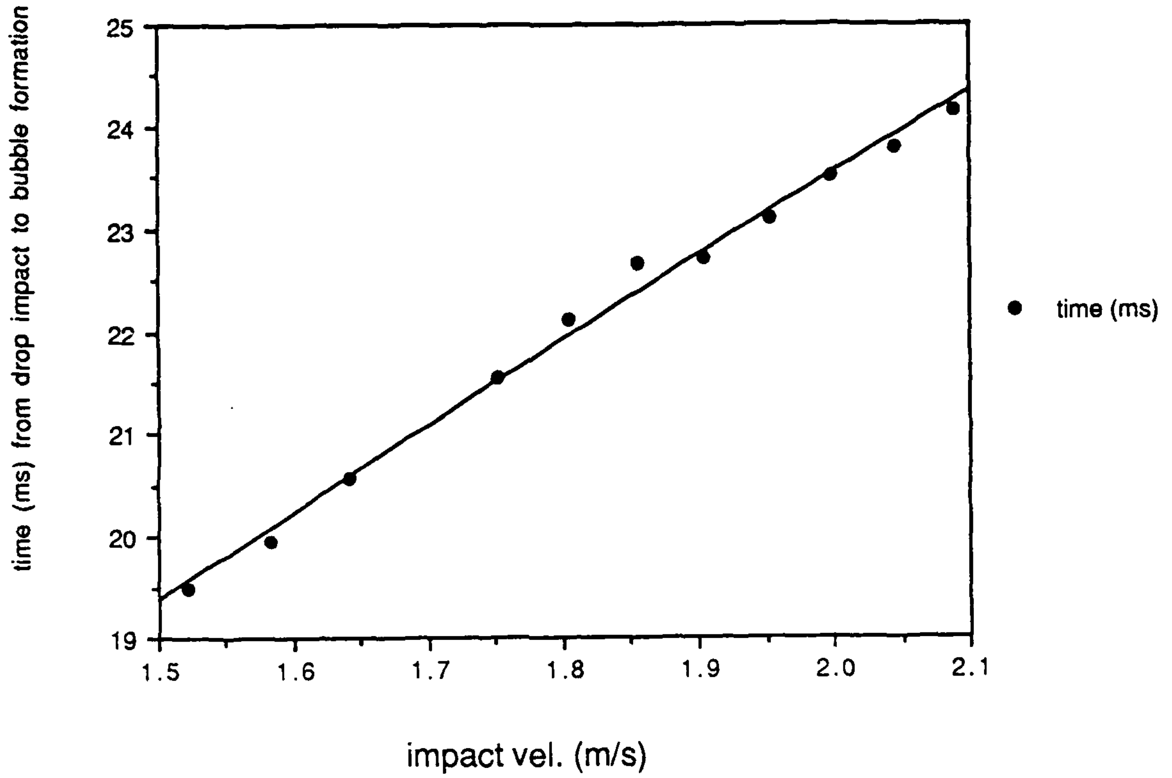

drop diameter = 3.13mm

y = 7.0770 + 8.2283x   R^2 = 0.991

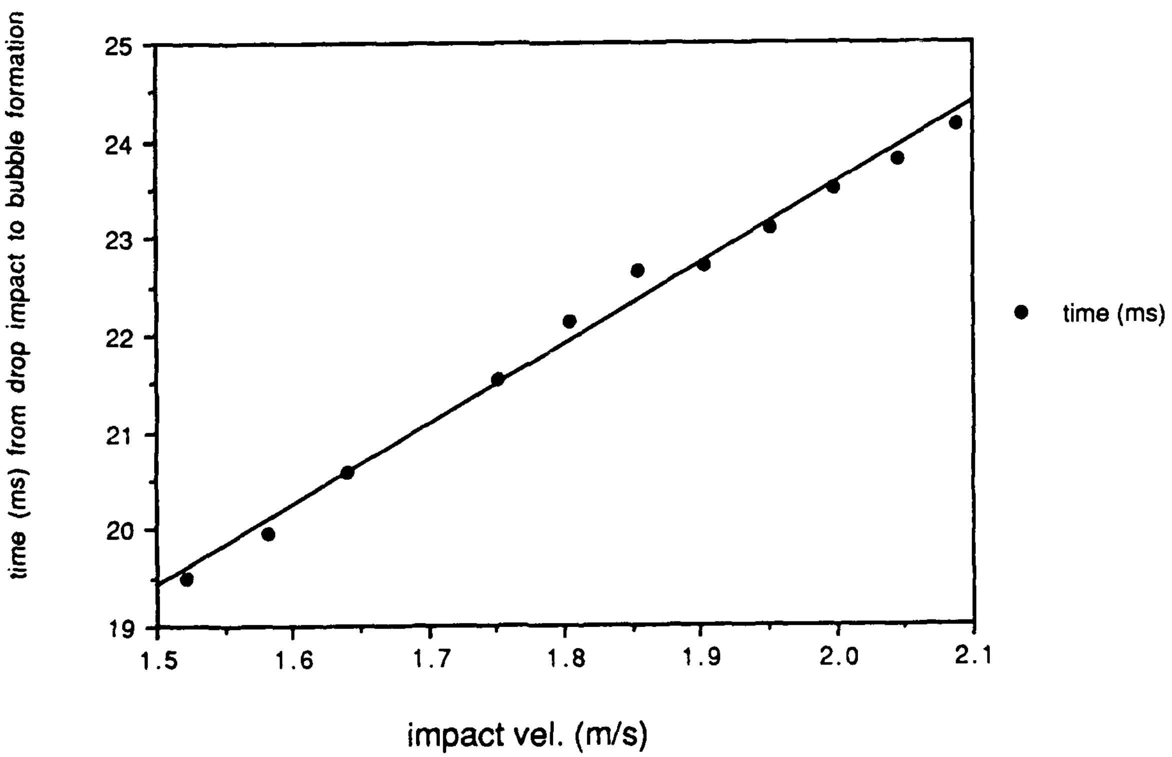

	impact vel.	time (ms)
1	1.246	19.340
2	1.321	20.480
3	1.391	21.126
4	1.458	21.936
5	1.522	22.446
6	1.583	23.276
7	1.642	23.508
8	1.698	24.072
9	1.753	24.580
10	1.805	24.992

drop diameter = 3.34mm

y = 16.357 * x^0.72379   R^2 = 0.996

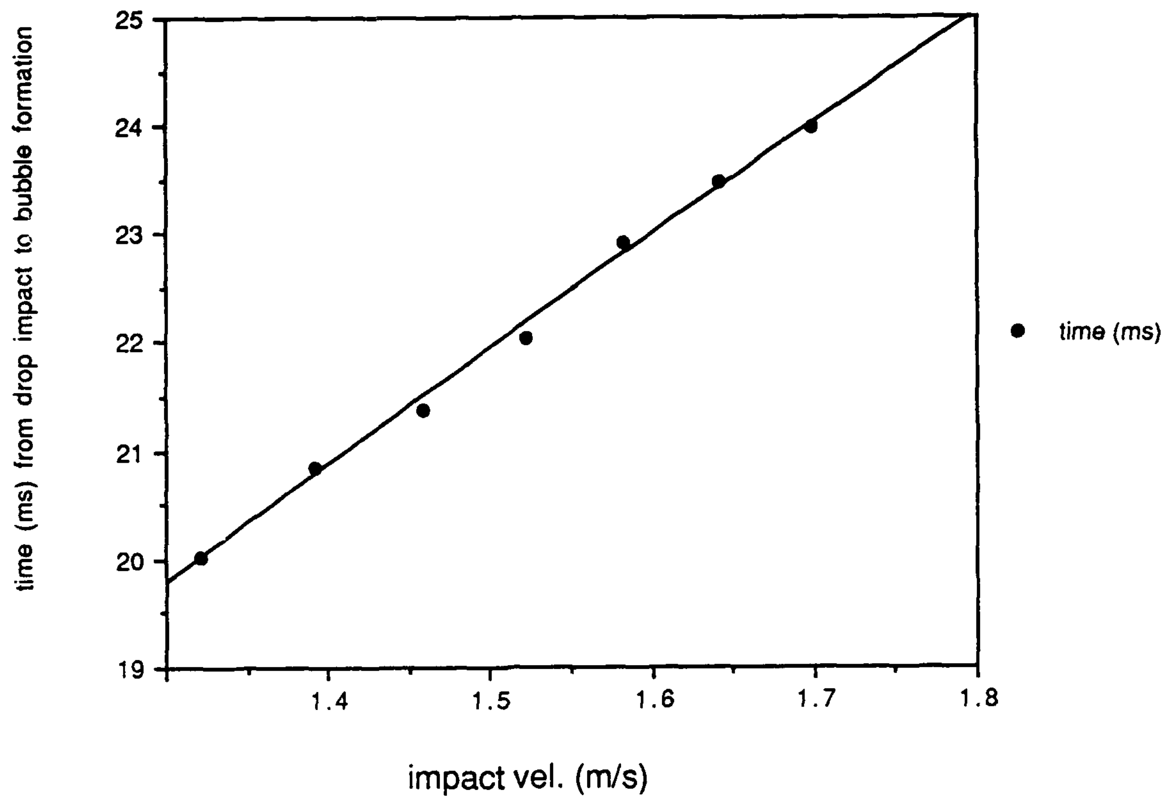

drop diameter = 3.34mm

y = 6.0346 + 10.591x   R^2 = 0.996

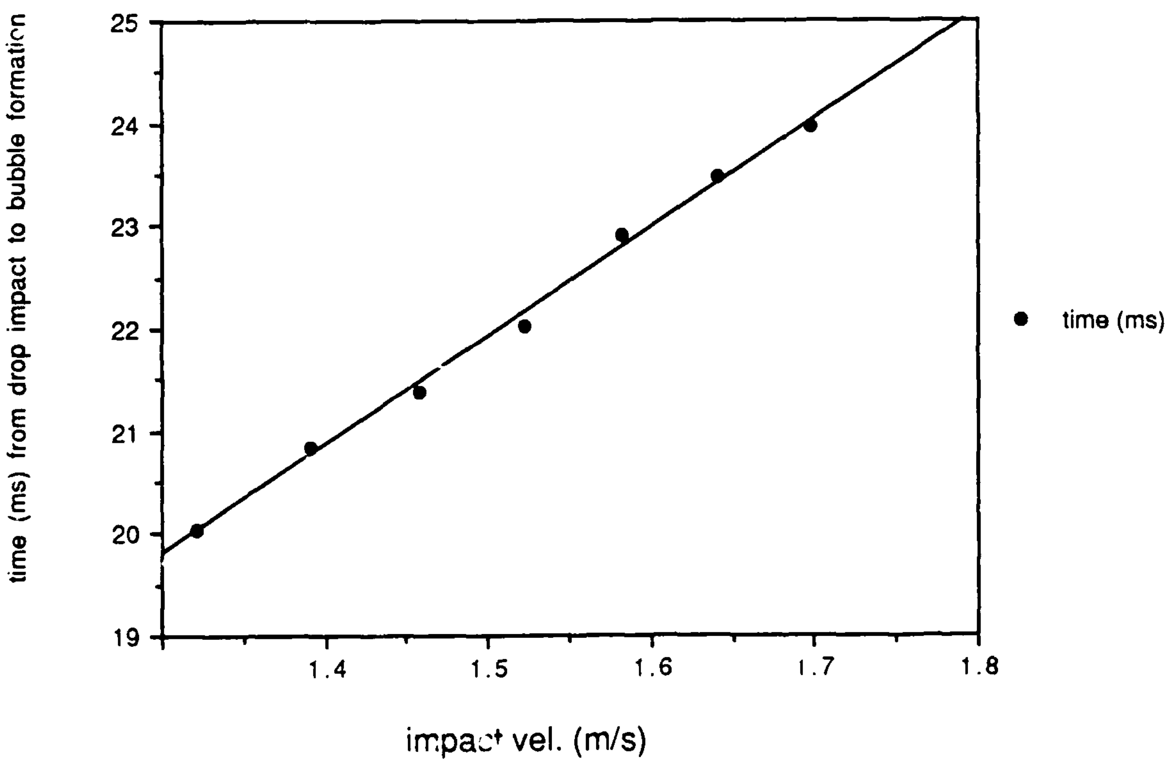

drop diameter = 3.73mm Thu, Jul 20, 1989 9:24 PM

	impact vel.	time (ms)
1	1.241	22.708
2	1.321	23.396
3	1.391	24.328
4	1.459	24.839
5	1.522	25.308
6	1.491	25.196
7	1.426	24.864
8	1.284	23.056
9	1.207	22.516

drop diameter = 3.73mm

y = 20.165 * x^0.55673   R^2 = 0.980

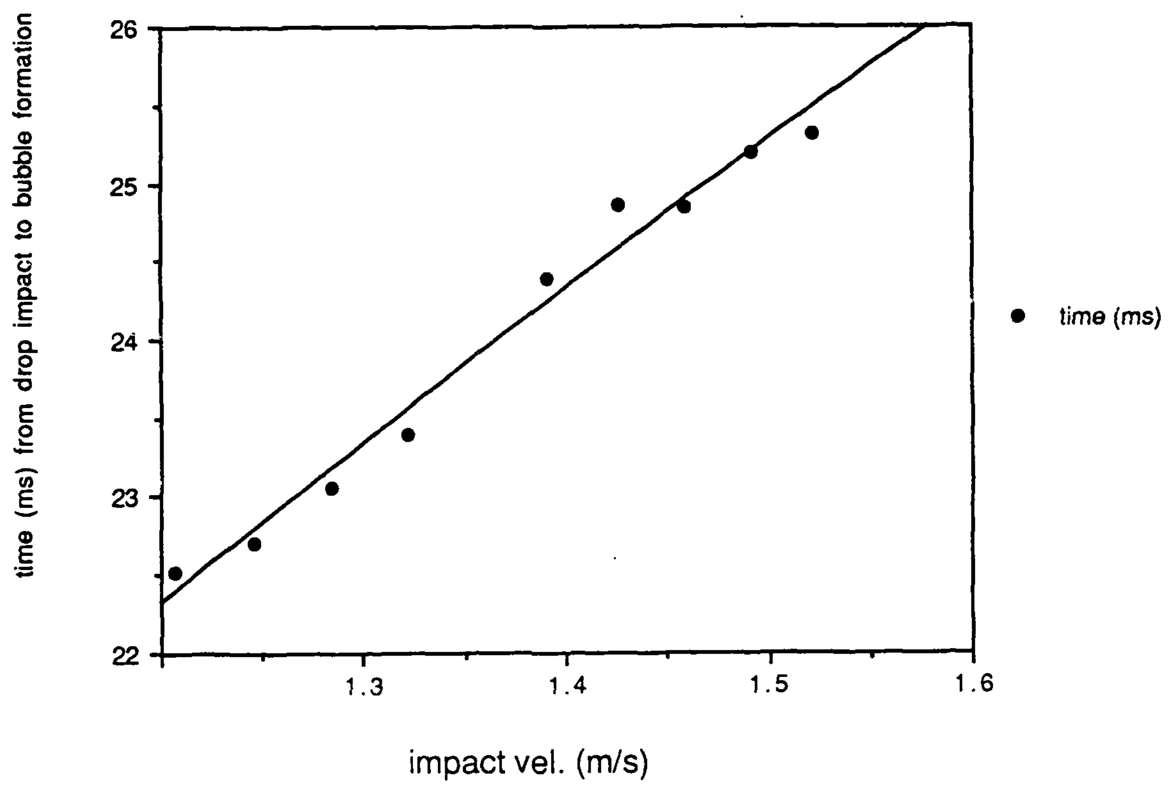

drop diameter = 3.73mm

y = 10.617 + 9.7767x   R^2 = 0.979

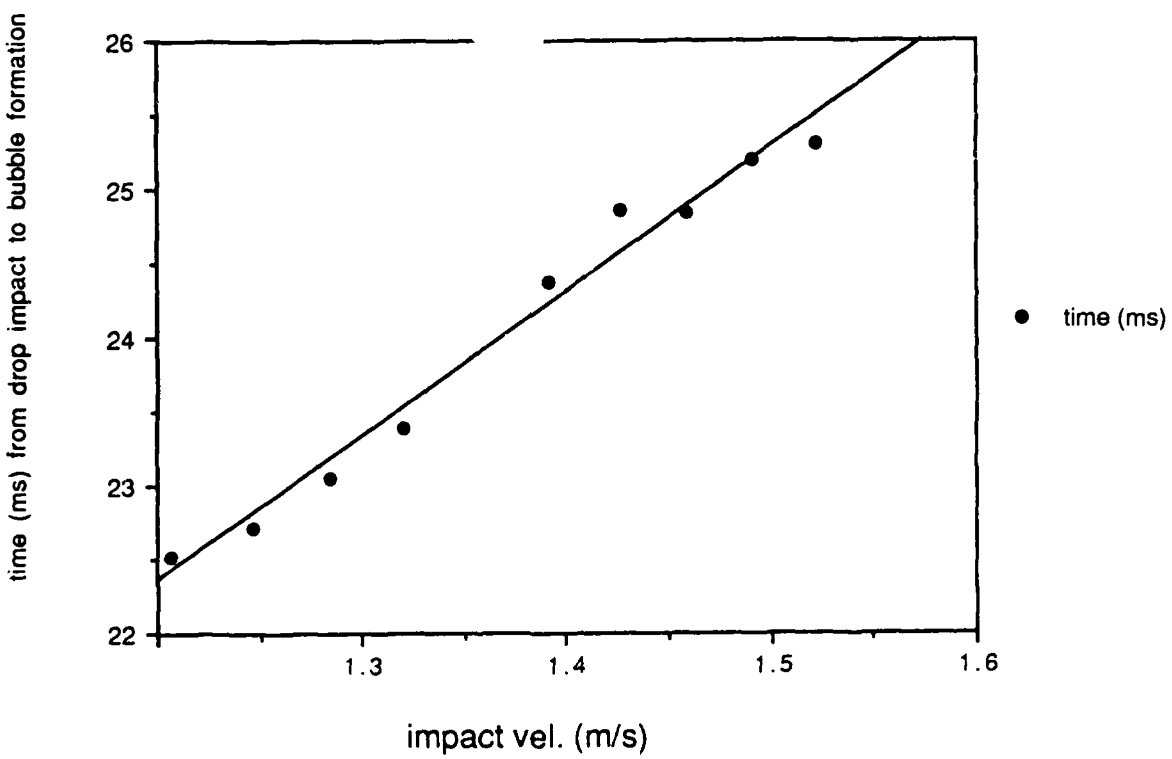

drop diameter = 3.99mm Fri, Jul 21, 1989 11:42 AM

	vel. (m/s)	time (ms)
1	1.266	23.600
2	1.321	24.200
3	1.392	24.700
4	1.426	25.500
5	1.459	25.700

drop diameter = 3.99mm

y = 20.421 * x^0.60644   R^2 = 0.969

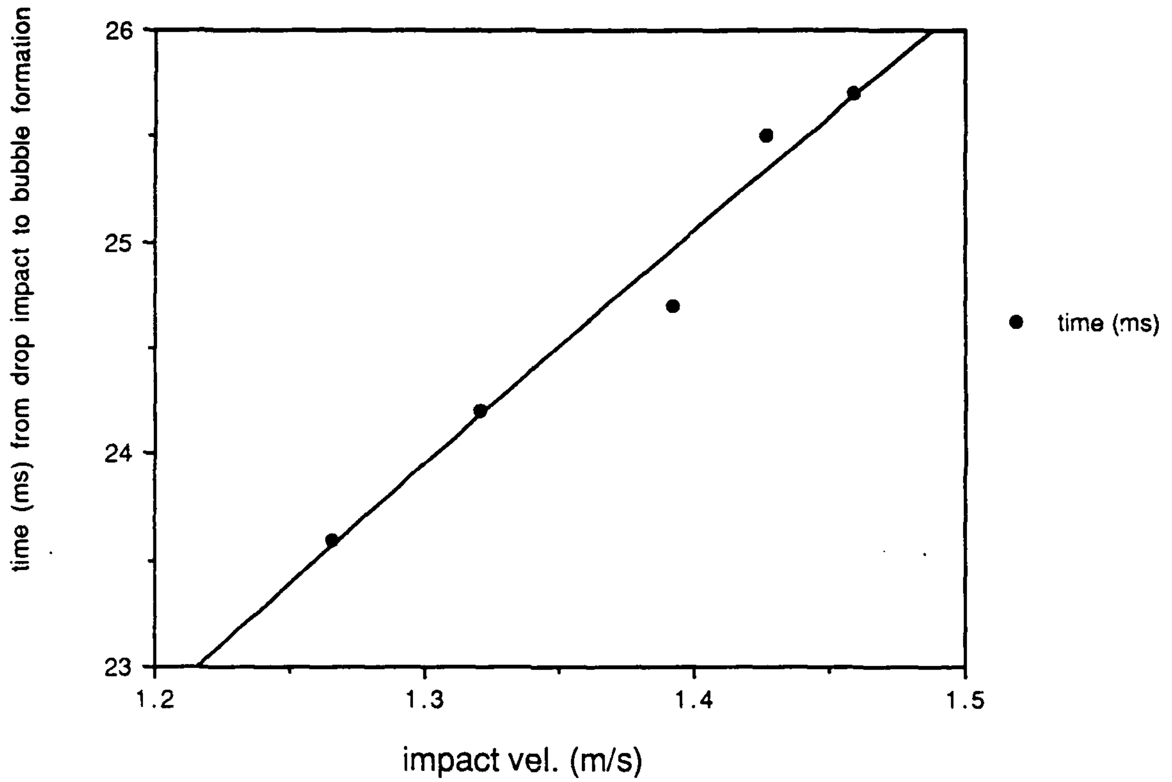

drop diameter = 3.99mm

y = 9.6262 + 11.009x   R^2 = 0.969

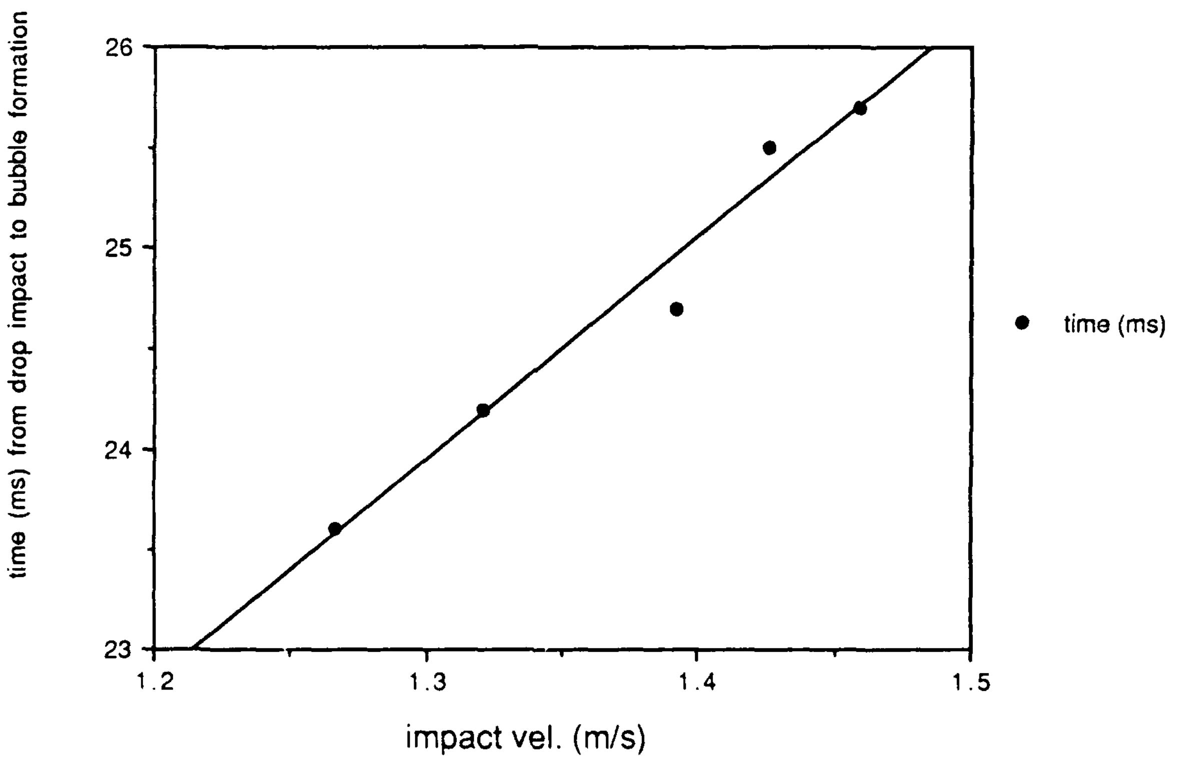

ANALYSIS OF DATA SET 2

Figure 13 is a comprehensive graph of data set 2. It shows that the time between drop impact and bubble formation increases monotonically as drop size or impact velocity increases.

OTHER OBSERVATIONS

Figures 2a and 8 both show the range of impact velocities and drop sizes for regular entrainment. However, there are other activities occurring in and around the region.

Just above the upper velocity bound for drops larger than 3.73 mm in diameter, there is a region of irregular entrainment. As the impact velocity steadily increases from the lowest entraining velocity, entrainment eventually ceases and a lull of bubble formation is observed. However, if the velocity is increased a little more, entrainment resumes. At first glance, the entrainment area appears to have a forked end. But what happens in these two areas is different. Below the lull, the water cavity is in the shape of a cone, and one bubble pinched off the bottom every time. Above the lull, the cavity is spherically shaped with bubbles being formed in an unpredictable manner. Many times there are several bubbles formed by one drop.

Another event occurs just below the lower velocity boundary for drops about 4.5 mm in diameter. Here, surface bubbles measuring about 7 mm diameter and oscillating at 1.3 to 1.4 kHz, are formed when the drop hits the water. However, the event is not a regular occurrence and seems to be dependent on contaminants in the water.

Finally, when a bubble is entrained from a drop falling at a velocity near the upper or lower velocity boundary, the bubble will occasionally exhibit second harmonics, as shown, for example, in Fig. 14. The exact nature of these higher harmonics is not yet clear, but the most likely reason is that the bubble's radius is behaving like a Duffing oscillator. However, shape oscillations may be occurring some of the time since frequency peaks not corresponding to harmonics have been observed in some of the bubble's FFT's. Their occurrence, however, is not common.

CONCLUSIONS

In summary, the characteristics of bubbles inside the observed boundaries of regular entrainment have been explored. When the drop diameter is kept constant and the changes in the bubble's radius, frequency, or initial dipole strength are observed as the impact velocity is continuously increased from the lowest to highest entraining velocities, an extrema is reached with the variance in the data points decreasing the closer they are to it. If the drop is large, (d > 3.79 mm), then any entrainment occurs marginally, and the graphs take on isotropic behavior. If the drop entrains a bubole at terminal velocity, only part of these trends will exist.

As the drop diameter is increased from the minimum to the maximum entrainment size, the frequency of the bubbles' oscillations decrease from 12 to 14 kHz to around 6 or 7 kHz . These results show that regular entrainment is the cause of the underwater noise produced by rain.

Also, bubbles have been shown to take longer to form after impact as the drop size or impact velocity is increased.

Finally, additional phenomena have been observed in and around the entrainment region: irregular entrainment, surface bubbles, and non-linear oscillations. Although, the details of regular entrainment has been extensively investigated, these other phenomena may prove to be sources of fruitful investigation for future researchers.

ACKNOWLEDGEMENTS

The principle author would like to thanks everyone who helped with this research: Dr. Hugh Pumphrey for guiding the research, being a constant source of help and information, and always willing to listen; Dr. Lawrence Crum and Dr. A. Prosperetti for directing the research, and providing many useful ideas and criticisms; and Dr. Suk Wang Yoon for his insight and helpful suggestions. I also wish to thank the faculty, staff, and graduate students at the Physics Department and the National Center for Physical Acoustics for making me feel comfortable and giving their friendship and help to me, especially Dr. Charlie Church, Dr. Glenn Holt, Dr. Ron and Nancy Roy, Adam Calabrese, Missy Carlisle, Mike Finn, Kimberly Frame, Milena and Felipe Gaitan, Steve Horsburgh (especially to you and Mike for curing the computers I unknowingly infected or injured), Joe Richardson, Sandra Smith, and Linnea Weddington. Finally, I wish to thank my undergraduate professors at Millsaps College, Dr. Robert McAdory and Dr. Asif Khandker, for the guidance both of you gave me thoughout my undergraduate studies, which made this research opportunity possible.

REFERENCES

Dingle, A. Nelson and Lee, Yean. "Terminal Fallspeeds of Raindrops." *Journal of Applied Meteorology*. **11** 877 (1972)

Franz, G.J. "Splashes as Sources of Sound in Liquids." *The Journal of the Acoustic Society of America*. **31** 150 (1959)

Gunn, R. and Kinser, G. D. "The Terminal Velocity of Fall for Water Droplets in Stagnant Air." *Journal of Meteorology*. **6** 243 (1949)

Longuet-Higgins, Michael S. "An Analytic Model of Sound Production by Rain-drops." *The Journal of the Acoustic Society of America*. (Submitted for Publication)

Longuet-Higgins, Michael S. "Bubble Noise Spectra." *The Journal of the Acoustic Society of America*. (Submitted for Publication)

Oguz, Hasan N. and Prosperetti, Andrea. "Bubble Entrainment by the Impact of Drops on Liquid Surfaces." *Journal of Fluid Mechanics*. (Submitted for Publication)

Pumphrey, Hugh C., Crum, L.A., and Bjørnø, L. "Underwater Sound Produced by Individual Drop Impacts and Rainfall." *The Journal of the Acoustic Society of A America*. **85** 1518 (1989)

Pumphrey, Hugh C. and Crum, L.A. *Sources of Ambient Noise in the Ocean: An Experimental Investigation*. University of Mississippi, Technical Report. NCPA LC.011989, 96 pp.

Scrimger, Joseph A. et al. "Underwater Noise Due to Rain, Hail, and Snow." *Journal of the Acoustical Society of America*. **81** 79 (1987)

FIGURE CAPTIONS

Figure 1: The sound spectrum of natural rainfall made at various windspeeds between 1.3 to 1.5 meters per second (Scrimger et al. 1987).

Figure 2a: A plot made in a previous study (Pumphrey, Crum, and Bjørnø 1989) of the impact velocities and drop diameters necessary for regular entrainment to occur. Anytime the drop diameter and impact velocity coordinates are located within the area bounded by the curves, regular entrainment will occur

Figure 2b: The graph plots the number of different sized water drop measured earlier (Scrimger et al. 1987) in natural rainfall on three different occasions.

Figure 3: A diagram of the experimental set-up used for this study.

Figure 4: The arrows mark the reference points in the bubble noise used to measure frequency.

Figure 5: The reference points in the bubble noise used to measure initial voltage. These points are marked by the tangential intersection of the vertical lines with the damped sine curve.

Figure 6: The arrows mark the reference points used along the drop's noise to measure the time between drop impact and bubble formation. These points are at the base of the initial impact noise and a reference point in the bubble formation sound.

Figure 7: A plot of two times the dipole strength versus frequency for 200 entrained bubbles. These bubbles were entrained from drops 2.57 mm in diameter striking the water at 2.29 m/s.

Figure 8: A plot made during this study of the impact velociti ... drop diameters necessary for regular entrainment to occur.

Figure 9: A plot made during this study of the kinetic energies and drop diameters necessary for regular entrainment to occur.

Figure 10: An enlargement of figure 5 showing the highest measured velocities for raindrops. The numbers to the sides show the average of thirty measured frequencies in kHz.

Figure 11: Contours of frequency or bubble radius are shown within the entrainment region up to a drop diameter of 3.07 mm.

Figure 12: Contours of initial dipole strength are shown within the entrainment region uo to a drop diameter of 3.07 mm.

Figure 13: Some of the graphs from data set 2 are shown plotted together. The drop diameters associated with each curve are listed beside them.

Figure 14: A marginally entrained bubble displaying primary and secondary harmonics. The top sweep is the acoustic pressure of the oscillation, while the bottom sweep is an enlarged view of its FFT. The numbers above the two peaks in the FFT correspond to the frequencies at those points.

figure 1

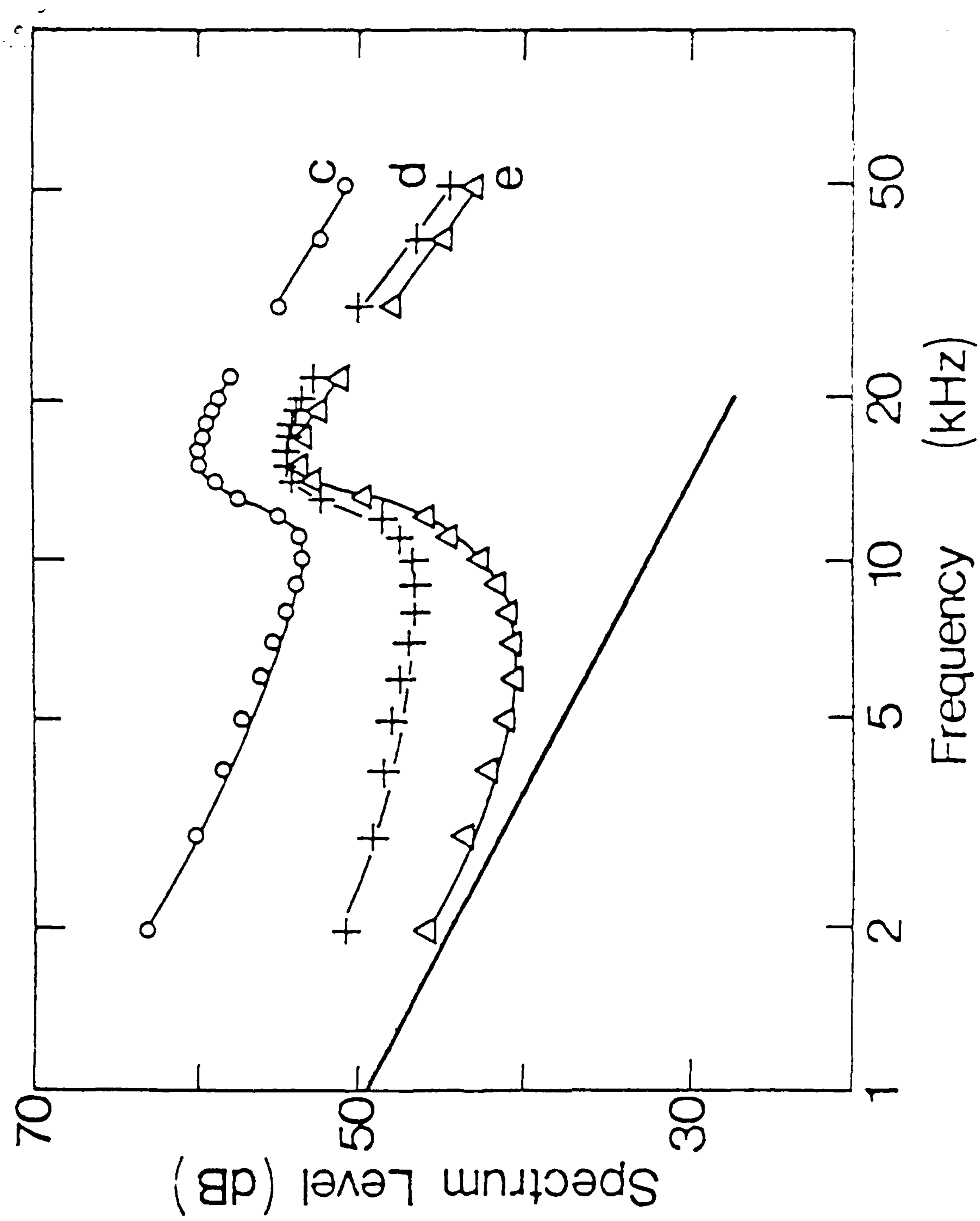

figure 2

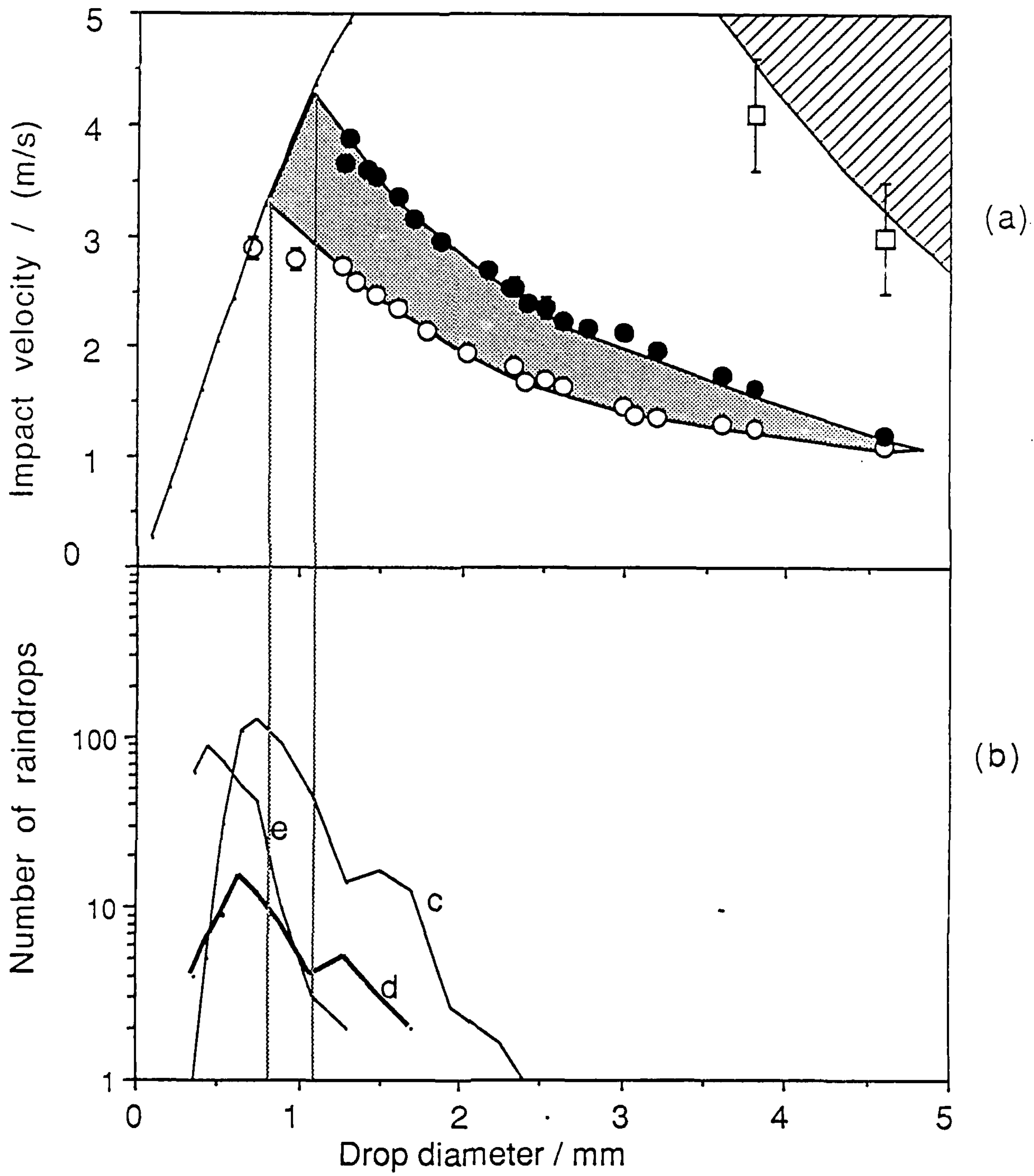

5
4
3
2
1
0
Impact velocity / (m/s)
(a)
100
10
1
Number of raindrops
e
c
d
(b)
0
1
2
3
4
5
Drop diameter / mm

figure 3

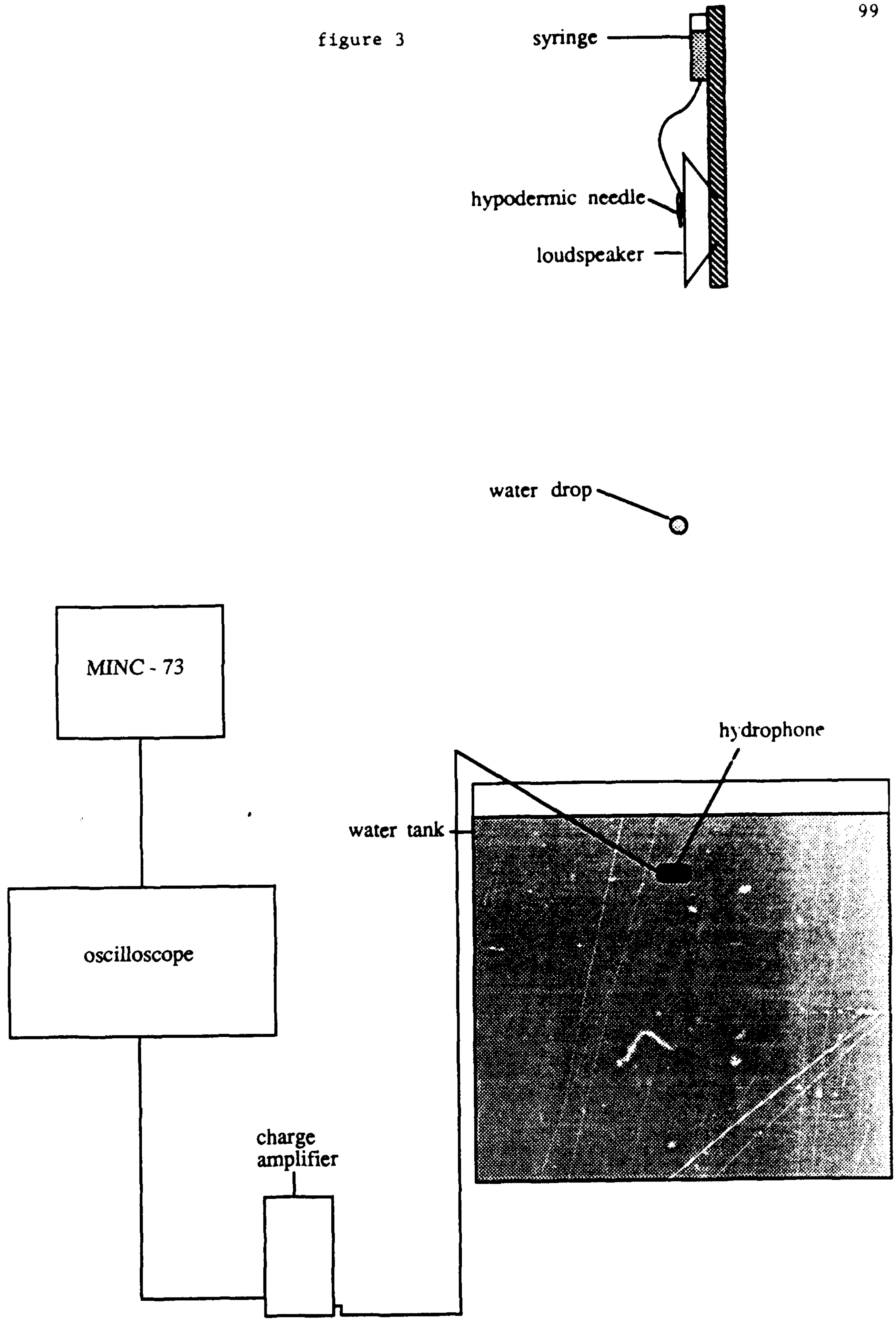
syringe
hypodermic needle
loudspeaker
water drop
MINC - 73
hydrophone
water tank
oscilloscope
charge
amplifier

figure 4

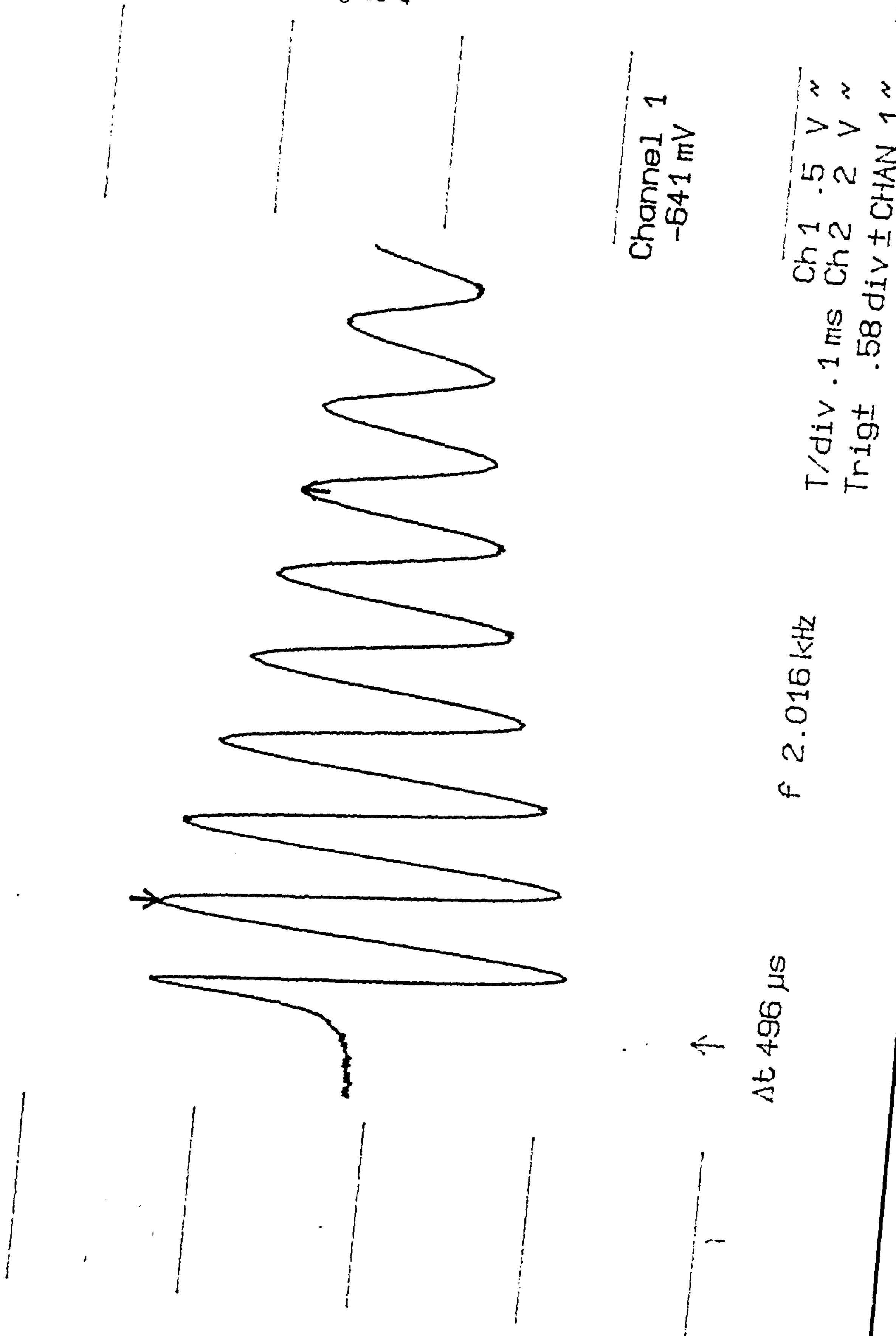
Channel 1
-641 mV
T/div .1 ms Ch 1 .5 V ~
Trig± .58 div ± CHAN 1 ~
Ch 2 2 V ~
f 2.016 kHz
Δt 496 μs

figure 5

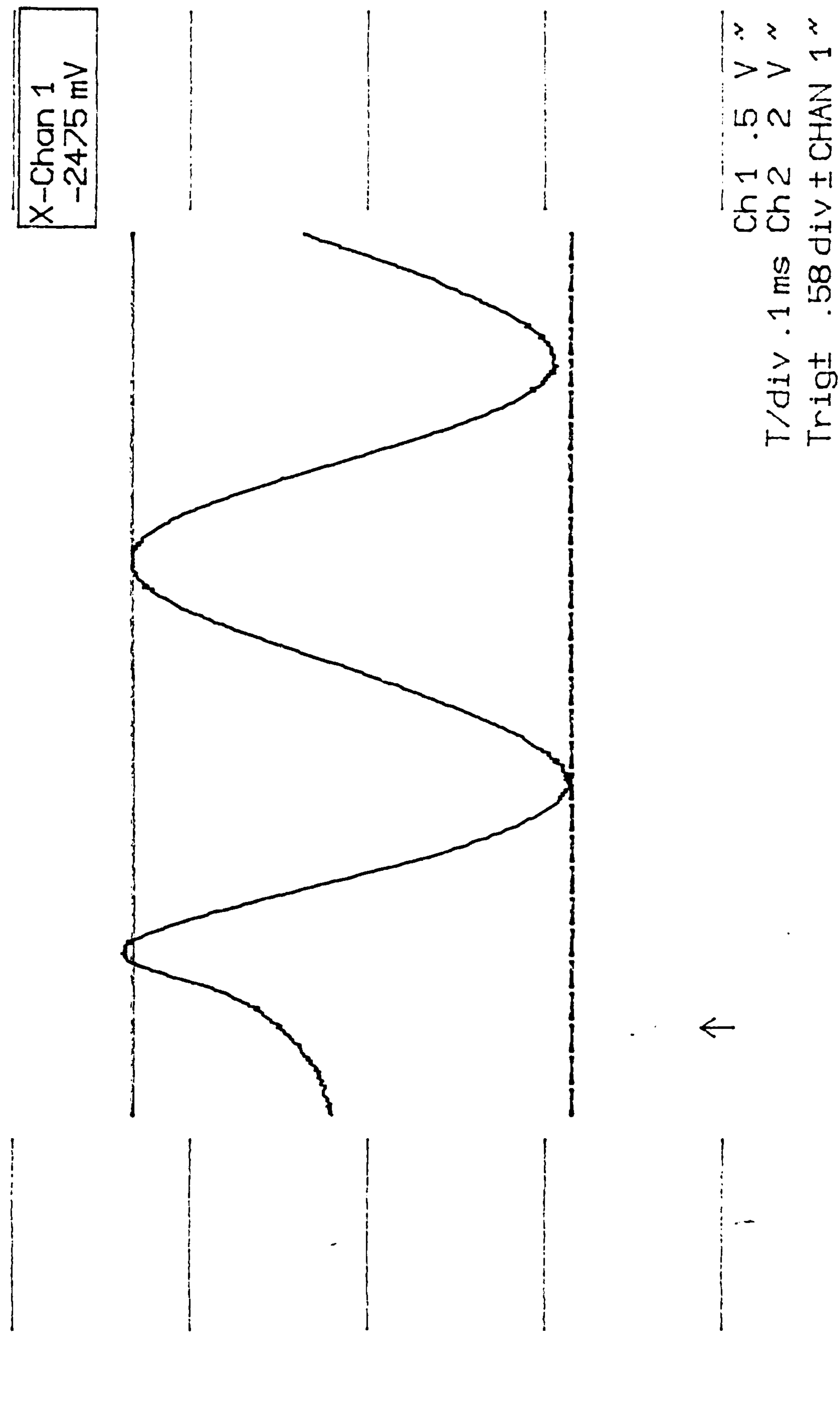

figure 6

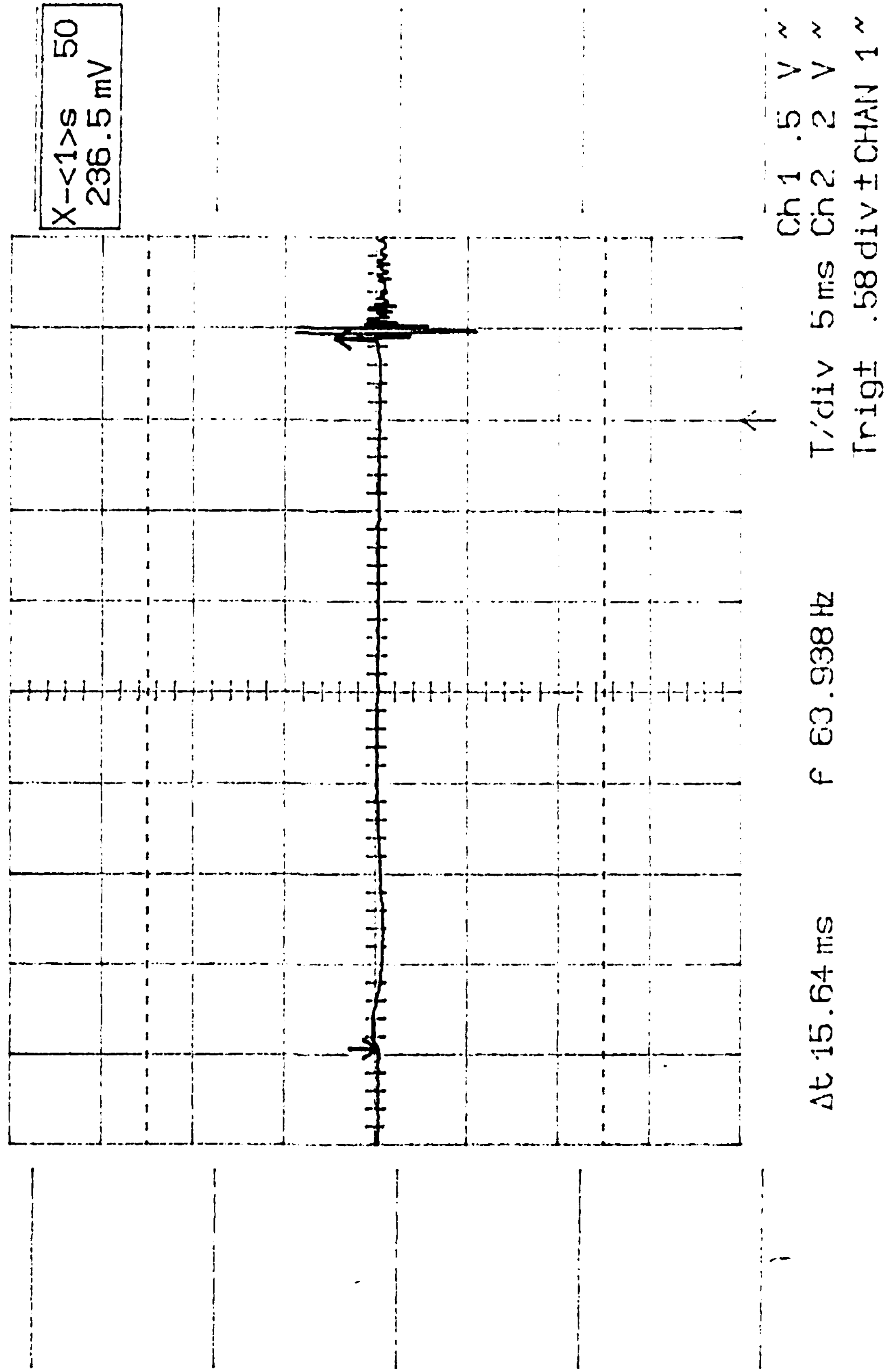
X-<1>s 50
236.5 mV
Ch1 .5 V ~ Ch2 2 V ~
T/div 5 ms
Trig± .58 div ± CHAN 1 ~
f 63.938 Hz
Δt 15.64 ms

figure 7

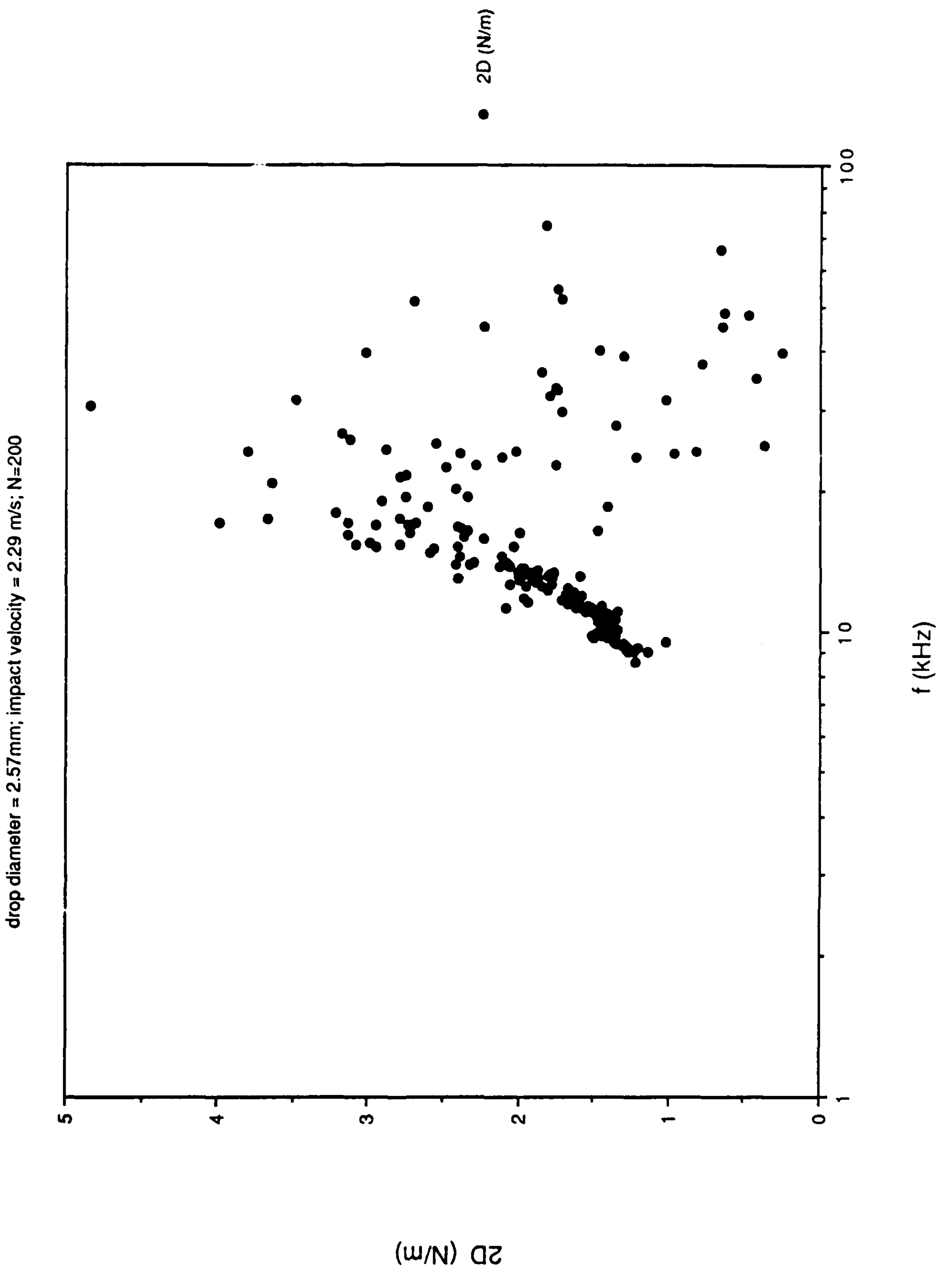
drop diameter = 2.57mm; impact velocity = 2.29 m/s; N=200
2D (N/m)
1
10
100
f (kHz)
0
1
2
3
4
5
2D (N/m)

figure 8

impact velocity vs. drop diameter

y = 7.3637 - 3.8671x + 0.94015x^2 - 8.5407e-2x^3   R^2 = 0.986

y = 5.1359 - 2.7258x + 0.66550x^2 - 5.7822e-2x^3   R^2 = 0.990

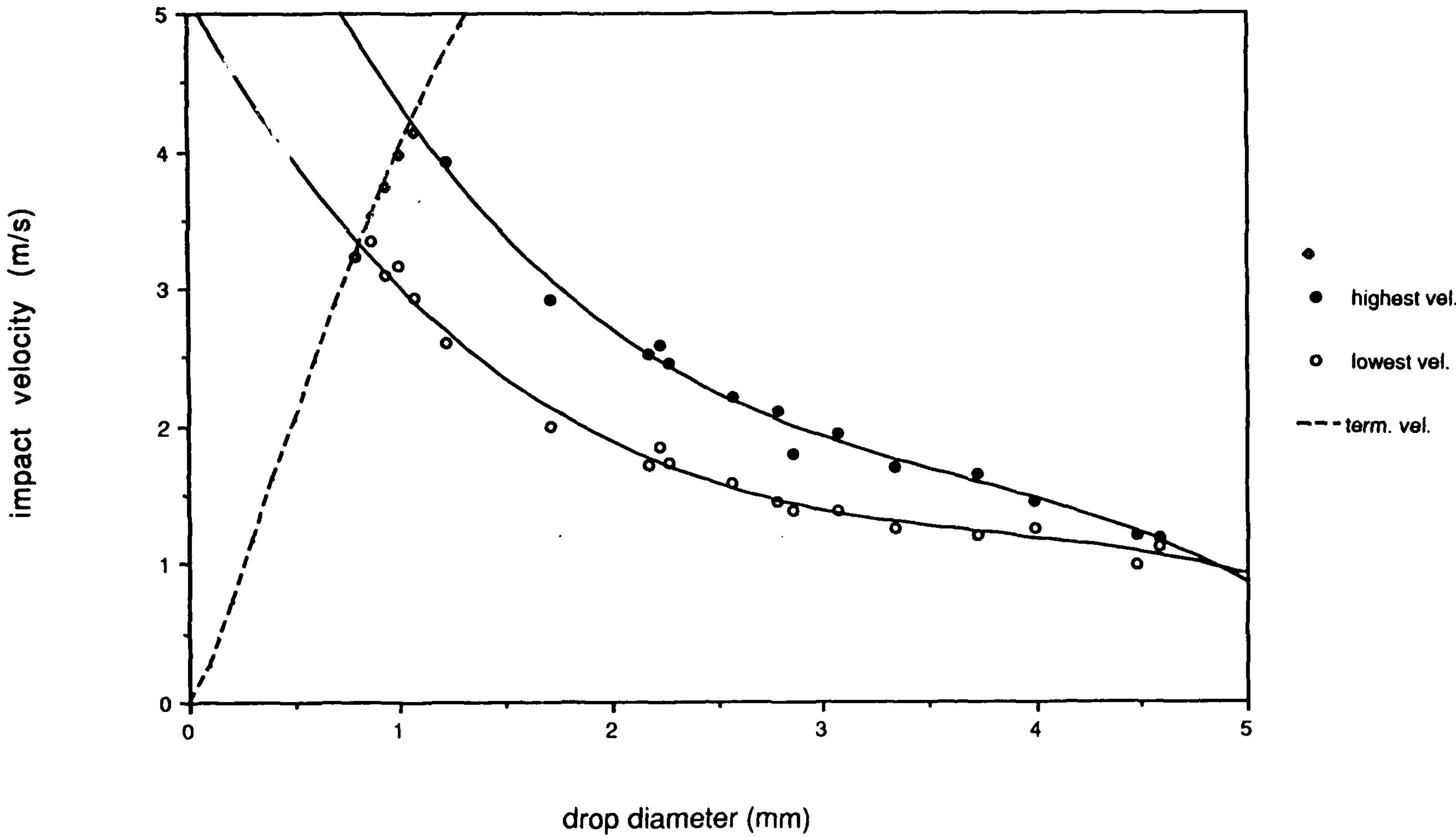

figure 9

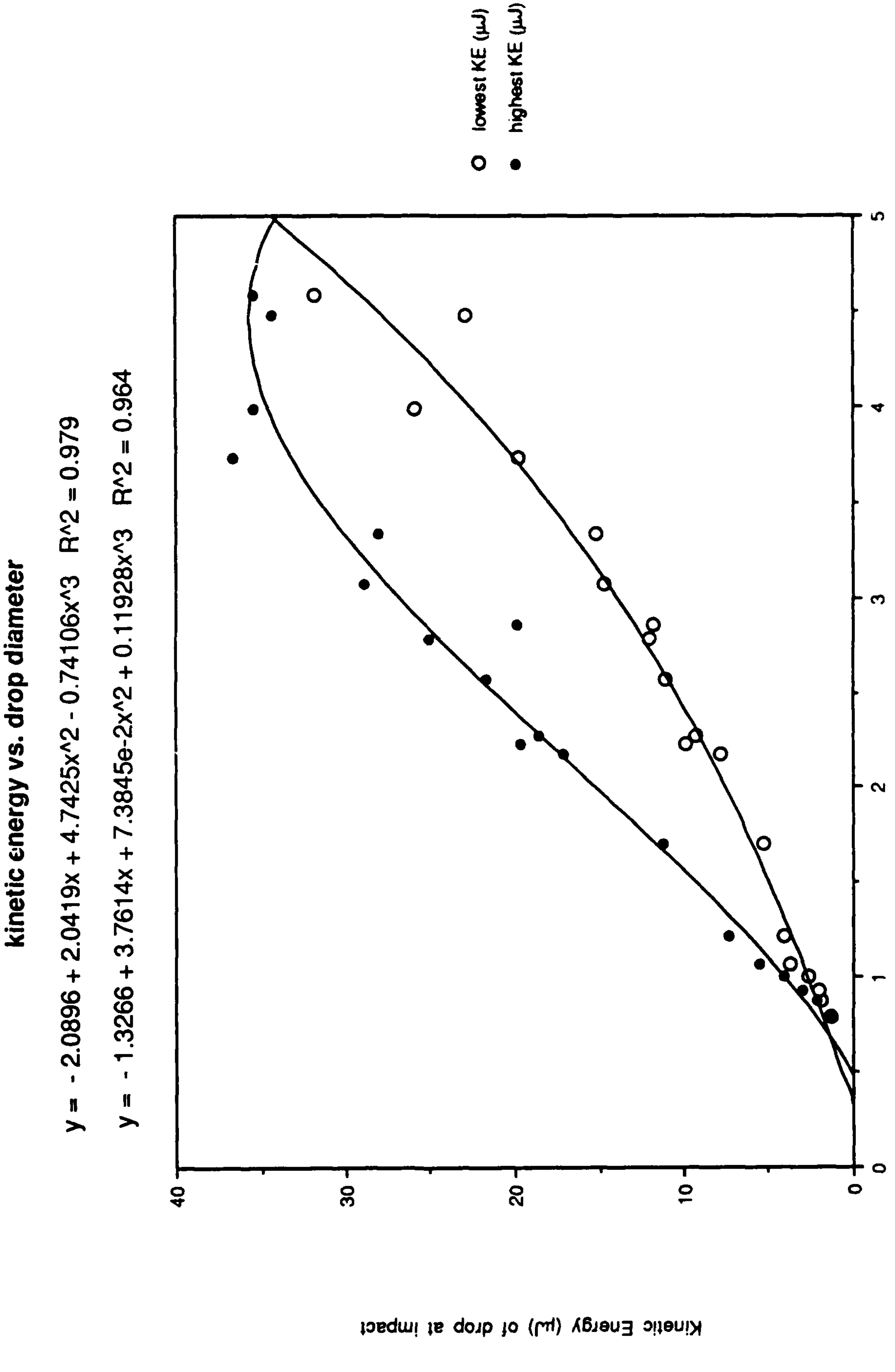
kinetic energy vs. drop diameter
y = - 2.0896 + 2.0419x + 4.7425x^2 - 0.74106x^3 R^2 = 0.979
y = - 1.3266 + 3.7614x + 7.3845e-2x^2 + 0.11928x^3 R^2 = 0.964
lowest KE (μJ)
highest KE (μJ)
Kinetic Energy (μJ) of drop at impact
drop diameter (mm)
0
10
20
30
40
0
1
2
3
4
5

figure 10

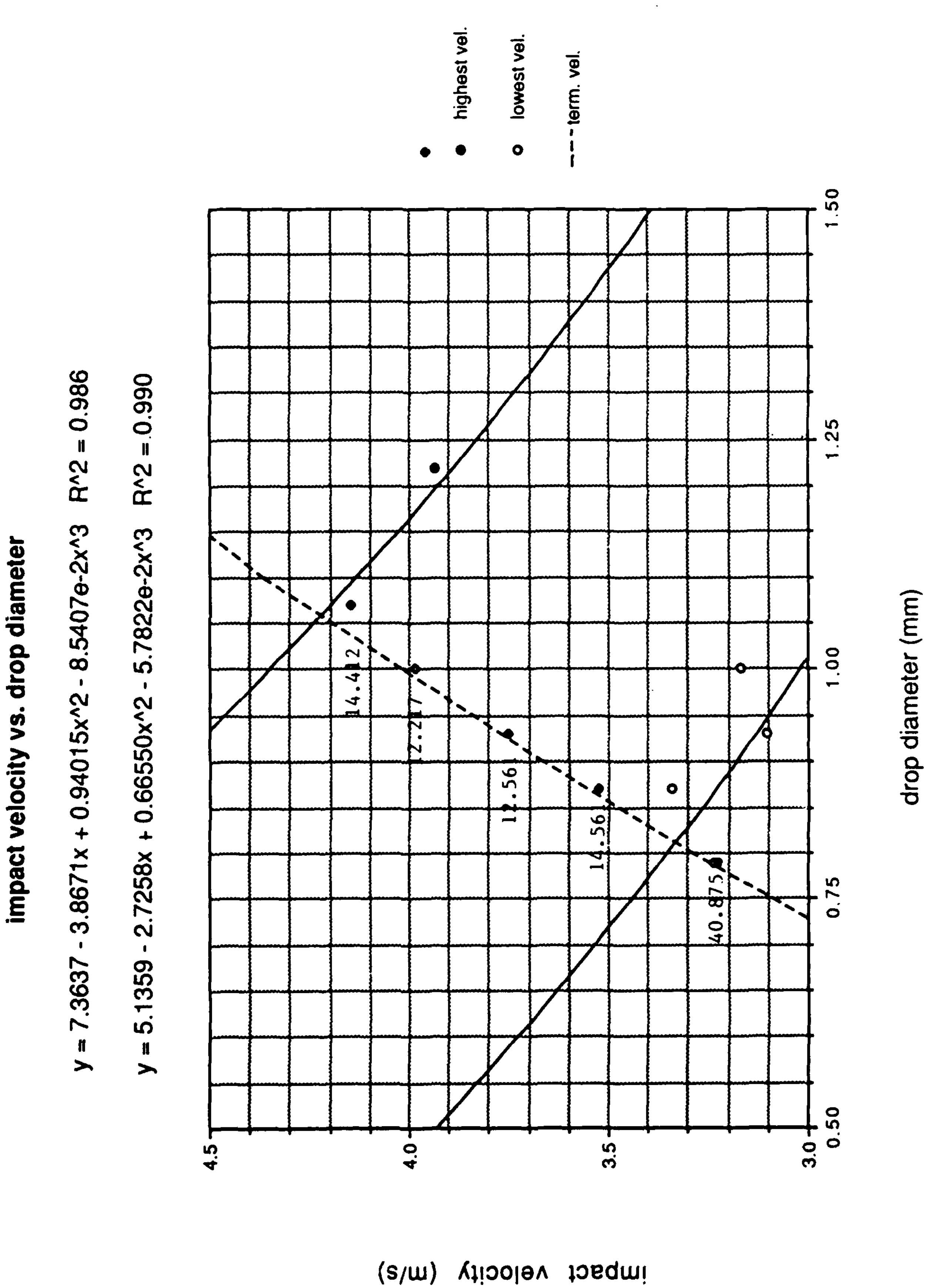
impact velocity vs. drop diameter
y = 7.3637 - 3.8671x + 0.94015x^2 - 8.5407e-2x^3   R^2 = 0.986
y = 5.1359 - 2.7258x + 0.66550x^2 - 5.7822e-2x^3   R^2 = 0.990
highest vel.
lowest vel.
term. vel.
14.412
2.217
12.56
14.56
40.875
4.5
4.0
3.5
3.0
0.50
0.75
1.00
1.25
1.50
drop diameter (mm)
impact velocity (m/s)

figure 11

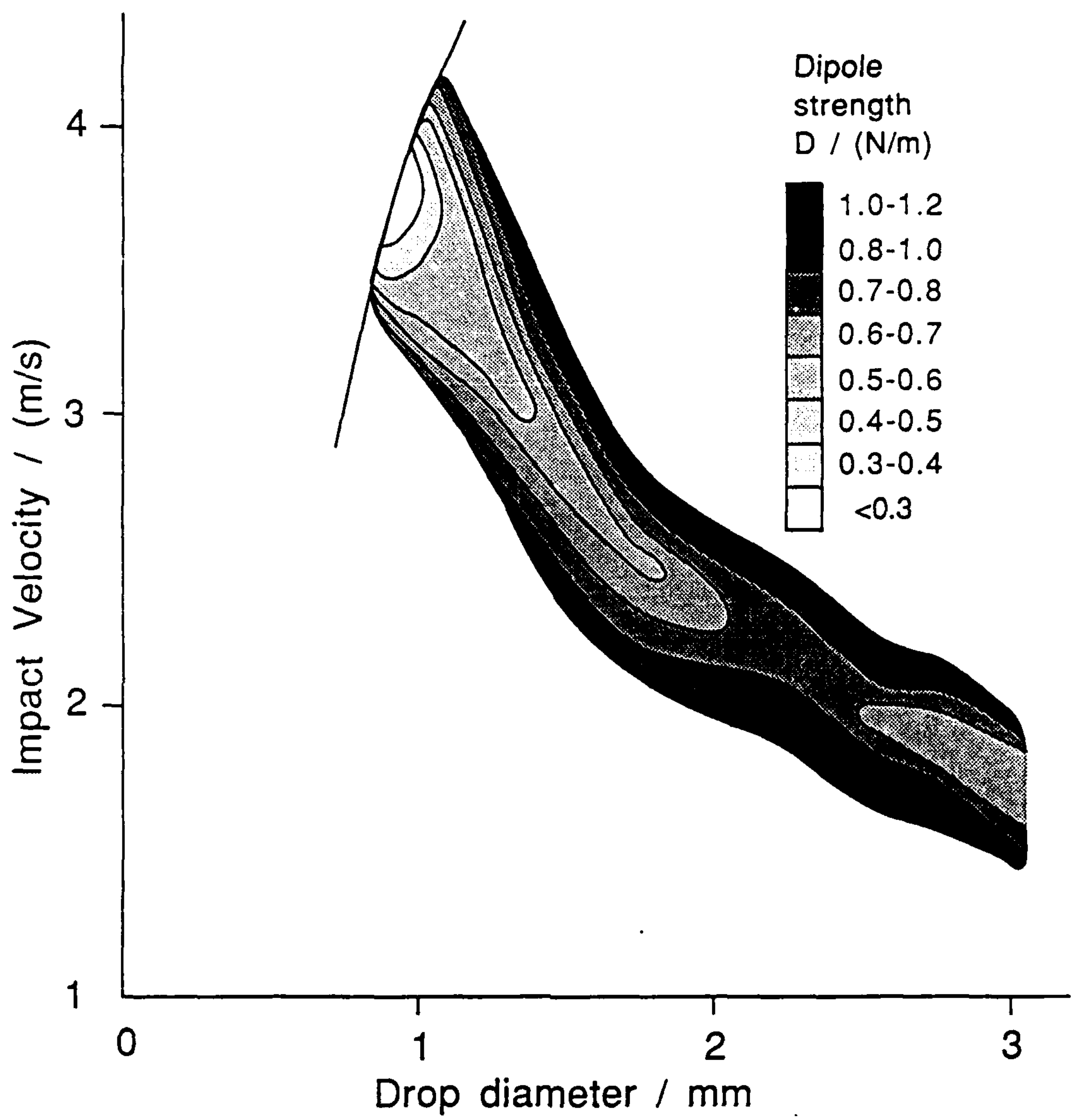
Dipole
strength
D / (N/m)
1.0-1.2
0.8-1.0
0.7-0.8
0.6-0.7
0.5-0.6
0.4-0.5
0.3-0.4
<0.3
Impact Velocity / (m/s)
1
2
3
4
0
1
2
3
Drop diameter / mm

figure 12

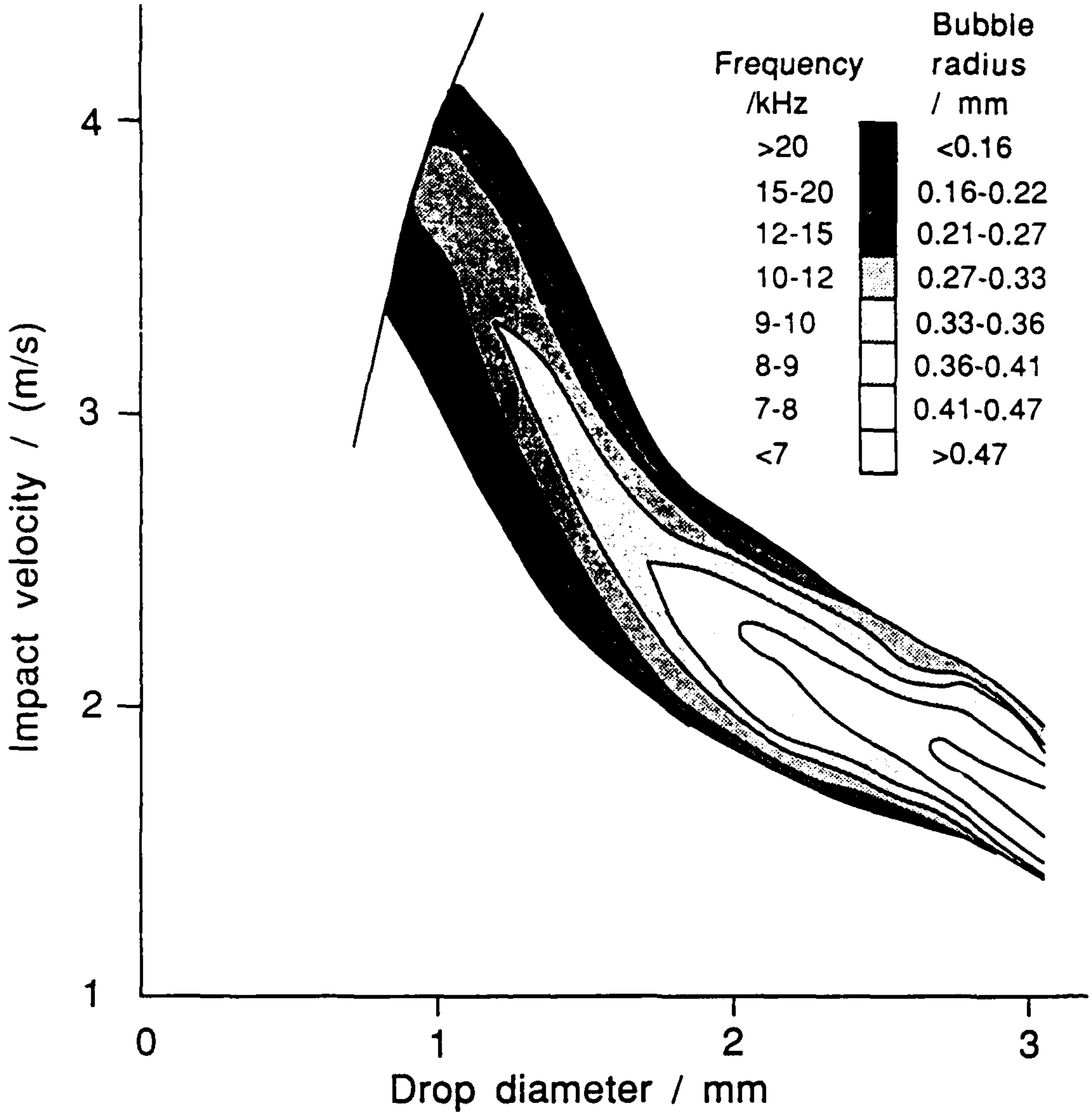
Frequency
/kHz
Bubble
radius
/ mm
>20
<0.16
15-20
0.16-0.22
12-15
0.21-0.27
10-12
0.27-0.33
9-10
0.33-0.36
8-9
0.36-0.41
7-8
0.41-0.47
<7
>0.47
Impact velocity / (m/s)
4
3
2
1
0
1
2
3
Drop diameter / mm

figure 13

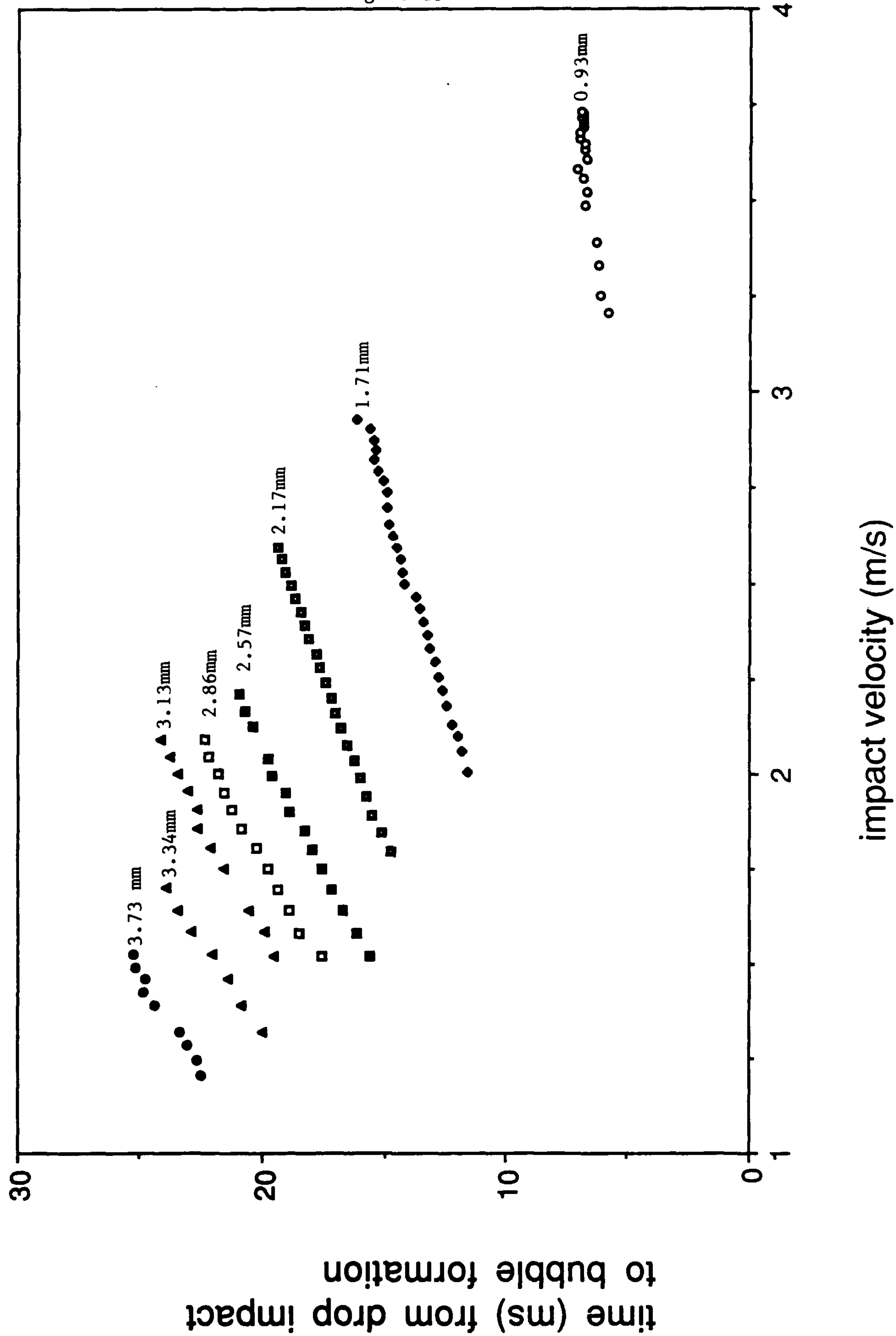
time (ms) from drop impact
to bubble formation
impact velocity (m/s)
0
10
20
30
1
2
3
4
3.73 mm
3.34mm
3.13mm
2.86mm
2.57mm
2.17mm
1.71mm
0.93mm

figure 14

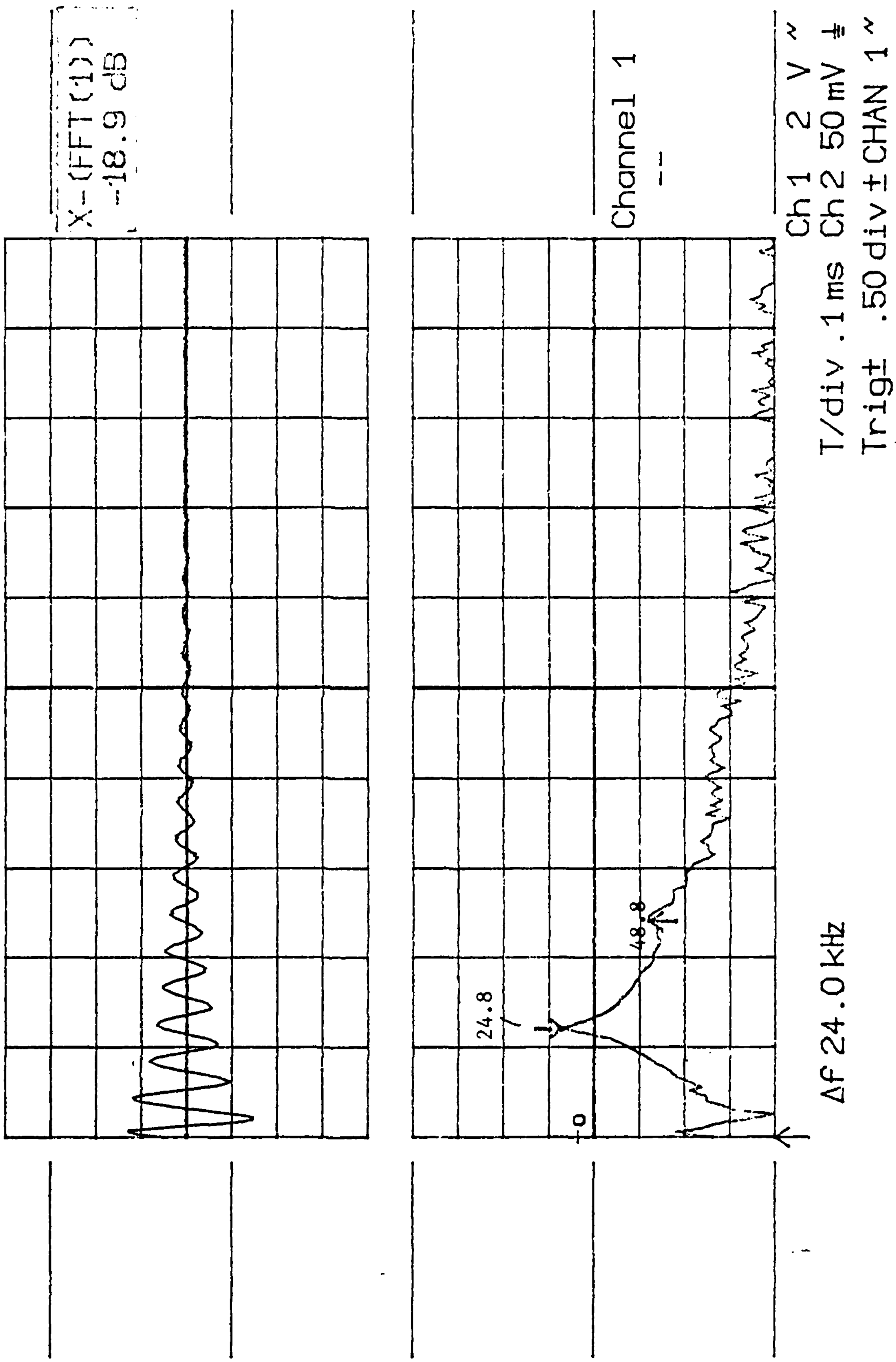
X-(FFT(1))
-18.9 dB
Channel 1
Ch 1 2 V
T/div .1 ms Ch 2 50 mV
Trig± .50 div ± CHAN 1
Δf 24.0 kHz
24.8
48.8
0

1	Chief of Naval Research Office of Naval Research Department of the Navy Arlington, VA 22219 Attn: Marshall Orr
2-5	Commanding Officer and Director Defense Technical Information Center Bldg. 5, Cameron Station 5010 Duke Street Alexandria VA 22314
6-8	Dr. L. A. Crum Associate Director of Basic Research National Center for Physical Acoustics University MS 38677
9	Professor M. S. Longuet-Higgins Center for Studies of Nonlinear Dynamics LaJolla Institute 10280 N. Torrey Pines Road, Suite 260 LaJolla CA 92037
10	Dr. A. Prosperetti Department of Mechanical Engineering The Johns Hopkins University Baltimore MD 21218
11	Dr. B. R. Kerman Atmospheric Environment Service 4905 Dufferin Street Downsview, Ontario, M3H 5T4 Canada
12	Dr. J. A. Nystuen Code 68Ny Department of Oceanography Naval Postgraduate School Monterey CA 93943
13	Dr. W. A. Kuperman Naval Research Laboratory Washington DC 20375
14	L. Bjørnø Industrial Acoustics Laboratory Technical University of Denmark Building 425, DK-2800 LYNGBY, Denmark
15-20	Paul A. Elmore P.O.Box 15094 Millsaps College Jackson, MS 39210